Endothelial colony-forming cells as a platform for early cardiovascular risk assessment

By

Cheryl Mei Jun Tan
BSc (Hons), MRes

Thesis presented for the degree of Doctor of Philosophy in Cardiovascular Medicine at the University of Oxford

St Hugh's College

Division of Cardiovascular Medicine
Radcliffe Department of Medicine
University of Oxford

Oxford Cardiovascular Clinical Research Facility
Level 1, John Radcliffe Hospital
Oxford, England. OX3 9DU

Supervisors:

Associate Professor Adam Lewandowski
Professor Paul Leeson
Assistant Professor Mariane Bertagnolli

Hilary term 2022

Approximate word count: 41, 638

Acknowledgements

This learning journey and research would not be possible without the support from several people. First, I would like to thank the Singapore private company scholarship for the funding and support for the research. I would also like to thank the British Heart Foundation and Wellcome Trust for supporting this research. I am ever so grateful to the University of Oxford, the Division of Cardiovascular Medicine department and my academic supervisors – Associate Professor Adam Lewandowski, Professor Paul Leeson and Assistant Professor Mariane Bertagnolli for the chance to work with you. Thank you, Professor Paul Leeson, for allowing me to be part of a wonderful team and giving me the opportunity to learn, grow my confidence, and the support I need to be where I am now. Thank you to Assistant Professor Mariane Bertagnolli for the guidance and support throughout my time at Oxford. Thank you for believing in me, showing me your passion for research, and for your invaluable guidance. Without your patience, insight and support, the work would not be possible. I am also so proud to witness all your wonderful achievements, you are truly amazing and someone that I aspire to be.

Thank you to Associate Professor Adam Lewandowski, for being there for me whenever I needed it. Your supervision and mentorship throughout my doctorate are vital to completing my thesis. You are a great role model, and I admire your work ethic, kindness, compassion, understanding and professionalism. Thank you for always supporting my “wild” research ideas. Thank you for believing in me. Thank you for everything, Adam (Jaco and Khaleesi). It is beyond words. A big thank you must also go to the volunteers that gave up their time to participate in the study. To the Oxford Cardiovascular Clinical Research family (Maryam, Afifah, Yvonne, Polly, Winok, Grace, Christina, Annabelle F., Annabelle M., Jamie, Wilby, Huck, Will, Cameron, Holger, Katie, Adam, Paul, Aggy, and Cate), thank you for being so welcoming and helpful throughout my time here. You guys have shown me the power of teamwork and the wonders of kindness. A special thanks to the Cardiovascular Medicine Laboratory team (Yiangos, My-Nhan, Charlotte, Naveed,

Daan, Alex, Letta, Lucia, Neelam, Kajus, Kate, Jillian, Paul, Chris, Nahla, Amy, Faseeha and Sandy) for being so kind and helpful, for teaching me different techniques and engage in not just in rigorous scientific discussions and collaborations and but also all the random pubs and waffles dates. I would also like to thank all my family and friends who have supported my journey.

To my fiancé, Kim Shen. Without your unconditional support, love, trust, and encouragement, this DPhil journey (and our long-distance relationship) would not have been possible. I am ever so thankful for you. We do make a great team.

Finally, I would like to express my gratitude to my family for always believing in me and for all the love, care, and support. I am so grateful for all sacrifices you have done to get me here and for always rooting for me. To my beloved papa, my biggest supporter, pillar of strength, and motivator, who sadly would not be able to witness my achievement. I hope I have done you proud. I could not have done this without your endless support and love. You taught me so much in life, and I am still learning even without you. Your wisdom and legacy will forever live on.

Dedication

For the man of my life, my best friend – my beloved papa.

It doesn't matter where you are, I will always look up to you.

我好愛你，好想你

爸爸。



Abbreviations

AcLDL	Acetylated low-density lipoprotein
ADMA	Asymmetric dimethylarginine
AVR	Arteriolar-to-venule ratio
BMI	Body mass index
BNP	Brain natriuretic peptide
BP	Blood pressure
BS-1	Bandeiraea simplicifolia lectin
CAC	Circulating angiogenic cell
CCRF	Cardiovascular clinical research facility
CD105	Endoglin
CFU-Hill	Colony-forming units-Hill
CPET	Cardio-pulmonary exercise testing
CRAE	Central retinal arteriolar equivalent
CRP	C-reactive protein
CRVE	Central retinal venular equivalent
CVD	Cardiovascular disease
EC	Endothelial cell
ECFC	Endothelial colony-forming cell
eNOS	Endothelial nitric oxide synthase
EPC	Endothelial progenitor cells
ECM	Extracellular matrix
FGF	fibroblast growth factor
Flk-1	Vascular endothelial growth factor receptor
GPx	Glutathione peroxidase
GWAS	Genome-wide association studies
HDL	High density lipoprotein
HUVEC	Human umbilical vein endothelial cell
ICAM-1	Intercellular cell adhesion molecules-1
IGF1	Insulin-like growth factor 1
IGF1R	Insulin-like growth factor 1 receptor
IL-1/IL-6	Interleukin-1 / -6
IRS	Insulin receptor substrate
LDL	Low density lipoprotein
MMP-9	Matrix-metalloproteinase-9
MNC	Mononucleated cell
NADPH	Nicotinamide adenine dinucleotide phosphate oxidase
NF-κB	Nuclear factor kappa B
NO	Nitric oxide
NOS	Nitric oxide synthase
PBMC	Peripheral blood mononucleated cell
PDGF	Platelet-derived growth factor

Peak VO_2	Maximum rate of oxygen consumption
PECAM-1/ CD31	Platelet-EC adhesion molecule 1
PWV	Pulse wave velocity
ROS	Reactive oxygen species
RV	Right ventricle
SDF-1	Stromal cell-derived factor 1
SOD	Superoxide dismutase
STEMI	ST-elevation myocardial infarction
TEK	Tunica intima EC kinase
TEPHRA	Trial of Exercise to Prevent HypeRtension in young Adults
Tie-2	Angiopoietin-1 receptor
TNF-α	Tumour necrosis factor-α
TOD	Target end-organ damage
UEA-1	Ulex Europeus Agglutinin-1
VE-cadherin or CD144	Vascular endothelial cadherin
VEGF	Vascular endothelial growth factor
VEGFR-2	Vascular endothelial growth factor receptor-2
vWF	von Willebrand factor

Abstract

Endothelial colony-forming cells as a platform for early cardiovascular risk assessment

Thesis presented for the degree of Doctor of Philosophy in Cardiovascular Medicine at the University of Oxford

Cheryl Mei Jun Tan

St Hugh's College, Hilary Term 2022

The human endothelial colony-forming cells (ECFCs), a subpopulation of endothelial progenitor cells (EPCs), offer a potential platform for cellular assessment due to their remarkable angiogenic expansion, regenerative, and self-renewable potentials *in vitro.* This thesis investigated how ECFC function and proteome profiles are altered in young adults with elevated cardiovascular disease (CVD) risk factors, including increased blood pressure (BP). It also demonstrated the effect of an exercise intervention on ECFC function and the potential to use ECFC to predict response to exercise intervention.

The main investigations of this thesis were based on a cohort of young adult participants aged 18 to 35 years, recruited through the **T**rial of **E**xercise to **P**revent **H**ypeRtension in young **A**dults (TEPHRA). Detailed clinical measurements, including BP measurements, retinal micro-vascular imaging, pulse wave velocity, blood biochemistry and lipid profiles, as well as ECFC culture and cellular assessments, were performed at baseline pre-exercise intervention. Measurements were repeated following a 16-week exercise intervention training period in a subgroup of participants. Our data presented a distinct proteomic signature with altered angiogenic mechanisms in dysfunctional ECFCs. An increase in CVD risks, including higher BP, body mass index and impaired lipid profile, were associated with a reduction in expansion and vasculogenic capacity in

dysfunctional ECFCs. Further analysis revealed that the young adults with elevated BP had significantly reduced ECFC functionality and presented a potentially adverse retinal micro-vascular structure and greater macro-vascular resistance. Although no significant changes were observed in the ECFCs after exercise intervention, we demonstrated that baseline ECFC functional characteristics might positively affect aerobic training response. In addition, baseline ECFC functional characteristics may predict response to exercise, suggesting that mechanisms or substances modulating ECFC colony formation and function may be essential factors that affect an individual's response to exercise.

List of publications & awards

Original manuscripts published during DPhil

Williamson, W., Lewandowski, A. J., Huckstep, O. J., Lapidaire, W., Ooms, A., **Tan, C.**, ... & Leeson, P. (2022). Effect of moderate to high intensity aerobic exercise on blood pressure in young adults: The TEPHRA open, two-arm, parallel superiority randomised clinical trial. EClinicalMedicine, 48, 101445.

Kitt, J., Frost, A., Mollison, J., Tucker, K. L., Suriano, K., Kenworthy, Y., McCourt A, Woodward W, **Tan C.,** . . . Leeson, P. (2022). Postpartum blood pressure self-management following hypertensive pregnancy: protocol of the Physician Optimised Post-partum Hypertension Treatment (POP-HT) trial. *BMJ open*, *12*(2), e051180.

Chuaiphichai, S., Yu, G., **Tan, C.,** Whiteman, C., Douglas, G., Dickinson, Y., . . . Channon, K. (2021). Endothelial GTP cyclohydrolase and tetrahydrobiopterin regulate gestational blood pressure, uteroplacental remodeling and fetal growth. *Hypertension*, *78*(6), 1871-1884.

Tan, C. M. J., Lewandowski, A. J., Williamson, W., Huckstep, O. J., Yu, G. Z., Fischer, R., . . . Bertagnolli, M. (2021). Proteomic signature of dysfunctional circulating endothelial colony-forming cells of young adults. *Journal of the American Heart Association*, *10*(15).

Alsharqi, M., Huckstep, O., Lapidaire, W., Williamson, W., Mohamed, A., **Tan, C.,** . . . Leeson, C. (2021). Left atrial strain predicts cardiovascular response to exercise in young adults with suboptimal blood pressure. *Echocardiography*, *38*(8), 1319-1326.

Ruane, P. T., **Tan, C. M. J**., Adlam, D. J., Kimber, S. J., Brison, D. R., Aplin, J. D., & Westwood, M. (2020). Protein O-GlcNAcylation Promotes Trophoblast Differentiation at Implantation. *Cells*, *9*(10), 2246.

Mohamed, A., Lamata, P., Williamson, W., Alsharqi, M., **Tan, C. M. J**., Burchert, H., . . . Lewandowski, A. J. (2020). Multimodality imaging demonstrates reduced right-ventricular function independent of pulmonary physiology in moderately preterm-born adults. *JACC: Cardiovascular Imaging*.

Huckstep, O., Burchert, H., Williamson, W., Telles, F., **Tan, C. M. J**., Bertagnolli, M., . . . Lewandowski, A. J. (2020). Impaired myocardial reserve underlies reduced exercise capacity and heart rate recovery in preterm-born young adults. *EHJ Cardiovascular Imaging / European Heart Journal - Cardiovascular Imaging*, *22*(5), 572-580.

Tan, C. M. J., & Lewandowski, A. (2019). The transitional heart: from early embryonic and fetal development to neonatal life. *Fetal Diagnosis and Therapy*.

Williamson, W., Huckstep, O., Frangou, E., Mohamed, A., **Tan, C.,** Alsharqi, M., . . . Leeson, P. (2018). Trial of exercise to prevent HypeRtension in young adults (TEPHRA) a randomised controlled trial: study protocol. *BMC cardiovascular disorders*, *208*(18).

Tan, C., Green, P., Tapoulal, N., Lewandowski, A., Leeson, P., & Herring, N. (2018). The role of neuropeptide Y in cardiovascular health and disease. *Frontiers in Physiology*, *9*, 1281.

Awards

British heart foundation Centre of Research Excellence Pump-Priming award – July 2020
Awarded to Associate Prof. Adam Lewandowski and Dr Christopher Toepfer

I proposed the research idea, established the protocol, drafted the first version of the proposal, and helped with the final editing and responses to reviewer comments.

***Project title**: The functional interaction and maturation of iPSC-cardiomyocyte organoids by co-culture with circulating endothelial colony-forming cells: towards bioengineering 3D cardiac-organoids for disease modelling and drug screening.*

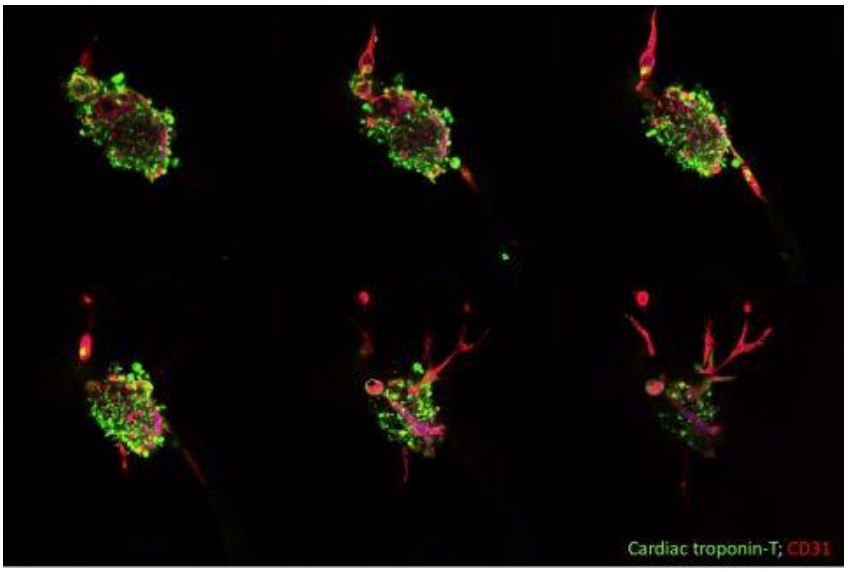
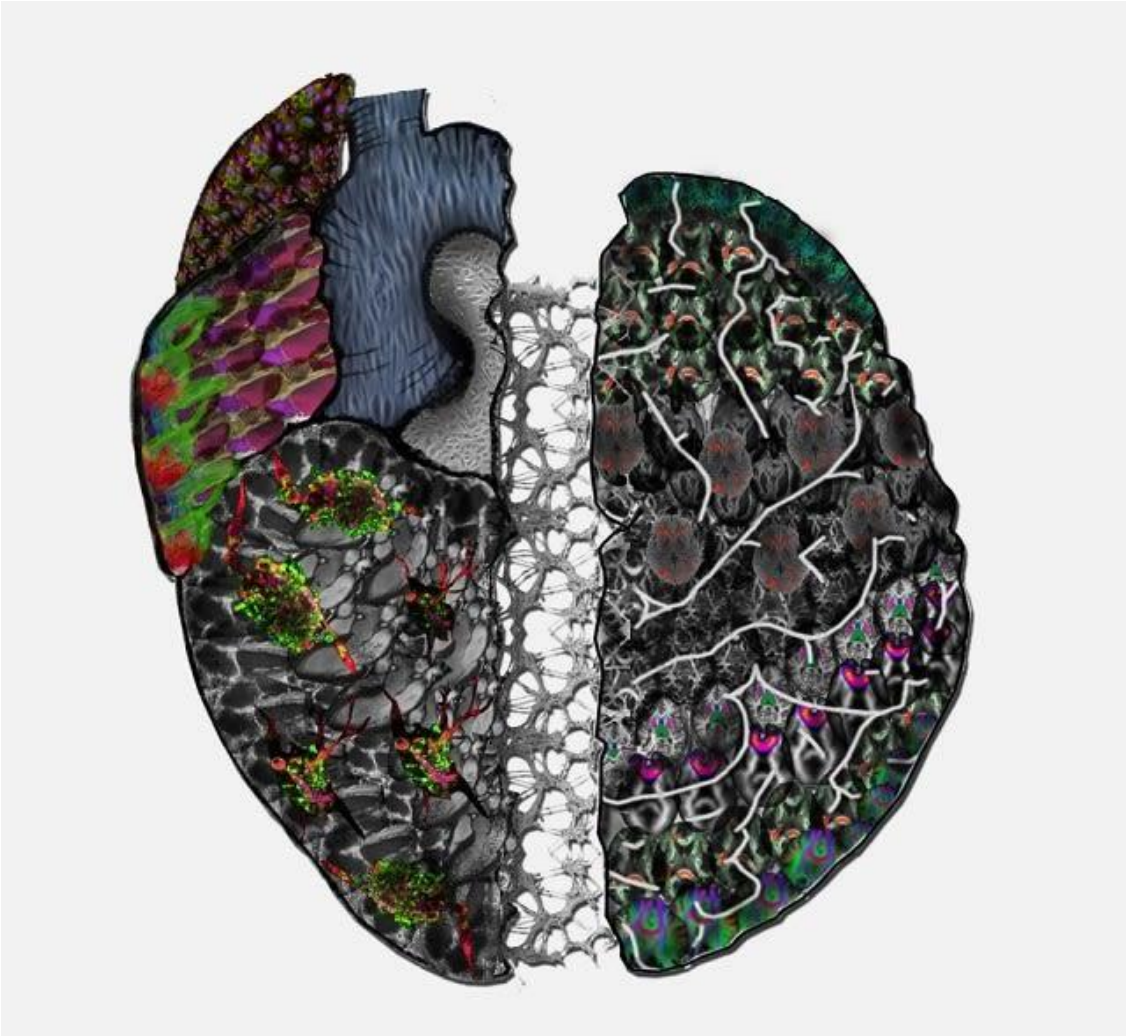


Image title: *Immunofluorescent imaging of a 3D endothelial colony-forming cell and human iPSC-cardiomyocyte organoid structure*

British heart foundation reflections of research image competition – 2019

Supporter's favourite

'THE HEART AND BRAIN AXIS'

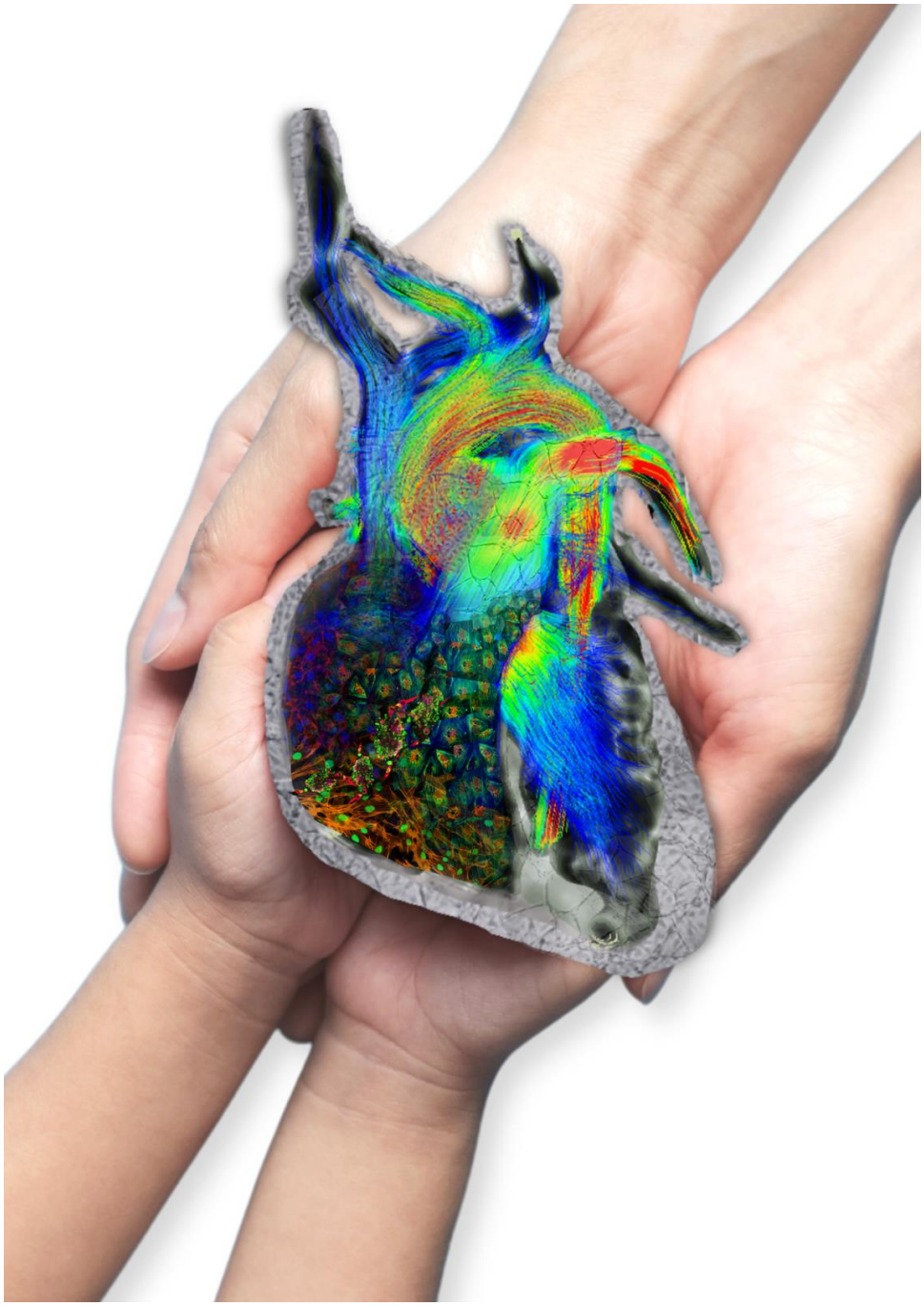


This image reflects the complex interaction between the heart and the brain, portraying some of the different imaging techniques that they use to investigate this relationship. These include magnetic resonance imaging of the heart and brain, ultrasound imaging of the heart, and fluorescent imaging of the heart and blood vessel cells.

Oxford British heart foundation Centre of Research Excellence Symposium Bench to Bedside Research - Image Competition – 2021

Winning image

'THE GROWING HEART- FROM MOTHER TO OFFSPRING'



This image reflects the complex cardiac developmental process of the offspring that begins during gestation. Several maternal factors during gestation could affect the cardiac development of the offspring, including genetics, epigenetics, nutrition, intrauterine environment, and pregnancy-related diseases such as hypertensive disorders of pregnancy. This image portrays some of the different imaging techniques used to investigate cardiac development and remodelling across critical developmental stages.

Contents

Acknowledgements ..... *ii*

Dedication ..... *iv*

Abbreviations ..... *v*

Abstract ..... *vii*

List of publications & awards ..... *ix*

Contents ..... *xiii*

List of Figures ..... *xvii*

List of Tables ..... *xix*

1. Introduction *2*

1.1 Endothelial colony-forming cells (ECFCs) – a subset of endothelial progenitor cells **2**

1.1.1 The origin of endothelial progenitor cells 3

1.1.2 The types of endothelial progenitor cells and isolation methods 3

1.2 Characteristics and therapeutics of ECFCs **6**

1.2.1 Angiogenesis and vascular regeneration 6

1.2.2 Therapeutic potential of ECFC extracellular vesicles 7

1.2.3 ECFC in diseases 8

1.2.4 Sex-specific differences in ECs 9

1.3 Hypertension **10**

1.3.1 Pathophysiology of hypertension – Microvascular and macro-vascular alterations 11

1.3.1.1 Microvasculature 11

1.3.1.1.1 In vitro micro-circulation - EC dysfunction 12

1.3.1.1.2 Retinal micro-vasculature – Fundoscopy 15

1.3.1.2 Macro-vasculature – Arterial stiffness and pulse wave velocity 17

1.3.2 Pathophysiology of hypertension interactions between micro-vascular and macro-vascular alterations 20

1.4 Exercise as a modulator of CVD risk **20**

1.4.1 The impact of exercise on vascular endothelium 23

1.4.1.1 Exercise-induced vasodilation on vascular endothelium 23

1.4.1.2 Exercise-induced anti-oxidative effects on vascular endothelium 24

1.4.1.3 Exercise-induced anti-inflammatory effects on vascular endothelium 25

1.4.1.4 Exercise-induced angiogenesis on vascular endothelium 25

1.4.2 The impact of exercise on endothelial progenitor cells (EPCs) 27

1.4.2.1 Exercise-induced EPCs mobilisation and proliferation 27

1.4.2.2 Exercise-induced EPCs angiogenesis 28

1.4.2.3 Exercise-induced EPC exosomes production 29

1.5 Thesis aims and hypotheses **29**

2. Study population *32*

2.1 Study background **33**

2.2 TEHPRA Study General aims and Hypotheses **34**

2.3 Overview of the study **35**

2.3.1 Participants and Recruitments 35
2.3.1.1 Inclusion and Exclusion 36
2.3.2 Trial design 36
2.3.2.1 Randomisation 37
2.3.2.1.1 Control allocation 37
2.3.2.1.2 Exercise intervention allocation 38
2.4 Thesis study cohort – THEPHRA cell study 40
2.4.1 Participants recruitment limitations 41
3. General methodology 43
3.1 Anthropometric measurements 44
3.2 Clinical BP measurements 44
3.3 Blood sample collection 44
3.3.1 Biochemistry analysis 45
3.3.2 ECFC isolation and culture 45
3.4 ECFC cellular assessments 46
3.4.1 Fluorescence-activated cell sorting (FACS) 46
3.4.2 Immunofluorescence staining 47
3.4.3 EdU proliferation assay 49
3.4.4 In vitro tube formation assay 49
3.4.5 Proteomic analysis on ECFCs 50
3.4.5.1 Sample digestion and de-saltation 50
3.4.5.2 Mass Spectrometry report system and conditions 50
3.4.5.3 Proteomics data availability and system biology analyses 50
3.5 Human umbilical vein endothelial cell (HUVEC) culture 51
3.6 Primary human dermal fibroblast culture 51
3.7 Statistical analysis 52
4. Characterising ECFC as an endothelial cell and a model for clinical in-vitro angiogenesis evaluation 54
4.1 Abstract 55
4.2 Introduction 59
4.2.1 Study hypotheses, aims and clinical significance 60
4.3 Methodology 61
4.3.1 Study population and general methods 61
4.3.2 ECFC functionality classification 62
4.3.3 Enriched ontology clustering 62
4.3.4 Molecular Complex Detection (MCODE) network analysis 63
4.3.5 Principal component analysis 63
4.3.6 Statistical analysis 63
4.4 Results 65
4.4.1 ECFC phenotype 65
4.4.2 Functional and dysfunctional ECFCs 71
4.4.3 Clinical characteristics of subjects with functional and dysfunctional ECFCs 75
4.4.4 Proteomic analysis of functional and dysfunctional ECFCs 77
4.4.4.1 Principal component analysis (PCA) of proteomic data 82
4.4.5 Sexual dimorphism in ECFC 83
4.4.5.1 Male vs Female ECFCs 83

4.4.5.2 Intra-sex proteome differences observed in same-sex individuals with different cell functionality 84

4.5 Discussion 94

4.5.1 ECFC isolation and characterisation 94
4.5.2 ECFC vs HUVECs 95
4.5.3 Proteome profiles of functional vs dysfunctional ECFCs 95
4.5.4 ECFC characteristics, clinical observations, and disease progression 97
4.5.5 Sex-dimorphism in ECFC 98
4.5.6 Study strengths and limitations 100

4.6 Conclusion 100

4.7 Supplemental materials 101

5. The association of ECFCs with micro-vasculature and macro-vasculature remodelling in young adults with elevated blood pressure 108

5.1 Abstract 109

5.2 Introduction 112

5.2.1 Study hypotheses, aims, and clinical significance 113

5.3 Methodology 114

5.3.1 Study population and general methods 114
5.3.2 Static retinal vessel analysis (SVA) 115
5.3.3 Vicorder measurements 116
5.3.4 Proteomics data analysis 117
5.3.4.1 Enriched gene ontology clustering 117
5.3.4.2 Principal component analysis 118
5.3.5 Statistical analysis 118

5.4 Results 120

5.4.1. Clinical characteristics of the study population 120
5.4.2. ECFC functional characteristics in subjects with normal versus elevated BP 123
5.4.3 Retinal micro-vasculature characteristics in subjects with normal versus elevated BP 125
5.4.3.1 Association between EC function and retinal micro-vasculature in subjects with normal and elevated BP 126
5.4.4 Macro-vascular resistance – pulse wave velocity characteristics in subjects with normal versus elevated BP 127
5.4.4.1 Association between EC function and macro-vascular resistance in subjects with normal and elevated BP 127
5.4.5 Relationship between systolic BP, EC function, micro-vasculature and PWV changes 128
5.4.5.1 Relationship between micro and macro-vascular changes 128
5.4.5.2 Relationship between systolic BP and ECFC, micro and macro-vascular changes 129
5.4.5.3 Multiple regression model of systolic BP 130
5.5.6 Proteomic signature of ECFCs from subjects with normal and elevated BP 132
5.5.6.1. Gene ontology, hierarchical and PCA analysis 132
5.5.6.2 Gene ontology analysis of top 5 Gene Ontology biological pathway 136

5.5 Discussion 142

5.5.1 Current findings 142
5.5.2 ECFC dysfunction, proteome, and elevated blood pressure 142
5.5.2.1 PCA reveals distinctive proteome between ECFC-derived from elevated BP vs normotensive individual. 143
5.5.2.2 ECFC dysfunction and extracellular vesicle transport 143
5.5.2.3 Role of GRB2 in the regulation ECFC function 144
5.5.3 Retinal micro-vasculature and blood pressure 146
5.5.3.1 Retinal micro-vasculature and endothelial colony-forming cell proliferation capacity 146

5.5.4 Arterial stiffness and blood pressure 147
5.5.4.1 Pulse wave velocity and endothelial colony-forming cell angiogenic capacity 148
5.5.4.2 Pulse wave velocity and retinal micro-vasculature 149
5.5.5 Study strengths and limitations 150
5.6 Conclusion 151
5.6 Supplemental materials 153
6. Effect of Exercise Training on ECFC function 172
6.1 Abstract 172
6.2 Introduction 175
6.2.1 Study hypotheses, aims and clinical significance 176
6.3 Methodology 177
6.3.1 Study population and general methods 177
6.3.2 ECFC functionality classification 177
6.3.3 Cardiopulmonary exercise testing 178
6.3.4 Randomisation - Exercise intervention and control group 180
6.3.5 Statistical analysis 181
6.4 Results 182
6.4.1 Study population 182
6.4.2 Clinical characteristics and ECFC phenotype 183
6.4.4 Baseline ECFC characteristics as a predictor of exercise response 190
6.4.5 Baseline ECFC functional group as a predictor of exercise response 195
6.5 Discussion 198
6.5.1 Effect of exercise intervention on clinical measurements 198
6.5.2 Impact of exercise on ECFC functionality 199
6.5.3 Baseline ECFC characteristics as a potential predictor to exercise response 199
6.5.3.1 ECFC cellular characteristics improve prediction of exercise responses 199
6.5.3.2 ECFC cellular functional group improve prediction of exercise responses 200
6.5.4 Study strengths and limitations 201
6.6 Conclusion 201
6.7 Supplemental materials 202
7. General conclusion 209
7.1 Main findings of the thesis 209
7.2 Experimental considerations and limitations 211
7.2.1 Impact of COVID-19 on research 211
7.3 Future work 212
7.3.1 Protein validation 212
7.3.2 ECFC extracellular vesicles assessments 212
7.3.3 Other clinical applications of ECFCs 213
7.3.3.1 ECFCs and pre-eclamptic pregnancy 213
7.3.3.2 3D ECFC-cardiomyocyte organoids (Cardiospheres) 214
References 217
Appendices 237

List of Figures

Figure 1.1. Common methodology of different types of endothelial progenitor cell culture and cellular characteristics. 5
Figure 1.2. Cellular characteristics of healthy and diseased endothelial colony-forming cells. 8
Figure 1.3. Comparison of American and European society definition of hypertension. 10
Figure 1.4. Potential pathways linking macro and micro-vasculature modifications to target organ damage in hypertension. 11
Figure 1.5. Schematic of the human arterial blood vessels and capillary. 13
Figure 1.6. Arteriole remodelling and pathophysiology of hypertension. 14
Figure 1.7. Comparison between normal and advanced micro-vascular ageing. 17
Figure 1.8. Role of large artery stiffness in health and diseases. 19
Figure 1.9. Model of systems control and factors that modulate response to physical activity. 22
Figure 1.10 Summary of the mechanisms through which exercise training improves endothelial dysfunction via modulation in the (a) vascular endothelium and (b) endothelial progenitor cells (EPCs). 26
Figure 2.1. Trial of Exercise to Prevent HypeRtension in young Adults (TEPHRA) study – General aims and hypotheses. 34
Figure 2.2. Trial of Exercise to Prevent HypeRtension in young Adults (TEPHRA) study design. 39
Figure 2.3. Flowchart of TEPHRA cell study participants. 41
Figure 3.1. Schematic representation of endothelial colony-forming cells (ECFCs) isolation and colony formation. 46
Figure 4.1. Fluorescence-activated cell sorting (FACS) of endothelial colony-forming cells (ECFCs) represented in dot plots and histograms. 67
Figure 4.2. Endothelial colony-forming cells (ECFCs) phenotype compared to human umbilical vein endothelial cells (HUVECs) and dermal fibroblasts and their respective isotype controls. 70
Figure 4.3. Endothelial colony-forming cells (ECFCs) functionality. 72
Figure 4.4. Proteomic comparisons and hierarchical clustering of endothelial colony-forming cells (ECFCs) versus human umbilical vein endothelial cells (HUVECs). 74
Figure 4.5. Proteomics analysis of functional and dysfunctional endothelial colony-forming cells (ECFCs). 78
Figure 4.6. Proteins identified in enriched gene ontology pathway - extracellular structure organisation that differently expressed between functional clusters of endothelial colony-forming cells (ECFCs). 79
Figure 4.7. Principal component analysis (PCA) of functional and dysfunctional endothelial colony-forming cells (ECFCs). 82
Figure 4.8. Protein intensities were analysed by 2-sided t-test. 84
Figure 4.9. Proteomics analysis of function and dysfunctional endothelial colony-forming cells (ECFCs) based on sex. 86
Figure 4.10. Proteomics analysis of overlapping proteins of intra-specific sex comparisons between function and dysfunctional endothelial colony-forming cells (ECFCs). 88
Figure 4.11. Proteomics analysis of non-overlapped proteins of intra-specific sex comparisons between function and dysfunctional endothelial colony-forming cells (ECFCs). 90
Figure 4.12. MCODE algorithm was applied to clustered enrichment ontology terms to identify neighborhoods where proteins are densely connected in (a) male-specific and (b) female-specific endothelial colony-forming cell (ECFC) proteins. 94
Figure S4.1. Heat maps based on log_2-transformed protein abundance of proteins in the top 10 enriched gene otology pathways. 103
Figure S4.2. Contribution of variables to principal component 1 to 3. 104
Figure 5.1. Schematic representation of retinal imaging and anatomy of the human eye. 116
Figure 5.2. Schematic representation of brachial-femoral pulse wave velocity (PWV). 117
Figure 5.3. Comparisons of endothelial colony-forming cells (ECFCs) functional features between subjects with normal versus elevated blood pressure (BP). 124
Figure 5.4. Retinal calibre assessment of subjects with normal versus elevated blood pressure (BP). 125

Figure 5.5. Linear regression between endothelial colony-forming cell (ECFC) functional parameters and retinal vascular calibre. 126
Figure 5.6. Linear regression between pulse wave velocity and endothelial colony-forming cells (ECFC) angiogenic capacity (closed tube formation). 128
Figure 5.7. Linear regression between pulse wave velocity (PWV) and retinal micro-vasculature calibre.... 129
Figure 5.8. Relationship between systolic blood pressure (BP) and endothelial colony-forming cell (ECFC) function, micro-vascular structure, and pulse wave velocity in young adults. 130
Figure 5.9. Proteomics analysis of normotensive and elevated blood pressure endothelial colony-forming cells (ECFCs). 133
Figure 5.10. Principal component analysis (PCA) of functional and dysfunctional endothelial colony-forming cells (ECFCs). 134
Figure 5.11. Contribution of variables to principal component 1 to 3. 135
Figure 5.12. Proteins identified in the top 5 enriched gene ontology (GO) pathways that are differently expressed between normotensive and elevated blood pressure (BP) of endothelial colony-forming cells (ECFCs). 139
Figure 5.13. Interaction diagrams of identified proteins from proteome that significantly correlated with ECFC function. 140
Figure 5.14. Gene Ontology enRIchement anaLysis and visuaLisAtion (GOrilla) reveals the gene ontology (GO) terms in biological process and cellular component GO domains, enriched with genes differentially expressed in elevated blood pressure endothelial colony cells (ECFCs) compared to normotensive ECFCs. .141
Figure 5.15. Summary of key findings - Association between endothelial colony-forming cell (ECFC) function, micro-vasculature, micro-vasculature and elevation in blood pressure. 152
Figure S5.1. Heatmaps of proteins identified from the String™ interactive pathway analysis. 170
Figure 6.1. Standard cardiopulmonary exercise testing (CPET) set-up (A) and TEPHRA CPET protocol (B)... 179
Figure 6.2. Schematic representation of TEPHRA cell study design. 181
Figure 6.3. Flowchart of TEPHRA cell study participants that were randomised into the trial. 182
Figure 6.4.Characteristics of endothelial colony-forming cells collected from participants in the control group (n=18) and exercise intervention group (n=19). 189
Figure 6.5. Classification of endothelial colony-forming cells (ECFCs) based on the cell functionality. Dysfunctional and functional cells were determined with a proliferation rate (% - Edu-stained cells/DAPI stained x 100) of below 20% and above 20%, respectively. 190
Figure 6.6. Relationship between ECFC characteristics to absolute change in clinical cardiopulmonary exercise testing parameters for oxygen uptake from baseline to 16-week follow up in control (red, circles) and intervention group (green, triangles). 195
Figure 6.7. Point-biserial correlation between endothelial colony-forming cell (ECFC) functional group and cardiopulmonary exercise test parameters post-exercise intervention. 197

List of Tables

Table 3.1. List of antibodies used with the respective application. 48
Table 4.1. Clinical characteristics of the study participants. 76
Table 4.2. Identified proteins of interest from the extracellular structure organisation (GO pathway). 81
Table 4.3. Clinical characteristics of the study participants based on sex. 83
Table S4.1. Clinical characteristics of the male study participants endothelial colony-forming cell (ECFC) based on cell functionality. 105
Table S4.2. Clinical characteristics of the female study participants endothelial colony-forming cell (ECFC) based on cell functionality. 106
Table 5.1. Clinical characteristics of the study population 122
Table 5.2. Vicorder assessment of participants 127
Table 5.3. Multiple linear regression with systolic blood pressure (BP) as dependent variable. 131
Table S5.1. Linear regression of endothelial colony-forming cell (ECFC) function and retinal micro-vascular and macro-vascular assessment 153
Table S5.2. Linear regression with systolic blood pressure as dependent variable. 156
Table S5.3. Clinical characteristics of the study population 157
Table S5.4. Endothelial colony-forming cells, retinal imaging and Vicorder characteristics of the study population 159
Table S5.5. Pearson correlation of proteins with endothelial colony-forming cell (ECFC) characteristics. 160
Table S5.6. Gene Ontology enRIchement anaLysis and visuaLisAtion (GOrilla) analysis with enriched GO biological pathway. 165
Table S5.7. Gene Ontology enRIchement anaLysis and visuaLisAtion (GOrilla) analysis with enriched GO cellular component pathway. 167
Table 6.1. Demographics and anthropometrics of the participants in TEPHRA study. 184
Table 6.2. Cardiopulmonary exercise test of the participants in TEPHRA study. 186
Table 6.3. Endothelial colony-forming cell (ECFC) characteristics of the participants in TEPHRA study 187
Table 6.4. Demographics and anthropometrics of the participants in TEPHRA study with Endothelial colony-forming cell (ECFC) cells growth at baseline. 191
Table 6.5. Baseline endothelial colony-forming cell (ECFC) characteristics of the participants in TEPHRA study. 193
*Table 6.6.The correlation and regression*analysis between baseline endothelial colony-forming cell (ECFC) characteristics to physical exercise parameters. 194*
Table 6.7. Baseline Endothelial colony-forming cells (ECFC) characteristics of the participants in the TEPHRA cell sub-study based on ECFC functional group. 196
Table 6.8. The point-biserial analysis between baseline endothelial colony-forming cell (ECFC) characteristics to physical exercise parameters. 197
Table S6.1. Demographics and anthropometrics of the control participants in TEPHRA study. 202
Table S6.2. Demographics and anthropometrics of the exercise intervention participants in TEPHRA study. 204
Table S6.3. Absolute change in demographics and anthropometrics of the participants in TEPHRA study based on endothelial colony-forming cell (ECFC) functional group. 206

1

Introduction



1. Introduction

1.1 Endothelial colony-forming cells (ECFCs) – a subset of endothelial progenitor cells

Strategically embedded between the tissues and blood, the vascular endothelium constitutes a highly heterogeneous, complex, and dynamic structure regulating critical physiological processes such as inflammation, vasomotor responses, mechano-sensing angiogenesis, and haemostasis[1-3]. Hence, impairment of the endothelial cells (ECs) and vascular endothelium can precede the development of cardiovascular diseases (CVDs), including hypertension, leading to further endothelial dysfunction[4, 5].

To this date, human umbilical vein endothelial cells (HUVECs) have been widely used as a gold standard for investigating EC biology and physiology[6-11]. However, it is not without limitations. HUVECs not only have a limited lifespan, proliferation, and angiogenic capacity, but also cannot account for lifestyle and environmental modifications occurring beyond birth[12]. Additionally, with the limited availability of umbilical cords, the cells' use for pathological studies is further restricted to the type of pregnancy and fetal complications. The usage of HUVECs as a platform for endothelial investigations in disease is sub-optimal and has been widely criticised.

There has been an increased interest in advancing experimental techniques that allow the isolation and primary culture of other types of ECs from vascular biopsies or peripheral blood[13]. Human endothelial colony-forming cells (ECFCs), a subpopulation of circulating endothelial progenitor cells (EPCs), offer a potential platform for cellular assessment due to their remarkable angiogenic expansion, regenerative, and self-renewable potentials *in vitro*[6, 14-21] and *in vivo*[22, 23].

1.1.1 The origin of endothelial progenitor cells

EPCs are likely originated in the bone marrow or from vessels and pools of progenitor cells in tissues[15]. These cells are isolated from relatively low volumes (10-25mL) of peripheral blood and present a well-characterised angiogenic phenotype, suggesting an important physiological role in re-endothelialisation and neovascularisation processes, which are disrupted during endothelial vascular dysfunction[14-16, 24-27]. Asahara *et al.* reported that EPCs could be cultured from a heterogeneous mononucleated cells (MNCs) population enriched for either the stem cell hematopoietic marker CD34, vascular endothelial growth factor receptor-2 (VEGFR-2), platelet-EC adhesion molecule 1 (PECAM-1 or CD31), vascular endothelial growth factor receptor (Flk-1), Tie-2 (angiopoietin-1 receptor), and E-selectin expression[15, 28]. However, despite many EPC populations co-express hematopoietic markers (CD34, CD133, CD117, and endoglin (CD105)), the relationship of EPCs to hematopoietic stem and progenitor cells remains in contention.

1.1.2 The types of endothelial progenitor cells and isolation methods

There are currently three distinct types of EPCs, and that includes (i) colony-forming units-Hill (CFU-Hill) EC; (ii) circulating angiogenic cells (CACs or "early-EPCs") and (iii) ECFCs ("late-EPCs" or "late outgrowth EPCs" or "blood outgrowth ECs" **(Figure 1.1)**. Each population display different phenotypical and functional characteristics. In general, *in vitro* EPC isolation and culture assays, peripheral blood mononucleated cells (PBMCs) are isolated and plated onto collagen I-coated plates in endothelial-specific growth media for up to 30 days; after which, the non-adherent fraction of cells is removed, resulting in a target adherent cell population[20, 29, 30]. The CFU-Hill cells are derived detween days 4-9 days, and display features of endothelial phenotype and function through binding of the endothelial-specific lectin Ulex Europeus Agglutinin-1 (UEA-1) and uptake of acetylated low-density lipoprotein (acLDL)[31]. These CFU-Hill EC also express von Willebrand

factor (vWF), CD31, VEGFR-2, vascular endothelial cadherin (VE-cadherin or CD144), Tie-2, TEK (tunica intima EC kinase), and bind Bandeiraea simplicifolia lectin (BS-1)[15].

The CACs emerge between day 4-7 of culture, and unlike CFU-Hill, CACs do not display colony morphology though the sprouting spindle-shaped cells from CFU-ECs are similar in shape to cultured CACs[15, 31, 32]. Furthermore, CACs comprise approximately 2% of the whole PBMC population, and therefore are collected from the culture in far greater numbers than CFU-ECs[33]. Both CFU-Hill and CACs do not have typical endothelial features such as the well-defined cobblestone morphology, adherent junctions and caveolae[34-36]. These two cell types have no or limited expansion potential with low proliferation capacity and no angiogenic capacity and no standard growth pattern[20, 35].Transcriptomic and proteomic analyses of CFU-Hills and CACs have reported to be hematopoietic cells with hematopoietic-specific transcripts expression with a molecular phenotype similar to monocytes[34].

The ECFC colonies emerge from the adherent cell population 10–21 days after plating (5–7 days if human umbilical cord blood MNCs are plated) and display a cobblestone appearance typical of ECs[12, 20]. Thus far, ECFCs have proven to be phenotypically indistinguishable from cultured ECs, with robust intrinsic clonal proliferative potential and capacity to contribute to *de novo* blood vessel formation capacity *in vivo*[16, 20, 22, 23, 29, 37, 38]. Although human ECFCs have not been shown to express any novel antigens that differentiate them from other non-proliferative vascular ECs, ECFCs can be identified by the expression of the cell surface proteins including CD31, CD34, vascular endothelial growth factor receptor 2 (VEGFR-2), VE-Cadherin, CD105, CD146, vWF. ECFC also have the ability to uptake acLDL, and they do not express the proteins CD45, CD14 and CD115[39, 40].

Apart from functional and morphological differences to other EPCs, comparative transcriptional and pro-teomic profiling has revealed that early EPCs and ECFCs show strikingly different gene and protein expression signatures, particularly in proteins regulating inflammation and angiogenic mechanisms[34] This same study[34] further provided evidence that ECFCs exhibit commitment to the endothelial lineage with the expression of transcripts involved in vascular

development and angiogenesis-related signalling pathways that supports endothelial repair and regeneration in injured vessels through largely paracrine mechanisms[34, 41].

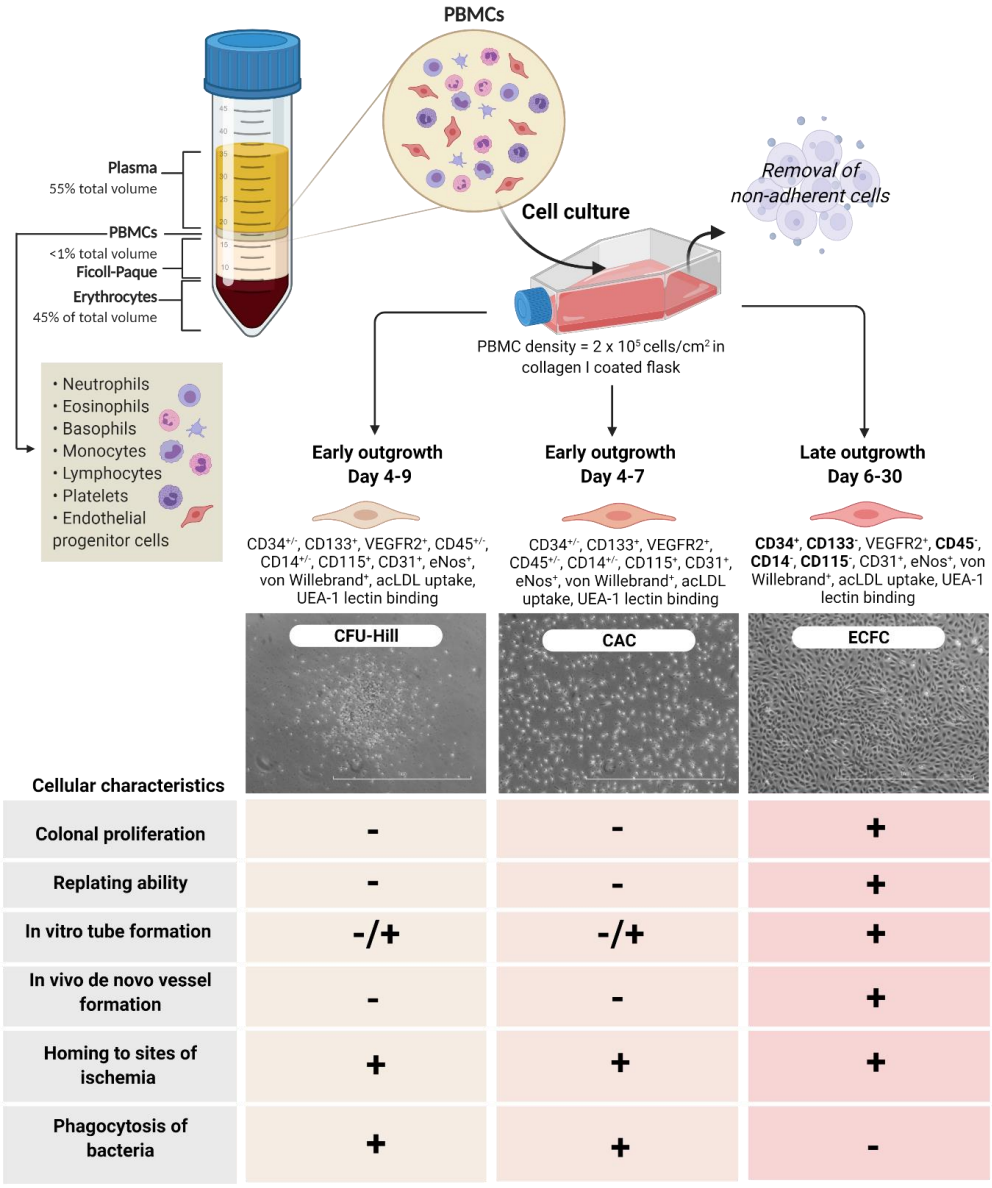


Figure 1.1. Common methodology of different types of endothelial progenitor cell culture and cellular characteristics.

Culture of the colony-forming unit–Hill cells (CFU-Hill), includes a 4-9-day process where adherent peripheral blood mononuclear cells (PBMCs) give rise to the colony. Circulating angiogenic cells (CAC) are the adherent mononuclear cells of a 4-7-day culture of PBMCs. CAC cultures typically do not display colony formation. Endothelial colony-forming cells (ECFCs) are derived from adherent PBMCs cultured for 6-30 days in endothelial conditions, and colonies display a cobblestone morphology. Cell characteristics are represented. Adherent cells that display the function are indicated by (+), that do not display the function by (−), and if the literature provides conflicting evidence (±). Those properties that distinguish cells in the ECFC assay from CFU-Hill and CAC assays are indicated in bold font. Only the ECFC and progeny display the full properties one would

attribute to an EPC. Vascular endothelial growth factor receptor 2 (VEGFR-2); aldehyde dehydrogenase (ALDH); Ulex europeaus agglutinin-1 (UEA-1); acetylated low-density lipoprotein (acLDL); endothelial nitric oxide synthase (eNOS). Images were collected using a Nikon light microscope (Scale bar=1um).

1.2 Characteristics and therapeutics of ECFCs

Pro-angiogenic ECFCs can infiltrate damaged blood vessels, release pro-angiogenic growth factors and exosomes to facilitate the repair process, and ultimately promote reperfusion and organ function at the site of ischemia[19, 42-46]. Additionally, ECFCs can provide trophic support to other therapeutically relevant cells[47]. These properties make them particularly attractive for cardiovascular investigation and therapeutic application to enhance vascular repair in ischemic diseases such as peripheral arterial disease, ischemic retinopathy, myocardial infarction, or stroke[48-52].

1.2.1 Angiogenesis and vascular regeneration

A growing body of evidence supports the use of ECFCs for cell-based regenerative and revascularisation therapy, with multiple suggested benefits in ischemic and vascular injuries, including peripheral arterial occlusion, cerebral ischemia, and acute renal injury[53]. The angiogenic and vascular regeneration of ECFCs has also been reported in several animal models of traumatic brain injury, stroke, and retinal ischemia[40, 54-56]. In a mouse model of traumatic brain injury, transplantation of human ECFCs increased the micro-vessel density angiogenesis and restored blood-brain barrier integrity, resulting in enhanced brain tissue viability function and significantly less neurologic disability[54]. In an ischaemic stroke rodent model with middle cerebral artery occlusion, intravenously administered ECFCs were found to home to the ischemic hemisphere and enhance functional recovery, angiogenesis, neurogenesis, and reduction in overall apoptosis[56-58]. It was also reported that Intravitreally-injected ECFCs prevented retinopathy in a murine model of hyperoxia-induced retinal avascularisation[59]. In addition, a study by Lin *et al.* reported that ECFCs

could also function as angio-paracrine mediators prior to the establishment of blood perfusion, modulating the regenerative potential and viability of human mesenchymal stem cells[47].

1.2.2 Therapeutic potential of ECFC extracellular vesicles

Extracellular vesicles (EVs) including apoptotic bodies, micro-vesicles, and exosomes, have emerged as a critical player in cell-to-cell communication in normal physiology and pathological conditions[60]. EVs convey these messages through their distinct cargoes consisting of cytokines, proteins, nucleic acids (mRNAs and microRNAs) to recipient cells and lipids, which they transport from the donor cell to the recipient cell[61-63], and have the ability to modulate EC behaviour[63-66] and angiogenesis *in vivo*[65, 67].

A recent study by Gomes *et al.* reported that ECFC-derived EV transport functional miRNAs, proteins, mRNAs, and lipids, playing a pivotal role in paracrine intercellular communication between cells, including ECs, and leading to ECFC-exosome-dependent angiogenesis and cardiac tissue repair[46]. The cardioprotective effects of ECFC-exosome were also evident in the murine model of myocardial infarction by preventing adverse cardiac remodelling and heart failure[53, 68, 69]. In addition, one other study indicated that ECFC-derived exosome treatment blocked hypoxia/reoxygenation-induced pro-inflammatory protein intercellular cell adhesion molecule-1 (ICAM-1) expression and EC apoptosis[70]. Vinas *et al.* specifically identified miR-486-5p enrichment in ECFC exosomes as a critical mediator of protecting kidney ischemia injury via targeting the phosphatase and tensin homolog protein and Akt pathway[62]. This suggests that using exosomes from ECFCs may be another strategy to protect against endothelial injury in animal models of acute kidney injury.

1.2.3 ECFC in diseases

Diseases including diabetes mellitus, hypertension, preeclampsia, venous thromboembolic disease, coronary artery disease and ischemic stroke have been associated with a deficiency in number, reduced colony formation, and compromised ECFC functionality, including reduced proliferation, tubulogenic capacity and reduced migration[6, 10, 19, 71-82] **(Figure 1.2)**. Bertagnolli *et al.* recently demonstrated that venous blood-derived ECFC dysfunction in preterm-born young adults was linked to elevated systolic blood pressure (BP) and bronchopulmonary dysplasia – a major prematurity-related neonatal chronic lung morbidity characterised by impaired vascular and alveolar growth[10]. Supporting this finding, an earlier study by Baker *et al.* demonstrated that preterm ECFCs appear in increased numbers and proliferate more rapidly but have an increased apoptotic susceptibility to hyperoxia – a contributor to bronchopulmonary dysplasia[83]. These studies indicate the reduced functionality of ECFCs in different clinical conditions and further suggest the importance of studying ECFC function in the pathophysiology of diseases to better facilitate the use of these cells for autologous cell therapy in the future.

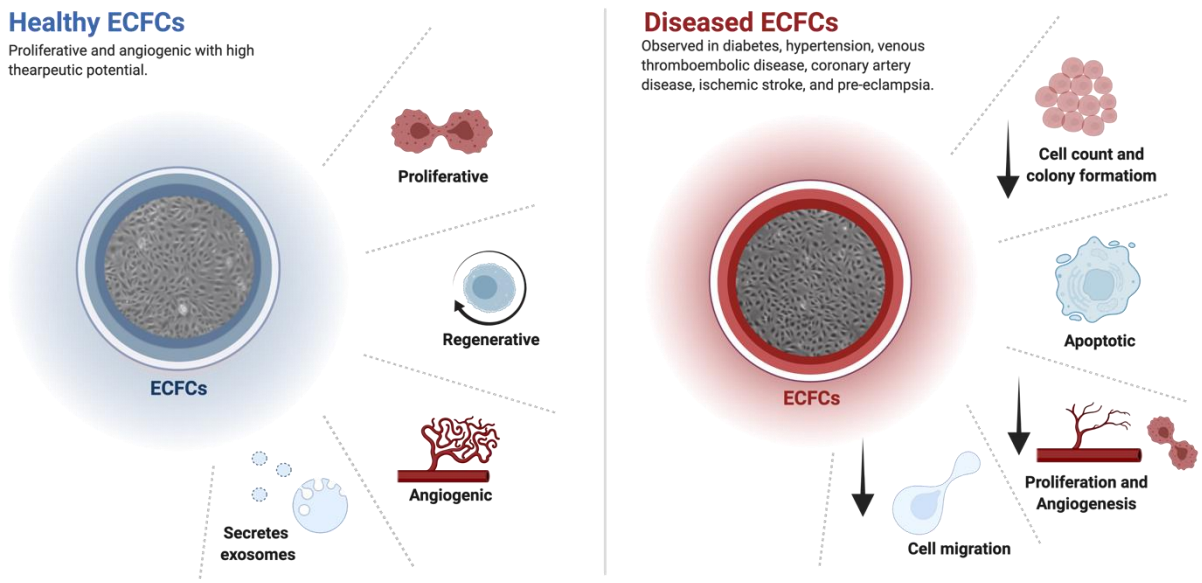


Figure 1.2. Cellular characteristics of healthy and diseased endothelial colony-forming cells.

1.2.4 Sex-specific differences in ECs

Sexual dimorphism is an important independent factor contributing to EC biology and CVD pathogenesis[84]. A large body of clinical and basic research has also documented sex-specific differences in endothelial dysfunction and CVD risk implicating a significant role for gonadal hormones[84-91]. Studies have reported the profound influence of sex on EC functional and physiological differences, including viability, migration, proliferation, angiogenesis and shear stress response, implying sex differences in the regulation of vital endothelial pathways, such as the redox system and endothelial nitric oxide synthase (eNOS) activity[92-97]. Transcriptomic and proteomic studies of female and male ECs revealed differentially expressed genes between sexes and their regulators, including the Y576/577 phosphorylation of angiogenic focal adhesion kinase and the expression of proteins DDX3X, UBA1, EIF1AX, and HDHD1, which were markedly enhanced in female HUVECs[93, 98]. Multiple genome-wide association studies (GWAS) of the twin model revealed that genes that present with an acquired sex difference in ECs are more likely to be influenced by sex steroids (oestrogens or androgens)[99].

Besides the actions of oestrogen, sex chromosome gene expression and programming effects also provoke this sexual dimorphism. miRNAs have emerged as regulators of HUVEC function with sex-dependent differences in barrier function and actin organisation[100]. Primary and established cell lines have provided almost all our knowledge about fundamental biological processes, but most of these studies disregarded the sex origin of cells as a relevant biological variable in preclinical research[101-103]. The asexual approach limits our understanding of the influence of sex not only in essential biological functions but especially in pathophysiological mechanisms[104, 105]. This underscores the need for treating sex as a biological variable and the need to achieve more effective and precise sex-oriented strategies for the prevention and therapy of diseases observed in the pathogenesis of CVDs and pathological angiogenesis[92].

1.3 Hypertension

Hypertension is a growing global public health concern. It identifies immediate primordial risk factors for CVDs that result in cardiovascular morbidity and mortality[106-108]. The lifetime risk of cardiovascular events is associated with modest increase in systolic BP above 115 mmHg[109]. Acknowledgement of these risks has prompted a recent review of international criteria for hypertension diagnosis in the United States, with several proposing stage 1 diagnosis to be lowered from the threshold of 140 mmHg systolic or 90 mmHg diastolic down to 130 mmHg systolic or 80 mmHg diastolic[110, 111] **(Figure 1.3)**.

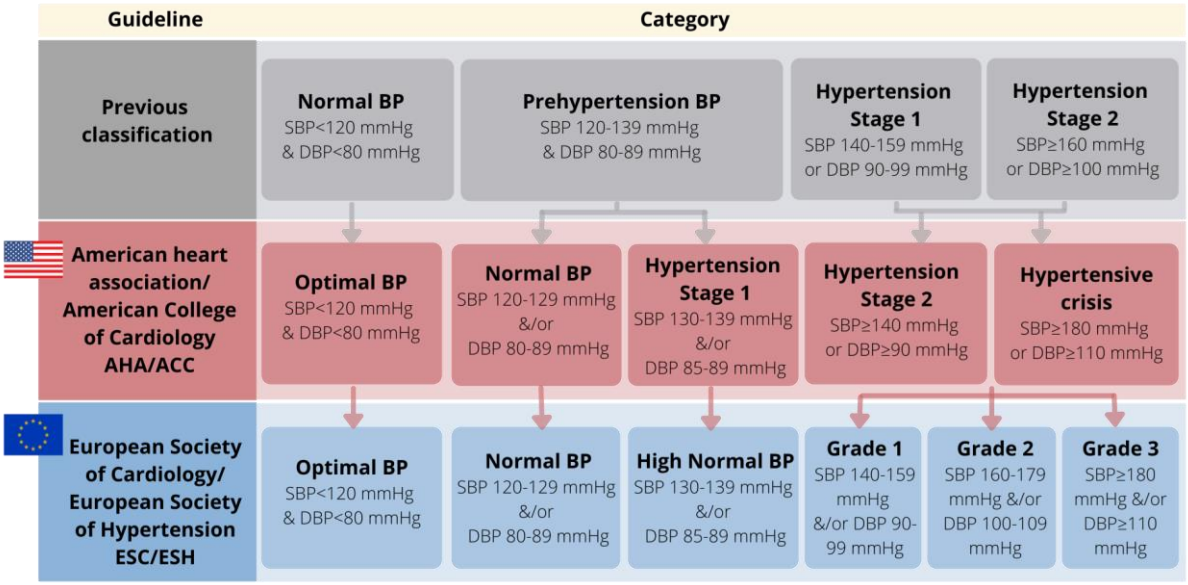


Figure 1.3. Comparison of American and European society definition of hypertension.

Based on the British Heart Foundation 2021 annual report, CVD and stroke are the underlying causes of up to 30% of global deaths and constitute one in four UK deaths, making it one of the leading causes of worldwide mortality[112]. The characteristics of hypertension involve anatomical and functional changes in cellular, micro- and macro-circulation throughout the body. It includes rarefaction of the micro-vasculature, vasoconstriction of the small vessels, as well as obstruction and reduced circulatory efficiency that ultimately contribute to organ dysfunction[107, 113, 114] **(Figure 1.4)**. There is substantial evidence that shows that an individual's risk of hypertension

and CVD may have etiologic origins to BP levels in early life[115, 116]. Based on the current findings, it has been hypothesised that elevated BP might cause structural damage to the vasculature in children and adolescents, which predisposes them to the subsequent development of clinical CVD[108, 116-119]. However, the exact pathophysiological mechanisms underlying these associations remain uncertain.

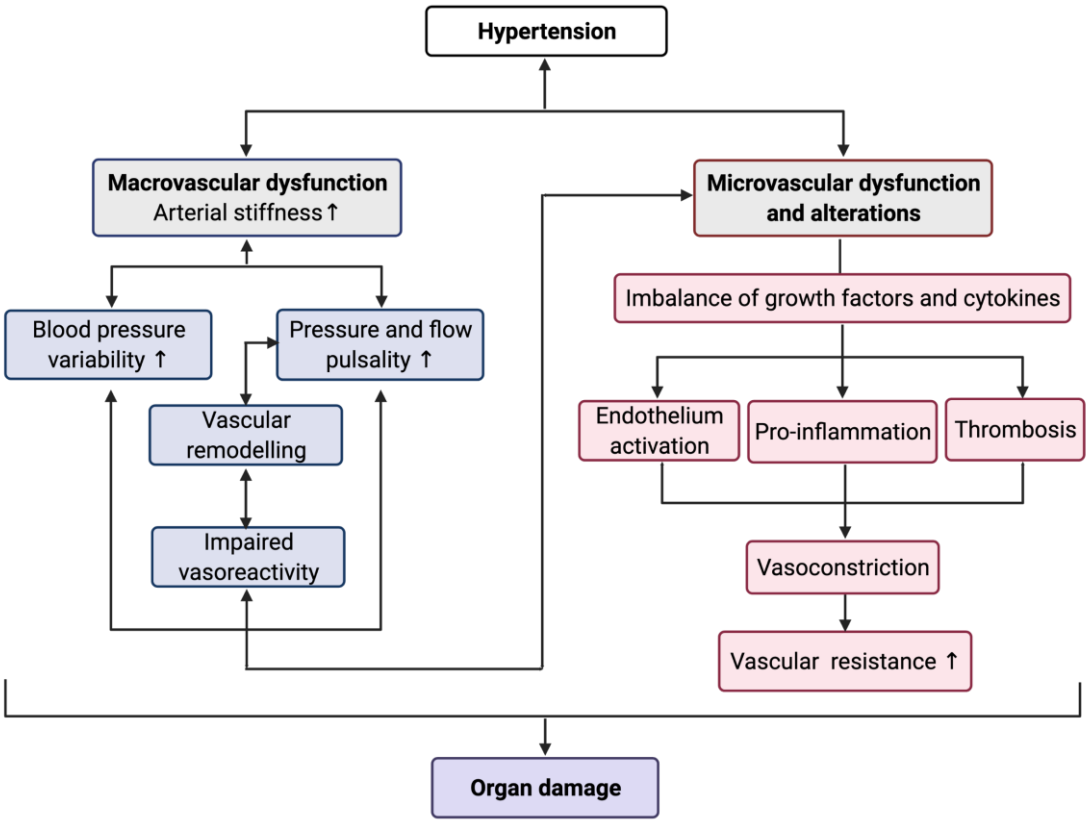


Figure 1.4. Potential pathways linking macro and micro-vasculature modifications to target organ damage in hypertension.

1.3.1 Pathophysiology of hypertension – Microvascular and macro-vascular alterations

1.3.1.1 Microvasculature

The micro-circulatory network is essential for tissue perfusion and organ function via three key mechanisms: (i) providing tissue nutrition in response to variations in demand; (ii) capillary protection against an increase in BP; and (iii) local and systemic peripheral resistance

determination[120]. Hypertension profoundly affects the micro-vasculature's functional and structural aspects, particularly in the smallest arteries, arterioles, capillaries, and venules. Modifications include vasoconstriction, rarefaction, and vessel narrowing[114, 121-125]. Consequently, alterations in micro-vasculature affect vascular resistance, tissue perfusion, metabolism, and susceptibility to ischaemia and may play a key role in the pathophysiology of hypertension, subsequently affecting the macro-vascular structures[125-130]. Furthermore, these micro-vascular modifications have been associated with target end-organ damage, such as CVD, stroke, left ventricular failure, and nephropathy seen in hypertension[124].

1.3.1.1.1 In vitro micro-circulation - EC dysfunction

The vascular wall is a dynamic organ and is formed by a variety of cells, including ECs, smooth muscle cells, and fibroblasts, interacting to form an autocrine-paracrine complex[128]. The inner layer of the blood vessel (tunica intima) is constituted of a single layer of ECs embedded between the interface blood vessel wall and parallel to the blood flow[1, 131] **(Figure 1.5)**. The endothelium has a metabolically active role by exchanging nutrients and other elements between the blood and the tissue layer, as well as by regulating different physiological processes, including vascular integrity maintenance, mechano-sensing angiogenesis and haemostasis[1-3]. The endothelium also responds to blood's fluid laminar shear stress, which elicits anti-coagulant, anti-atherosclerotic and anti-thrombotic pathways, particularly via endothelial-derived nitric oxide (NO)[132, 133]. NO is a major vasodilating and pro-angiogenic factor that modulates local vasomotor responses and BP regulation. It stimulates the release of vascular endothelial growth factor (VEGF) to control vasculogenesis and vascular remodelling in response to shear stress[132, 133].

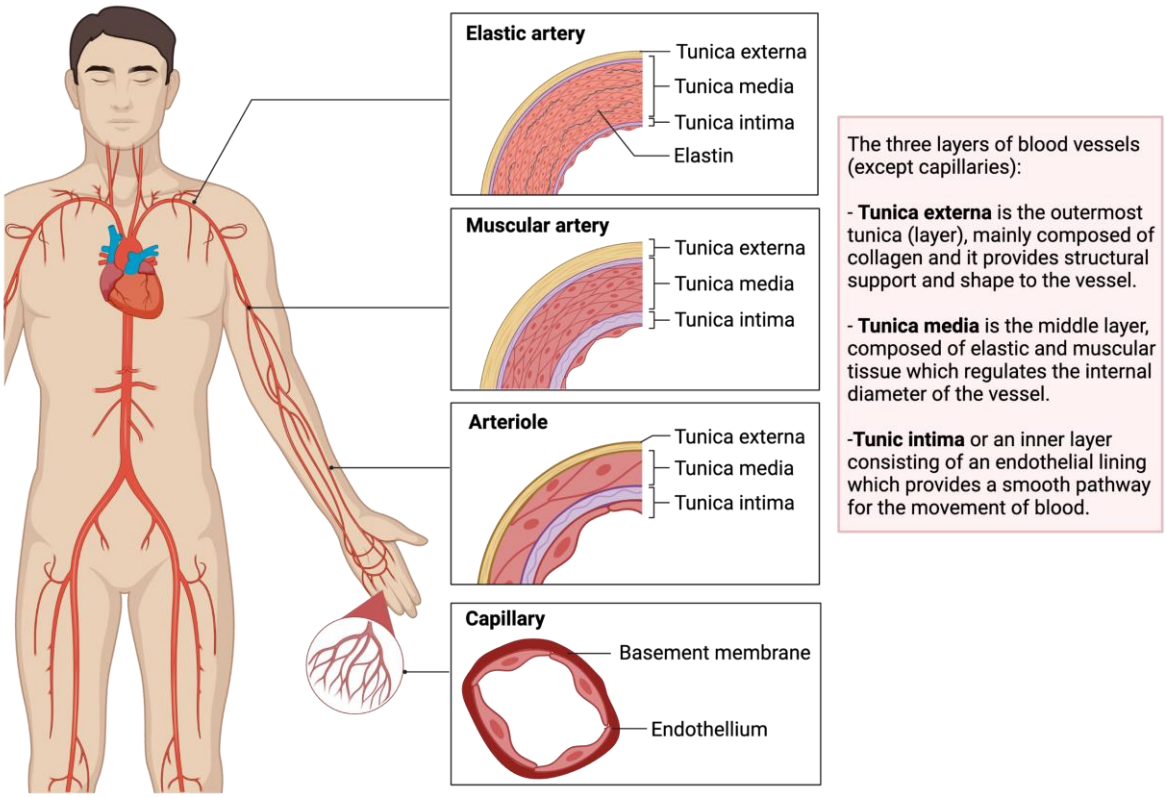


Figure 1.5. Schematic of the human arterial blood vessels and capillary.

The structure of the blood vessels is well-adapted to its function. There are two main types of arteries found in the body: elastic arteries and muscular arteries. Elastic arteries are those nearest the heart (aorta and pulmonary arteries) with an abundance of elastic tissue and less smooth muscle in the tunica media than muscular arteries. This feature of the elastic arteries allows them to maintain a relatively constant pressure gradient despite the constant pumping action of the heart. The arterioles provide blood to the organs and regulate systemic vascular resistance. Except for capillaries, all blood vessels have three main layers (tunica externa, tunica media, and tunica intima). The capillaries are thin-walled vessels composed of a single endothelial layer. Because of the thin walls of the capillary, the exchange of nutrients and metabolites occurs primarily via diffusion[131].

Under normal conditions, the endothelium is quiescent and genetically stable[134]. However, cumulative metabolic burden and chronic oxidative stress may lead to chronic EC injury and activation, resulting in hydrogen peroxide accumulation, redox signalling, inflammation, endothelial dysfunction, DNA damage and reduction in NO bioavailability[127, 129, 134-136]. These affect EC and smooth muscle cell proliferation, angiogenesis, apoptosis, attract inflammatory cells, coagulation, thrombosis, and affect vasoactivity to restore homeostasis[127, 129, 135].

Prolonged or chronic activation of the endothelium leads to EC dysfunction, loss of homeostatic functions, pathological pro-thrombotic, pro-inflammatory, and pro-constrictive vascular remodelling, hypertrophy, and micro-vascular rarefaction[113, 127, 137, 138]. In hypertension, vascular remodelling is characterised by alterations in vasoconstriction, endothelium activation, synthesis or degradation of extracellular matrix, inflammation, thrombosis lesions and neointima formation, which leads to the muscularisation, elevation in vascular resistance and ultimately occlusion of the lumen of arteries by the formation of vascular lesions[127-130, 139, 140] **(Figure 1.6)**. Modifications to capillary rarefaction and structural changes of arterioles are also hallmarks of the metabolic syndrome, including obesity, hyperglycaemia, hypertension, and diabetes[141, 142].

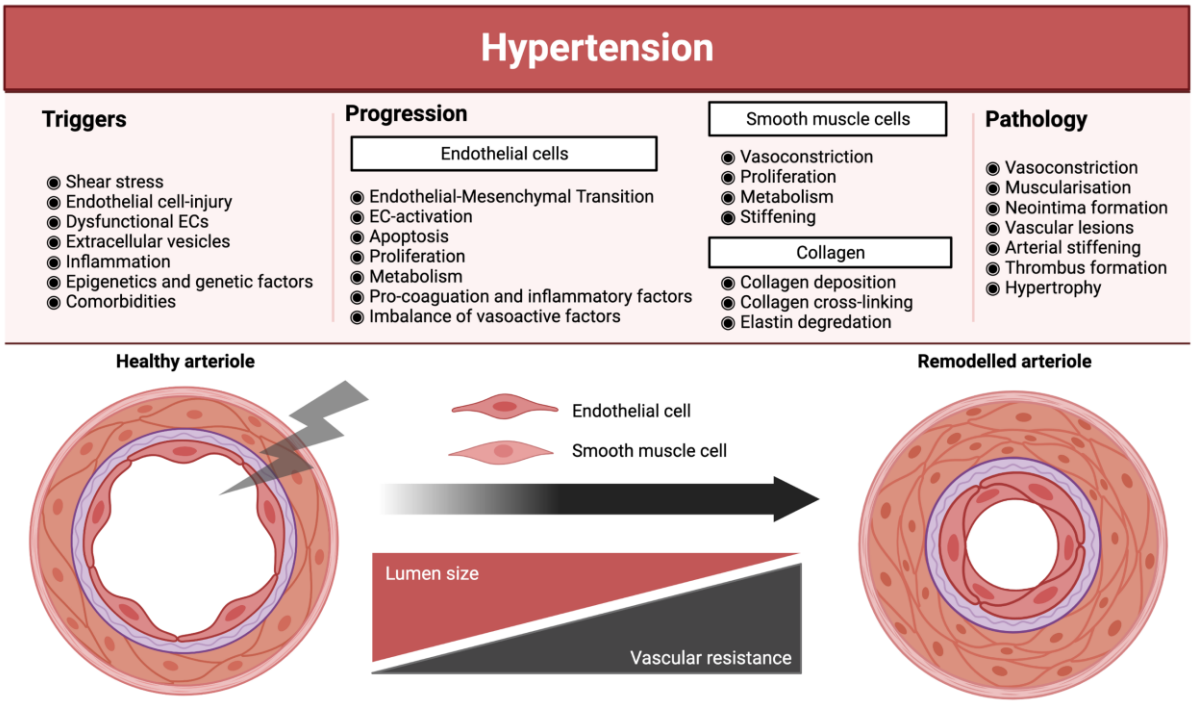


Figure 1.6. Arteriole remodelling and pathophysiology of hypertension.

Hypertension may be induced by a progressive increase in vascular resistance caused by micro-vascular remodelling. Molecular mechanisms behind remodelling are still not fully elucidated, but endothelial cell (EC) injury is considered one of the early triggers. EC injury can be induced via shear stress, hypoxia, and inflammation. Host factors such as genetic mutations, sex, epigenetic factors, and comorbidities are essential in EC dysfunction. EC dysfunction leads to disease progression, including alterations in cell processes endothelial-mesenchymal transition, apoptosis, and proliferation. In addition, changes are found in cell metabolism and the secretion of vasoactive, coagulation and thrombotic factors. Additionally, vascular smooth muscle cells and collagen display

a diseased cellular phenotype, including elastin degradation, collagen deposition, collagen-elastin cross-linking. This results in vasoconstriction, thrombus formation, neointima formation, muscularisation, and the development of vascular lesions as lumen size decreases, pulmonary vascular resistance increases and induces right ventricle (RV) hypertrophy and eventual RV failure.

1.3.1.1.1.1 Endothelial colony-forming cell dysfunction

Human ECFCs offer a promising platform for cellular assessment as they present substantial angiogenic, expansion, regenerative and self-renewable potentials in vitro[15, 26, 27, 37, 143, 144]. The function of ECFCs suggests an important physiological role in re-endothelialisation and neovascularisation processes, known to be disrupted in cases of endothelial vascular dysfunction[14-16, 24-27, 71-73, 75, 145]. Studies on human ECFCs have highlighted compromised cellular functionality in several conditions, including metabolic diseases such as hypertension and diabetes[76, 77]. Furthermore, early EC dysfunction has been observed in pre-diseased states, including pre-hypertension and pre-diabetes, suggesting a potential disease risk[146, 147]. Recent study highlighted dysfunctional ECFCs are associated with distinct proteome profiles and common cardiovascular risk factors like cholesterol levels, body mass index, and BP[148].

Current findings further support that impairment of the ECs and vascular endothelium can precede the initiation and progression of CVDs, including hypertension and may be an early precursor for macro and micro-vascular dysfunction[5, 26, 149-152]. Despite identifying the distinct phenotype of ECFCs with elevated CVD risk, including elevated BP, there is a lack of detailed knowledge regarding associations between markers reflecting endothelial function with other parameters of micro-vascular and macro-vascular assessments.

1.3.1.1.2 Retinal micro-vasculature – Fundoscopy

Advances in fundus photography and retinal image analysis techniques have enabled a highly reliable, reproducible, and non-invasive in-vivo method for direct visualisation of retinal micro-vasculature, thereby offering a means to accurately conduct a quantitative assessment of

retinal vasculature[107, 108, 153-155]. Furthermore, retinal fundoscopy not only offers a unique window for monitoring the macro-circulatory system but also offers a potential platform to assess its relationship with other clinical measurements, including BP, endothelial and arterial compliance, the sympathetic nervous system and the hypothalamic-pituitary-adrenal axis[107]. The morphology of retinal micro-vasculature is represented by a series of parameters such as the calibre of retinal arterioles and venules represented as central retinal arteriolar equivalent (CRAE) and central retinal venular equivalent (CRVE), respectively, and their tortuosity, branching angle and fractal dimension[125, 156].

Over the past few decades, extensive population-based studies have shown that retinal vascular calibres are a potentially valuable and reliable site for a pre-clinical assessment tool to underlie early life factors related to CVDs[157]. This is due to the ability of fundoscopy to reflect a wide range of risk factors, including lifestyle (active or inactive), ageing, elevation in BP, atherosclerosis, hyperglycaemia, dyslipidaemia, inflammation and endothelial dysfunction; and appear to predict the incidence of CVDs, including stroke and heart diseases, and are related to vascular and metabolic conditions including diabetes[156, 158-168].

A substantial number of studies on children and pre-adolescents showed that the pathological micro-vascular adaptations in early life underlie its influence on advanced micro-vascular ageing, cardiovascular health, and disease[118, 169, 170]. Some of the pathological changes have been identified as retinal arteriolar narrowing and venular widening[154] **(Figure 1.7)**. Constriction of retinal arteriolar and venular calibres is associated with elevated BP and higher risk of hypertension in childhood, with the strongest association for retinal arteriolar calibre[118, 169, 170]. Retinal arteriolar tortuosity was positively associated with levels of cholesterol, triglyceride, high sensitivity c-reactive protein and systolic and diastolic BP[171, 172]. Furthermore, a wider retinal venular calibre was associated with lower systolic BP, mean arterial pressure, pulse pressure and higher carotid-femoral pulse wave velocity (PWV)[118]. These observations for retinal vascular remodelling in childhood were comparable to those observed in adults[9, 172, 173].

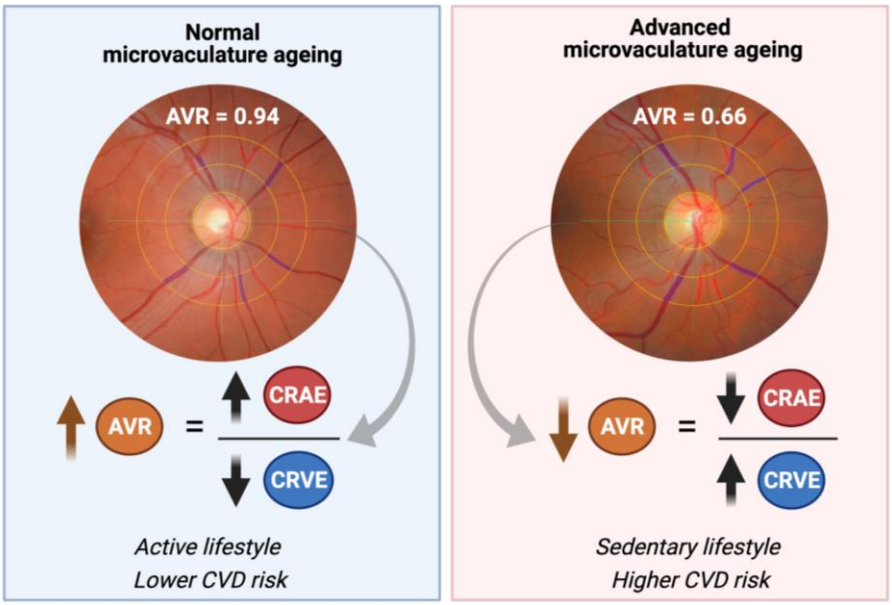


Figure 1.7. Comparison between normal and advanced micro-vascular ageing.

Fundoscopic images can be used to determine the central retinal arteriolar (CRAE), venular (CRVE) diameter equivalents and the arteriolar-to-venular diameter ratio (AVR). Healthy individuals with normal vascular ageing are associated with higher AVR (wider CRAE, narrower CRVE) than healthy sedentary and at-risk individuals, that are presented with lower AVR (narrower CRAE, wider CRVE). Lower AVR has been associated with increased cardiovascular disease (CVD) events.

Even though retinal imaging is recognised as a promising imaging modality to evaluate the pathogenesis of CVDs, most of the large population-wide cohort studies were performed in children and middle-aged individuals[155, 162, 174-176]. Evaluating the pathophysiological changes between retinal vasculature and classical systemic, environmental, and genetic CVD risk factors in the specific high CVD-risk group of young adults is still lacking. Furthermore, it remains elusive whether arteriolar narrowing precedes and contributes to the development of hypertension or is only a consequence of long-standing elevated BP[124, 177].

1.3.1.2 Macro-vasculature – Arterial stiffness and pulse wave velocity

Macro-vasculature modifications in the form of aortic stiffening is associated with increased vascular resistance[108]. The bidirectional relationship between aortic stiffness and systolic

hypertension is well supported by epidemiologic evidence, suggesting a precursor role of aortic stiffening in the incident hypertension[178]. A healthy aorta exerts protective cushioning, limiting arterial pulsatility and protecting the micro-vasculature from harmful pressure and blood flow[179]. Stiffening of the arterial wall occurs following a reduction in vascular distensibility due to increased calcification and elastin degeneration, which occurs with ageing and various pathologic states, including hypertension[119, 180].

The first direct measurement of arterial stiffness is through PWV[180, 181]. PWV represents the speed at which the arterial pulse/pressure waves generated upon each heart contraction propagate a specific point in the arterial circulation[179]. PWV is measured using the Bramwell-Hill equation. The ratio is derived from the distance between two measuring sites and the time delay of the arterial pulse between these sites, known as the pulse transit time and is expressed in m/s[180]. Based on the European guidelines, the clinical reference method is carotid-femoral PWV, measured from these two easily accessible measuring sites, but several other variants exist [182, 183].

Stiffness increases PWV and is thought to result in an earlier return of the reflected pulse wave to the proximal aorta, thus increasing the afterload on the heart, decreasing diastolic pressure, coronary perfusion pressure, and deeper penetration of the pulse wave into the micro-circulation that supply blood to high-flow, low resistance end organs[178-180, 184]. Thereby increasing organ damage and dysfunction **(Figure 1.8).** Stiffness promotes inward remodelling of small arteries, increasing resistance, BP, and central artery stiffness, thus creating a feedback loop[180]. Arterial stiffening may also cause substantial BP variability and elevated in pulsatile load that will affect the function of organs with low-resistance micro-vascular beds, including the brain, kidneys and placenta[108, 179]. In addition, elevation in PWV can result in increased left systolic ventricular load and abnormal ventricular and arterial interactions resulting in left ventricular hypertrophy, dysfunction, and fibrosis[108, 179]. In addition, large artery stiffness is recognised as a risk factor and prognostic index of several increasingly prevalent disorders, including hypertension[149, 185], diabetes

mellitus[186], renal failure[187], inflammatory and pulmonary disorders[188], coronary artery disease[189], stroke[190], myocardial infarction, and general cardiovascular events[191].

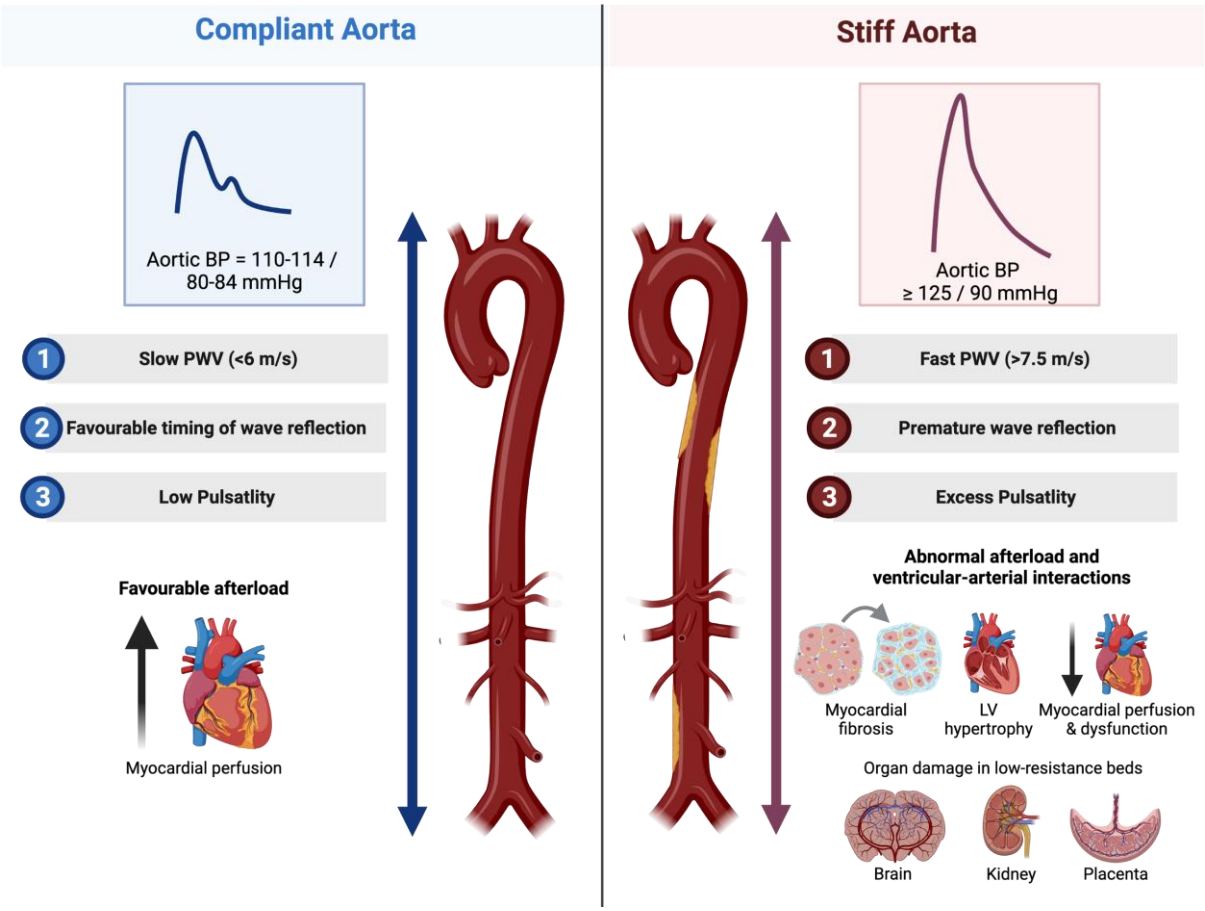


Figure 1.8. Role of large artery stiffness in health and diseases.

The left side represents what occurs with a highly compliant aorta, as occurs in young, healthy adults; the right side represents a very stiff aorta, as occurs in the elderly and/or in the presence of various disease states. In healthy young adults, a compliant aorta (left): 1) effectively buffers excess pulsatility caused by the intermittent left ventricular ejection; and 2) exhibits a slow PWV, which allows pulse wave reflections to arrive at the heart during diastole, increasing diastolic coronary perfusion pressure but not systolic ventricular load. A stiff aorta is associated with a high-amplitude forward wave and a faster PWV, determining faster forward and backward (reflected) wave speeds. This determined an earlier arrival of wave reflections to the aorta, with progressive loss of diastolic pressure augmentation and increased late systolic augmentation. These hemodynamic changes result in adverse patterns of pulsatile load to the left ventricle in systole and reduced coronary perfusion pressure in diastole, ultimately promoting myocardial remodelling, dysfunction, failure, and a reduced perfusion reserve (even in the absence of epicardial coronary disease). This adverse hemodynamic pattern also results in excessive pulsatility in the aorta, which is transmitted preferentially to low-resistance vascular beds (such as the brain, kidney and placenta) because, in these organs, micro-vascular pressure is more directly coupled with aortic artery pressure

fluctuations resulting in end-organ damage. Blood pressure (BP); backward wave (BW); forward wave (FW); pulse wave velocity (PWV).

1.3.2 Pathophysiology of hypertension interactions between micro-vascular and macro-vascular alterations

Studies have discovered associations with the macro-vasculature and micro-vasculature, indicating that micro-vessel remodelling parallels large vessel remodelling[192-196]. The remodelling of the circulatory network seems to be a common denominator contributing to end-organ damage in individuals with elevated BP[178]. Several studies have shown associations between retinal vessel morphology, BP, and arterial stiffness index with more substantial evidence in patients with CVDs or at-risk patients[117, 193, 197]. Other studies have shown similar interactions between ECs and increased arterial stiffness. The response includes changing cells migration, proliferation, transcriptome, VEGF signalling, stress fibre formation and barrier integrity, thus contributing to the emergence of these pathologies[198-200]. These observations further highlight the interplay between EC behaviour, micro-vasculature and macro-vasculature in preclinical disease processes. However, the complex temporal relationship between aortic stiffening, micro-vasculature networks, as well as their interactions leading to CVD development and progression have not yet been fully clarified. Examining their associations could enhance our understanding of whether assessing both could improve cardiovascular risk prediction and have significant therapeutic implications.

1.4 Exercise as a modulator of CVD risk

The existing hypertension phenomenon highlights the urgency to adopt an early and population-level preventive approach targeting the younger population to improve hypertension and CVD risk factors. Physical inactivity accounts for 3.2 million global annual deaths, with 0.7 million deaths (aged below 60 years)[201]. Compliance with physical activity guidelines for both

muscle-strengthening and aerobic exercises as a lifestyle intervention may reduce up to a quarter of all-cause mortality among the healthy population and almost half of the mortality among people with chronic comorbidities[202, 203]. Exercise training is vital for maintaining physical fitness, including building muscle mass during development and preserving musculoskeletal function during ageing[204]. Furthermore, it is widely accepted that regular exercise has enormous health benefits and can positively contribute to sustaining and promoting physiological well-being and as a non-drug therapeutic strategy to use both in disease prevention and treatment[205, 206]. The cardio-metabolic benefits of exercise in many CVDs have been well documented in epidemiological and clinical studies[207, 208]. Exercise promotes cardiometabolic wellness, improves cognitive performance, and effectively aids in the prevention and treatment of a variety of health conditions, including CVD, diabetes and other disorders of metabolism and neurological disease[209-212].

Exercise broadly impacts the sophisticated crosstalk between a multi-system organism's physiological and metabolic network from subcellular to different organ-system states. It challenges homeostasis in every organ system and activates acute and long-term compensatory mechanisms to preserve and/or re-establish homeostasis[213] **(Figure 1.9)**. Moreover, because exercise produces a strong systemic physiological stimulus, the circulatory blood may yield unique molecular footprints associated with the specific biological effects[214, 215]. The exercise-induced subcellular molecular effects may affect all body cells and tissues in numerous ways depending on the type and intensity of activity. Other factors that may influence response to exercise include inherent (sex, genetics and epigenetics) and acquired (age, fitness, nutrition, environment and disease state) factors[216].

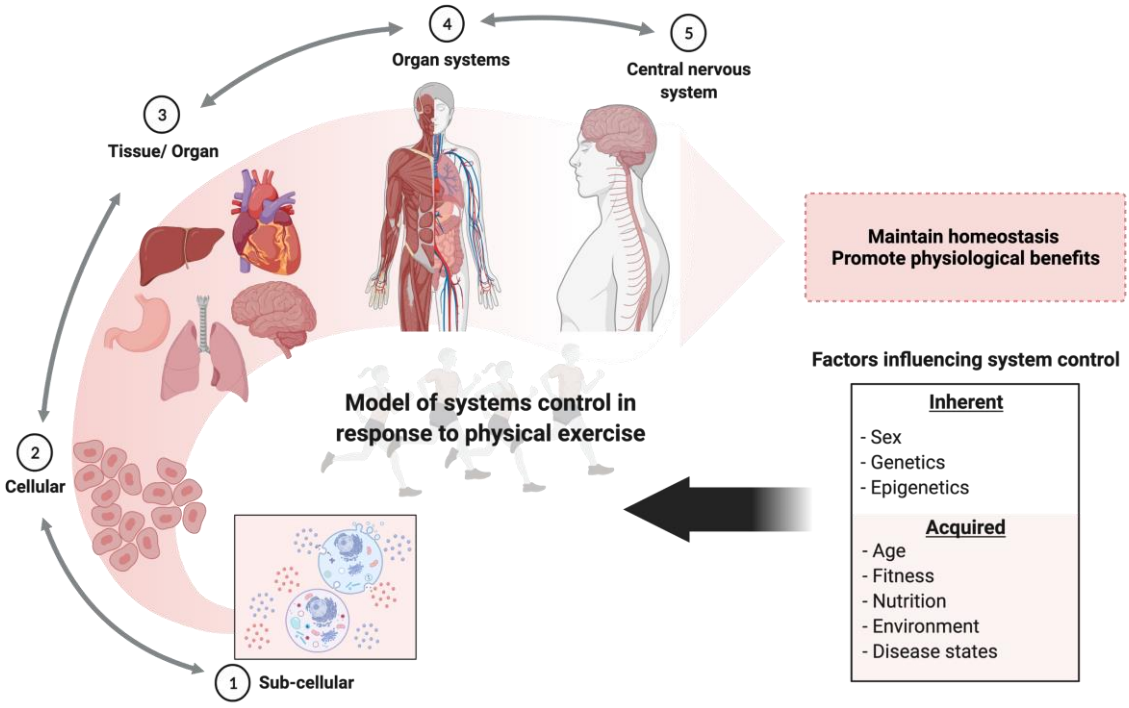


Figure 1.9. Model of systems control and factors that modulate response to physical activity.

Physiological activation with physical exercise and crosstalk between the different systems were illustrated. Other inherent and acquired factors that may affect the interaction between the systems and the response to exercise were highlighted.

The majority of the studies have emphasised the benefits of aerobic exercise, a lifestyle intervention, on individual's general cardiovascular health, including beneficial effects on circulating blood (endothelial-derived vasoactive agents and endothelial progenitor cells), vascular structure and functions, resting peripheral BP, brachial artery flow-mediated dilation, attenuates left ventricular (LV) dilation, regresses cellular hypertrophy, and slows the progression of coronary artery disease within the middle-aged and above subpopulation[26, 211, 217-221]. Additionally, it is well established that physical exercise can modulate the cardiovascular system and other physiological systems, such as the musculoskeletal and the nervous system[222]. Numerous clinical trials and animal models showed that exercise exerts endothelial protection and helps retain endothelial function[223, 224]. Despite indisputable evidence of the myriad physiological benefits conferred by regular physical activity, the exact molecular mechanisms by which physical activity promotes

human health remain nearly uninvestigated and remain poorly understood, particularly in young adults.

1.4.1 The impact of exercise on vascular endothelium

Regular physical exercise promotes a favourable cardiovascular state and has been shown to preserve and improve endothelium and endothelial function via several mechanisms[205, 225]. Blood flow and laminar shear stress augmentations increase NO production and bioavailability, regulating vasodilation[226]. Beneficial effects of training on vascular function also can be mediated via several ways, including synthesis of other molecular and neurohormonal mediators and oxidant-antioxidant homeostasis[205]. In addition, physical exercise can also elicit systemic molecular pathways connected with chronic anti-inflammation and angiogenesis with modulating endothelial function[225]. However, it is worth noting that the benefit is dependent on the type and intensity of training[205] **(Figure 1.10a)**.

1.4.1.1 Exercise-induced vasodilation on vascular endothelium

The endothelium is constantly exposed to haemodynamic forces from the blood flow varying in magnitude and direction, depending on the anatomy of the blood vessel and the blood viscosity, creating a frictional force that exerts shear stress on the surface of the endothelium[227]. An important physiologic stimulus to eNOS and tetrahydrobiopterin (BH4) production is increased intravascular blood flow as the endothelium tends to normalise shear stress through NO-mediated vasodilation, vascular remodelling and blood vessel formation[228-233]. These shear-stress mediated effects may explain the observation that a single session of exercise elicited an acute increase in NO formation, both in athletes and healthy, non-athletic participants[234]. In experimental studies conducted in rats, a 2-to 4-week exercise training programme increased NO synthesis and flow-

mediated dilatation (FMD) in skeletal muscle arteries, increased eNOS protein levels in aortic tissue, and enhanced acetylcholine-induced aortic vasodilatation.

In addition, in situations of haemodynamic overload, growth factors, including insulin-like growth factor 1 (IGF1) are released, and IGF1-IGF1 receptor (IGF1R)-insulin receptor substrate (IRS) is capable of activating the PI3K-AKT signalling pathway, which plays a key role in maintaining optimal vascular function[235]. After binding to IGF1R, IGF1 subsequently recruits the IRS1/IRS2, which activates PI3K-AKT signalling and increases AKT-mediated eNOS phosphorylation and NO production. On the contrary, animal studies showed that inhibition of NO synthase (NOS) resulted in reduced blood flow within exercising skeletal muscles and decreased exercise capacity[236]. Furthermore, reduced NO bioavailability causes abnormal blood flow within the working skeletal muscles and is associated with impaired exercise capacity measured by peak VO_2 in humans, which could be used as a predictor of vasculature damage[237, 238]. Besides from vasodilation, eNOS mediates key aspects of cardiac and vascular remodelling via orchestrating the mobilisation, migration, recruitment, and differentiation of vascular and cardiac progenitor cells, in part by regulating the stabilisation and transcriptional activity of hypoxia-inducible factor in normoxia and hypoxia[232] .

1.4.1.2 Exercise-induced anti-oxidative effects on vascular endothelium

During exercise, the skeletal muscle undergoes aerobic respiration to produce energy, an elevation in respiration rate, heart rate, cardiac contractility, BP, blood flow, and endothelium-dependent vasodilation is observed to meet energy demands[237]. Studies have underlined the non-exhaustive exercise-induced redox signalling via transient oxidative stress and the simultaneous elevation of anti-oxidative capacity adaptations of the vascular wall, thereby modulating muscle contractility and BP[231, 239]. It is known that laminar shear stress can also regulate other enzymes, such as superoxide dismutase (SOD) and glutathione peroxidase (GPx), which are responsible for

reactive oxygen species (ROS) scavenging[231, 239, 240]. The overall net effect of long-term exercise will ultimately improve oxidative stress tolerance and mitigate the oxidative burden[231, 239].

Exercise-induced shear stress promotes NO bioavailability, which plays a critical role in regulating ischaemic metabolites in skeletal muscle during exercise[241]. Experimental studies in healthy animals demonstrated that aerobic exercise suppresses nicotinamide adenine dinucleotide phosphate oxidase (NADPH) protein expression, increases expression of anti-oxidant enzymes, improves mitochondrial biogenesis, activates mitochondrial anti-oxidant defence system, enhanced ATP formation and reduced mitochondrial swelling[242, 243]. Observed changes in mitochondrial health were accompanied by improvement in endothelium-mediated arterial relaxation.

1.4.1.3 Exercise-induced anti-inflammatory effects on vascular endothelium

Aerobic exercise duration and intensity regulate levels of vascular inflammatory markers. Although a single bout of exercise increased circulating levels of interleukin-1 (IL-1), IL-6, interferon-γ, tumour necrosis factor-α (TNF-α), transcription factor nuclear factor kappa B (NF-κB) and C-reactive protein (CRP), regular aerobic exercise is associated with a reduction in serum concentration of pro-inflammatory cytokines[225, 239, 244-248]. This translates to an increased expression of anti-inflammation. Other studies have reported the benefits of regular exercise because it promotes the expression of adhesion molecules modulation of the inflammatory response[248].

1.4.1.4 Exercise-induced angiogenesis on vascular endothelium

Angiogenesis has been shown to be an adaptation to exercise training; it is mediated mainly by various types of circulating growth factors, including VEGF, FGF and platelet-derived growth factor (PDGF)[207, 249, 250]. In particular, VEGF is involved in extracellular matrix (ECM) changes, EC proliferation and improvement in EC function[251]. Improvements in endothelial function not only depend on the cells that reside in the vessel wall but can also be modified by bone marrow-derived

EPCs[233]. These stem cells have been shown to enhance angiogenesis, promote vascular repair, improve endothelial function, inhibit atherosclerosis, and increase ventricular function after myocardial infarction[252]. The increased NO production during exercise has been proposed to be the main stimulator for releasing EPCs[233].

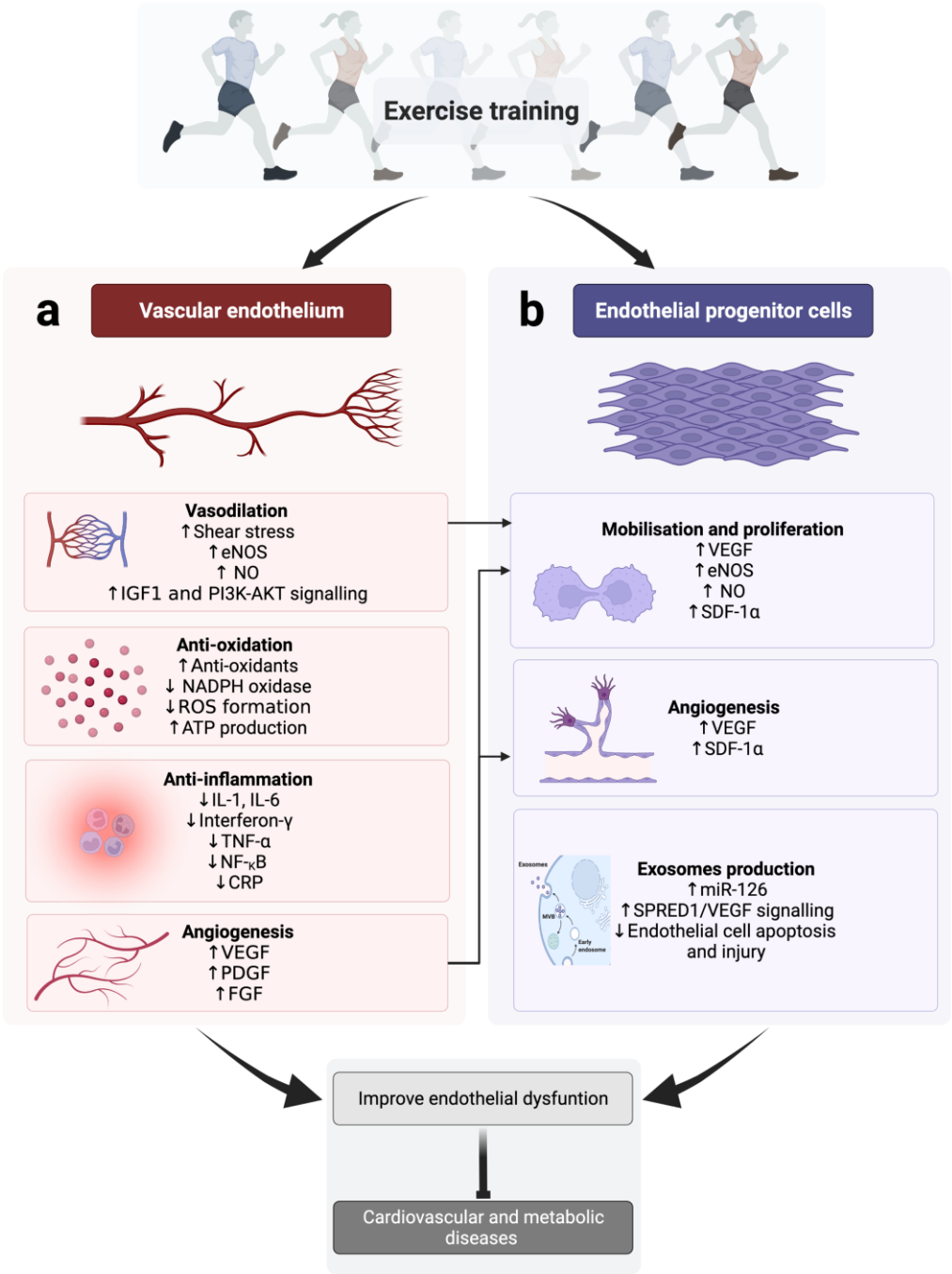


Figure 1.10 Summary of the mechanisms through which exercise training improves endothelial dysfunction via modulation in the (a) vascular endothelium and (b) endothelial progenitor cells (EPCs).

The changes induced by exercise training in vascular endothelium and EPC coincided with improvements in endothelial function and prevented cardiometabolic disease progression. Nitric oxide (NO); endothelial nitric oxide synthase (eNOS); insulin-like growth factor 1 (IGF1); nicotinamide adenine dinucleotide phosphate oxidase (NADPH); reactive oxygen species (ROS); interleukin-1 (IL-1); tumour necrosis factor-α (TNF- α); nuclear factor kappa B (NF-κB); C-reactive protein (CRP); vascular endothelial growth factor (VEGF); platelet-derived growth factor (PDGF); fibroblast growth factor (FGF); and stromal cell-derived factor 1α (SDF-1α).

1.4.2 The impact of exercise on endothelial progenitor cells (EPCs)

The endothelium is a self-renewing system. However, disruption in the injury and repair balance of the endothelium leads to the pathophysiology of vascular diseases[236]. Endothelial injury can be rescued by mechanisms including EC proliferation, angiogenesis, EPC mobilisation and EPCs to EC differentiation[232, 233, 253-255]. The extent of the circulating EPC pool is considered as a mirror of cardiovascular health[256]. High levels of EPCs have been associated with prolonged event-free survival from adverse cardiovascular events. In contrast, low levels and impaired activity of circulating EPCs have been shown to be independent predictors of morbidity and mortality in patients with CVD[257, 258] **(Figure 1.10b)**.

1.4.2.1 Exercise-induced EPCs mobilisation and proliferation

Several studies demonstrated that regular physical activity positively affects the levels of circulating EPCs by inducing EPC mobilisation and proliferation from the bone marrow niche[217, 218, 258, 259]. Exposure to an intermittent hypoxic environment during exercise promotes homing of EPC to damaged vascular sites in healthy individuals and those with CVDs, and eventually counteracts endothelial dysfunction and CVD risk[26, 259-270]. A single bout of exercise was sufficient to induce a release of circulatory EPCs from bone marrow for up to 72 hours post-physical activity in healthy individuals[271].

The mechanisms by which exercise mobilises EPCs is complex and includes upregulation of VEGF serum that in turn activates matrix-metalloproteinase-9 (MMP-9), stimulating stem cells to migrate from a quiescent bone marrow niche to the vascular zone[272, 273]. The increased number of

circulating EPCs demonstrates the beneficial effects of a 12-week supervised exercise training programme on the endothelium, elevated NO production, and improved FMD of the brachial artery in the training group for patients with coronary artery disease and/or cardiovascular risk factors[274]. In another clinical trial, patients diagnosed with the peripheral arterial disease that underwent six months of exercise training increased the number of circulating EPCs and decreased the plasma levels of asymmetric dimethylarginine (ADMA, an inhibitor of NOS), both reflecting improved endothelial function[275]. Consistently, after regular exercise training, the number and the migration capacity of EPCs were increased was accompanied by a reduction in brain natriuretic peptide (BNP) level and improvement in the maximum rate of oxygen consumption (peak VO_2) in patients with ST-elevation myocardial infarction (STEMI)[261].

1.4.2.2 Exercise-induced EPCs angiogenesis

Pro-angiogenic factors such as VEGF and stromal cell-derived factor 1α (SDF-1α) promote the activity and recruitment of EPCs to promote vascularisation that may serve as a physiologic repair or compensation mechanis[32, 262, 273, 276, 277]. A study conducted by Tan *et al.* showed that after eight weeks, the number of CFU-Hills was significantly increased in the exercise group compared to the control group and that the exercise intervention enhanced tube-formation capacity of EPCs and increased phosphorylation levels of eNOS and PI3K-AKT signalling[278]. A 3-month aerobic exercise training programme in older men improved EPC number and function nearly two-fold[265], while a 12-week exercise markedly enhanced the re-endothelialisation capacity of EPCs in older adults[279]. In most clinical trials assessing the chronic effects of exercise, elevations in circulating EPCs coincides with an improvement in aerobic capacity including peak VO_2, 6 minutes walking test, maximal walking distance[262, 273, 280-285]. However, the role of circulating EPCs in improving aerobic capacity is not clear. Mezzani *et al.* suggested EPCs possibly had a positive effect on peak VO_2 by mediating changes in the altered micro-vasculature, which improved oxygen utilisation and aerobic power[284].

1.4.2.3 Exercise-induced EPC exosomes production

Recent evidence suggests that exercise increases the level of total EPC-derived exosomes containing miR-126 and enhances EPC-derived exosomes's effects on protecting EC against injury[286-289]. In addition, EPC-derived exosomes have been shown to enhance angiogenesis of human pancreatic islets and protect kidneys from ischaemia/reperfusion injury through their carried miR-126 and miR-296[290]. It is well understood that miR-126 modulates angiogenesis and vascular integrity. Previous reports have also shown that miR-126 can target the SPRED1/VEGF pathway to decrease endothelial apoptosis[291, 292].

Taken together, data presented in the literature shed light on physical exercise as an efficient tool for reducing global cardiovascular risk and improving vascular endothelium and endothelial progenitor cells. However, no studies have yet investigated the effect of exercise training in young adults and the specific subtype of EPCs – ECFCs.

1.5 Thesis aims and hypotheses

Currently, no studies have yet investigated the proteomic profiles in ECFCs with different functionality and explored the impact of sex dimorphism. This knowledge is critical to justify their use in clinical investigations and target the discovery of disease-related endothelial mechanisms. In addition, little is known about the function of how ECFCs interact with other clinical measurements linked to CVD risk, including micro-vascular and macro-vascular changes and high BP, particularly in young adults. Besides, several studies have shown that exercise is a CVD risk modulator that exerts endothelial protection and helps retain endothelial function[223, 224, 259-266]. However, the effect of exercise on ECFCs has yet to be investigated. To address the research gaps, the thesis sets out to address the following general aims and hypotheses:

Aims	Hypotheses
1 To demonstrate the feasibility of ECFC isolation and culture; to describe their endothelial, angiogenic phenotype and proteomic signatures of circulating ECFCs; and to investigate the influence of sex on ECFCs function and proteomic profiles.	ECFCs can be used as a tool for clinical in-vitro angiogenesis evaluation that displays distinctive proteome profile and clinical characteristics based on ECFC functionality and sex.
2 To describe the baseline characteristics in individuals of varying blood pressure profiles and investigate the relationship between ECFC, micro-vasculature, macro-vascular remodelling in blood pressure regulation and understand these interactions.	An increase in CVD risk factors, including elevation in blood pressure, adversely affects young adults' cellular, micro-and macro-vascular function.
3 Outline the ECFC function pre-and post-exercise intervention and correlate it with clinical measurements, and investigate if ECFC functionality can predict the change in clinical measures after exercise intervention.	Exercise intervention as a CVD risk modulator will improve ECFC function and its relationship with other clinical measurements. ECFC cellular function (proliferative and angiogenic capacity) can predict response to exercise intervention.

2

Study population



2. Study population

Trial of Exercise to Prevent HypeRtension in young Adults (TEPHRA) study

ECFCs were collected from a pre-existing study that my supervisors and seniors had established and designed – The Trial of Exercise to Prevent HypeRtension in young Adults (TEPHRA) study (Ethics no. 16/SC/0016; Clinicaltrials.gov registration number NCT02723552)[293]. TEPHRA is an open, parallel-arm randomised control trial with three study visits (baseline visit, 16-weeks follow-up and 52 weeks follow-up). ECFCs were collected from participants during the baseline visit and 16-week follow-up in our attempt to investigate baseline and post-exercise effects on ECFC functionality. As part of the trial, I assisted in the study recruitment and data collection, which included over 120 participant screening visits and over 300 full study visits during a two year period. I was also responsible for managing the daily study operation and administrative work, including organising and chairing the bi-weekly meetings, major trial committee meetings, trial rostering, training, data extraction and organisation. I also successfully submitted a study amendment for the trial **(Appendix Figure 1)**, presented on the trial for our Departmental meeting day, and organised a booth at the hospital to promote recruitment. Furthermore, I was the leading wet laboratory researcher who managed the lab's day-to-day operation and handled blood sample collection, storage, and analysis.

2.1 Study background

Hypertension affects over 1 in 4 adults (approximately 31% of men; 25% of women). More than 13.5 million people are diagnosed with hypertension, and it contributed to 75,000 deaths in England based on the National Institute for Health and Care Excellence (NICE) report from 2019. Based on the current guidelines, it is estimated that over 30-40% of the adults aged 18 to 39 are within diagnostic criteria (BP ≥ 130 mmHg systolic or 80 mmHg diastolic) for hypertension leading to a three-fold increase in prevalence[294-296]. A global increase in hypertension incidence in young adults represents a rising risk of cardiovascular events and, if untreated, up to 50% of those with elevated BP may transition to hypertensive levels in as little as five years[294, 296-298].

The existing hypertension phenomenon underlines the urgency to adopt an early and population-level preventive approach targeting the younger population to improve hypertension and CVD risk factors. The benefits of anti-hypertensive medications in young adults are unclear[299]. Therefore, first-line management is typically a lifestyle intervention with advice to increase aerobic exercise[300]. Compliance with physical activity guidelines for muscle-strengthening and aerobic exercises as a lifestyle intervention has shown to reduce up to a quarter of all-cause mortality among healthy adults and almost half of the mortality among people with chronic comorbidities[202]. In addition, a systematic review by Williamson *et al.* has emphasised the benefits of aerobic exercise, a lifestyle intervention, for non-, pre- and hypertensive individuals' general cardiovascular health, including BP control and weight loss within middle-aged populations[219]. Young adult hypertension may have a distinct pathophysiology and risk factor profile compared to older adult hypertension. Furthermore, there remains a lack of understanding in terms of physiological and cardiovascular remodelling in response to exercise training for BP management in the young adult population.

Further to this, unique early developmental history, including preterm birth or pregnancy hypertension, relates to distinct cardiovascular phenotypes and risk of BP elevation[301-308]. Thus, the

TEPHRA study is a randomised controlled trial that was designed to investigate the effect of a prescribed exercise intervention supported by physical activity self-monitoring and motivational coaching in BP, on the behavioural and physiological modifications in young adults with elevated BP[293].

2.2 TEHPRA Study General aims and Hypotheses

TEPHRA is an open-label, single-blinded, parallel-arm, randomised controlled trial in young adults with elevated BP to investigate the effectiveness of a structured exercise intervention to lower BP in young adults with pre-hypertension and hypertension with varying birth histories. A total of 540 participants were recruited, of which 203 participants underwent randomisation, 178 participants (88%) returned for the 16-week follow-up, and 160 participants (76%) returned for the 52-week follow-up visit. The overall aims and hypotheses of TEPHRA are listed in **Figure 2.1**, which are published and investigated alongside with other team members.

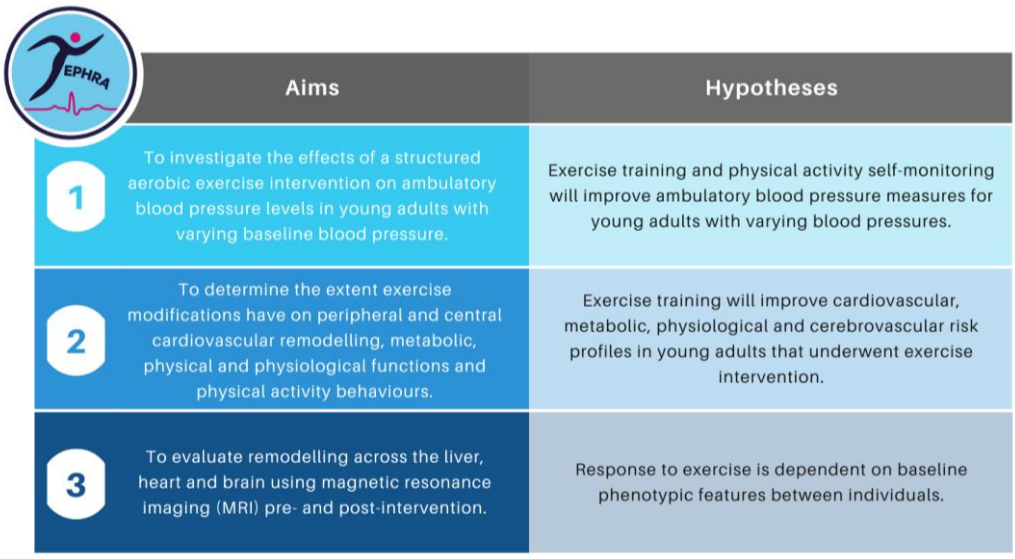


Figure 2.1. Trial of Exercise to Prevent HypeRtension in young Adults (TEPHRA) study – General aims and hypotheses.

Study funding and Ethics approval

The study was supported with funding from the Wellcome Trust (105741/Z/14/Z) and British Heart Foundation (PG/17/13/32860) and approved by the Oxford B Research Ethic Committee (Reference 16/SC/0016).

2.3 Overview of the study

2.3.1 Participants and Recruitments

The randomised controlled trial was conducted in the Oxford Cardiovascular Clinical Research Facility (CCRF), John Radcliffe Hospital, Oxford, England[293]. Participants were recruited through an invitation from hospital birth registers, GP records, local practice recruitment, open recruitment at primary advertising locations that included Oxford University Hospitals NHS Foundation Trust, the University of Oxford Colleges and Oxford Brookes University, targeted web-based advertising via social media platforms including Google, LinkedIn, Facebook, Instagram, and Twitter, or invitation following participation in previous studies.

Before the screening visit, participants completed a pre-screening questionnaire via a secure online platform (Trialspark). The questionnaire included information such as the sex, age, birth history, pregnancy status, medical history, self-reported current physical activity levels, and willingness to alter physical activity and attend a 16-week supervised exercise training at Oxford. A trained clinical research investigator reviewed the online questionnaire to determine the eligibility for study participation. Potentially eligible participants were invited to attend a screening visit at CCRF. articipants were provided with written and verbal versions of the information leaflet during the screening visit. Informed consent was taken from the participant before any study-specific procedures were performed.

2.3.1.1 Inclusion and Exclusion

Individuals were deemed eligible if they met the inclusion criteria:

- Able and willing to give informed consent and comply with all study requirements;
- Aged between 18-35 years old;
- Had a verifiable birth history of preterm birth (<37 weeks) or full-term birth (≥37 weeks),
- A body mass index <35 kg/m^2;
- A clinic and 24-hour awake ambulatory systolic and/or diastolic BP ≥115/75 mmHg, but <159/99mmHg;
- Had access to a computer and the internet;
- And no prescription or previously prescribed hypertension medications.

Participants were considered ineligible if any of the following applied:

- Unable to give informed consent and comply with all study requirements;
- Above the BMI or age limit;
- Clinic BP >159/99mmHg;
- 24 hours awake BP >150/95mmHg;
- Unable to walk at a brisk pace on the flat surface for 15 minutes;
- Current levels of cardiovascular fitness and activity are higher than intervention;
- Hypertension diagnosis and/or on anti-hypertensive medication;
- Any other evidence of CVDs or abnormalities;
- Or currently pregnant.

2.3.2 Trial design

After the screening visit, eligible and consented participants attended the first baseline study visit. Detailed multi-model study measurements were taken from the participants, including demographics, anthropometrics, 24-hour ambulatory BP monitoring, micro-vascular assessments,

cardio-pulmonary exercise testing (CPET), blood sample collection, and cardiac imaging **(Figure 2.2)**. Trained study investigators conducted all measurements. Each participant was randomised into either an exercise group (16-month exercise intervention) or usual care (control group). Participants were requested to return for two more follow-up study visits at 16 weeks and 52 weeks with repeated measurements of the parameters at baseline. More detailed study objectives, outcome measures and measurement time-points are listed in the **Appendix Table 1**.

2.3.2.1 Randomisation

Participants meeting the main study inclusion criteria were randomly allocated 1:1 to the two arms using a secure web-based randomisation program (Sealed Envelope™) following completion of baseline study measures. A minimisation algorithm (with a random element) was used to ensure balanced allocation across treatment groups for key prognostic factors: sex, age, and gestational age of participants. Due to the nature of the intervention, participants were not blinded. To eliminate potential bias, primary and secondary outcome data were analysed remotely by operators blinded to the participant identifiers and randomisation and results were verified by a second blinded research team member.

2.3.2.1.1 Control allocation

Participants in the control group were instructed to maintain and continue the regular physical activity. They were sign-posted to educational materials produced by the British Heart Foundation explaining hypertension, hypertension prevention and recommended lifestyle behaviours to maintain heart health (https://www.bhf.org.uk/informationsupport/heart-matters-magazine).

2.3.2.1.2 Exercise intervention allocation

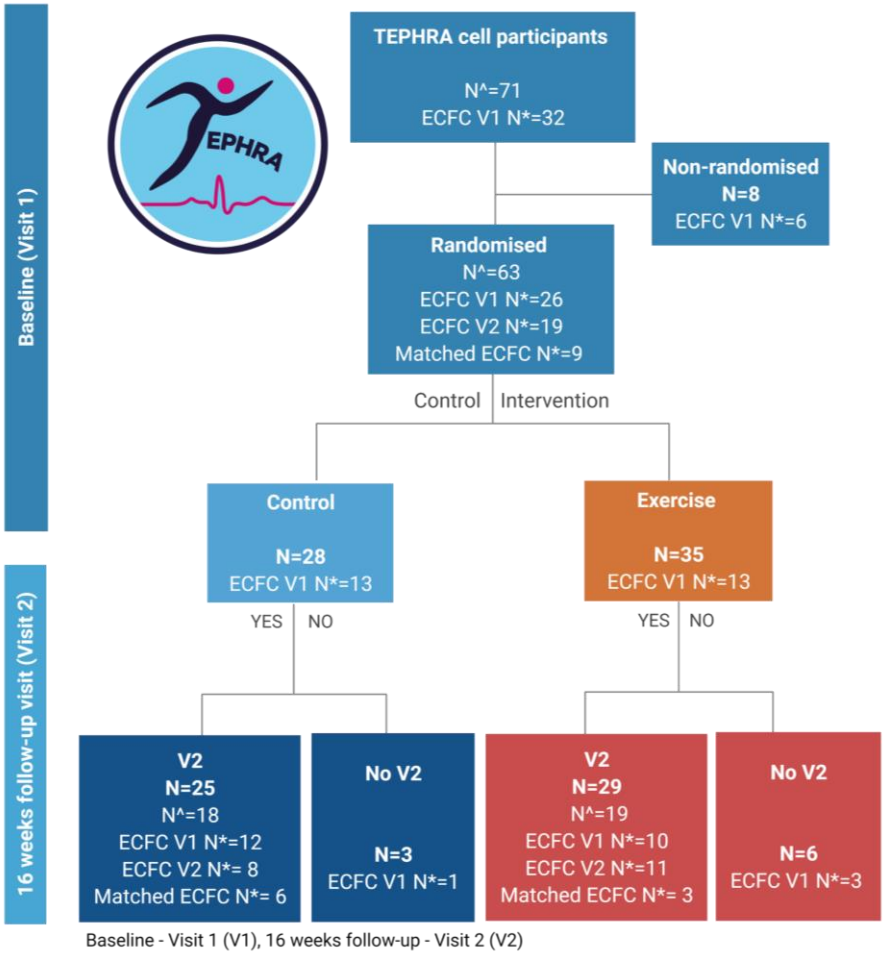
Participants in the exercise intervention group were expected to complete three supervised 60-minute aerobic training sessions per week at 60-80% peak heart rate based on their CPET test measurements at the baseline visit. This intervention replicates effective exercise strategies for BP reduction as outlined in the systematic review[219]. The training sessions were held at a dedicated gym at the Movement Science Department of Oxford Brookes University. The intervention team were completely independent of the research study team and included a physician, physiologists, physiotherapists, and a clinical nurse trained in motivational coaching. Participants were gifted a wrist-worn heart rate and activity monitor (Fitbit Charge HR) that they were encouraged to wear daily to aid in self-monitoring their activity. Upon completing 16 weeks of training, participants received a motivational coaching session to encourage them to set long-term physical activity goals to maintain cardiovascular fitness until a 52-week follow-up. The physical activity of participants in the intervention group was tracked using the wrist-worn activity monitor on the Fitabase data management platform.



Figure 2.2. Trial of Exercise to Prevent HypeRtension in young Adults (TEPHRA) study design.

2.4 Thesis study cohort – THEPHRA cell study

As part of the thesis, Assistant Professor Mariane Bertagnolli and I attempted collection of ECFCs from 71 participants at the baseline visit and repeated collection from 37 participants at the 16-week follow-up visit **(Figure 2.3)**. Participants were recruited concurrently with the main TEPHRA study. The rates of successful ECFCs isolation are between 52.4% based on our study. This isolation rate has been supported by other studies that have shown the efficiency of ECFC colonies to be between 30 - 62%[10, 309-311]. To detect an effect of blood pressure on ECFC functionality, powered to 90% at P=0.05 with the effect size of 1.33 requires a total sample size of 26 and with 1:1 randomisation this would require 13 in each group. For a required power of 90% at P=0.05 with the effect size of 2.29, a sample size of at least 5 per group (repeated measurement at V1 and V2) was required to detect the change in ECFC function based on exercise. Power calculations were conducted using G*Power Version 3.1.



Baseline - Visit 1 (V1), 16 weeks follow-up - Visit 2 (V2)

Figure 2.3. Flowchart of TEPHRA cell study participants.

TEPHRA cell participants were recruited alongside the main TEPHRA trial; 71 and 37 participants had their blood taken for ECFC isolation at baseline and 16-week follow-up visits, respectively. **N** (bold) represents the number of participants that participated in the visit. N^ represents the number of participants with blood collected for ECFC culture. N* represents the number of ECFC successfully isolated from participants in the baseline visit (visit 1) or 16-week follow-up (visit 2).

2.4.1 Participants recruitment limitations

The recruitment of the participants was hindered by several factors described below:

- Pause in TEPHRA cell recruitment due to insufficient human resources during the trial transition – the departure of key investigators and research team members. Our focus was to ensure trial recruitment and primary data collection.
- Blood sample for TEPHRA cell was an optional component, and not all participants wanted additional blood volume drawn for cell analysis.
- Several participants opted out of blood collection or withdrew consent for blood collection at the follow-up visit.
- Furthermore, I was the sole person working on cell isolation once Assistant Professor Bertagnolli moved back to Montreal. I had limited capacity as I had to assist in conducting the study visits and trial management, alongside cell sample isolation.

3

General methodology



3. General methodology

The following chapter examines the methods that were used to: (i) collect clinical measurements, including BP, anthropometry, and blood sampling; (ii) isolate and culture ECFCs; (iii) investigate ECFC functionality in young adults from TEPHRA; and finally, (iv) the general statistical analysis tests used in the thesis. In addition, the method for culturing the positive and negative control cell types (HUVECs and primary dermal fibroblast, respectively) will be described. This methodology chapter forms the basis of the methods used for the entire thesis, while specific experimental methods will be discussed in each respective chapter.

3.1 Anthropometric measurements

Height and weight were measured to the nearest 0.1 cm and 0.1 kg using a Seca measuring station (Seca, Birmingham, United Kingdom) with footwear removed. Body mass index was calculated using the formula = $\frac{Weight\ (kg)}{Height\ (m^2)}$. A bioelectrical impedance InBody 720 body composition analyser was used to determine body composition. Manual waist circumference was measured with a measuring tape at 2cm above the iliac crest, and the manual hip circumference was measured at the widest portion near the level of the greater trochanter of the femur or mid-buttock. Waist-hip circumference ratio was then calculated.

3.2 Clinical BP measurements

Resting brachial BP was measured after a 5-minute acclimation period in a seated position using an automated oscillometer device (Dinamap V100, GE Healthcare, Chalfont St. Giles, United Kingdom) by trained investigators and clinical staff. Three readings were taken from the left arm, with the last two readings averaged and subsequently used for further analyses.

3.3 Blood sample collection

Participants were instructed to have fasted at least 4 hours prior to blood sample collection. They were encouraged to drink water during the fast. A total volume of 50 ml of peripheral venous blood was collected per individual from the antecubital fossa by venepuncture. Blood samples were centrifuged within 30 minutes of collection at 3,000g for 15 minutes at 4°C, and the separated plasma and serum were stored at -80°C for further analysis.

.

3.3.1 Biochemistry analysis

Fasting lipid, cholesterol and metabolic profiles were measured at the Oxford Hospital Biochemistry John Radcliffe Hospital Biochemistry Laboratory using routine clinical quality validated assays with clinical level quality controls. Insulin resistance was calculated using the homeostasis model assessment calculator[312].

3.3.2 ECFC isolation and culture

The process of ECFC isolation from PBMCs is illustrated in **Figure 3.1.** . The protocol used for PBMC isolation was previously described [10]. Briefly, 15 ml of fasted whole blood was diluted 1:1 with Dulbecco's phosphate-buffered saline (PBS; Gibco by Life technologies). PBMCs were separated from the diluted blood using 10 ml Ficoll-Paque PLUS (GE Healthcare Life Sciences, Pittsburgh, PA, USA) density gradient following 30 minutes of 400g centrifugation at room temperature (RT) and then washed once with PBS.

PBMCs were either frozen down in 10% dimethyl sulfoxide (Sigma Aldrich) fetal bovine serum (FBS; Gibco by Life Technologies, New York, USA) or immediately plated on collagen I-coated (Corning, New York, USA) 25 cm^2 tissue culture-treated Falcon flasks (Thermo Fisher Scientific, Waltham, MA, USA) at a density of $5.0x10^6$ cells/flask. Cultured cells were maintained in a standard cell culture condition (humidified chamber, at 37°C with 21% O_2 and 5% CO_2), using complete EC growth basal medium-2 (EBM™-2 plus SingleQuots™ of Growth Supplements, Lonza, Basel, Switzerland) supplemented with 1% penicillin/streptomycin (Gibco by Life Technologies) and 10% fetal bovine serum (FBS).

Media was changed every 2 or 3 days, and cells were maintained for up to 30 days in culture. Cultured cells were observed daily from day 6 to 30 to determine the first day of cobblestone patterned ECFC colony formation **(Figure 3.1.).** Once ECFC colonies were observed, they were passaged and expanded under the same conditions. ECFC phonotype, clonogenic and

functional assessments were assessed using cells from the second passage. The remaining PBMCs and ECFCs were frozen in 10% dimethyl sulfoxide (Sigma Aldrich) FBS and stored in liquid nitrogen for later analysis.

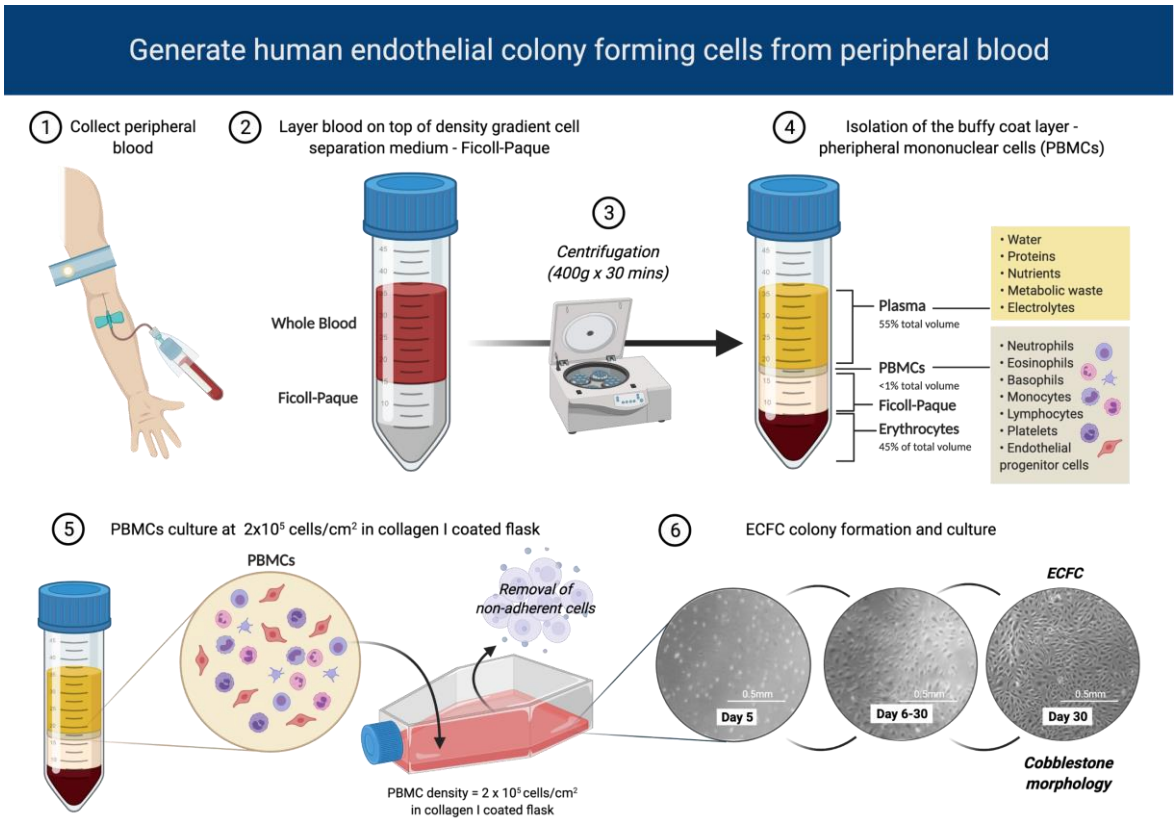


Figure 3.1. Schematic representation of endothelial colony-forming cells (ECFCs) isolation and colony formation.

Peripheral blood mononuclear cells (PBMCs) isolated from peripheral blood undergo cell culture and were observed daily from day 6 to 30 to determine the first day of cobblestone-pattern ECFC colony formation (phase contrast fluorescence microscope, magnification 5x).

3.4 ECFC cellular assessments

3.4.1 Fluorescence-activated cell sorting (FACS)

ECFCs were detached with accutase and washed with PBS. Cells were fixed and permeabilised with 4% paraformaldehyde (PFA) and 0.2% triton-x100, respectively for 10 minutes. Cells were then blocked with 3% FBS for 15 minutes at RT. Cells were incubated with conjugated

antibodies for 30 minutes at RT **(Table** 3.1**)**. Stained and unstained cells were washed with eBioscience flow cytometry staining buffer and analysed on a Fortessa flow cytometer. Cells were stained with FITC-PECAM-1, PE-VE-Cadherin, APC-vascular endothelial growth factor-2 (VEGFR-2) along with fluorescence minus one control. A total of N=8 cells were analysed.

3.4.2 Immunofluorescence staining

Antibodies and dilutions used are summarised in **Table 3.1.** Cells (ECFCs, HUVECS and fibroblasts) were fixed in 4% PFA, permeabilised with 0.2% Triton-X100 for 10 minutes at RT and blocked with blocking buffer (PBS with 10% FBS; 30 min, at RT). The samples were incubated with primary antibodies (overnight, 4°C). The cells were washed thrice at a 5-minutes interval with wash buffer (PBS and 0.05% Tween-20; Thermo Fisher Scientific). Cells were incubated with an appropriate secondary antibody, and nuclei were stained with TOPRO™-3 Iodide (1:500) (1 hour, RT). Stained cells were washed thrice at a 5-minutes interval with wash buffer and mounted in SlowFade™ Gold anti-fade mountant (Thermo Fisher Scientific). Cells were visualised using a Leica DM6000 CFS confocal microscope with three main fluorochromes – Alexa Fluor 488, Alexa Fluor 555 and Alexa Fluor 647 were used to capture 12-bit resolution images were captured with Leica application suite (Version 2.7.3.9723). Appropriate isotype controls were used.

Table 3.1. List of antibodies used with the respective application.

Antigen	Spices	Dilution	Supplier	Application
PECAM-1, PAb	Rabbit	1:200	Thermo-Fisher, PA5-14372	IF
CD34, MAb	Mouse	1:200	Thermo Fisher, MA1-10202	IF
eNOS, PAb	Rabbit	1:200	Thermo Fisher, PA5-16887	IF
VE-Cadherin, MAb	Rabbit	1:200	Cell signaling technology, 2500S	IF
Lectin (UEA-1) Fit-C conjugate	-	1:200	Vector laboratories, B-1065	IF
VEGF-R2, MAb	Rabbit	1:200	Stratech Scientific Ltd, 50998-R004-P	IF
CD133 (Prominin-1), MAb	Mouse	1:100	eBioscience, 14-1331-80	IF
Purified anti-human CD45, MAb	Mouse	1:100	BioLgend, 304001	IF
TO-PRO™-3 Iodide (642/661)	-	1:500	Invitrogen, T3605	IF
ActinGreen™ 488 ready probes™ reagent	-	1 drop/ 0.5ml	Thermo Fisher, R37110	IF
AlexaFlour™ 555 anti-rabbit IgG(H+L)	Goat	1:400	Invitrogen, A27039	IF, Flow cytometry
AlexaFlour™ 546 anti-mouse IgG	Mouse	1:400	Invitrogen A11018	IF
AlexaFlour™ 488 anti-mouse IgG	Goat	1:400	Invitrogen, A1101	IF, Flow cytometry
Human VE-Cadherin (D87F2) XP® PE Conjugate, MAb	Rabbit	1: 150	Cell Signalling Technology, 89426S	Flow cytometry
Human PECAM-1 Fit-C conjugate, MAb	Mouse	1:20	Bio Legend Inc, 303104	Flow cytometry
Human VEGF R2 (Clone 89106), MAb	Mouse	1:20	Bio-Techne (R&D Systems); FAB357A	Flow cytometry
Mouse IgG1 kappa Isotype Control	Mouse	1:200	Invitrogen; 14-471482	IF
Rabbit IgG Isotype Control	Rabbit	1:200	Life technologies, 086199	IF

Monoclonal Antibody (MAb); Polyclonal Antibody (PAb); Immunofluorescence imaging (IF)

3.4.3 EdU proliferation assay

The proliferation rate was assessed by quantifying 5-ethynyl-2'-deoxyuridine (EdU) cellular incorporation using the Click-iT™ EdU Alexa Fluor™ 488 Imaging kit (Thermo Fisher Scientific). ECFC with a cell density of $4.0x10^4$ were plated on collagen-coated flasks 1.86 cm^2 surface area, maintained with complete EBM™-2 media and grown for 24 hours. Cells were then incubated with 10 µM EdU in complete EBM™-2 media for 4.5 hours at 37°C, then fixed with 3.7% formaldehyde in PBS, permeabilised with 0.5% Triton X-100 in PBS, and stained according to the kit instructions. Assays were performed in triplicates and, cell images were obtained using a fluorescence microscope (Leica, Germany) and a 10x objective. The number of cells under proliferation and incorporating EdU into their DNA, stained positive for EdU (green, AlexaFluor 488), were counted in three to five full pictures per assay, as well as the total number of cells with nuclei stained with DAPI (blue); the percentage of proliferating cells was then calculated using the formula: proliferation rate = $\frac{EdU\ stained\ cells}{DAPI\ stained\ cells} \times 100\%$.

3.4.4 In vitro tube formation assay

Vascular tube formation was assessed *in vitro* by plating $1.5x10^4$ cells on 50 µL of growth factor reduced basement membrane matrix (Matrigel) in a 96-well plate. Cells were imaged using a Leica DMIL inverted trinocular phase contrast fluorescence microscope (Leica, Germany) and 5x objective after 6 hours of incubation under standard culture conditions. Assays were performed in triplicates, and the number of closed tubes and branches formed (not necessarily forming closed tubes) were quantified in three to six random images per participant using ImageJ software (NIH, USA).

3.4.5 Proteomic analysis on ECFCs

3.4.5.1 Sample digestion and de-saltation

ECFCs from normotensive and elevated BP subjects (total n=11) were used for proteomic analysis at passage number two. Cell pellets containing approximately 2.0 x10^5 were re-suspended in lysis buffer (50 mM Tris-HCl pH 8.5, 4% sodium dodecyl sulfate (SDS) and 50 mM dithiothreitol), boiled for 5 minutes and incubated for 30 minutes at room temperature for protein solubilisation. Total protein (~250 µg) was digested and desalted after two rounds of chloroform-methanol precipitation, reduction/alkylation with DTT/Iodoacetamid[313]. Digested and desalted proteins were dissolved in 0.1% formic acid and loaded into the nano-LC-MS/MS system (Orbitrap Fusion Lumos, Thermo Fisher Scientific) in collaboration with the Oxford Target Discovery Institute.

3.4.5.2 Mass Spectrometry report system and conditions

Mass spectrometry (MS) analysis was performed in the Target Discovery Institute MS (TDI MS) laboratory led by Benedikt M. Kessler (University of Oxford, UK). Peptides were separated with a gradient of 2-35% acetonitrile in 0.1% formic acid/5% DMSO on an EasySpray column (50 cm x 75 µm) over 60 minutes and with a flow rate of 250 nl/min. The MS data were acquired on an Orbitrap Fusion Lumos using a standard method as described previously[314].

3.4.5.3 Proteomics data availability and system biology analyses

Peptides and proteins were identified by searching the MS raw files against the Human SwissProt database downloaded on 11/2015 (containing 20,268 human sequences). MASCOT data outputs were filtered by applying a 20-ion cutoff and 1% False Discovery Rate (FDR) above the identity or homology threshold. The raw MS proteomics data have been deposited to the ProteomeXchange Consortium (http://www.proteomexchange.org) via the PRIDE partner repository with the dataset identifier: PXD020677 and project DOI: 10.6019/PXD020677.

Perseus (Max Planck Institute of Biochemistry, Germany) was used for quantitative analysis of the log-transformed (normalised protein abundance) after label-free quantitation as performed in Progenesis QI (Waters) using default settings. The data were filtered per row for 70% of the valid values, followed by imputation of missing values and ≥ 2 identified peptides. Student's T-tests were used to make comparisons between the groups and genes satisfying a difference of $-1.5 < \log_2(\text{fold change}) > 1.5$, and FDR-corrected p-value (named q-value) < 0.05 were considered statistically significant. As part of the proteomic analysis, all the p-values were expressed as FDR-corrected p-value (q-value) unless stated otherwise. Gene Ontology enrichment among cluster enriched, differential genes, was computed and retrieved with the following ontology sources: KEGG Pathway, GO Biological Processes, Reactome Gene Sets, Canonical Pathways, and CORUM using Metascape (http://www.metascape.org)[315]. Functional protein association networks of identified proteins were created using STRING (http://www.string-db.org) and InstantClue software[316].

3.5 Human umbilical vein endothelial cell (HUVEC) culture

Four samples of primary HUVECs derived from healthy mothers were obtained from the Oxford Cardiovascular Tissue Bioresource of the umbilical-derived cell (Ethics reference: 09/H0606/68, 07/H0606/148, 15/SC/0027, 11/SC/0230). HUVECs were cultured in the same media and standard conditions as ECFCs. HUVEC functional assessments were performed using cells after the second passage. Further details of HUVEC isolation were described elsewhere[8, 317].

3.6 Primary human dermal fibroblast culture

Normal human dermal fibroblasts (Lonza, Basel, Switzerland; Lot no.: 0000520141) were cultured in fibroblast growth medium-2 (FGM™-2) supplemented with FGM™-2 SingleQuots™ supplements (Lonza, Basel, Switzerland). These cells were used as an immunofluorescence negative staining control.

3.7 Statistical analysis

Statistical analysis was performed using SPSS (version 25, IBM, North Castle, NY, USA). Shapiro-Wilk testing and visual inspection were used to assess whether variables were normally distributed. Dependent on the normality of sample distribution, comparisons between two groups were performed by either parametric independent t-test or non-parametric Mann-Whitney U test. A parametric 2-way analysis of variance (ANOVA) or non-parametric Kruskal-Wallis test was performed with a Bonferroni post hoc test for comparisons between more than two groups. $\chi 2$ or Fisher's Exact tests were used to make the comparison between categorical variables. Results are presented as mean ± standard deviation (SD) unless stated otherwise. Linear regression modelling was performed using forced entry with missing data excluded pairwise. Standardised regression coefficients (β) are presented for multivariate linear regressions. Pearson correlations (r) were used for bivariate associations with 95% confidence intervals estimated by Bootstrap analysis. P values ≤ 0.05 were considered statistically significant. When appropriate, p-values were adjusted for sex and indicated as such.

4

Characterising ECFC as an endothelial cell and a model for clinical *in-vitro* angiogenesis evaluation



4. Characterising ECFC as an endothelial cell and a model for clinical *in-vitro* angiogenesis evaluation

This chapter is based on:

"Proteomic Signature of Dysfunctional Circulating Endothelial Colony-Forming Cells of Young Adults."

By

Cheryl M J Tan, Adam J Lewandowski, Wilby Williamson, Odaro J Huckstep, Grace Z Yu, Roman Fischer, Jillian N Simon, Maryam Alsharqi, Afifah Mohamed, Paul Leeson and Mariane Bertagnolli

Journal of American Heart Association (2021); 10(15): e021119.

4.1 Abstract

Background

A subpopulation of endothelial progenitor cells called endothelial colony-forming cells (ECFCs) may offer a platform for cellular assessment in clinical studies due to their remarkable angiogenic and expansion potentials in vitro. Although EC function has been shown to be influenced by CVD risk factors and, more recently, the sex dimorphism in ECs, no studies have yet provided a comprehensive proteomic profile to distinguish functional – more angiogenic and expansive cells, versus dysfunctional circulating ECFCs derived from peripheral blood of young adults with no pre-existing CVDs and to explore the effect of sex in cellular biological functions. Therefore, this chapter aims to demonstrate the feasibility of ECFC isolation and culture, describe their endothelial, angiogenic phenotype proteomic signatures of functional and dysfunctional circulating ECFC and investigate the potential influence of sex in function and proteomic profile ECFCs.

Methods

Peripheral blood ECFCs were isolated from 11 subjects (45% male, 27±5 years old) using the Ficoll density gradient centrifugation isolation method. ECFCs were characterised via phenotypic assessment via light microscopy, cell surface biomarkers via immunofluorescence microscopy and fluorescence cell sorting, EdU proliferation assay and Matrigel *in-vitro* tube formation assay. ECFCs were deemed dysfunctional if <1 closed tube formed during the in vitro tube formation assay and proliferation rate <20%. All cells were processed and used for proteomics analysis. Metascape tools executed the Gene Ontology (GO) analysis. Cytoscape and STRING were employed to identify crucial protein-protein interactions and networks. MCODE, a plug-in of the Cytoscape software, was used for module analysis.

Results

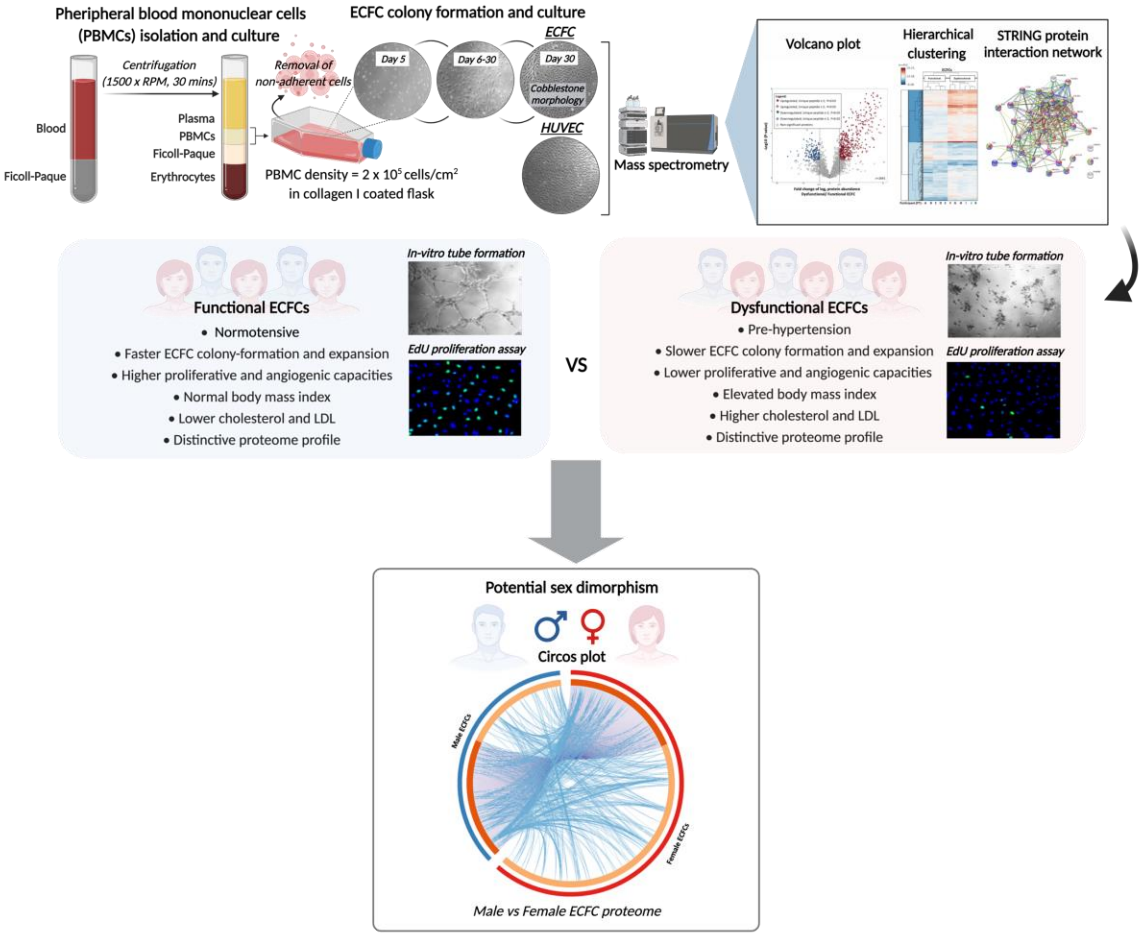
ECFCs expressed endothelial and progenitor surface markers and displayed cobblestone-patterned morphology with clonal and angiogenic capacities in vitro as observed in established ECs (human umbilical vein cells). Additionally, functional ECFCs with higher angiogenic capacity exhibit a greater proteome similarity with HUVECs than dysfunctional ECFCs. Subjects with dysfunctional circulating ECFCs have higher BP, body mass index and impaired lipid profile than subjects with functional ECFCs. Hierarchical functional clustering revealed distinct ECFC proteomic signatures between functional and dysfunctional ECFCs with changes in cellular mechanisms involved in exocytosis, vesicle transport, ECM organisation, cell metabolism and apoptosis. Targeted anti-angiogenic proteins in dysfunctional ECFCs included SPARC, CD36, LUM and PTX3. However, due to a limited study sample size, we could not observe the effect of sex in ECFC functionality and proteome profiles. Nonetheless, our investigations revealed the potential intra-sex- dimorphism in ECFC when comparing functionality. Intra-sex comparison of proteome profile of functional and dysfunctional ECFCs revealed similar enrichment in GO pathways, including ECM organisation, VEGF signalling pathway, wound healing, neutrophil degranulation, vesicle-mediated transport, negative regulation of catalytic pathway, IGF transport and uptake in both male and female. Distinct differences in GO biological pathways were identified in intra sex-specific comparison between functional and dysfunctional ECFCs in males (predominantly inflammation related pathway) and females (predominantly angiogenic pathway).

Conclusion

Circulating ECFCs with impaired angiogenesis and expansion capacities have a distinct proteomic profile and significant phenotype changes compared to highly angiogenic ECs. Dysfunctional ECFCs with a significant impairment of angiogenesis and expansion capacities may underlie the link between endothelial dysfunction and CVD risks in young adults. However, more studies are needed to validate our targeted mechanisms and investigate the potential of sex dimorphism of ECFCs in larger populations to

enhance our understanding of the physiological function of ECFCs and their potential clinical applications in CVDs.

Graphical abstract



4.2 Introduction

Strategically embedded between the tissues and blood, the vascular endothelium constitutes a highly heterogenic, complex, and dynamic structure regulating critical physiological processes such as inflammation, vasomotor responses, mechano-sensing angiogenesis, and hemostasis[1-3]. Therefore, impairment of the ECs and vascular endothelium can precede the initiation and progression of CVDs, including hypertension, leading to further endothelial dysfunction[4, 5, 10].

The human ECFCs, a subpopulation of EPCs, offer a potential platform for cellular assessment due to their remarkable angiogenic, expansion, regenerative, and self-renewable potentials *in vitro*[6, 14-20, 35]. However, the literature lacks essential information on the main mechanisms that intrinsically or extrinsically regulate angiogenesis in these cells. This is critical because clinical studies have pointed out that dysfunctional ECFCs, particularly in babies and young adults, may be related to lifelong illnesses [10, 317, 318]. Despite this, the phenotype of dysfunctional ECFCs is not well known. Likely originated in the bone marrow or from vessels and pools of progenitor cells in tissues, ECFCs can be isolated from relatively low volumes (10-25 ml) of peripheral blood[14-16, 37]. Unlike hematopoietic progenitor cells, ECFCs do not express CD45 and CD133[36]. However, ECFC expresses endothelial surface markers including PECAM-1, CD105, melanoma cell adhesion molecule (MCAM, or CD146), eNOS, VE-cadherin, in addition to progenitor cell antigens and are also characterised by the uptake of AcLDL[29, 36].

In addition, a large body of clinical and basic research has also documented sex-specific differences in endothelial dysfunction[85-91]. Studies have shown the profound influence of sex on EC functional and physiological differences, including viability, migration, proliferation, angiogenesis and shear stress response, imply sex differences in the regulation of key endothelial pathways, such as the redox system and eNOS activity[92-97]. However, no studies have yet elucidated the impact of sex on ECFC biological functions and the involvement in disease pathophysiological mechanisms[104, 105].

4.2.1 Study hypotheses, aims and clinical significance

Despite the low number of ECFCs circulating in the blood, animal and clinical studies have shown that in vitro angiogenic and expansion potential can relate to clinical characteristics, disease risk, and repair capacity[6, 10, 12, 19, 73, 78, 318-321]. However, no study has yet provided a comprehensive molecular characterisation and description of disrupted mechanisms in less angiogenic ECFCs, also classified as dysfunctional cells and the effect of sex. This knowledge is critical to justify their use in clinical investigations and to target the discovery of disease-related EC mechanisms.

Thus, this chapter seeks to compare the phenotype and proteomic signatures of functional and dysfunctional circulating ECFCs derived from peripheral blood of young adults with no pre-existing CVDs and explore the influence of sex in cellular biological functions. We hypothesised that:

1. A distinctive proteome profile and clinical characteristics are observed in individuals with dysfunctional ECFCs compared to functional ECFCs.
2. Sex dimorphism of cell function and proteome signatures in ECFCs.
3. ECFC to be a model for clinical in vitro angiogenesis evaluation.

To address the hypotheses, we aimed to:

1. *Demonstrate the feasibility of ECFC isolation and culture;*
2. *Describe their endothelial, angiogenic phenotype and proteomic signatures of functional and dysfunctional circulating ECFCs;*
3. *To investigate the influence of sex on ECFCs function and proteomic profiles.*

This chapter will enhance our biological understanding of ECFCs to facilitate the study of these cells in diseases and therapies.

4.3 Methodology

4.3.1 Study population and general methods

Participants were recruited as part of a baseline assessment visit for an Oxford Cardiovascular Clinical Research Facility study. Ethical approval was provided by the Oxford Research Ethics Committee (Ethics reference: 16/SC/0016). For this study, we included 11 young adults (five males and six females) aged between 18-35 years, body mass index (BMI) <30 kg/m2, clinical BP <159 mmHg systolic and/or 99 mmHg diastolic BP without any clinical diagnosis of CVDs and medications. All participants provided written consent for the collection and subsequent experimental use of samples under appropriate ethical approvals.Details of the study are outlined in **Chapter 2 – Study population, Section 4.1.**

The following methods that were used for this chapter are described in detail in **Chapter 3**:

3.1 Anthropometric measurements

3.2 BP measurements

3.3 Blood sample collection and biochemistry analysis

3.4 ECFC isolation and cellular assessments

- 3.4.1 Fluorescence-activated cell sorting (FACS)
- 3.4.2 Immunofluorescence staining
- 3.4.3 EdU proliferation assay
- 3.4.4 In vitro tube formation assay
- 3.4.5 Proteomic analysis of ECFCs

3.5 Human umbilical vein endothelial cell (HUVEC) culture

3.6 Primary human dermal fibroblast culture

4.3.2 ECFC functionality classification

Cellular proliferation and angiogenic capacity were assessed to classify the functionality of ECFCs. Specifically, ECFCs with less than one closed tube formed on Matrigel and less than 20% proliferation rate was deemed dysfunctional[10]. The 20% proliferation cutoff was established based on the capacity of ECFCs to sufficiently expand in culture to form cobblestone-shaped colonies after the first or second passages and reach at least 30% confluence[10]. As a result, both functional, phenotype and proteomic tests were performed using cells obtained from no more than two passages after PBMC culture.

4.3.3 Enriched ontology clustering

The proteomic data were filtered per row for 70% of the valid values, followed by imputation of missing values and ≥ 2 identified peptides. Student's T-tests were used to make comparisons between the groups and genes satisfying a difference of $-1.5 < \log_2(\text{fold change}) > 1.5$, and FDR-corrected p-value ((named q-value) were calculated using the Benjamini-Hochberg procedure to account for multiple testing) <0.05 were considered statistically significant. Statistically significant proteins were used to identify all statistically enriched GO/KEGG terms and network reconstruction using the Metascape tool (http:// metascape.org). Imputing the gene set obtained from statistical significant proteins, pathway and enrichment analyses were carried out selecting the genomics sources: KEGG Pathway, GO Biological Processes, Reactome Gene Sets, Canonical Pathways, and CORUM[322].

The remaining significant terms were then hierarchically clustered into a tree network layout based on Kappa-statistical similarities (using a 0.3 kappa score threshold to cast the tree into term clusters) among their gene memberships. More specifically, each term was represented by a circle node, where its size was proportional to the number of input genes that fell into that term, and its colour represented its cluster. Terms with a similarity score > 0.3 were linked by an edge (the thickness of the

edge represents the similarity score). The network was visualised with Cytoscape (v3.1.2) with a "force-directed" layout and with edge bundled for clarity[323].

4.3.4 Molecular Complex Detection (MCODE) network analysis

Subsequently, using Metascape default parameters, based on Protein-protein interaction (PPI) enrichment analysis, we ran a module network reconstruction based on the selected genomics databases. The resulting network was constructed containing the subset of proteins that form physical interactions with at least one other list member. Subsequently, utilising Molecular Complex Detection (MCODE) algorithm, we first identified densely connected network components. A pathway and process enrichment analysis was applied to each MCODE component independently, and the five best-scoring (by p-value) terms were retained as the functional description of the resulting modules. Each MCODE network was assigned a unique colour. GO enrichment analysis was applied to each MCODE network to assign representative GO pathways to the network component using Metascape[315].

4.3.5 Principal component analysis

The logarithm values of protein expression were submitted to principal component analysis (PCA) and in the R-package "FactoMineR" and "FactoExtra" with the generation of graphical output. Analysis was completed with the help of DPhil student Daan Paget.

4.3.6 Statistical analysis

All statistical analyses were performed using SPSS version 25 (IBM, North Castle, NY, USA). Shapiro-Wilk normality test was used to assess the normality of variables. Dependent on the normality of sample distribution, comparisons between two groups were performed by either parametric independent

t-test or non-parametric Mann-Whitney U test. The Kruskal-Wallis test was performed with the Bonferroni post hoc test to compare HUVEC, both ECFC groups (functional and dysfunctional) and sexes. Categorical variables were compared by $\chi 2$ or Fisher Exact tests. Results are presented as mean ± standard deviation (SD) unless stated otherwise. Pearson correlations (r) were used for bivariate associations. P values ≤ 0.05 were considered statistically significant.

4.4 Results

4.4.1 ECFC phenotype

ECFCs were isolated from the peripheral blood of 11 participants. FACS analysis confirmed that >99% of the ECFCs were negatively stained for hematopoietic biomarkers CD45, CD133 and positively stained for the endothelial biomarkers PECAM-1 and VEGFR-2 **(Figure 4.1 a-f)**. These findings were further confirmed by immunofluorescence staining of ECFCs, HUVECs (an EC positive control) and human dermal fibroblast (negative control) against common endothelial surface biomarkers including VEGFR-2, VE-Cadherin, eNOS, PECAM-1, Ulex Europaeus Agglutinin-1 (UEA-1) and AcLDL up-take **(Figure 4.2 a-k)**. ECFCs also stained positive for progenitor biomarker CD34. Phase-contrast images also showed that ECFCs and HUVECs similarly exhibited cobblestone-patterned endothelial-like morphology.

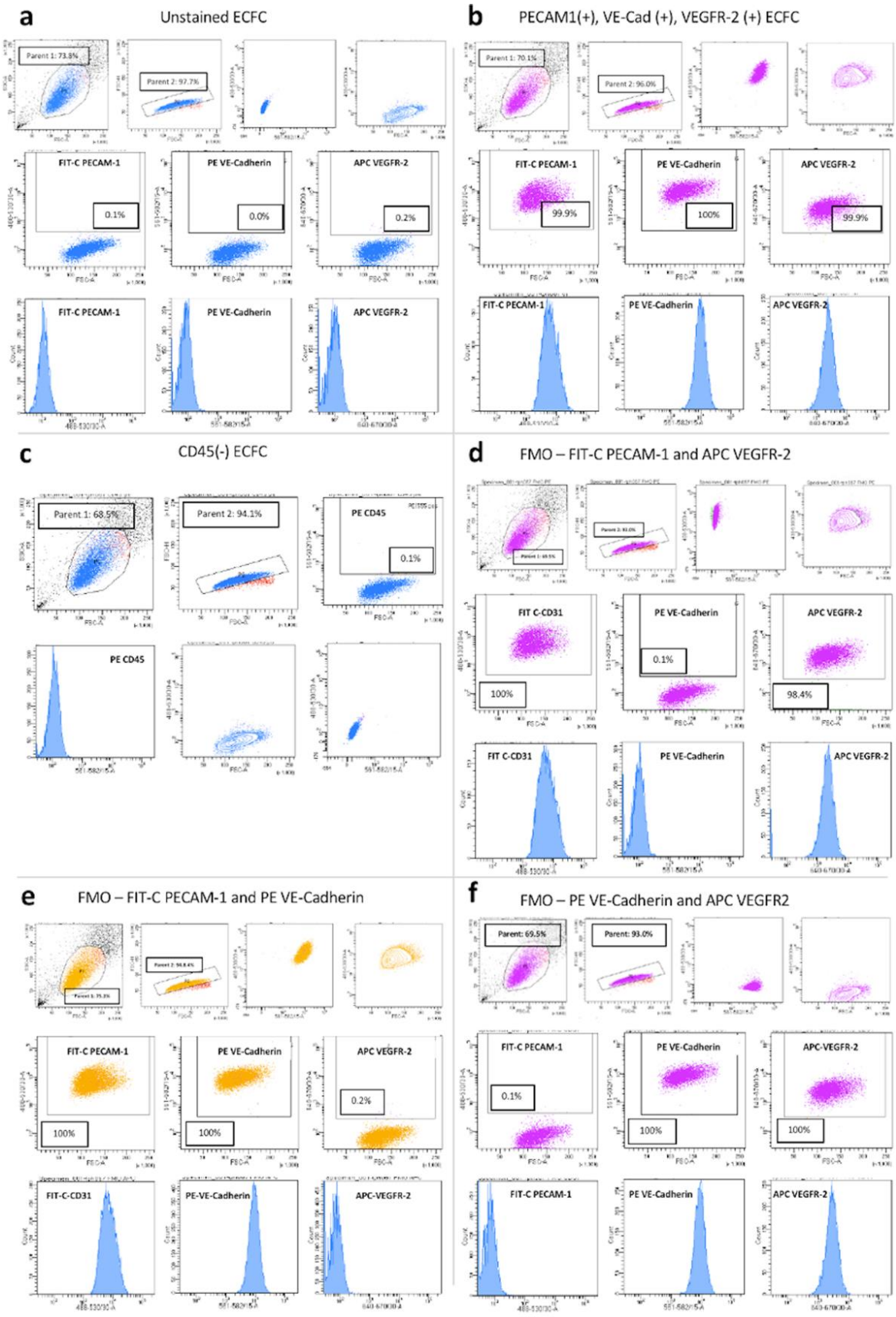
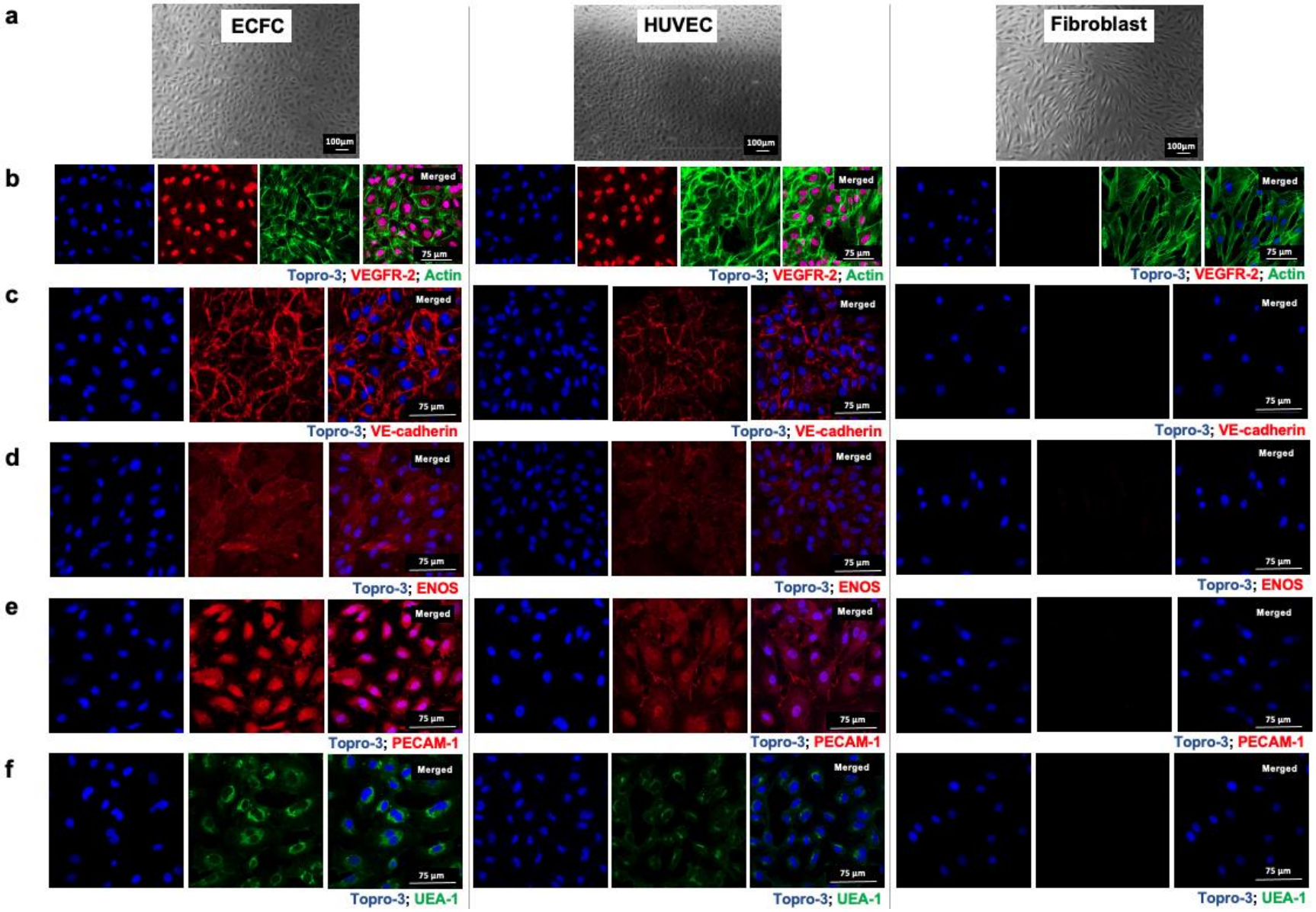

a
Unstained ECFC
Parent 1: 73.8%
Parent 2: 97.7%
FIT-C PECAM-1
PE VE-Cadherin
APC VEGFR-2
0.1%
0.0%
0.2%
b
PECAM1(+), VE-Cad (+), VEGFR-2 (+) ECFC
Parent 1: 70.1%
Parent 2: 96.0%
99.9%
100%
99.9%
c
CD45(-) ECFC
Parent 1: 68.5%
Parent 2: 94.1%
PE CD45
0.1%
d
FMO – FIT-C PECAM-1 and APC VEGFR-2
FIT C-CD31
PE VE-Cadherin
APC VEGFR-2
100%
0.1%
98.4%
e
FMO – FIT-C PECAM-1 and PE VE-Cadherin
100%
100%
0.2%
f
FMO – PE VE-Cadherin and APC VEGFR2
Parent: 69.5%
Parent: 93.0%
0.1%
100%
100%

Figure 4.1. Fluorescence-activated cell sorting (FACS) of endothelial colony-forming cells (ECFCs) represented in dot plots and histograms.

(a) Unstained ECFCs. **(b)** Cells were stained with EC surface biomarkers, including FITC-PECAM-1, PE-VE-Cadherin, APC-VEGFR-2, and **(c)** with a hematopoietic cell lineage surface marker PE-CD45. FACS immunophenotype showed that ECFC expressed PECAM-1, VE-Cadherin, VEGFR-2 but were negative for CD45. The overall percentage is based on *Parent 2*. Fluorescence minus one control (FMO) for ECFCs is represented in dot plots and histograms. Cells were stained with **(d)** FIT-C PECAM-1 and APC VEGFR-2; **(e)** FIT-C PECAM-1 and PE VE-Cadherin; and **(f)** PE VE-Cadherin and APC-VEGFR-2.


a
ECFC
HUVEC
Fibroblast
100μm
b
Merged
75 μm
Topro-3; VEGFR-2; Actin
c
Topro-3; VE-cadherin
d
Topro-3; ENOS
e
Topro-3; PECAM-1
f
Topro-3; UEA-1

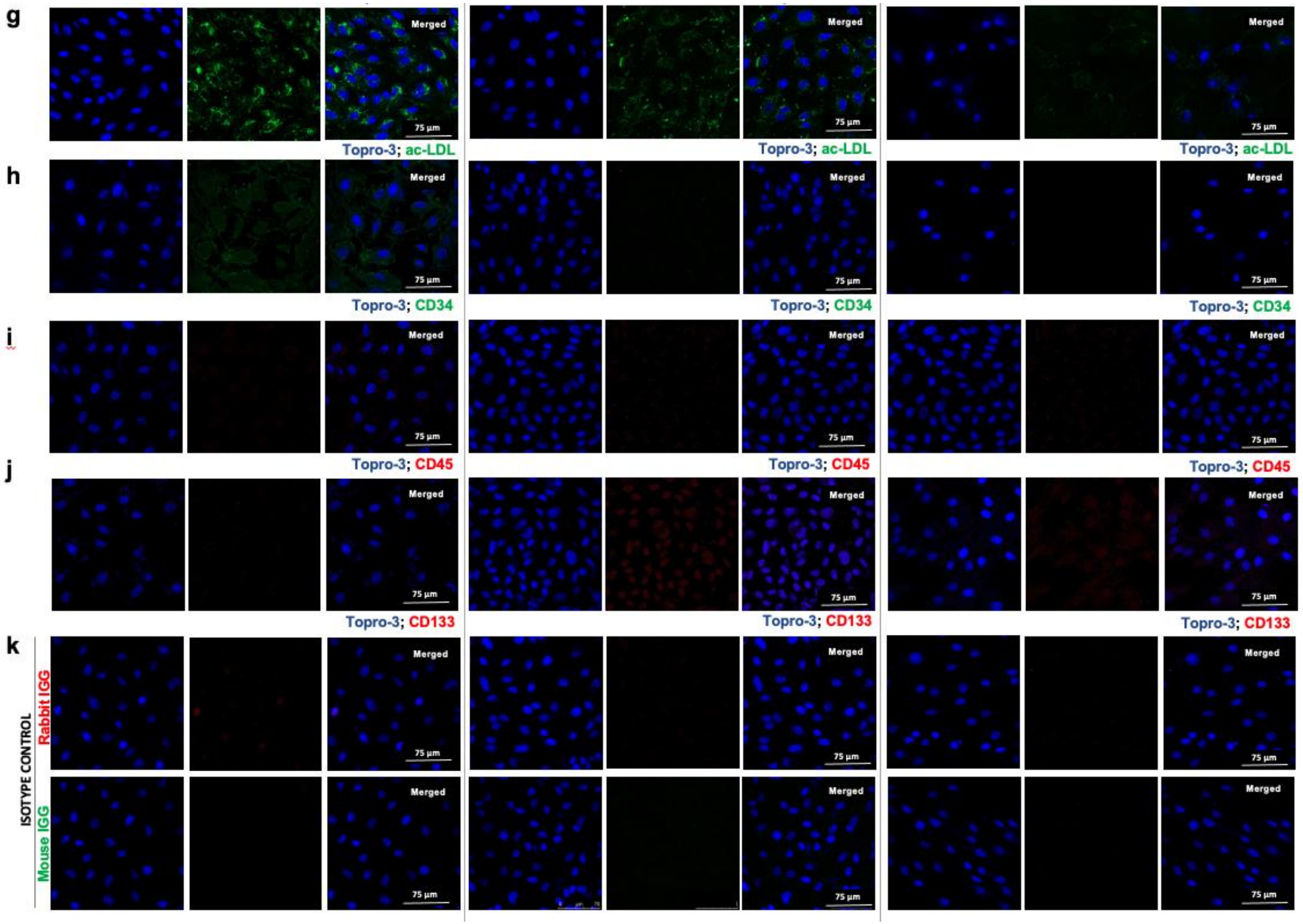

g
Merged
75 µm
Topro-3; ac-LDL
h
Topro-3; CD34
i
Topro-3; CD45
j
Topro-3; CD133
k
ISOTYPE CONTROL
Rabbit IGG
Mouse IGG

Figure 4.2. Endothelial colony-forming cells (ECFCs) phenotype compared to human umbilical vein endothelial cells (HUVECs) and dermal fibroblasts and their respective isotype controls.

HUVECs and fibroblasts served as positive and negative controls. Light microscope images of ECFCs, HUVECs and fibroblasts were obtained using a Nikon light microscope. All cells were stained with surface biomarkers including **(a)** vascular endothelial growth factor receptor 2 (VEGFR-2; AlexaFluor 555, red) and actin (AlexaFluor 488, green); **(b)** VE-Cadherin (AlexaFluor 555, red); **(c)** endothelial nitric oxide synthase (eNOS; AlexaFluor 555, red); **(d)** PECAM-1 (AlexaFluor 555, red); **(e)** Ulex Europaeus-1 (UEA-1) lectin (AlexaFluor 488, green); **(f)** acetylated low density lipoprotein up-take (ac-LDL; AlexaFluor 488, green); **(g)** progenitor cell surface marker CD34 (AlexaFluor 488, green); **(i)** hematopoietic biomarker CD45 (AlexaFluor 555, red) **(j)** CD133 (AlexaFluor 555), red. Nuclei were stained with Topro-3 iodide (blue) in confocal microscope magnification: x63. Immunoglobulin isotype controls, including **(k)** rabbit IGG (green) and mouse IGG control (red), were stained negative on all the cells.

4.4.2 Functional and dysfunctional ECFCs

The comparison of ECFC functional characteristics revealed that, in subjects with dysfunctional ECFCs, the number of days for ECFC colony formation was longer (20.3±3.0 versus 13.2±1.9 days, P<0.001), the proliferation rate was lower (7.2±8.2 versus 40.3±10 %, P<0.001), and the angiogenic capacity was reduced as indicated by the number of tube branching (5.4±3.3 versus 32.3±9.9 branches, P<0.001) and the number of closed tubes formed *in vitro* (0 versus 16.2±6.8 closed tubes, P<0.001) **(Figure 4.3 a-f**). When comparing ECFCs to HUVECs, we found that functional ECFCs displayed a similar proliferation rate to HUVECs (40.3 ± 10.0% versus 49.3±7.8%, respectively), although they had lower angiogenic capacity demonstrated by reduced branching (32.3±9.9 versus 54.3±8.0 branches, P<0.001) and the number of closed tubes (16.2±6.8, 21.0±6.4 closed tubes, P<0.001) **(Figure 4.3 d-f**).

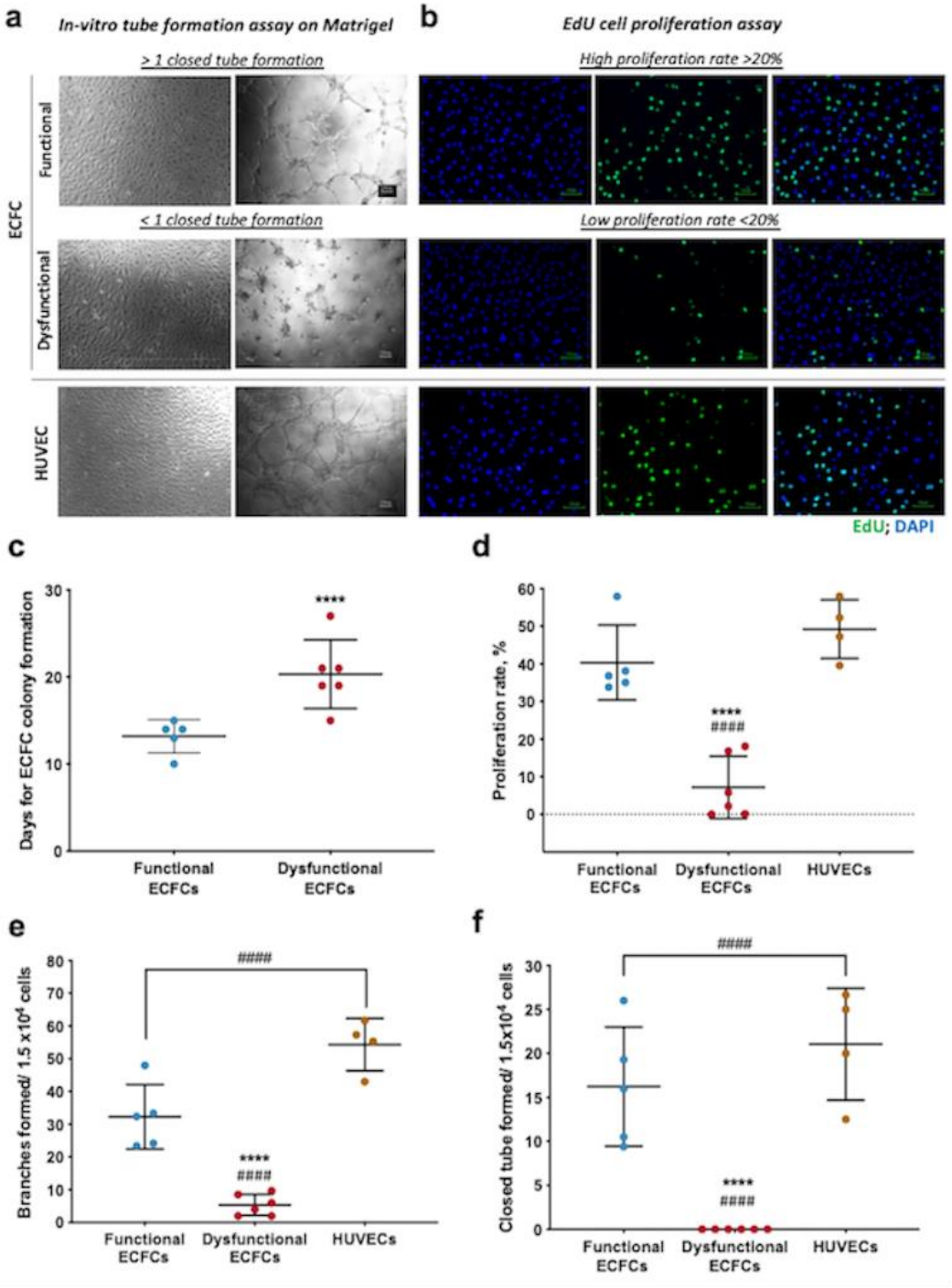


Figure 4.3. Endothelial colony-forming cells (ECFCs) functionality.

(a) ECFC (functional and dysfunctional) and human umbilical vein endothelial cells (HUVECs) (positive endothelial control) tube formation capacity were assessed using Matrigel tube formation assay with the numbers of total branches and closed tubes formed quantified in phase-contrast images (5x objective).

ECFCs with less than 1 closed tube formed were considered to be dysfunctional, as depicted in the phase-contrast images. **(b)** Proliferation rate was determined by DNA Edu incorporation (AlexaFluor 488, green), with nuclei counterstained with 4',6-diamidino-2-phenylindole (DAPI, blue) (10x objective). Dysfunctional and functional cells were determined with a proliferation rate (% - Edu-stained cells/DAPI stained x 100) of below 20% and above 20% respectively. Scatter plots representing respective ECFC clusters and HUVECs for each of the following cell characteristics: **(c)** days for ECFC colony formation, **(d)** proliferation rate (%), **(e)** total branching formed per $1.5x10^4$ cells, and **(f)** total closed tubes formed per $1.5x10^4$ cells. Functional ECFCs (n=5), dysfunctional ECFCs (n=6) and HUVECs (n=4). ****P<0.0001 versus cluster 1; ### P<0.001 and ####P<0.0001 versus HUVECs. Mann-Whitney U test (panel c) or Kruskal-Wallis test with Bonferroni post hoc test (panels d, e, f).

A comparative proteomic analysis between overall ECFCs with HUVECs further confirmed a very similar proteomic profile between these two types of ECs. Hierarchical clustering comparing ECFCs and HUVECs revealed that functional ECFCs exhibited a greater proteome similarity with HUVECs, (99.1±0.16% matched pairs, Pearson correlation = 0.77±0.07, R2 = 0.59±0.11) than dysfunctional ECFCs (96.9±1.27% matched pairs, Pearson correlation = 0.54±0.04, R2 = 0.30±0.04) **(Figure 4.4).**

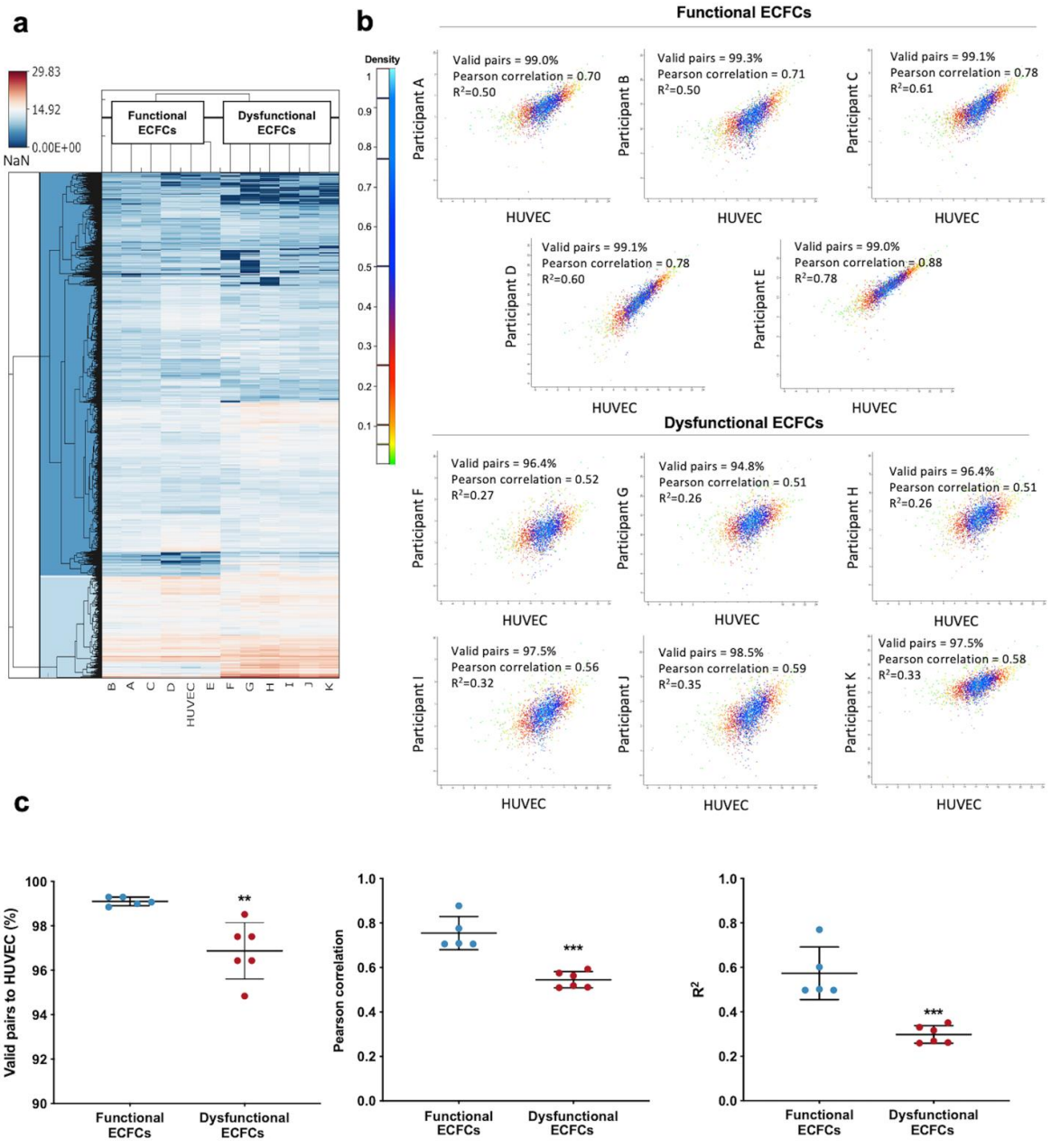


Figure 4.4. Proteomic comparisons and hierarchical clustering of endothelial colony-forming cells (ECFCs) versus human umbilical vein endothelial cells (HUVECs).

(a) A total of 2691 proteins were expressed among two distinct ECFC functional clusters. Results are represented as a heatmap displaying protein expression levels on a logarithmic scale. Red indicates high expression, while dark blue indicates low or no expression. **(b)** Scatter plots of normalised protein abundance in ECFCs against HUVECs. **(c)** Scattergram of % of valid matched protein pairs between ECFCs and HUVECs. Functional ECFCs displayed highly similar protein expression (%) compared to HUVECs (99.1±0.16%, Pearson correlation = 0.77±0.07, R2 = 0.59±0.11) while dysfunctional ECFCs had lower

degree of similarity and correlation to HUVECs (96.9±1.27%, Pearson correlation = 0.54±0.04, R2 = 0.30±0.04). Mean±SD; **P<0.01, ***P<0.001.

4.4.3 Clinical characteristics of subjects with functional and dysfunctional ECFCs

The clinical characteristics of the 11 participants are presented in **Table 4.1**. No differences were observed for male/female numbers, age, height, and weight between functional versus dysfunctional ECFC groups. However, systolic, and mean BPs, as well as BMI, were significantly higher in subjects with dysfunctional ECFCs. Diastolic BP and heart rate were similar between the groups **(Table 4.1)**. In addition, differences in blood lipid profile were observed with higher total cholesterol and low-density lipoprotein in subjects with dysfunctional ECFCs compared to subjects with functional ECFCs, with no significant differences observed for triglycerides, high-density lipoprotein, glucose, insulin, Homeostasis Model Assessment (HOMA) β-cell, HOMA β-cell sensitivity and HOMA insulin resistance between groups **(Table 4.1)**.

Table 4.1. Clinical characteristics of the study participants.

Clinical characteristics	Total (n=11)	Functional ECFC (n=5)	Dysfunctional ECFC (n=6)	P-Value
Male, n (%)	5 (45%)	2 (40%)	3 (50%)	>0.99
Age, years	26.55 ± 4.63	24.8 ± 1.64	28.0 ± 5.93	0.245
Height, cm	171.63 ± 8.72	173.8 ± 10.71	169.83 ± 7.19	0.482
Weight, kg	70.9 ± 11.89	63.96 ± 7.84	76.68 ± 12.05	0.074
BMI, kg/m^2	24.12 ± 4.07	21.16 ± 1.81	26.56 ± 3.79	0.016*
Systolic BP, mmHg	130.4 ± 13.75	122.0 ± 8.6	137.3 ± 13.81	0.050*
Diastolic BP, mmHg	84.0 ± 11.97	77.2 ± 14.4	89.67 ± 6.62	0.089
Mean arterial pressure, mmHg	101.55 ± 12.82	93.6 ± 11.8	108.17 ± 10.83	0.032*
Heart rate, beats per min	73.18 ± 10.51	72.8 ± 10.83	73.5 ± 11.26	0.789
Blood biochemistry	**Total (n=11)**	**Functional ECFC (n=5)**	**Dysfunctional ECFC (n=6)**	**P-Value**
Triglyceride, mmol/l	1.13 ± 0.8	0.86 ± 0.3	1.36 ± 1.04	0.328
Cholesterol, mmol/l	4.85 ± 0.78	4.21 ± 0.64	5.38 ± 0.38	0.004*
High density lipoprotein, mmol/l	1.39 ± 0.26	1.41 ± 0.21	1.38 ± 0.32	0.838
Low density lipoprotein, mmol/l	2.63 ± 0.76	2.1 ± 0.53	3.17 ± 0.66	0.027*
Glucose, mmol/l	4.89 ± 0.41	4.78 ± 0.32	4.99 ± 0.49	0.433
Insulin, pmol/l	49.81 ± 14.05	45.94 ± 10.42	53.03 ± 16.74	0.433
HOMA β-cell function, %	96.41 ± 24.31	95.36 ± 19.31	97.28 ± 29.7	0.904
HOMA insulin sensitivity, %	116.36 ± 33.44	123.12 ± 31.32	110.73 ± 36.99	0.569
HOMA IR (insulin resistance)	0.92 ± 0.26	0.85 ± 0.19	0.99 ± 0.31	0.37

Data are expressed as mean ± standard deviation (SD). *P<0.05 between functional clusters. Independent t-test or χ^2 -test.

4.4.4 Proteomic analysis of functional and dysfunctional ECFCs

Proteomic comparison of ECFCs further identified 2691 proteins with 519 differentially expressed proteins between functional and dysfunctional clusters with unique peptides ≥ 2 and either $\log_2$(fold change) ≥ 1.5 or ≤ -1.5 (388 upregulated and 131 downregulated proteins) **(Figure 4.5 a and b)**. The analysis of gene ontology revealed the top 10 enriched pathways being the following: regulated exocytosis, vesicle-mediated transport, metabolism of RNA, wound healing, ECM organisation, generation of precursor metabolites and energy, post-translational protein modification, apoptosis, regulation of peptidase activity and regulation of cellular protein localisation **(Figure 4.5 c and Supplementary Figure S4.1)**.

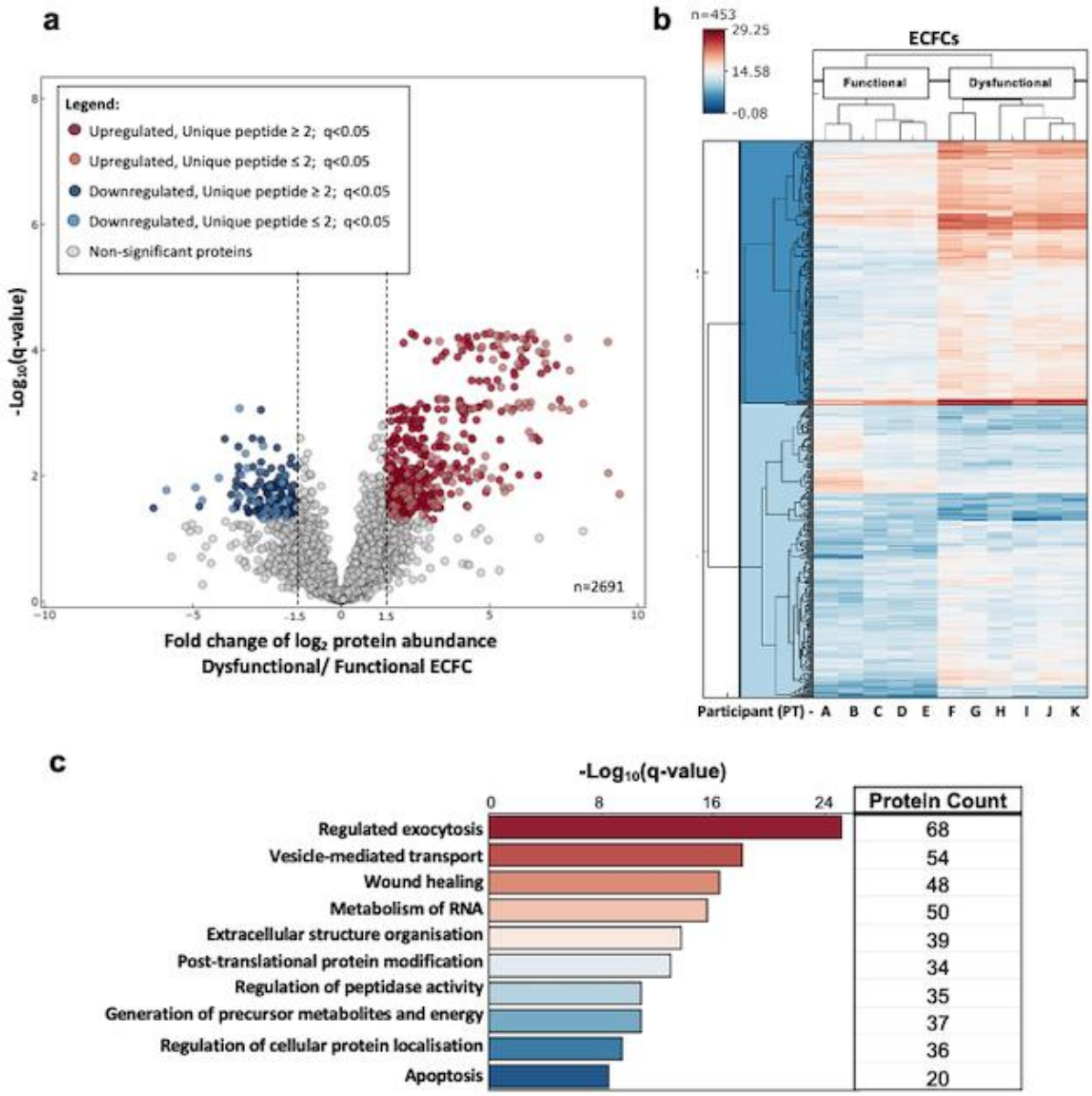
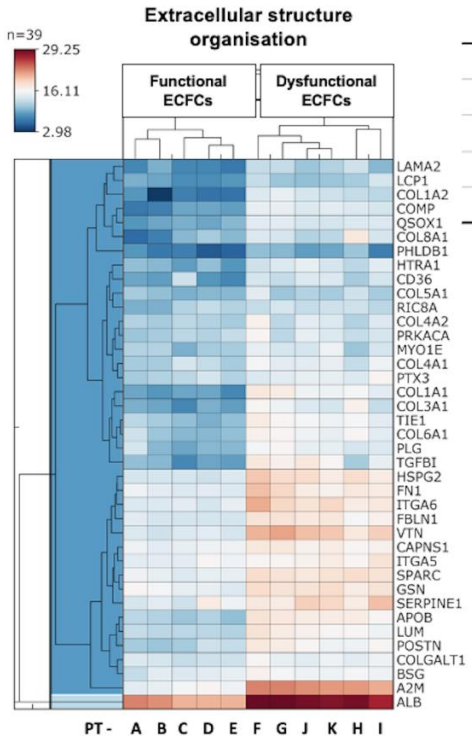


Figure 4.5. Proteomics analysis of functional and dysfunctional endothelial colony-forming cells (ECFCs).

(a) Volcano plot shows significantly regulated proteins between dysfunctional and functional ECFCs, after Student's t-test and FDR correction for multiple testing. A total of 2,691 proteins were quantified, with 453 proteins demonstrating significant differential abundance between the compared conditions based on proteins with unique peptides ≥ 2 and $\log_2$(fold change) ≥ 1.5 or ≤ -1.5 (357 upregulated and 96 downregulated proteins). **(b)** Unsupervised hierarchical clustering (Euclidean distance) distinguishes samples according to their group and shows distinct protein abundance profiles indicative of grouping. **(c)** Significantly changed proteins show enrichment gene ontology biological pathways. Protein count represents the number of proteins involved in the respective biological pathway.

Detailed proteomic investigation of the impaired functionality in dysfunctional ECFCs revealed significant differences in 42 proteins involved in the extracellular structural organisation **(Figure 4.6 a and b**). Four proteins of interest have been identified within the identified enriched gene ontology pathway. These proteins include Secreted Protein Acidic and Cysteine Rich (SPARC), also known as osteonectin (OSN), pentraxin-related protein PYX3 (PTX3), Lumican (LUM), and CD36 **(Table 4.2)**. However, after adjusting for BMI and systolic BP, only SPARC and LUM remained significantly different between functional and dysfunctional ECFCs **(Table 4.2)**.

a



b

Functional enrichments in the String network

Enriched gene ontology pathway	Count	False discovery rate	Legend
Cellular component organisation	34	8.1E-13	
Response to stimulus	33	5.4E-07	
Extracellular structure organisation	31	8.7E-44	
Vasculature development	16	3.3E-13	
Cell adhesion	14	2.8E-08	

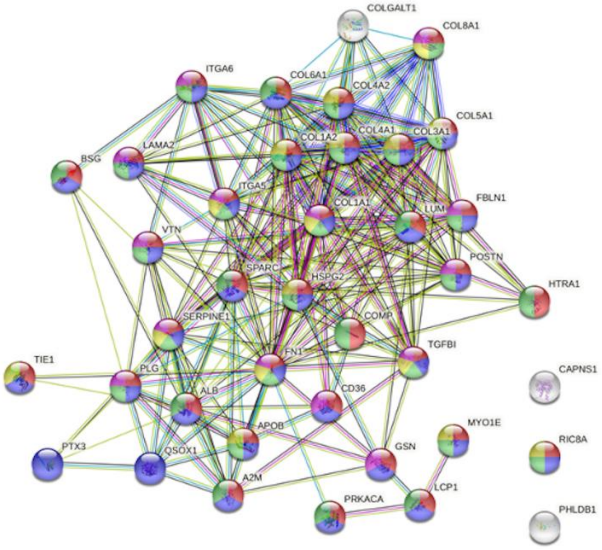


Figure 4.6. Proteins identified in enriched gene ontology pathway - extracellular structure organisation that differently expressed between functional clusters of endothelial colony-forming cells (ECFCs).

(a) Heatmap of proteins involved in the extracellular structure organisation biological pathway. Results are represented as a heatmap displaying protein expression levels on a logarithmic scale. Red indicates high expression, while dark blue indicates low or no expression. **(b)** String™ interactive pathway analysis of proteins involved in extracellular structure organization (n=39).

Table 4.2. Identified proteins of interest from the extracellular structure organisation (GO pathway).

Proteins of interest	Functional description	ECFCs log_2protein expression ± SD	Dysfunctional ECFCs log_2protein expression ± SD	Dysfunctional/ Functional log_2protein expression fold change	Unique peptide count	$-Log_{10}$P-value*	P-Value*^
Secreted protein acidic and cysteine rich (SPARC)	Anti-angiogenesis; anti-proliferation; anti-adhesion; regulates EC migration, VEGFR signalling, ECM structural constituent, remodelling, collagen and calcium binding	15.0±0.5	18.2±0.5	3.21	12	6.14	0.0003
Pentraxin-related protein PTX3 (PTX3)	Anti-angiogenesis; inhibits vascular regeneration; regulates ECM remodelling, inflammation, nitric oxide biosynthesis and phagocytosis	12.3.5±0.9	14.9±0.7	2.64	8	3.34	0.065
Lumican (LUM)	Anti-angiogenesis; ECM organisation, keratan sulfate biosynthesis and catabolic processes; RNA transcription; and regulation of transforming-growth factor-β1 production	12.4±0.4	16.8±0.8	4.38	3	5.65	<0.0001
CD36	Anti-angiogenesis, regulates cell adhesion, inflammatory response, fatty acid metabolism, cholesterol metabolism and platelet degranulation	9.6±2.2	13.3±1.1	3.7	2	2.25	0.13

*Independent T-test comparison after correction for False Discovery Rate (FDR) by applying the Benjamini and Hochberg algorithm. #Independent t-test. ^P-value corrected for BMI and SBP.

4.4.4.1 Principal component analysis (PCA) of proteomic data

We applied PCA tools to further evaluate the proteome profile with the functionality of the cells. The analyses confirmed the difference in protein profiles of individuals with functional and dysfunctional ECFCs **(Figure 4.7)**. The contribution of variables to the principal component 1 to 3 is highlighted in **Supplementary Figure S4.2**.

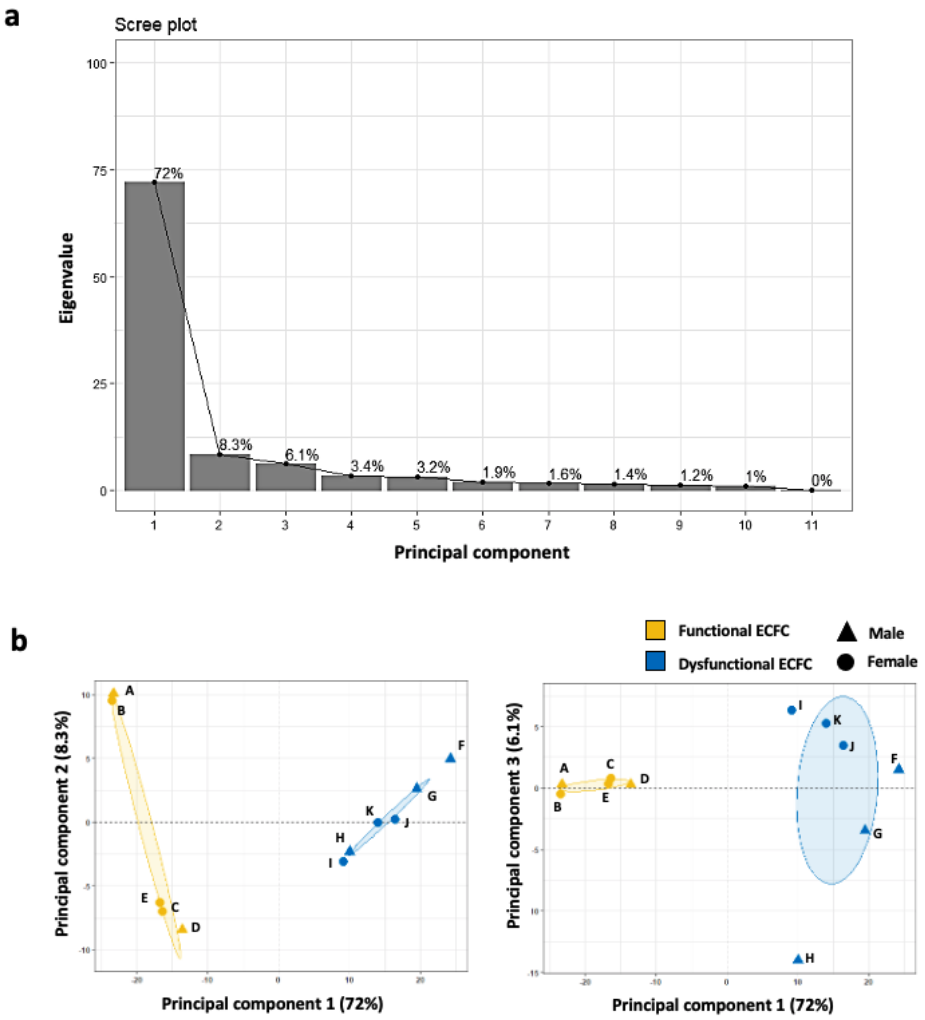


Figure 4.7. Principal component analysis (PCA) of functional and dysfunctional endothelial colony-forming cells (ECFCs).

(a) Scree plots showing the eigenvalue (%) of all the principal components for the analysis. **(b)** The PCA plot represents 11 participants that indicated clear proteomics profile differences between functional and

dysfunctional ECFC are represented in yellow and blue colours respectively and sex are represented in matching symbols (male – triangle and female – circle).

4.4.5 Sexual dimorphism in ECFC

4.4.5.1 Male vs Female ECFCs

No significant differences were observed in the ECFC and clinical characteristics apart from glucose levels (5.17 ± 0.35 mmol/l vs 4.66±0.33 mmol/l; male vs female) **(Table 4.3)**.

Table 4.3. Clinical characteristics of the study participants based on sex.

Clinical characteristics	Total (n=11)	Male (n=5)	Female (n=6)	P-Value*
Age, years	26.55 ± 1.4	26.6 ± 5.5	26.5 ± 4.32	0.974
Height, cm	171.64 ± 2.63	178.6 ± 6.11	165.83 ± 5.78	0.006*
Weight, kg	70.9 ± 3.58	76.8 ± 12.08	65.98 ± 10.1	0.139
BMI, kg/m^2	24.12 ± 1.23	24.18 ± 4.4	24.07 ± 4.19	0.967
Systolic BP, mmHg	129.91 ± 4.21	124.6 ± 8.5	134.33 ± 16.73	0.271
Diastolic BP, mmHg	83.64 ± 3.63	79.4 ± 13.39	87.17 ± 10.63	0.310
Mean arterial pressure, mmHg	101.55 ± 3.86	97.2 ± 10.85	105.17 ± 14.13	0.330
Heart rate, beats per min	73.18 ± 3.17	76 ± 13.11	70.83 ± 8.28	0.446
Blood biochemistry	**Total (n=11)**	**Male (n=5)**	**Female (n=6)**	**P-Value***
Triglyceride, mmol/l	1.13 ± 0.24	1.41 ± 1.12	0.9 ± 0.37	0.317
Cholesterol, mmol/l	4.85 ± 0.24	4.89 ± 0.46	4.82 ± 1.03	0.883
High density lipoprotein, mmol/l	1.39 ± 0.08	1.33 ± 0.35	1.44 ± 0.18	0.530
Low density lipoprotein, mmol/l	2.63 ± 0.23	2.5 ± 0.66	2.73 ± 0.89	0.640
Glucose, mmol/l	4.89 ± 0.12	5.17 ± 0.35	4.66 ± 0.33	0.034*
Insulin, pmol/l	49.81 ± 4.23	45.8 ± 13.18	53.15 ± 15.04	0.416
HOMA β-cell function, %	96.41 ± 7.33	81.94 ± 23.25	108.47 ± 19.13	0.067
HOMA insulin sensitivity, %	116.36 ± 10.08	122.94 ± 32.37	110.88 ± 36.32	0.579
HOMA IR (insulin resistance)	0.92 ± 0.26	0.86 ± 0.24	0.98 ± 0.29	0.494
ECFC characteristics	**Total (n=11)**	**Male (n=5)**	**Female (n=6)**	**P-Value***
Days for ECFC colony formation	17.09 ± 1.45	18 ± 6.24	16.33 ± 3.67	0.594
Proliferation rate (%)	22.25 ± 5.83	23.72 ± 23.76	21.03 ± 17.1	0.832
Closed tube formed, n per 1.5x10^4	7.38 ± 2.87	5.96 ± 8.73	8.57 ± 10.77	0.674
Branches formed, n per 1.5x10^4	17.61 ± 4.69	14.4 ± 13.69	20.28 ± 17.76	0.561

Homeostatic model assessment (HOMA); endothelial colony-forming cell (ECFC). Data are expressed as mean ± standard deviation (SD). *P<0.05 between functional clusters. Independent t-test.

To explore the protein intensities difference between sex, 2-sided t-test were performed on the proteomic data. It showed that no significant protein with unique peptides ≥ 2 and $\log_2$(fold change) ≥ 1.5 or ≤ -1.5, and P<0.05 were identified when comparing between the male and female participants **(Figure 4.8)**.

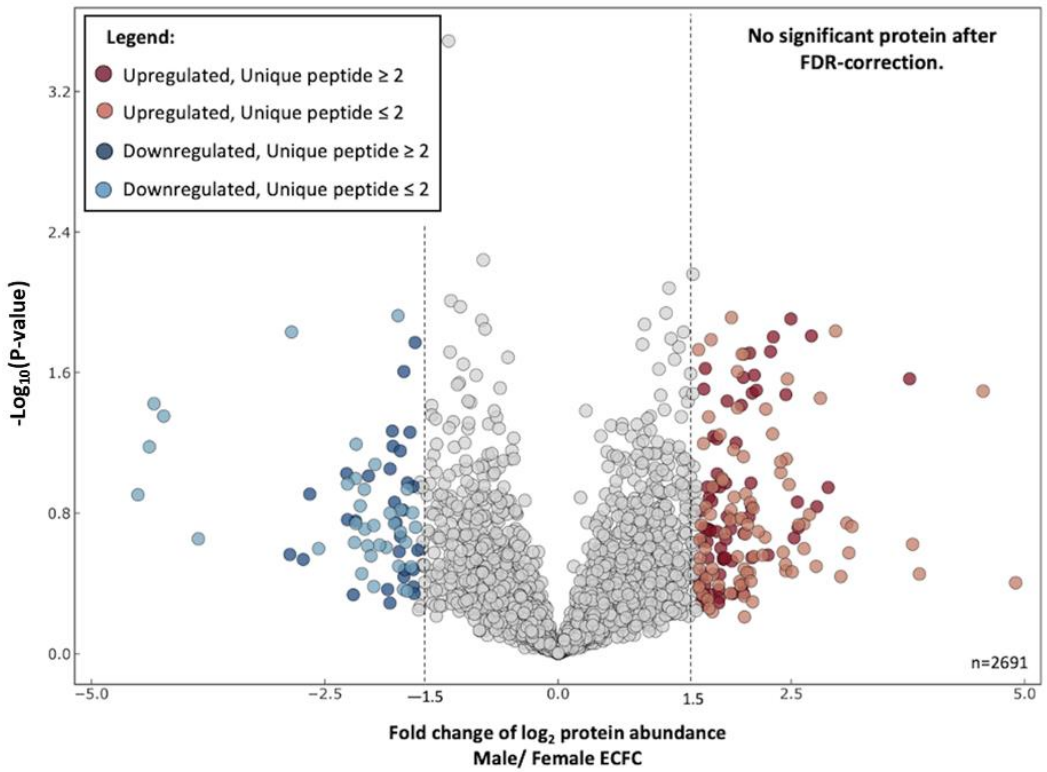


Figure 4.8. Protein intensities were analysed by 2-sided t-test.

Results are represented as a volcano plot. Student T-test was used to analyse the data and P-values were False Discovery Rate (FDR)-adjusted. No significant proteins identified (proteins with unique peptides ≥ 2 and $\log_2$(fold change) ≥ 1.5 or ≤ -1.5, and P<0.05 were considered statistically significant).

4.4.5.2 Intra-sex proteome differences observed in same-sex individuals with different cell functionality

Following this, we investigated the intra-sex differences between individuals with different cell functionality. In ECFC isolated from males, no significant differences in clinical characteristics were observed in the comparison between functional and dysfunctional ECFCs except for height (184.5±3.54cm

vs 174.67±3.21cm, P<0.048) **(Supplemetary Table S4.1)**. Whereas, females with dysfunctional ECFCs presented significantly higher cholesterol levels compared to females with functional ECFCs (5.72±0.1mmol/l vs 3.92±0.43mmol/l, P<0.002) **(Supplementary Table S4.2)**.

A comparison of the proteomic profile was made to assess the effect of the functionality of ECFCs within each sex. Over 231 proteins were identified with 204 downregulated and 27 upregulated proteins in male functional vs dysfunctional ECFCs **(Figure 4.9 a and b)**. The top enriched gene ontology pathways included platelet degranulation, wound healing, neutrophil degranulation, ECM organisation and VEGF signalling pathway **(Figure 4.9 c)**. Similarly, a comparison between functional and dysfunctional female ECFCs identified over 399 proteins (309 downregulated and 90 upregulated proteins) and revealed comparable enriched GO pathways, including VEGF signalling, ECM organisation, and metabolism of RNA and wound healing **(Figure 4.9 d-f).**

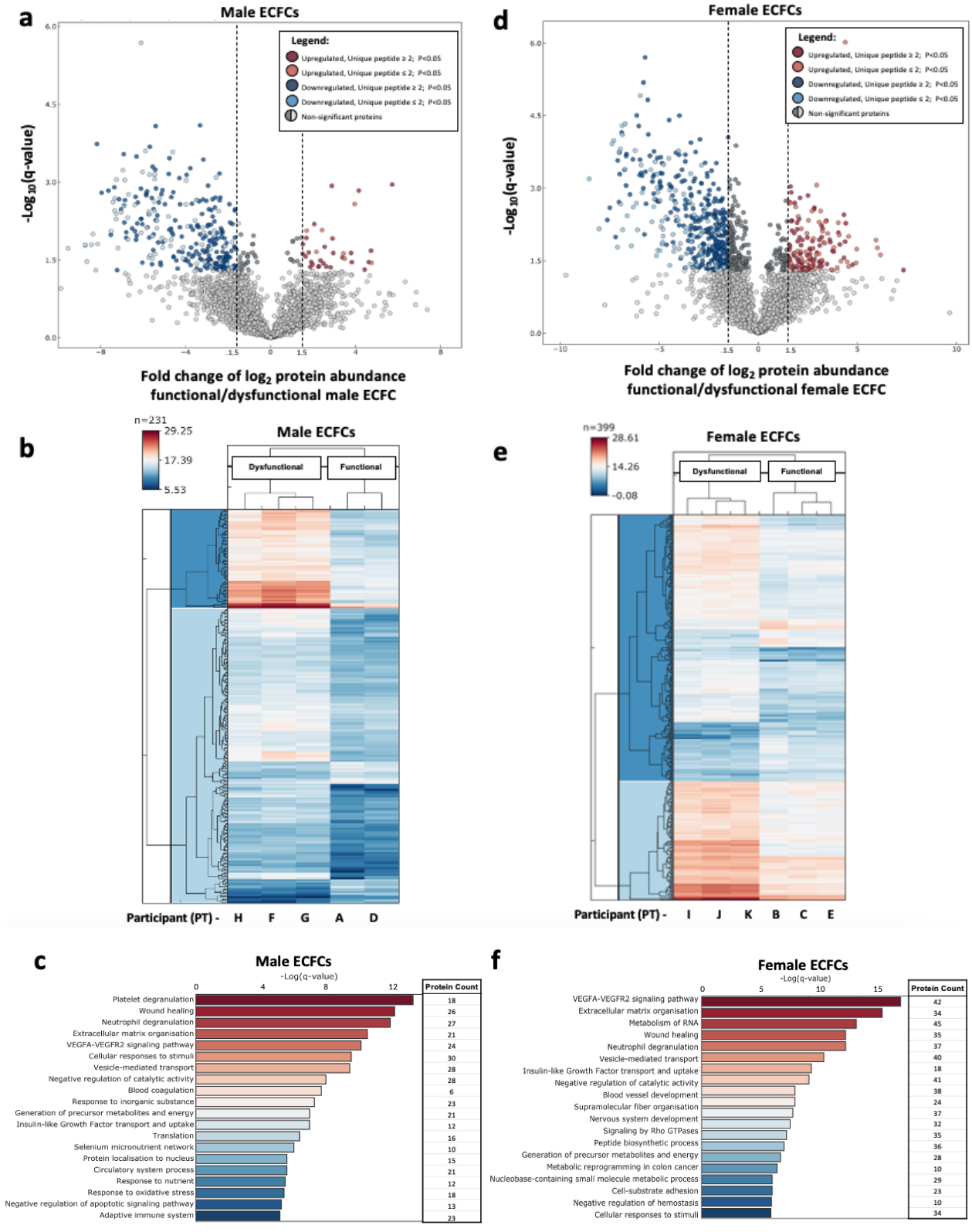
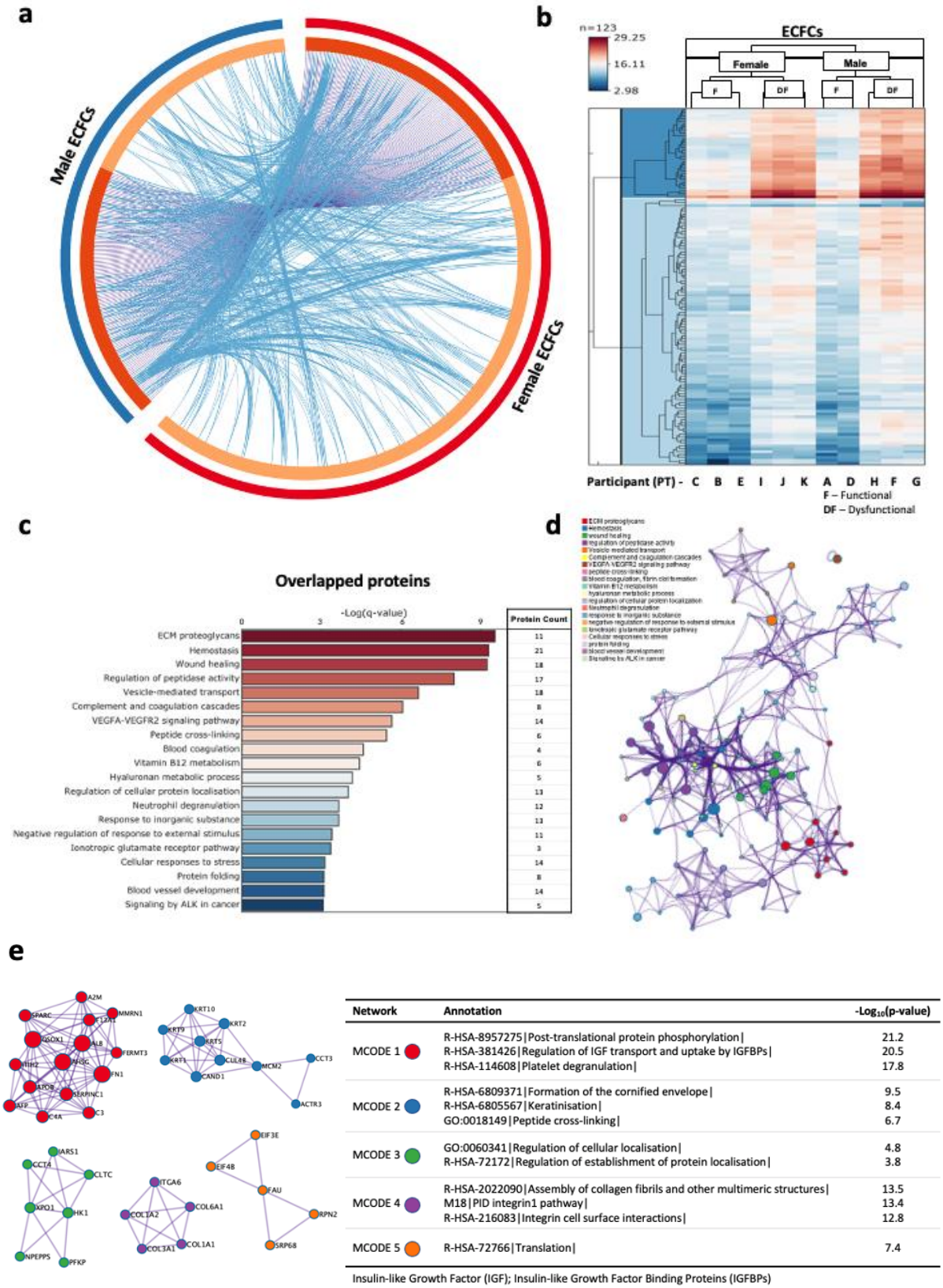


Figure 4.9. Proteomics analysis of function and dysfunctional endothelial colony-forming cells (ECFCs) based on sex.

Volcano plots show significantly regulated proteins between functional and dysfunctional ECFCs in **(a)** male and **(d)** female, after Student's t-test and FDR correction for multiple testing. Unsupervised hierarchical clustering (Euclidean distance) distinguishes samples according to their group and shows distinct protein abundance profiles indicative of grouping demonstrated in the form of heatmaps. The heatmaps showing a total of 231 proteins and a total of 399 proteins demonstrating significant differential abundance between the compared conditions based on proteins with unique peptides ≥ 2 and $\log_2$(fold change) ≥ 1.5 or ≤ -1.5 in dysfunctional and functional **(b)** male and **(e)** female ECFCs respectively. Significantly changed proteins show enrichment gene ontology biological pathways in **(c)** male and **(f)** female ECFCs. Protein count represents the number of proteins involved in the respective biological pathway.

Intra-sex comparison of functional and dysfunctional ECFCs identified over 123 overlapping proteins between the males and females with 3 upregulated and 120 downregulated proteins **(Figure 4.10 a and b)**. GO Enrichment analysis of overlapping proteins revealed top 20 biological pathways including ECM proteoglycans, haemostasis, wound healing, regulation of peptidase activity and vesicle-mediated transport **(Figure 4.10 c and d).**

The MCODE enrichment analysis revealed top 5 densely connected PPI network modules in the identified overlapped proteins **(Figure 4.10 e)**. Among the enriched terms of Module 1 (15 proteins - AFP, APOB, A2M, AHSG, ALB, F13A1, SERPINC1, C3, C4A, FN1, ITIH2, QSOX1, SPARC, MMRN1 and FERMT3), the main functional GO pathways include post-translational protein phosphorylation, regulation of IGF transport and uptake by IGFBPs and platelet degranulation. The top list of enriched categories for Module 2 (10 proteins - KRT1, KRT2, KRT5, KRT9, KRT10, CUL48, CAND1, MCM2, ACTR3 and CCT3) includes formation of the cornified envelope, Keratinisation and peptide cross-linking. The top list of enriched categories for Module 3 (7 proteins – IARS1, CLTC, CCT4, XPO1, HK1, NPEPPS and PFKP) included regulation of cellular localisation and regulation of establishment of protein localisation. The top list of enriched categories for Module 4 (5 proteins – ITGA6, COL6A1, COL1A2, COL3A1, COL1A1) includes assembly of collagen fibrils and other multimeric structures, PID integrin 1 pathway and integrin cell surface interactions. Translation was the main enriched GO pathway for Module 5 (5 proteins – EIF3E, EIF48, FAU, SRP68 and RPN2).



Network	Annotation	-Log$_{10}$(p-value)
MCODE 1	R-HSA-8957275|Post-translational protein phosphorylation|	21.2
	R-HSA-381426|Regulation of IGF transport and uptake by IGFBPs|	20.5
	R-HSA-114608|Platelet degranulation|	17.8
MCODE 2	R-HSA-6809371|Formation of the cornified envelope|	9.5
	R-HSA-6805567|Keratinisation|	8.4
	GO:0018149|Peptide cross-linking|	6.7
MCODE 3	GO:0060341|Regulation of cellular localisation|	4.8
	R-HSA-72172|Regulation of establishment of protein localisation|	3.8
MCODE 4	R-HSA-2022090|Assembly of collagen fibrils and other multimeric structures|	13.5
	M18|PID integrin1 pathway|	13.4
	R-HSA-216083|Integrin cell surface interactions|	12.8
MCODE 5	R-HSA-72766|Translation|	7.4

Insulin-like Growth Factor (IGF); Insulin-like Growth Factor Binding Proteins (IGFBPs)

Figure 4.10. Proteomics analysis of overlapping proteins of intra-specific sex comparisons between

function and dysfunctional endothelial colony-forming cells (ECFCs).

(a) A Circos plot shows how genes from the input gene lists of male and female ECFCs. Dark orange represents the genes that appear in both male and female gene lists, and light orange represents genes that are unique to that gene list. Purple lines link the same gene that is shared by multiple gene lists. Blue lines link the different genes where they fall into the same ontology term. **(b)** A total of 123 were identified as significantly overlapped proteins demonstrating significant differential abundance between the compared conditions based on proteins with unique peptides ≥ 2 and $\log_2$(fold change) ≥ 1.5 or ≤ -1.5 in dysfunctional vs functional male and female ECFCs. Unsupervised hierarchical clustering (Euclidean distance) distinguishes samples according to their group and shows distinct protein abundance profiles indicative of grouping. **(c)** Significantly changed proteins show enrichment gene ontology biological pathways in the overlapped proteins. Protein count represents the number of proteins involved in the respective biological pathway. **(d)** Based on Kappa-statistical similarities among their gene memberships, significant and enriched terms were hierarchically clustered into a tree. Then 0.3 kappa score was applied as the threshold to cast the tree into term clusters. **(e)** Molecular Complex Detection (MCODE) algorithm was applied to clustered enrichment ontology terms to identify neighbourhoods where proteins are densely connected in overlapped proteins of male and female ECFCs. Each MCODE network is assigned a unique colour. Protein-protein interaction (PPI) MCODE component. GO enrichment analysis was applied to each MCODE network to assign "meanings" to the network component.

Distinct differences in GO biological pathways were identified in intra sex-specific comparison between functional and dysfunctional ECFCs **(Figure 4.11).** Over 108 significant proteins were identified in male ECFCs with top 20 enriched GO biological pathways, including neutrophil degranulation, selenoamino acid metabolism, circulatory system process, IL-10 anti-inflammatory signalling pathway and antigen processing-cross presentation **(Figure 4.11 a and b).** On the other hand, over 276 significant proteins were identified in female ECFCs with top 20 enriched GO biological pathways including the metabolism of RNA, VEGFA-VEGFR-2 signalling pathway, neutrophil degranulation, translation and axon guidance **(Figure 4.11 a and b).**

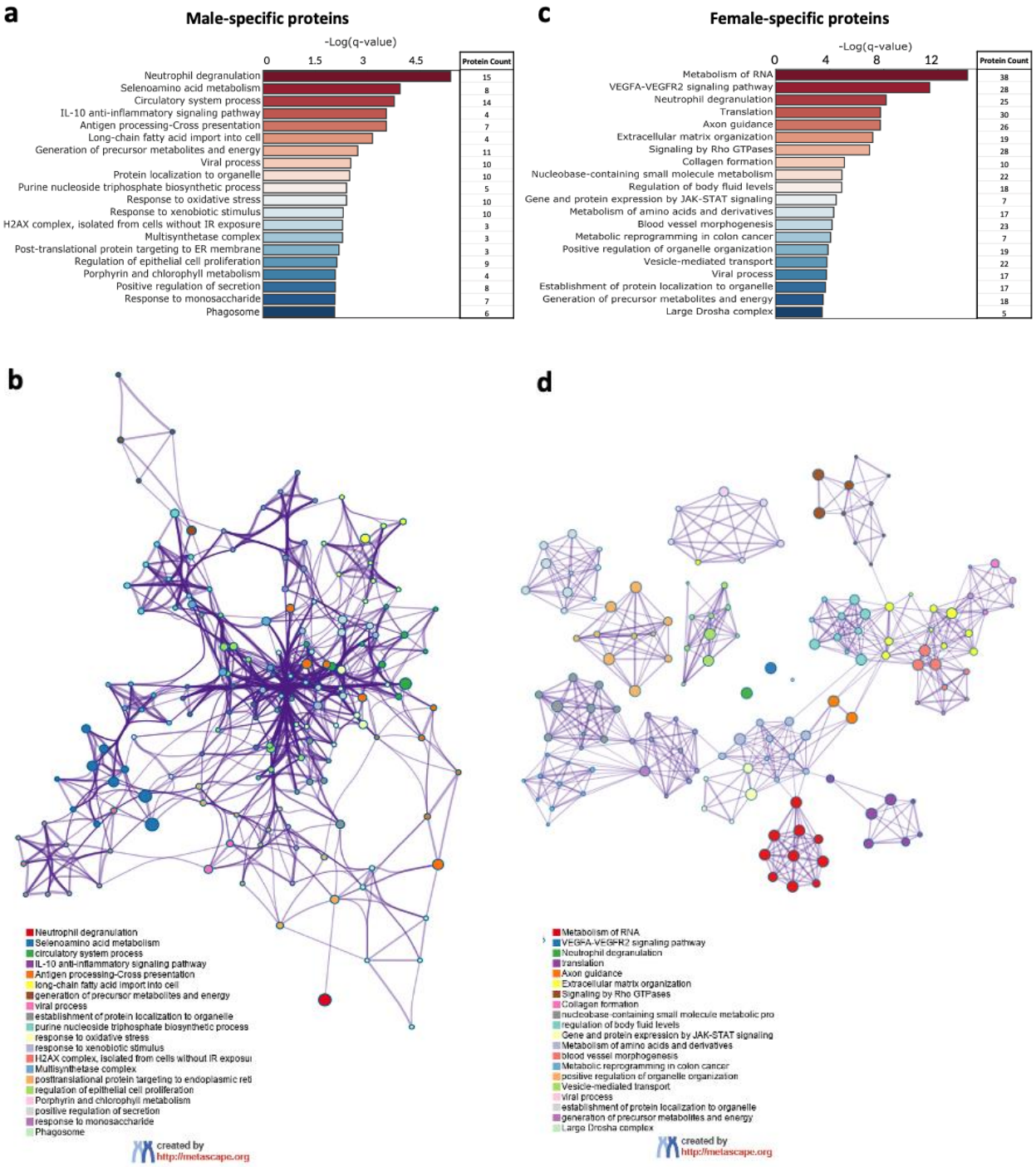


Figure 4.11. Proteomics analysis of non-overlapped proteins of intra-specific sex comparisons between function and dysfunctional endothelial colony-forming cells (ECFCs).

Significantly changed sex-specific proteins show enrichment gene ontology biological pathways in **(a)** male and **(c)** female ECFCs. Significant and enriched terms were hierarchically clustered into a tree based on

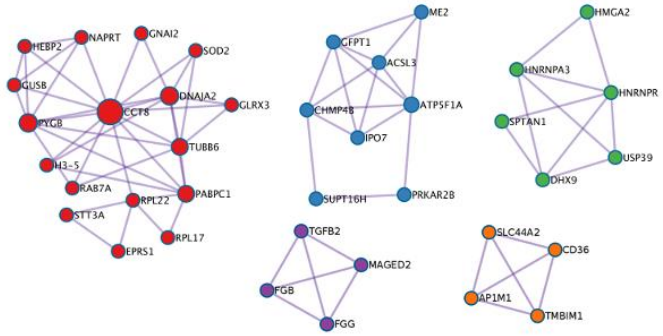
Kappa-statistical similarities among their gene memberships in **(b)** male and (**d)** female. Then 0.3 kappa score was applied as the threshold to cast the tree into term clusters.

The top 5 MCODE enrichment modules were identified based on PPI enrichment analysis in male-specific proteins **(Figure 4.12 a)**. Among the top list of enriched terms of Module 1 (17 proteins – GNAI2, NAPRT, HEBP, GUSB, PYGB, CCT8, DNAJA, SOD2, GLRX3, TUBB6, H3-5, RAB7A, PABPC1, RAB7, RPL22, RPL17, STT3A and EPRS1), three major GO pathways were identified, this includes neutrophil degranulation, translation, and nonsense Mediated Decay (NMD). The top list of enriched categories for Module 2 (8 proteins – ME2, GFPT1, ACSL3, CHMP4B, ATP5F1A, IPO7, SUPT16H and PRKAR2B) includes the generation of precursor metabolites and energy, nucleobase-containing small molecule metabolic process and monocarboxylic acid metabolic process. The top list of enriched categories for Module 3 (6 proteins – HMGA2, HNRNPA3, HNRNPR, SPTAN1, USP39 and DHX9) included mRNA Splicing and processing of capped intron-containing pre-mRNA. The top list of enriched categories for Module 4 (4 proteins – TGFB2, MAGED2, FGB and FGG) included platelet degranulation, response to elevated platelet cytosolic Ca^{2+} and platelet activation, signalling and aggregation. The top list of enriched categories for Module 5 (4 proteins – SLC44A2, CD36, AP1M1 and TMBIM1) included neutrophil degranulation.

The top 5 MCODE enrichment modules were identified in female-specific proteins **(Figure 4.12 b)**. Among the top list of enriched terms of Module 1 (28 proteins – P4HA1, P4HA2, COL8A1, COL18A1, COL4A2, ITGB3, COL4A1, PLOD1, COLGALT1, PLOD2, ITGA5, THBS1, GNB2, TCP1, PRKACA, RUVBL2, PSMD4, PSMB5, PSME2, IDH1, TKT, GLRX, RCC2, DSTN, PGD, AHCY, RCC1 and TARS1) include 3 GO pathways, including ECM organisation, collagen biosynthesis and modifying enzymes and collagen formation. The top list of enriched categories for Module 2 (24 proteins – TARDBP, IDH3A, PGM1, BCAT2, GAPDH, GDJ1, VARS1, PSMD2, YWHAG, KDELR2, KLC1, PFKL, RPA1, PSMD12, DCTN2, COPE, TMED10, CAPZB, MRPL12, NONO, MRPL41, MRPS35, TMED9, KIF5B and CAPZB) includes Golgi-to-ER retrograde transport, intra-Golgi and retrograde Golgi-to-ER traffic and membrane trafficking. The top list of enriched

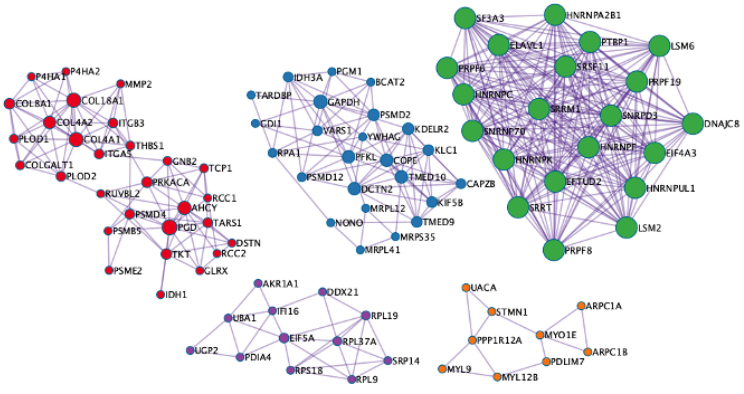
categories for Module 3 (21 proteins – SF3A3, ELAVL1, PRPF6, HNRNPA2B1, HNRNPC, SNRNP70, SRRM1, SRSF11, PTBP1, LSM6, PRPF19, SNRPD3, HNRNPF, EFTUD2, SRRT, HNRNPK, PRPF8, LSM2, HNRNPUL1, EIF43A and DNAJC8) includes mRNA Splicing and processing of capped intron-containing pre-mRNA. The top list of enriched GO pathways for Module 4 (12 proteins – AKR1A1, UBA1, UGP2, IFI16, PDIA4, DDX21, EIF5A, RPS18, RPL37A, RPL19, RPL9 and SRP14) includes Nop56p-associated pre-rRNA complex, SRP-dependent co-translational protein targeting to membrane and major pathway of rRNA processing in the nucleolus and cytosol. The top list of enriched GO pathways for Module 5 (9 proteins – UACA, STMN1, PPP1R12A, MYL9, MYL12B, MYO1E, PDLIM7, ARPC1A and ARPC1B) included regulation of actin cytoskeleton and EPH-Ephrin signalling.

a **Male-specific proteins**



Network	Annotation	-Log$_{10}$(p-value)
MCODE 1	R-HSA-6798695|Neutrophil degranulation|	6.8
	R-HSA-72766|Translation|	4.7
	R-HSA-975956|Nonsense Mediated Decay (NMD)|	4.7
MCODE 2	GO:0006091|generation of precursor metabolites and energy|	3.7
	GO:0055086|nucleobase-containing small molecule metabolic process|	3.5
	GO:0032787|monocarboxylic acid metabolic process|	3.4
MCODE 3	R-HSA-72163|mRNA Splicing - Major Pathway|	7.7
	R-HSA-72172|mRNA Splicing|	7.6
	R-HSA-72203|Processing of Capped Intron-Containing Pre-mRNA|	7.2
MCODE 4	R-HSA-114608|Platelet degranulation|	9.5
	R-HSA-76005|Response to elevated platelet cytosolic Ca2+|	9.4
	R-HSA-76002|Platelet activation, signalling and aggregation|	8.3
MCODE 5	R-HSA-6798695|Neutrophil degranulation|	7.2

b **Female-specific proteins**



Network	Annotation	-Log$_{10}$(p-value)
MCODE 1	R-HSA-1474244|Extracellular matrix organization|	18.4
	R-HSA-1650814|Collagen biosynthesis and modifying enzymes|	17.1
	R-HSA-1474290|Collagen formation|	15.9
MCODE 2	R-HSA-8856688|Golgi-to-ER retrograde transport|	13.1
	R-HSA-6811442|Intra-Golgi and retrograde Golgi-to-ER traffic|	11.6
	R-HSA-199991|Membrane Trafficking|	10.6
MCODE 3	R-HSA-72163|mRNA Splicing - Major Pathway|	47.1
	R-HSA-72172|mRNA Splicing|	46.7
	R-HSA-72203|Processing of Capped Intron-Containing Pre-mRNA|	44.3
MCODE 4	CORUM:3055|Nop56p-associated pre-rRNA complex|	11.9
	R-HSA-1799339|SRP-dependent co-translational protein targeting to membrane|	9.3
	R-HSA-6791226|Major pathway of rRNA processing in the nucleolus and cytosol|	8.2
MCODE 5	ko04810|Regulation of actin cytoskeleton|	8.7
	R-HAS-04810|Regulation of actin cytoskeleton|	8.5
	R-HSA-2682334|EPH-Ephrin signalling|	8.0

Figure 4.12. MCODE algorithm was applied to clustered enrichment ontology terms to identify neighborhoods where proteins are densely connected in (a) male-specific and (b) female-specific endothelial colony-forming cell (ECFC) proteins.

Each MCODE network is assigned a unique color. Protein-protein interaction (PPI) MCODE component. GO enrichment analysis was applied to each MCODE network to assign "meanings" to the network component.

4.5 Discussion

4.5.1 ECFC isolation and characterisation

This study is the first to describe a distinct proteomic signature and to target altered angiogenic mechanisms in dysfunctional ECFCs with significant reduction in both expansion and vasculogenic capacities. In addition, we also provide evidence that specific proteomic changes in dysfunctional cells were associated with a distinct ECFCs phenotype and proteome profile in comparison to another highly angiogenic EC population of HUVECs.

In order to properly run such comparisons, our study performed a comprehensive characterization of ECFCs showing the expression of classic EC surface markers including PECAM-1, VE-Cadherin, VEGFR-2, eNOS, lectin (UEA-1), but also key progenitor cell markers such as AcLDL and CD34 in ECFCs. Specifically, we showed that ECFCs stained negative for CD133 and CD45 that are expressed in other EPCs. These findings are in line with others supporting the use of a combination of PECAM-1/VE-cadherin/VEGFR-2 positive and CD45 and CD133 negative surface markers when quantifying ECFCs from blood or PBMC pools by flow cytometry[12, 20, 39]. In addition, our study confirmed the expression of CD34, a marker of progenitor cells in ECFCs.

4.5.2 ECFC vs HUVECs

Comparative proteome analysis revealed similar proteomic profiles between overall ECFCs and HUVECs, although this degree of similarity varied according to ECFC functionality. These data are consistent with recent findings from Kutikhin *et al.* that showed similar proteome profiles between ECFCs and HUVECs, particularly in the expression of specific endothelial lineage, ECM and basement membrane markers including NRP-2, PECAM-1, COL1A1, COL1A2, COL4A1, COL4A2[324]. In contrast to our findings, the authors demonstrated higher proliferative potential in ECFCs than HUVECs [324]. This may be due to differences in baseline clinical characteristics of the study population or to sex differences since they assessed ECFCs obtained only from male subjects.

4.5.3 Proteome profiles of functional vs dysfunctional ECFCs

Proteomic studies have been conducted to define molecular mechanisms and markers in CVDs and regeneration, both experimentally and clinically. Proteins involved in angiogenesis, vasoconstriction, inflammation, and matrix degeneration have been repeatedly found in such studies[325]. However, to this date, the main mechanisms impairing angiogenesis in primary cultured ECFCs are not entirely elucidated. Therefore, our proteomic findings are among the first to identify mechanisms significantly altered in less angiogenic and proliferative ECFCs. This is also supported by the PCA. The PCA analyses confirmed the great discrepancy between protein profiles of functional and dysfunctional cells. The gene ontology of distinct proteomic signatures between functional clusters revealed the activation of mechanisms driving exocytosis regulation and vesicle-mediated transport processes in dysfunctional ECFCs, which are critical processes involved in the formation and secretion of micro and nanovesicles in ECs[326].

In response to injury and stress, ECs can undergo exocytosis by releasing numerous hemostatic and pro-inflammatory factors into the bloodstream, further regulating vascular thrombosis and inflammatory responses[327]. One of the main factors released by ECs is the pro-thrombotic protein vWF[327,

[328]. Some studies have shown that patients with increased vWF levels have a higher incidence of adverse cardiovascular events, including coronary artery disease, myocardial infarction and thrombosis[329, 330]. In addition, animal studies have also highlighted the relationship between exocytosis and endothelial dysfunction. In mice, a study by Zhang *et al.* outlined the impact of excessive exocytosis of lysosomal-related organelles, which hindered endothelial mechano-transduction and nitric oxide production, leading to EC dysfunction[331].

Furthermore, our proteomic analysis also identified changes in mechanisms essential for maintaining the vascular tree, including ECM organisation and regulation of apoptosis[60, 332, 333]. These biological functions are also critical for capillary sprouting and wound healing[334]. In addition, we identified changes in the main mechanisms regulating RNA metabolism, as well as the generation of precursor metabolites and energy in cells, indicating significant metabolic and energetic changes in dysfunctional ECFCs.

We also identified targeted proteins that were differently expressed between functional clusters of ECFCs. Top-ranked proteins upregulated in the group of dysfunctional ECFCs were SPARC, CD36, LUM and PTX3. It is beyond the scope of this study to review the functions of these proteins extensively, but these are briefly described in **Table 4.2**. Interestingly, CD36 and SPARC are cellular receptors to thrombospondin-1, an essential anti-angiogenic focal adhesion glycoprotein with cellular effects that can inhibit cell migration and tube formation in ECs[335, 336]. In addition, SPARC is shown to reduce ECs proliferation mainly by antagonising VEGF and inhibiting the phosphorylation of MAPKs and fibroblast growth factor[337].

Similarly, LUM is a small leucine-rich proteoglycan that binds to the α2 integrin I domain and significantly reduces the expression of matrix metalloproteinases (MMP), particularly MMP-14, inhibiting cell adhesion and migration in ECs[338]. Furthermore, LUM is a novel mediator of angiostasis by promoting

fibrillogenesis and the stabilisation of collagen fibers. It is also reported to inhibit tumour angiogenesis and growth by activating the pro-apoptotic Fas pathway in ECs[339].

Interestingly, after adjusting the top-ranked proteins by the participants' BMI and systolic BP, we found that only SPARC and LUM remained significantly different between functional and dysfunctional ECFCs, while PTX3 and CD36 were no longer significantly different. These findings suggest a closer relationship between the latter two proteins with BMI and systolic BP variations. PTX3 is a soluble pattern recognition receptor produced mainly by monocytes and ECs. It binds with high affinity to fibroblast growth factor-2 (FGF2) and heparan sulfate proteoglycans, thus inhibiting angiogenesis and cell proliferation[340, 341]. Elevated PTX3 levels were also reported in various CVDs, including pulmonary arterial hypertension[342], acute coronary syndrome[343], heart failure[344], and in advanced atherosclerotic plaque[345].

4.5.4 ECFC characteristics, clinical observations, and disease progression

Our findings and others' suggest that the disruption of these candidate anti-angiogenic proteins and mechanisms could contribute to the progression of CVDs in subjects[337-344]. Emerging evidence suggests that ECFCs play an active role in stimulating processes of capillary sprouting and angiogenesis during wound healing and tissue development, as well as by contributing to the maintenance and remodelling of main vessels in physiological processes during pregnancy and diseases such as hypertension[4, 5, 19, 49, 73, 152, 321, 346, 347]. Deficiency in the number and activity of circulating overall EPCs and ECFCs were previously associated with reduced arterial elasticity in humans with advancing ageing and common cardiovascular risk factors like diabetes, hypertension, heart failure, ischemic stroke, angina, atherosclerotic coronary artery lesions and hyperlipidemia[71-74, 348, 349]. In addition, the strong association between ECFC dysfunction and higher BP was also reported in preterm-born young adults, particularly in those exposed to bronchopulmonary dysplasia as newborns, which is a comorbidity marked by severe micro-vascular growth arrest in newborn lungs[10, 318]. These studies corroborate our findings showing

impaired proliferative and angiogenesis potentials in subjects with dysfunctional ECFCs also presenting higher BP values. ECFC dysfunction could represent a key mechanism to the initiation of the pathogenesis of CVDs with associated endothelial dysfunction in these subjects.

Furthermore, higher BMI was also observed in participants with dysfunctional ECFCs. This finding was also evident in studies conducted by MacEneaney *et al.* and Tobler *et al.* that revealed a reduction in circulating overall EPCs and ECFCs, with premature cell senescence and impaired ECFC colony-forming and proliferative capacity in overweight and obese adult subjects[350, 351]. A reduction in EPC number in obese individuals was also evident in several studies, including patients with obesity-related hypercholesterolemia[352, 353]. The mechanisms promoting EPC, particularly ECFC, dysfunction in obesity and dyslipidemia, are still unclear. However, it may involve the increase in adiposity observed in these individuals, which could prevent EPCs from releasing pro-angiogenic factors (including VEGF and granulocyte colony-stimulating factor) while stimulating the release of pro-apoptotic caspase-3, thereby compromising their reparative potential[354].

4.5.5 Sex-dimorphism in ECFC

Several studies have observed sex-specific differences in intracellular proteome and genome of human ECs that may contribute to EC function[84, 93, 97, 98]. Due to a limited study sample size, we could not observe the effect of sex in ECFC functionality and proteome profiles. However, our investigations revealed the potential intra-sex- dimorphism in ECFC when comparing functionality. For the first time, we showed the intra-sex comparison of proteome profile of functional and dysfunctional ECFCs to be similar with enrichment in GO pathways, including ECM organisation, VEGF signalling pathway, wound healing, neutrophil degranulation, vesicle-mediated transport, negative regulation of catalytic pathway, IGF transport and uptake in both male and female. Further proteomic analysis revealed for the first time sex-

specific changes between functional and dysfunctional ECFCs. We observed that in males, the comparison between functional and dysfunctional ECFC, dysregulation in proteome was observed predominantly in immune response including neutrophil degranulation, IL-10 anti-inflammatory signalling pathway and antigen processing-cross presentation. Furthermore, MCODE Module 1 (17 proteins – GNAI2, NAPRT, HEBP, GUSB, PYGB, CCT8, DNAJA, SOD2, GLRX3, TUBB6, H3-5, RAB7A, PABPC1, RAB7, RPL22, RPL17, STT3A and EPRS1) also identified three major GO pathways were identified, this includes neutrophil degranulation, translation, and nonsense Mediated Decay (NMD). Whereas, in comparing the female functional and dysfunctional ECFCs, the alterations in proteome were observed mainly in angiogenesis-related pathways, including VEGFA-VEGFR-2 signalling pathway. This is supported by the top list of enriched terms of MCODE Module 1 (28 proteins – P4HA1, P4HA2, COL8A1, COL18A1, COL4A2, ITGB3, COL4A1, PLOD1, COLGALT1, PLOD2, ITGA5, THBS1, GNB2, TCP1, PRKACA, RUVBL2, PSMD4, PSMB5, PSME2, IDH1, TKT, GLRX, RCC2, DSTN, PGD, AHCY, RCC1 and TARS1) include 3 GO pathways, including ECM organisation, collagen biosynthesis and modifying enzymes and collagen formation. These data further supported that ECFC may have intra-sex dimorphism that is dependent on cell functionality. Studies have shown the profound influence of sex on EC functional and physiological differences, including viability, migration, proliferation, angiogenesis and shear stress response, imply sex differences and the influence of sex steroids (oestrogens or androgens) in regulation of vital endothelial pathways, such as the redox system, inflammation and angiogenesis pathways[92-97, 99].

As the sample size is small, the sexual dimorphism of ECFC should be further evaluated to aid in understanding physiological and mechanical differences and achieve more effective strategies for the prevention and therapy of disease-associated with an impaired endothelial function, including CVD. Overall, our investigations align with others suggesting a closed link between underlying CVD risks and on EC dysfunction. More extensive studies are needed to confirm and validate the main observations and mechanisms, establishing a connection between our experimental findings with clinical characteristics.

This proteomic approach has successfully identified a novel ECFC proteomic signature and targeted proteins potentially driving ECFC angiogenic (dys)function.

4.5.6 Study strengths and limitations

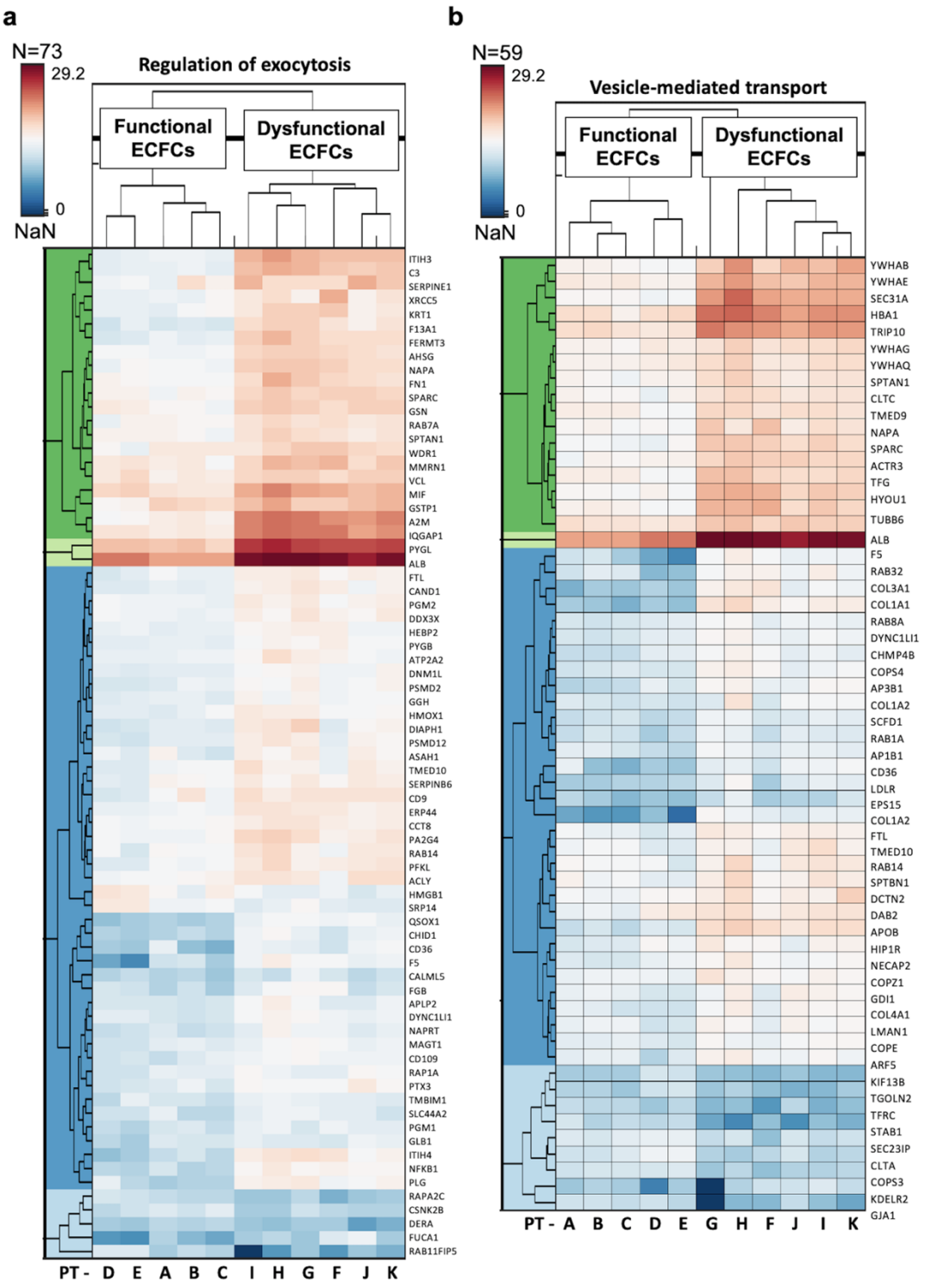
Despite a limited sample size, our investigations are in line with others suggesting a close link between underlying CVD risks and EC dysfunction. Several studies have observed sex-specific differences in the intracellular proteome and genome of human ECs, affecting EC function[84, 93, 97, 98]. Sex-based ECFC differences are still unclear. Additional studies are needed to confirm and validate the main observations and mechanisms, establish a connection between our experimental findings and clinical characteristics, and considering potential sex differences. This proteomic approach has successfully identified a novel ECFC proteomic signature and targeted proteins potentially driving ECFC angiogenic (dys)function.

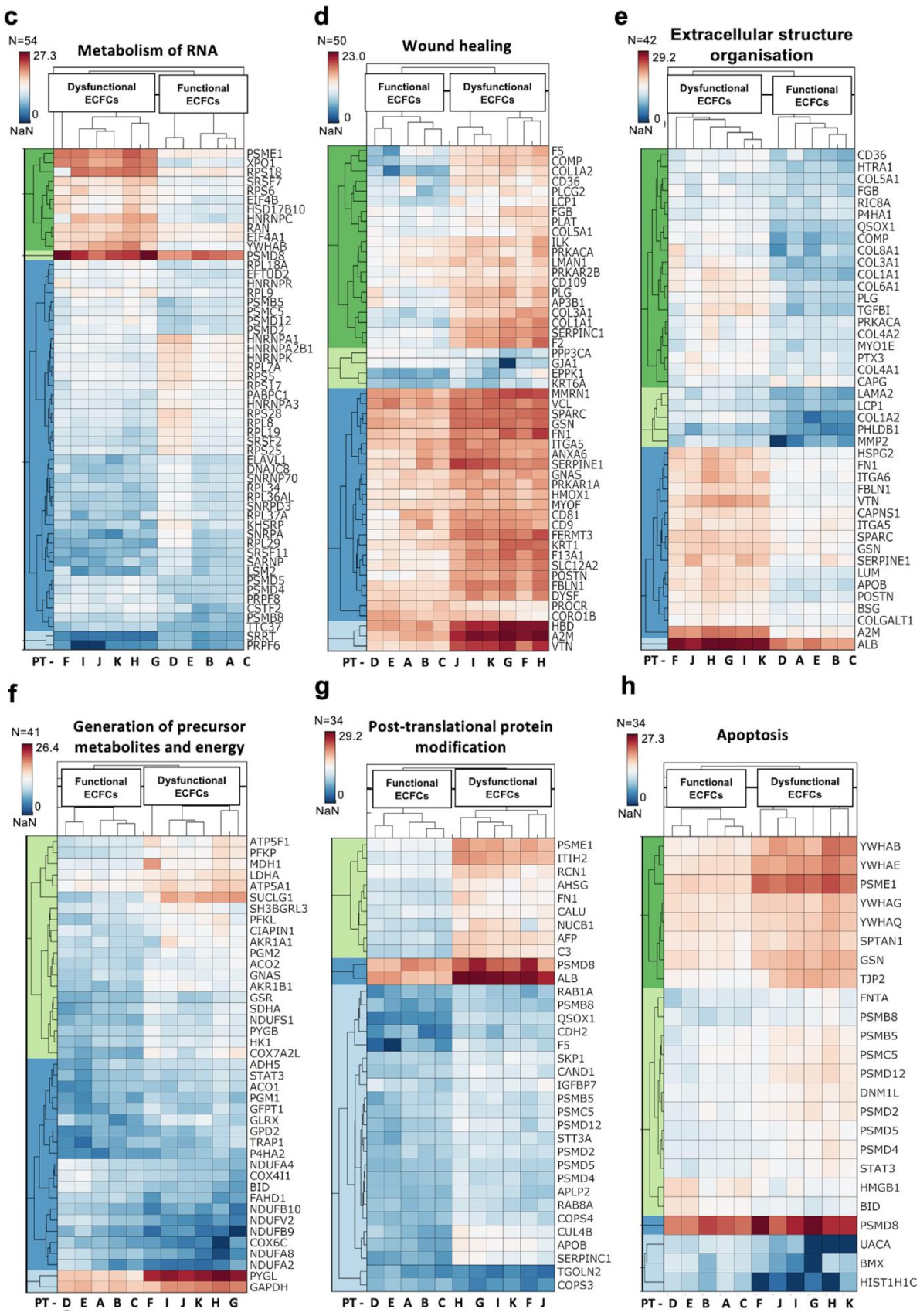
4.6 Conclusion

In conclusion, circulating ECFCs with impaired angiogenesis and expansion capacities have a distinct proteomic profile and phenotype than highly angiogenic ECFCs and HUVECs. The disruption of key cellular mechanisms involved mainly in exocytosis and vesicle transport and in ECM organisation, cell metabolism and apoptosis were identified in dysfunctional ECFCs, in addition to targeted anti-angiogenic proteins. These findings suggest a potential relationship between specific anti-angiogenic mechanisms and EC dysfunction. However, more studies are needed to validate our targeted mechanisms and investigate the potential of sex dimorphism of ECFCs in larger populations to enhance our understanding of the physiological function of ECFCs and their potential clinical applications in CVD.

4.7 Supplemental materials

Supplementary Figure S4.1




c
N=54
27.3
0
NaN
Metabolism of RNA
Dysfunctional ECFCs
Functional ECFCs
PSME1
XPO1
RPS18
SRSF7
RPS6
EIF4B
HSD17B10
HNRNPC
RAN
EIF4A1
YWHAB
PSMD8
RPL18A
EFTUD2
HNRNPR
RPL9
PSMB5
PSMC5
PSMD12
PSMD7
HNRNPA1
HNRNPA2B1
HNRNPK
RPL7A
RPS5
RPS17
PABPC1
HNRNPA3
RPS28
RPL8
RPL19
SRSF2
RPS25
ELAVL1
DNAJC8
SNRNP70
RPL34
RPL36AL
SNRPD3
RPL37A
KHSRP
SNRPA
RPL29
SRSF11
SARNP
LSM2
PSMD5
PSMD4
PRPF8
CSTF2
PSMB8
TTC37
SRRT
PRPF6
PT- F I J K H G D E B A C
d
N=50
23.0
0
NaN
Wound healing
Functional ECFCs
Dysfunctional ECFCs
F5
COMP
COL1A2
CD36
PLCG2
LCP1
FGB
PLAT
COL5A1
ILK
PRKACA
LMAN1
PRKAR2B
CD109
PLG
AP3B1
COL3A1
COL1A1
SERPINC1
F2
PPP3CA
GJA1
EPPK1
KRT6A
MMRN1
VCL
SPARC
GSN
FN1
ITGA5
ANXA6
SERPINE1
GNAS
PRKAR1A
HMOX1
MYOF
CD81
CD9
FERMT3
KRT1
F13A1
SLC12A2
POSTN
FBLN1
DYSF
PROCR
CORO1B
HBD
A2M
VTN
PT- D E A B C J I K G F H
e
N=42
29.2
0
NaN
Extracellular structure organisation
Dysfunctional ECFCs
Functional ECFCs
CD36
HTRA1
COL5A1
FGB
RIC8A
P4HA1
QSOX1
COMP
COL8A1
COL3A1
COL1A1
COL6A1
PLG
TGFBI
PRKACA
COL4A2
MYO1E
PTX3
COL4A1
CAPG
LAMA2
LCP1
COL1A2
PHLDB1
MMP2
HSPG2
FN1
ITGA6
FBLN1
VTN
CAPNS1
ITGA5
SPARC
GSN
SERPINE1
LUM
APOB
POSTN
BSG
COLGALT1
A2M
ALB
PT- F J H G I K D A E B C
f
N=41
26.4
0
NaN
Generation of precursor metabolites and energy
Functional ECFCs
Dysfunctional ECFCs
ATP5F1
PFKP
MDH1
LDHA
ATP5A1
SUCLG1
SH3BGRL3
PFKL
CIAPIN1
AKR1A1
PGM2
ACO2
GNAS
AKR1B1
GSR
SDHA
NDUFS1
PYGB
HK1
COX7A2L
ADH5
STAT3
ACO1
PGM1
GFPT1
GLRX
GPD2
TRAP1
P4HA2
NDUFA4
COX4I1
BID
FAHD1
NDUFB10
NDUFV2
NDUFB9
COX6C
NDUFA8
NDUFA2
PYGL
GAPDH
PT- D E A B C F I J K H G
g
N=34
29.2
0
NaN
Post-translational protein modification
Functional ECFCs
Dysfunctional ECFCs
PSME1
ITIH2
RCN1
AHSG
FN1
CALU
NUCB1
AFP
C3
PSMD8
ALB
RAB1A
PSMB8
QSOX1
CDH2
F5
SKP1
CAND1
IGFBP7
PSMB5
PSMC5
PSMD12
STT3A
PSMD2
PSMD5
PSMD4
APLP2
RAB8A
COPS4
CUL4B
APOB
SERPINC1
TGOLN2
COPS3
PT- D E A B C H G I K F J
h
N=34
27.3
0
NaN
Apoptosis
Functional ECFCs
Dysfunctional ECFCs
YWHAB
YWHAE
PSME1
YWHAG
YWHAQ
SPTAN1
GSN
TJP2
FNTA
PSMB8
PSMB5
PSMC5
PSMD12
DNM1L
PSMD2
PSMD5
PSMD4
STAT3
HMGB1
BID
PSMD8
UACA
BMX
HIST1H1C
PT- D E B A C F J I G H K

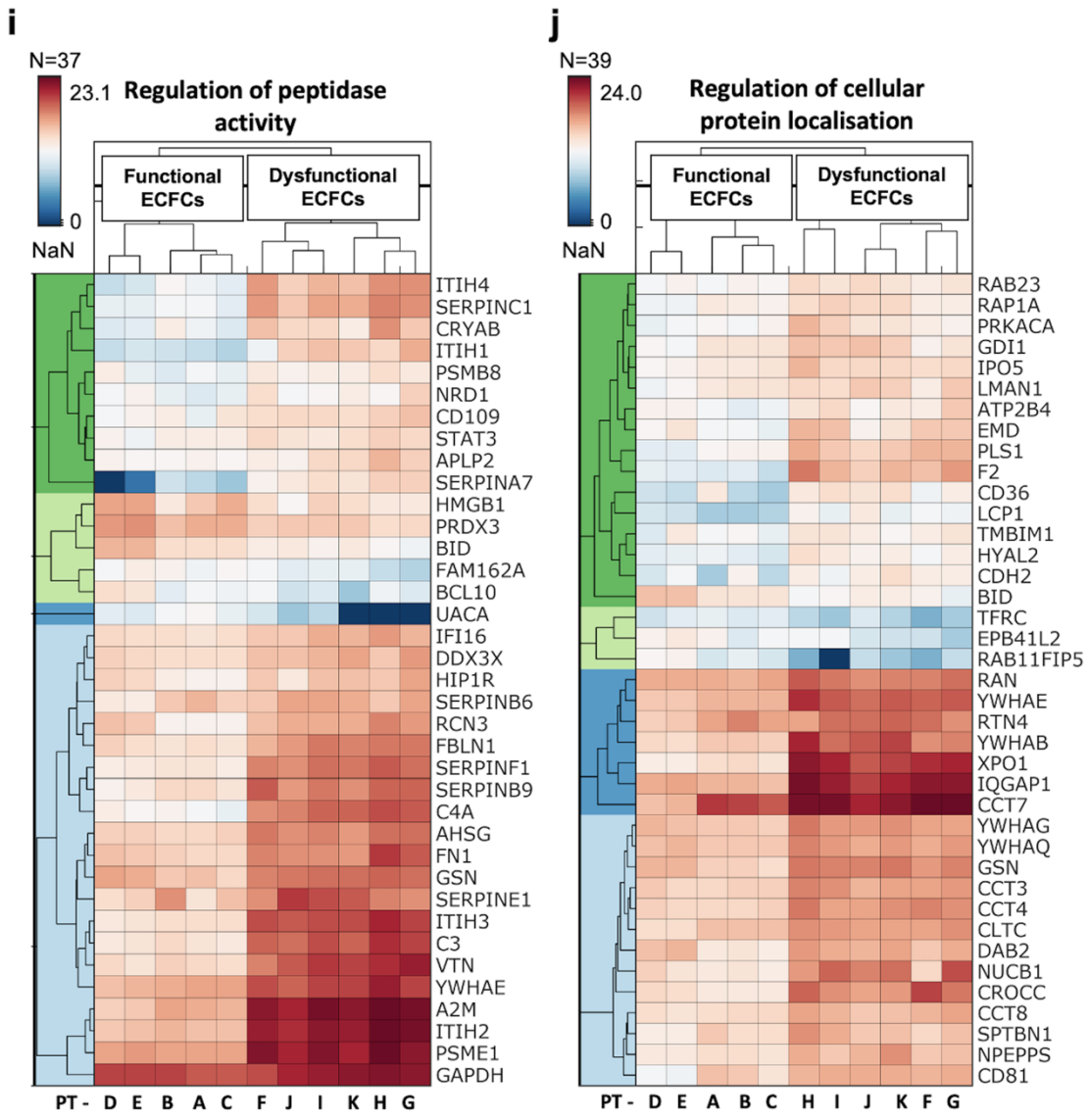


Figure S4.1. Heat maps based on log_2-transformed protein abundance of proteins in the top 10 enriched gene otology pathways.

This includes **(a)** regulated exocytosis; **(b)** vesicle-mediated transport; **(c)** metabolism of RNA; **(d)** wound healing; **(e)** extracellular structure organization; **(f)** generation of precursor metabolites and energy; **(g)** post-translational protein modification; **(h)** apoptosis; **(i)** regulation of peptidase activity and **(j)** regulation of cellular protein localisation.

Supplementary Figure S4.1

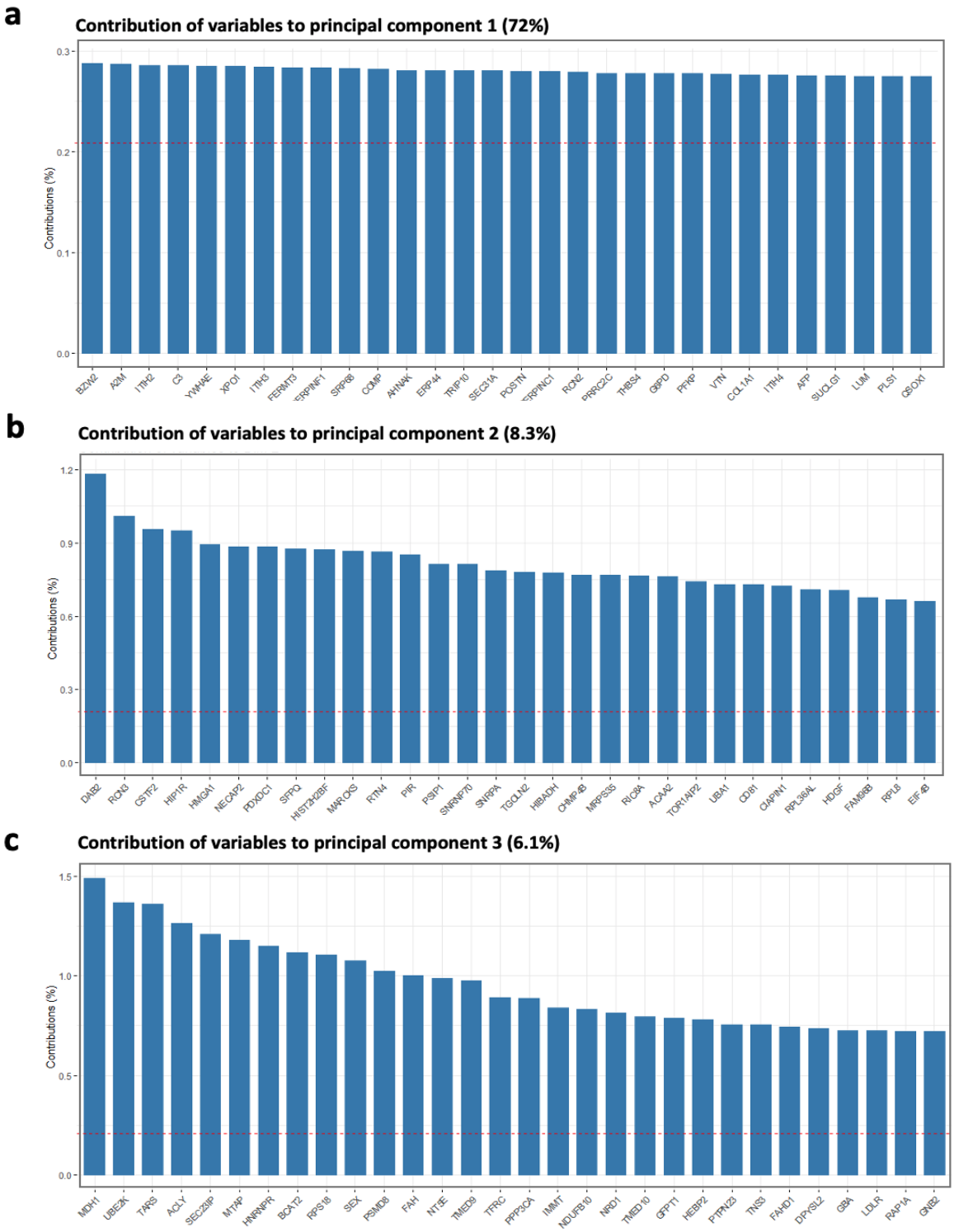


Figure S4.2. Contribution of variables to principal component 1 to 3.

The red dashed line on the graph above indicates the expected average contribution.

Supplementary Table S4.1

Table S4.1. Clinical characteristics of the male study participants endothelial colony-forming cell (ECFC) based on cell functionality.

Clinical characteristics	Total (n=5)	Functional ECFC (n=2)	Dysfunctional ECFC (n=3)	P-Value
Age, years	26.6 ± 5.5	23.5 ± 2.12	28.67 ± 6.51	0.376
Height, cm	178.6 ± 6.11	184.5 ± 3.54	174.67 ± 3.21	0.048*
Weight, kg	76.8 ± 12.08	69.95 ± 2.19	81.37 ± 14.53	0.372
BMI, kg/m^2	24.18 ± 4.4	20.57 ± 1.43	26.59 ± 4.01	0.146
Systolic BP, mmHg	124.6 ± 8.5	121 ± 8.49	128.67 ± 8.39	0.392
Diastolic BP, mmHg	79.4 ± 13.39	71 ± 18.38	86.33 ± 7.57	0.436
Mean arterial pressure, mmHg	97.2 ± 10.85	91 ± 15.56	101.33 ± 7.09	0.367
Heart rate, beats per min	76 ± 13.11	79 ± 5.66	74 ± 17.69	0.736
Blood biochemistry	**Total (n=5)**	**Functional ECFC (n=2)**	**Dysfunctional ECFC (n=3)**	**P-Value**
Triglyceride, mmol/l	1.41 ± 1.12	0.92 ± 0.16	1.74 ± 1.45	0.503
Cholesterol, mmol/l	4.89 ± 0.46	4.65 ± 0.78	5.05 ± 0.15	0.601
High density lipoprotein, mmol/l	1.33 ± 0.35	1.25 ± 0.21	1.39 ± 0.46	0.725
Low density lipoprotein, mmol/l	2.5 ± 0.66	2.1 ± 0.85	2.77 ± 0.49	0.333
Glucose, mmol/l	5.17 ± 0.35	4.97 ± 0.49	5.3 ± 0.23	0.371
Insulin, pmol/l	45.8 ± 13.18	49 ± 9.9	43.67 ± 16.77	0.72
HOMA β-cell function, %	81.94 ± 23.25	94.55 ± 28.92	73.53 ± 19.96	0.397
HOMA insulin sensitivity, %	122.94 ± 32.37	111.15 ± 19.16	130.8 ± 40.99	0.585
HOMA IR (insulin resistance)	0.86 ± 0.24	0.91 ± 0.16	0.83 ± 0.31	0.25
ECFC characteristics	**Total (n=5)**	**Functional ECFC (n=2)**	**Dysfunctional ECFC (n=3)**	**P-Value**
Days for ECFC colony formation	18 ± 6.24	12.5 ± 3.54	0.83 ± 0.31	0.101
Proliferation rate (%)	23.72 ± 23.76	47.36 ± 14.94	21.67 ± 4.62	0.033*
Closed tube formed, n per $1.5x10^4$	5.96 ± 8.73	14.9 ± 6.22	7.95 ± 9.22	0.02*
Branches formed, n per $1.5x10^4$	14.4 ± 13.69	28.75 ± 6.43	0 ± 0	0.011*

Homeostatic model assessment (HOMA); endothelial colony-forming cell (ECFC). Data are expressed as mean ± standard deviation (SD). *P<0.05 between cell functionalities. Independent t-test.

Supplementary Table S4.2

Table S4.2. Clinical characteristics of the female study participants endothelial colony-forming cell (ECFC) based on cell functionality.

Clinical characteristics	Total (n=6)	Functional ECFC (n=3)	Dysfunctional ECFC (n=3)	P-Value
Age, years	26.5 ± 4.32	25.67 ± 0.58	27.33 ± 6.66	0.707
Height, cm	165.83 ± 5.78	166.67 ± 5.69	165 ± 7	0.765
Weight, kg	65.98 ± 10.1	59.97 ± 7.78	71.98 ± 9.28	0.161
BMI, kg/m^2	24.07 ± 4.19	21.55 ± 2.23	26.59 ± 4.46	0.155
Systolic BP, mmHg	134.33 ± 16.73	122.67 ± 10.5	146 ± 13.45	0.077
Diastolic BP, mmHg	87.17 ± 10.63	81.33 ± 12.7	93 ± 4.36	0.207
Mean arterial pressure, mmHg	105.17 ± 14.13	95.33 ± 12.1	115 ± 7.94	0.078
Heart rate, beats per min	70.83 ± 8.28	68.67 ± 12.42	73 ± 1.73	0.608
Blood biochemistry	**Total (n=6)**	**Functional ECFC (n=3)**	**Dysfunctional ECFC (n=3)**	**P-Value**
Triglyceride, mmol/l	0.9 ± 0.37	0.82 ± 0.4	0.98 ± 0.42	0.655
Cholesterol, mmol/l	4.82 ± 1.03	3.92 ± 0.43	5.72 ± 0.1	0.002*
High density lipoprotein, mmol/l	1.44 ± 0.18	1.52 ± 0.15	1.36 ± 0.21	0.353
Low density lipoprotein, mmol/l	2.73 ± 0.89	2.1 ± 0.46	3.37 ± 0.75	0.067
Glucose, mmol/l	4.66 ± 0.33	4.65 ± 0.15	4.67 ± 0.5	0.933
Insulin, pmol/l	53.15 ± 15.04	43.9 ± 12.36	62.4 ± 12.49	0.142
HOMA β-cell function, %	108.47 ± 19.13	95.9 ± 18.07	121.03 ± 10.69	0.107
HOMA insulin sensitivity, %	110.88 ± 36.32	131.1 ± 39.23	90.67 ± 23.07	0.199
HOMA IR (insulin resistance)	0.98 ± 0.29	0.80 ± 0.23	1.14 ± 0.26	0.158
ECFC characteristics	**Total (n=6)**	**Functional ECFC (n=3)**	**Dysfunctional ECFC (n=3)**	**P-Value**
Days for ECFC colony formation	16.33 ± 3.67	13.67 ± 0.58	1.15 ± 0.26	0.157
Proliferation rate (%)	21.03 ± 17.1	35.67 ± 2.19	19 ± 3.46	0.025*
Closed tube formed, n per $1.5x10^4$	8.57 ± 10.77	17.13 ± 8.36	6.39 ± 9.1	0.024*
Branches formed, n per $1.5x10^4$	20.28 ± 17.76	34.67 ± 12.36	0 ± 0	0.018*

Homeostatic model assessment (HOMA); endothelial colony-forming cell (ECFC). Data are expressed as mean ± standard deviation (SD). *P<0.05 between cell functionalities. Independent t-test.

5

The association of ECFCs with micro-vasculature and macro-vasculature remodelling in young adults with elevated blood pressure.



5. The association of ECFCs with micro-vasculature and macro-vasculature remodelling in young adults with elevated blood pressure

This chapter is based on:

"The association of circulating endothelial colony-forming cell dysfunction with micro-vascular structural changes in young adults with elevated blood pressure."

By

Cheryl M. J. Tan; Adam J. Lewandowski, Henner Hanssen, Lukas Zahner, Odaro J. Huckstep,

Roman Fischer, Maryam Alsharqi, Afifah Mohamed, Wilby Williamson,

Paul Leeson and Mariane Bertagnolli

Unpublished - in review (2022)

5.1 Abstract

Background

Hypertension involves anatomical and functional changes in the micro and macro-circulation. It includes endothelial dysfunction, micro-vascular rarefaction, vasoconstriction of the small arteries and arterioles in the peripheral circulation, obstruction, reduced circulatory efficiency, and increased susceptibility to ischemia, contributing to organ dysfunction. However, there is still an important gap in the knowledge of mechanisms linking endothelial and micro-vascular changes with high BP, particularly in young adults with elevated BP before the onset of hypertension. This chapter investigates associations between EC dysfunction and micro- or macro-vascular modifications in young adult subjects with elevated BP, also describing molecular mechanisms potentially involved in vascular changes.

Methods

Participants (n=32; 53% male, 28± 4 years old) with BP ≥120/80 mmHg were included in the elevated BP group, whereas ≤120/80 mmHg were deemed normotensive. Peripheral blood ECFCs were isolated using the Ficoll-density gradient centrifugation isolation method. Microvascular retinal assessment of retinal arterioles and venules was performed via static retinal vessel analyser. Macro-vascular modifications in the form of arterial stiffness were assessed via PWV measurements.

Results

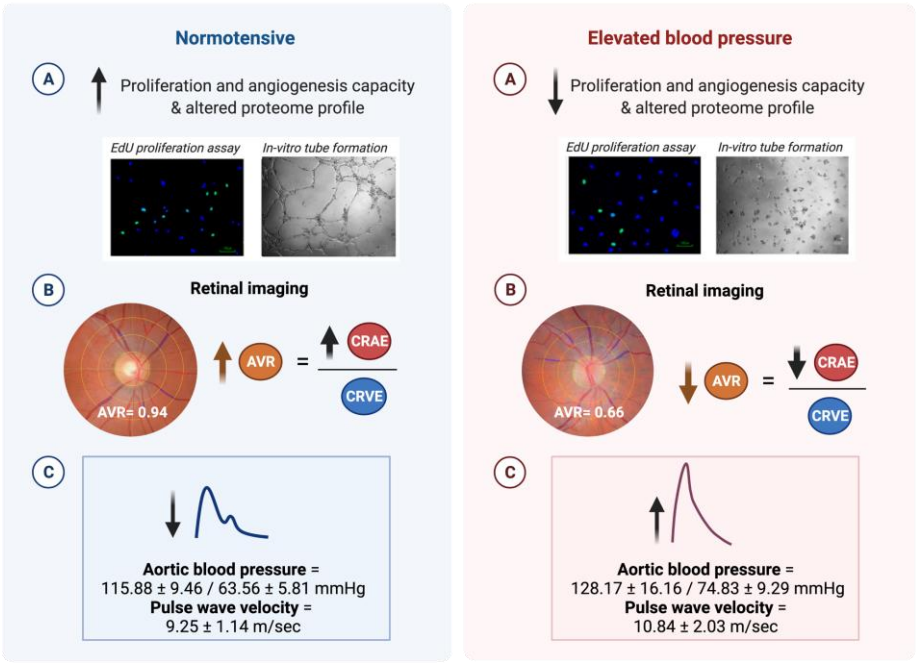
Subjects with elevated BP have significant (i) ECFC dysfunction (compromised proliferation and vasculogenic potentials), (ii) narrower retinal arteriole and (iii) increased macro-vascular resistance (increased PWV). Variation in the ECFC functionality, arteriolar-to-venular diameter ratio (AVR), CRAE and PWV were inversely correlated to systolic BP. Hierarchical functional clustering revealed distinct ECFC proteomic signatures between normotensive and elevated-BP ECFCs with changes in cellular mechanisms involved in exocytosis and vesicle transport. Further functional

enrichment analysis indicated a central role of the growth factor receptor-bound protein-2 (GRB2) gene in regulating ECFC function in young adults with elevated BP.

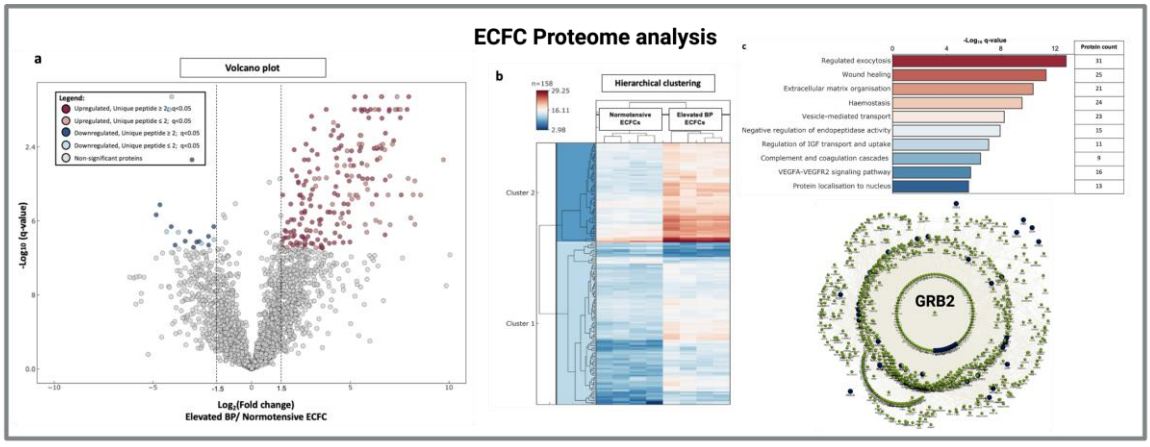
Conclusion

Our findings may implicate early EC dysfunction with altered EVs transport on micro-vasculature modifications in hypertension disease progression in young adults, which may represent a novel target for therapeutic and preventive intervention. Furthermore, the retinal micro-vascular network may represent a promising therapeutic and preventive target, considering the vital role of micro-circulation on EC function, macro-vascular dysfunction and potentially on incident hypertension.

Graphical Abstract



Abbreviations: ECFC, endothelial colony-forming cells; AVR, arteriolar to venular diameter ratio; CRAE, central retinal arteriolar equivalent; CRVE, central retinal venular equivalent (CRVE)



5.2 Introduction

Hypertension is a growing global public health concern. It identifies primary primordial risk factors for CVDs that result in cardiovascular morbidity and mortality[106-108]. The characteristics of hypertension involve anatomical and functional changes in cellular, micro-circulation and macro-circulation throughout the body. It includes micro-vascular rarefaction, vasoconstriction of the small arteries and arterioles in the peripheral circulation, obstruction, reduced circulatory and efficiency, increased susceptibility to ischemia, thereby contributing to organ dysfunction[107, 113, 114]. It is becoming increasingly well-supported that alteration on the EC, micro- and macro-vessels dysfunction to be associated with BP alterations and CVD risk factors such as hypertension[8, 76, 77, 119, 180, 355, 356].

A growing number of studies have suggested the participation of ECs in the pathogenesis of endothelial vascular dysfunction in hypertension[113, 148, 317]. However, the evaluation of ECs in clinical studies is still limited by methodological issues. Recently, we have observed ECFC dysfunction in pre-hypertension individuals and found that ECFC functionality to be associated with distinct proteome profiles and standard cardiovascular risk factors like cholesterol levels, body mass index, and BP [148]. Current findings further support that impairment of the ECs and vascular endothelium can precede the initiation and progression of CVDs, including hypertension and may be an early precursor for macro and micro-vascular dysfunction[5, 26, 149-152].

Micro-circulation dysfunction involves abnormal alteration of blood vessels characterised by a pro-thrombotic, pro-inflammatory, and pro-constrictive phenotype in the arterioles, capillaries and venules[114, 121-126]. By using dorsal finger venous occlusion capillaroscopy, several studies revealed that individuals with borderline hypertension and normotensive individuals with familial predisposition exhibit decreased numbers of dermal vessels, suggesting that rarefaction may be an early structural abnormality in essential hypertension[357-359]. BP-induced changes are prominent in peripheral dermal capillaries, including rarefaction of capillary, increased looping formation, transcapillary filtration and capillary resistance[360-362]. Similar is observed in retinal

micro-vasculature, where pathological changes have been identified as retinal arteriolar narrowing (lower CRAE) and retinal venular widening (higher CRVE), which result in an overall reduction of AVR have been shown to be associated with elevated BP[9, 118, 154, 164, 169, 170, 172, 173].

Macro-vasculature modifications in the form of aortic stiffening are associated with increased vascular resistance (PWV), which depends on micro-vascular density, tone, and structure[108, 180, 181]. The bidirectional relationship between aortic stiffness and systolic hypertension is well supported by epidemiologic evidence, suggesting a precursor role of aortic stiffening in incident hypertension[178]. Furthermore, arterial stiffening may also cause substantial BP variability and abnormal ventricular and arterial interactions that promote left ventricular hypertrophy, dysfunction, and fibrosis[108, 179].

The remodelling of the circulatory network seems to be a common denominator contributing to end-organ damage in individuals with elevated BP[178]. However, the complex relationship between endothelial dysfunction, micro-, macro-circulation, and hypertension in terms of cause and effect remains unclear. It is partly because of the multiplicity of causal factors potentially implicated in their pathophysiology, including vascular ageing, genetic, epigenetic, environmental, nutritional, and metabolic factors and the lack of investigation[178].

5.2.1 Study hypotheses, aims, and clinical significance

Studies have shown that impairment of blood supply to large arteries via the vasa vasorum leads to large artery remodelling and arterial stiffening[363]. This suggests that micro-circulatory abnormalities may further represent an indirect marker of macro-vascular alterations with an increase in arterial stiffness via an increase in peripheral resistance, mean arterial BP, central systolic and pulse pressure[178, 364-366]. However, there is still an important gap in the knowledge of mechanisms linking EC, micro-, macro-vascular changes and high BP, particularly in young adults with elevated BP.

Thus, this chapter seeks to uncover the relationship between EC function, retinal micro-vascular, macro-vascular resistance (arterial stiffness, PWV) and BP changes. We hypothesised that elevation in BP would result in adverse modifications in:

I. ECFC functions and proteome profiles.
II. Retinal micro-vasculature remodelling including the narrowing of retinal arterioles and widening of retinal venules
III. Macro-vasculature in the form of increased macro-vascular resistance (PWV).

To address the hypotheses, we aimed to:

I. Describe differences in ECFC function, micro-vascular and macro-vascular remodelling in individuals with elevated BP and correlations between cellular and vascular changes.
II. Identifying molecular mechanisms in ECFC that may associate with vascular changes in subjects with elevated BP.

Understanding the interactions will not only allow a better understanding about vascular alterations in incident hypertension but also provide new insights for a preventive and therapeutic target for hypertension.

5.3 Methodology

5.3.1 Study population and general methods

The study population selected for this chapter includes all 32 young adults with ECFCs isolated and had completed baseline visit 1. Details of the study are outlined in **Chapter 2 – Study population, Section 4.1.**

The following methods that were used for this chapter are described in detail in **Chapter 3**:

3.1 Anthropometric measurements

3.2 BP measurements

3.3 Blood sample collection and biochemistry analysis

3.4 ECFC isolation and cellular assessments

3.4.1 Fluorescence-activated cell sorting (FACS)

3.4.2 Immunofluorescence staining

3.4.3 EdU proliferation assay

3.4.4 In vitro tube formation assay

3.4.5 Proteomic analysis of ECFCs

5.3.2 Static retinal vessel analysis (SVA)

Static Retinal Vessel Analyzer (SVA-T, Imedos Systems, Germany) was used to capture three valid images of the retina of the left and the right eye, with the optic disk in the centre for static retinal vessel analysis **(Figure 5.1 a and b)**. The detailed procedure was described previously[367]. Briefly, retinal arterioles and venules, coursing through an area of 0.5–1 disc diameter from the margin of the optic disc, were identified semi-automatically using an analyzing software identifying retinal vessels in ring-zones (Vesselmap 2, Visualis, Imedos Systems UG **(Figure 5.1 c)**. Diameters were averaged to CRAE and CRVE using the Parr-Hubbard formula[162]. CRAE and CRVE values were used to calculate the AVR, taking the mean of the right and left eye results.

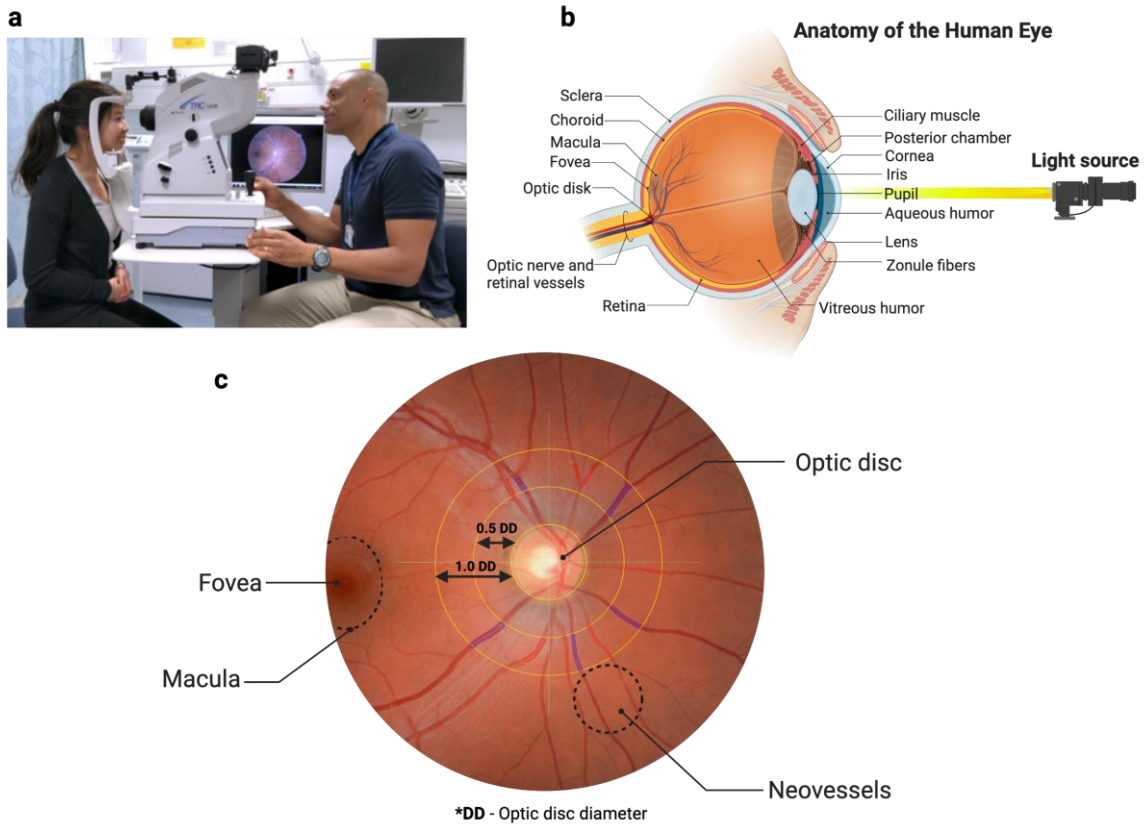


Figure 5.1. Schematic representation of retinal imaging and anatomy of the human eye.

(a) The setup for retinal imaging using Static Retinal Vessel Analyzer (SVA-T, Imedos Systems UG, Jena, Germany). **(b)** Image representation of the human eye. **(c)** All retinal arterioles (red) and venules (blue) that pass completely through the circumferential zone 0.5 to 1 disc diameter from the optic disc margin are evaluated. The retinal vascular calibres are calculated using the revised Parr-Hubbard formulas using the Vesselmap 2, Visualis, Imedos Systems software.

5.3.3 Vicorder measurements

Resting measures of brachial-femoral PWV and aortic BP were derived using sphygmomanometer-derived indices (Vicorder, Skidmore Medical, Taunton, UK) with cuffs placed around brachial and femoral arteries to identify pulse arrival times as described[368, 369] **(Figure 5.2)**. PWV was derived from recording the time delay between the two measurement sites relative to the distance between the predefined landmarks.

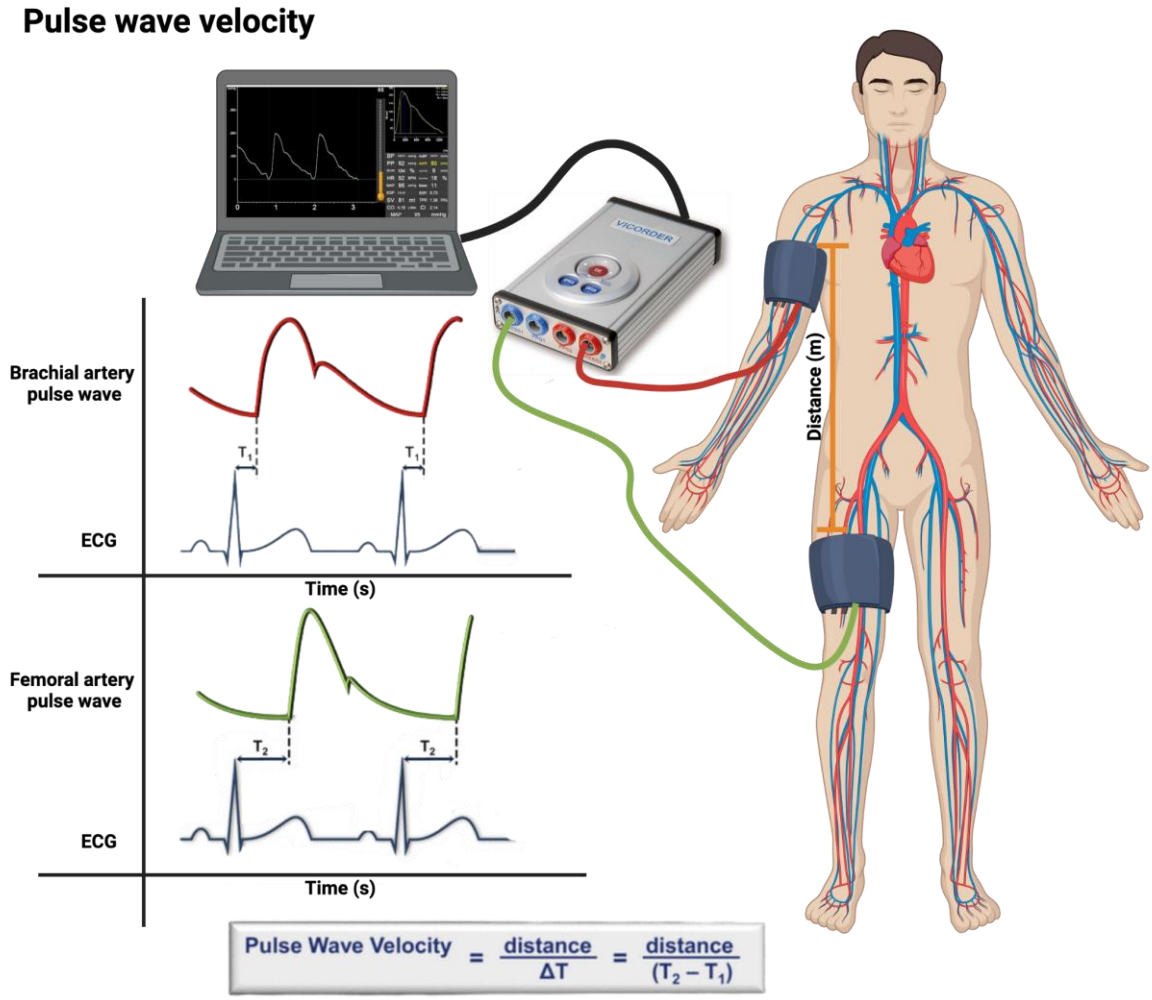


Figure 5.2. Schematic representation of brachial-femoral pulse wave velocity (PWV).

Waveform are sequentially obtained from the right brachial arteries and femoral arteries using Vicorder® apparatus. PWV is estimated as the distance between the brachial and femoral sampling sites divided by the time delay between the 2 waveforms.

5.3.4 Proteomics data analysis

5.3.4.1 Enriched gene ontology clustering

The proteomic data were filtered per row for 70% of the valid values, followed by imputation of missing values and ≥ 2 identified peptides. Student's T-tests were used to make comparisons between the groups and genes satisfying a difference of -1.5< $\log_2$(fold change) >1.5, and FDR-corrected p-value (named q-value) were calculated using the Benjamini-Hochberg procedure to account for multiple testing) <0.05 was considered statistically significant. Statistically

significant proteins were used to identify all statistically enriched GO/KEGG terms and network reconstruction using the Metascape tool (http://metascape.org). Imputing the gene set obtained from statistical significant proteins, pathway and enrichment analyses were carried out by selecting the genomics sources: KEGG Pathway, GO Biological Processes, Reactome Gene Sets, Canonical Pathways, and CORUM[322]. Functional protein association networks of identified proteins were created using STRING (http://www.string-db.org) and InstantClue software[316]. Gene Ontology enRIchement anaLysis and visuaLisAtion (Gorilla) (http://cbl-gorilla.cs.technion.ac.il/) was used for identifying and visualising enriched GO terms in ranked lists of genes[370].

5.3.4.2 Principal component analysis

The logarithm values of protein expression were submitted to principal component analysis (PCA) and in the R-package "FactoMineR" and "FactoExtra" with the generation of graphical output. Analysis was completed with the help of the DPhil student Daan Paget.

5.3.5 Statistical analysis

Statistical analysis was performed using SPSS (version 25, IBM, North Castle, NY, USA). Shapiro-Wilk testing and visual inspection were used to assess whether variables were normally distributed. Dependent on the normality of sample distribution, comparisons between normotensive and elevated BP groups were performed by either parametric independent t-test or non-parametric Mann-Whitney U test. Categorical variables were compared by $\chi 2$ or Fisher Exact tests. Comparisons between groups were performed by ANCOVA statistical test having only sex or sex and glucose as covariates. Linear regression modelling was performed using forced entry with missing data excluded pairwise. Model analyses were performed using multiple linear regression, with systolic BP being the dependent variable. Standardised regression coefficients (β) are

presented for multivariate linear regressions. Results are presented as mean ± standard deviation (SD) unless stated otherwise. P values ≤ 0.05 were considered statistically significant.

Results are presented as mean ± standard deviation (SD) unless stated otherwise. A p-value ≤ 0.05 was considered statistically significant, and a 95% confidence interval was used. When appropriate, p-values were adjusted for sex.

5.4 Results

5.4.1. Clinical characteristics of the study population

The rates of successful ECFCs isolation are between 45.1% (32/71 participants) based on our study. Based on our analysis, no significant changes in clinical measurements were observed between individuals with or without ECFC colony formation **(Supplemental Table S1)**. The clinical characteristics of our study population are presented in

Table 5.1**.** No difference was observed between groups for the number of male/female subjects or their age, height, weight, and BMI. Significant differences were observed between groups in resting systolic (114±8 versus 133±10 mmHg, P<0.001), diastolic (69±7 versus 87±7 mmHg, P<0.001), and mean BP (86±6 versus 104±7 mmHg, P<0.001). Both groups displayed similar blood biochemistry profiles, with no significant differences observed in triglycerides, lipid profiles, insulin, Homeostasis Model Assessment (HOMA) β-cell, HOMA β-cell sensitivity and HOMA insulin resistance between groups, apart from a higher fasting glucose level in the elevated BP group (4.7±0.2 versus 5.1±0.4 mmol/L, P=0.038).

Table 5.1. Clinical characteristics of the study population

Demographics and anthropometrics	Total (n=32)	Normotensives (n=16)	Elevated BP (n=16)	P-Value*
Male, n	17	8	9	<0.999
Female, n	15	8	7	
Age, years	28.12 ± 4.4	28.06 ± 4.65	28.19 ± 4.28	0.75
Height, cm	172.96 ± 9.89	172.18 ± 7.7	173.75 ± 11.9	0.90
Weight, kg	75.7 ± 14.25	73.2 ± 11.5	78.21 ± 16.55	0.29
BMI, kg/m^2	25.18 ± 3.34	24.64 ± 3.11	25.71 ± 3.59	0.21
Total body fat, %	25.66 ± 9.67 (28)	26.34 ± 9.65 (13)	25.06 ± 9.99 (15)	0.86
Total fat mass, kg	25.33 ± 3.19 (28)	24.67 ± 2.75 (13)	25.89 ± 3.52 (15)	0.50
Total fat free mass, kg	56.63 ± 12.19 (28)	53.75 ± 9.3 (13)	59.13 ± 14.07 (15)	0.33
Waist-hip ratio	0.88 ± 0.31 (30)	0.93 ± 0.42	0.82 ± 0.07 (14)	0.63
Gestational age, weeks	37.88 ± 3.43	37.25 ± 3.79	38.5 ± 3.03	0.16
Clinic seated BP				
Systolic BP, mmHg	**123.91 ± 13.24**	**114.37 ± 8.36**	**133.44 ± 9.94**	**<0.001**
Diastolic BP, mmHg	**77.84 ± 11.2**	**69.19 ± 7.07**	**86.5 ± 7.01**	**<0.001**
Mean arterial BP, mmHg	**95.12 ± 11.52**	**85.88 ± 6.11**	**104.38 ± 7.39**	**<0.001**
Heart rate, beats per min	70.81 ± 10.91	71.06 ± 12.35	70.56 ± 9.65	0.79
Blood biochemistry				
Triglyceride, mmol/l	1.07 ± 0.65	0.91 ± 0.4 (14)	1.21 ± 0.8	0.25
Cholesterol, mmol/l	4.58 ± 0.73	4.45 ± 0.75 (14)	4.7 ± 0.71	0.25
High density lipoprotein, mmol/l	1.39 ± 0.3	1.45 ± 0.29 (14)	1.34 ± 0.3	0.51
Low density lipoprotein, mmol/l	2.59 ± 0.67	2.51 ± 0.65 (14)	2.66 ± 0.71	0.24
Glucose, mmol/l	**4.9 ± 0.36**	**4.73 ± 0.24 (14)**	**5.06 ± 0.38**	**0.038**
Insulin, pmol/l	49.23 ± 26.7	47.97 ± 22.56 (14)	50.33 ± 30.57	0.74
HOMA β-cell, %	93.54 ± 25.99 (28)	98.58 ± 22.66 (13)	89.18 ± 28.61 (15)	0.51
HOMA β-cell sensitivity, %	126.39 ± 54.32 (28)	127.74 ± 54.79 (13)	125.21 ± 55.8 (15)	0.91
HOMA Insulin resistance	0.96 ± 0.49 (28)	0.93 ± 0.4 (13)	0.99 ± 0.57 (15)	0.67
C-reactive protein, mg/l	2.6 ± 4.38 (28)	2.8 ± 5.75 (13)	2.43 ± 2.94 (15)	0.84

Data are expressed as mean ± standard deviation (SD). BP, blood pressure; BMI, body mass index; HOMA, Homeostasis Model Assessment. * Comparison between normotensive and Elevated-blood pressure (BP) participants and P-values corrected for sex. Independent t-test or χ^2 test. Mean ± standard deviation (SD).

5.4.2. ECFC functional characteristics in subjects with normal versus elevated BP

Comparisons of ECFCs functional characteristics between groups revealed that subjects with elevated BP have slower ECFC colony growth (18.3 ± 5.4 versus 13.9 ± 3.9 days, P=0.016, **(Figure 5.3 c)**. Some ECFCs have grown small colonies in the first 30 days in culture but did not reach enough confluence to perform additional functional tests. From those reaching a successful expansion, ECFCs of subjects with elevated BP have a significantly lower proliferation rate (13.9 ± 17.7 versus 26.8 ± 13.3 % of total cells, P=0.037, **Figure 5.3 d**), and reduced angiogenic capacity indicated by the number of closed tubes formed *in vitro* (2.9 ± 7.2 versus 9.0 ± 7.9 number of closed tubes per 1.5 x 10^4 cells, P=0.034, **Figure 5.3 e**) and the number of tube branching (10.2 ± 13.0 versus 24.1 ± 17.1 number of branches per 1.5 x 10^4 cells, P=0.017, **Figure 5.3 f)** compared to normotensive subjects. However, after adjusting these comparisons for sex and glucose levels, we found that the days to form ECFC (P=0.023) and proliferation rate (P=0.033) remained statistically significantly different. However, the numbers of closed tubes (P=0.092) and branches formed (P=0.059) were no longer significantly different.

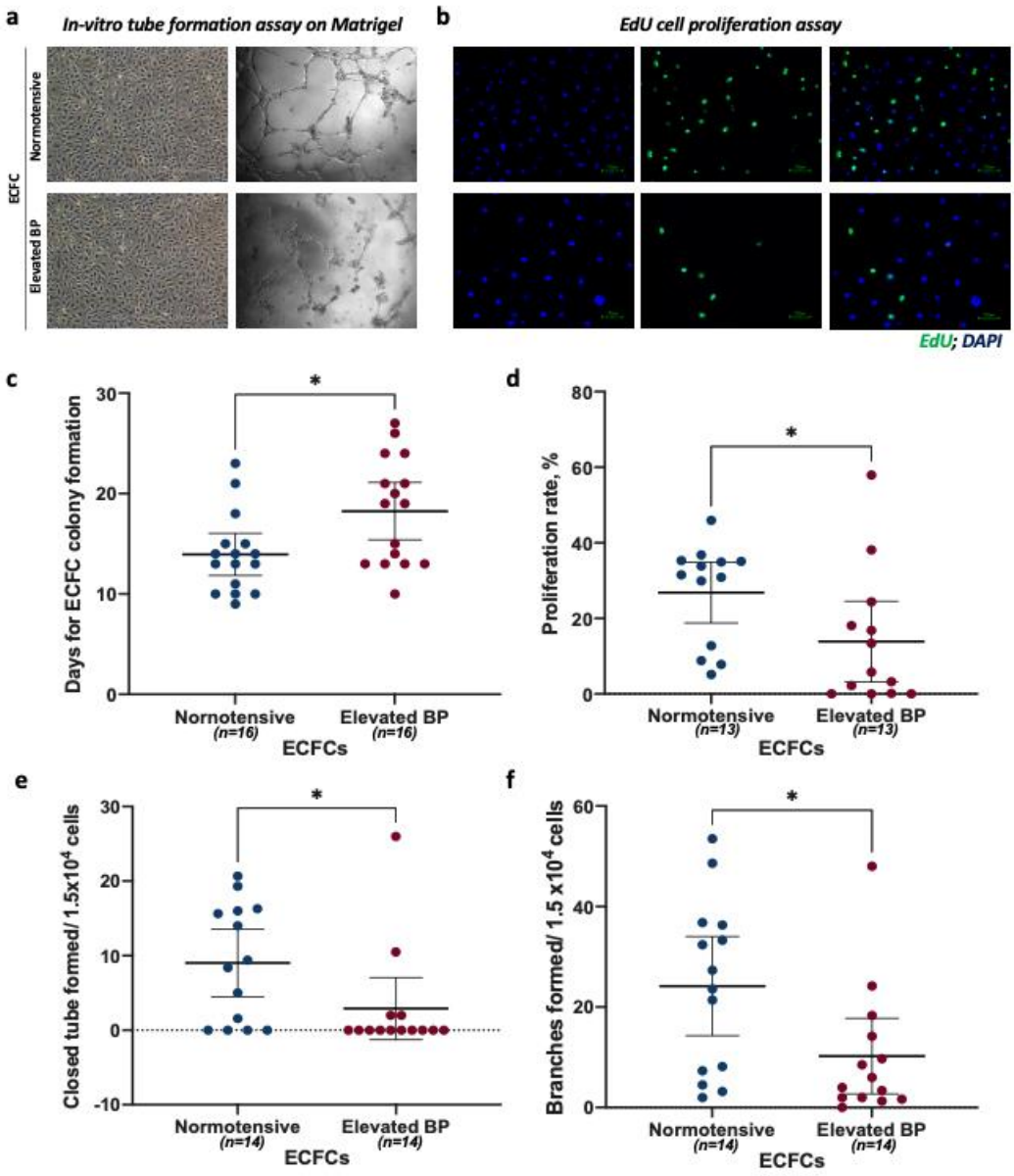


Figure 5.3. Comparisons of endothelial colony-forming cells (ECFCs) functional features between subjects with normal versus elevated blood pressure (BP).

(a) ECFC tube formation capacity was assessed using Matrigel tube formation assay with the numbers of total branches and closed tubes formed quantified in phase-contrast images (5x objective). **(b)** Proliferation rate was determined by DNA Edu incorporation (AlexaFluor 488, green), with nuclei counterstained with 4',6-diamidino-2-phenylindole (DAPI, blue) (10x objective) **(c-f)**. Scatter plots representing respective ECFC clusters for each of the following cell characteristics: **(c)** days for ECFC colony formation, **(d)** proliferation rate (%), **(e)** total closed tubes formed per $1.5x10^4$ cells, and **(f)** total branching formed per $1.5x10^4$ cells. Comparison between normotensive and elevated BP groups by ANCOVA having sex as a covariate. Data presented as mean ± standard deviation (SD). * $P<0.05$.

5.4.3 Retinal micro-vasculature characteristics in subjects with normal versus elevated BP

Fundoscopy of both left and right eyes of the participants revealed that the group of subjects with elevated BP has reduced CRAE (169.1 ± 20.0 µm vs 187.2 ± 11.2 µm, P<0.01, **Figure 5.4 a**) without significant difference in CRVE values between groups (**Figure 5.4 b**). Consequently, AVR was significantly lower in subjects with elevated BP (0.81 ± 0.07 vs. 0.88 ± 0.07, P<0.001, **Figure 5.4 c**). Differences on CRAE and AVR remained statistically significant after adjustment for sex and glucose levels.

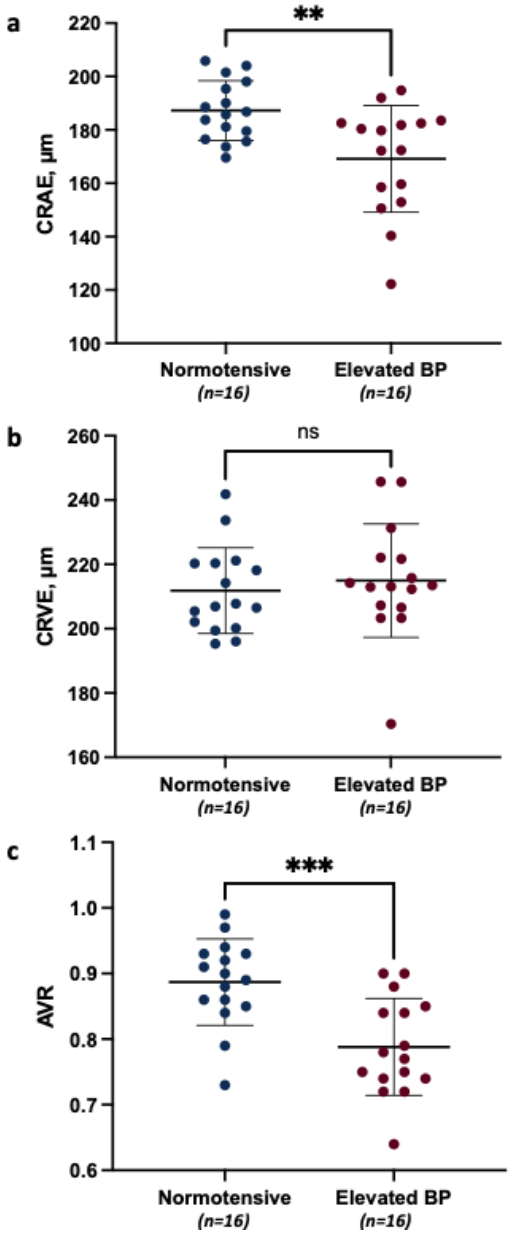


Figure 5.4. Retinal calibre assessment of subjects with normal versus elevated blood pressure (BP).

Fundoscopy was used to assess (**a**) central retinal arteriolar equivalent (CRAE), (**b**) central retinal venular equivalent (CRVE), and (**c**) arteriole–venular ratio (AVR). Comparison between normotensive and elevated BP groups by ANCOVA having sex as covariate (n=16 per group). Data presented as mean ± standard deviation (SD). ** P<0.01 and *** P<0.001.

5.4.3.1 Association between EC function and retinal micro-vasculature in subjects with normal and elevated BP

We used linear regression analyses to assess correlations between ECFC function and micro-vascular changes (complete data in **Supplementary Table S5.1**). Our results were adjusted for sex and demonstrated negative correlations between the number of days taken for ECFC colony formation and arterioles diameter represented by CRAE (r^2= 0.19, P=0.021, **Figure 5.5 a**) and AVR (r^2= 0.12, P=0.019, **Figure 5.5 b**). Adjustments for glucose levels has not changed the significance of these correlations.). Our results were adjusted for sex and demonstrated negative correlations between the number of days taken for ECFC colony formation and arterioles diameter represented by CRAE (r^2= 0.19, P=0.021, **Figure 5.5 a**) and AVR (r^2= 0.12, P=0.019, **Figure 5.5 b**). Adjustments for glucose levels has not changed the significance of these correlations.

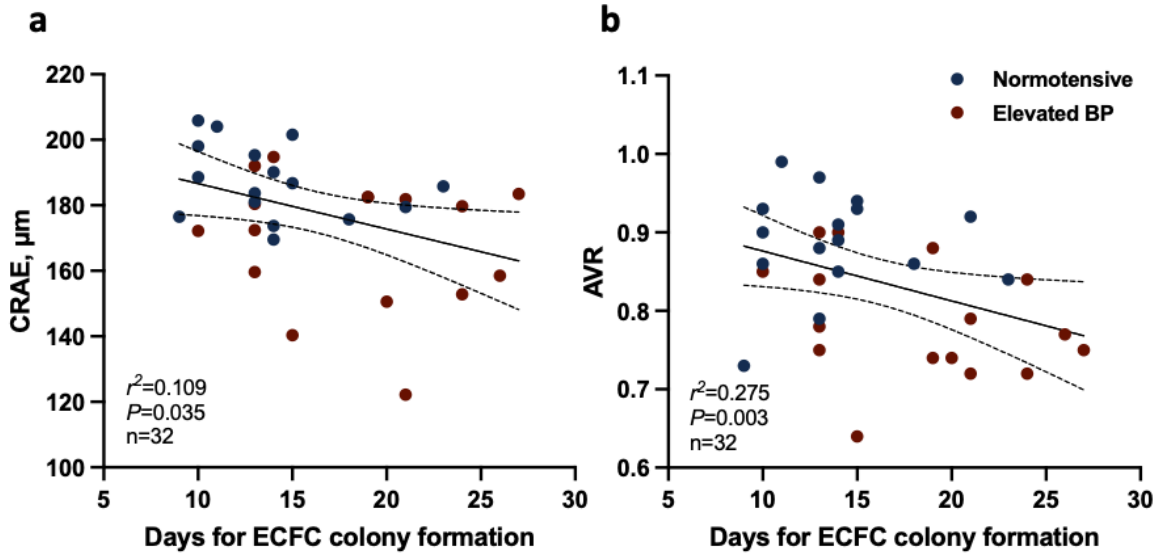


Figure 5.5. Linear regression between endothelial colony-forming cell (ECFC) functional parameters and retinal vascular calibre.

The days taken for ECFC colony formation is negatively correlated with (**a**) central retinal arteriolar equivalent (CRAE) (r^2= 0.185, P=0.016) and (**b**) arteriole–venular ratio (AVR) (r^2= 0.12, P=0.019). Linear regression adjusted for sex. Normotensive and elevated blood pressure (BP) individuals are represented by blue and red circles, respectively.

5.4.4 Macro-vascular resistance – pulse wave velocity characteristics in subjects with normal versus elevated BP

Consistent with other findings, we showed that elevated BP individuals had significantly higher peripheral and central aortic systolic and diastolic BP **(Table 5.2)**. Furthermore, we showed that participants with high BP to have higher macro-vascular resistance (PWV = 10.84 ± 2.03 m/sec) as compared to normotensives (PWV = 9.98 ± 1.79 m/sec) (P<0.022). Differences in Vicorder parameters, including peripheral systolic BP, peripheral diastolic and central aortic BP, remained statistically significant after adjustment for sex and glucose levels. Missing data was due to machine malfunction, no data acquired or data loss during data transfer (n=6).

Table 5.2. Vicorder assessment of participants

Vicorder parameters	Total (n=32)	Normotensives (n=16)	Elevated BP (n=16)	P-Value*
Peripheral systolic BP, mmHg	128 ± 14.28 (28)	121.81 ± 10.05	136.25 ± 15.26 (12)	0.007
Peripheral diastolic BP, mmHg	68.39 ± 9.28 (28)	63.56 ± 5.81	74.83 ± 9.29 (12)	0.001
Central aortic systolic BP, mmHg	121.14 ± 13.95 (28)	115.88 ± 9.46	128.17 ± 16.16 (12)	0.021
Central aortic diastolic BP, mmHg	68.39 ± 9.28 (28)	63.56 ± 5.81	74.83 ± 9.29 (12)	0.001
Pulse wave velocity, m/sec	9.98 ± 1.79 (26)	9.25 ± 1.14 (15)	10.84 ± 2.03 (11)	0.022

Data are expressed as mean ± standard deviation (SD). *Comparison between normotensives and elevated blood pressure (BP) participants and P-values corrected for sex. Independent t-test.

5.4.4.1 Association between EC function and macro-vascular resistance in subjects with normal and elevated BP

Complete linear regression data of systolic BP and ECFCs function or macro-vascular changes (PWV) are presented in **Supplementary Table S5.2**, and the significant relationship is summarised in **Figure 5.6**. Our data demonstrated that PWV to be negatively associated to ECFC angiogenic capacity (the numbers of ECFC closed formation) (r2= 0.268, p=0.017) **(Figure 5.6).** Differences in PWV and ECFC branches were statistically insignificant after sex and glucose levels adjustment.

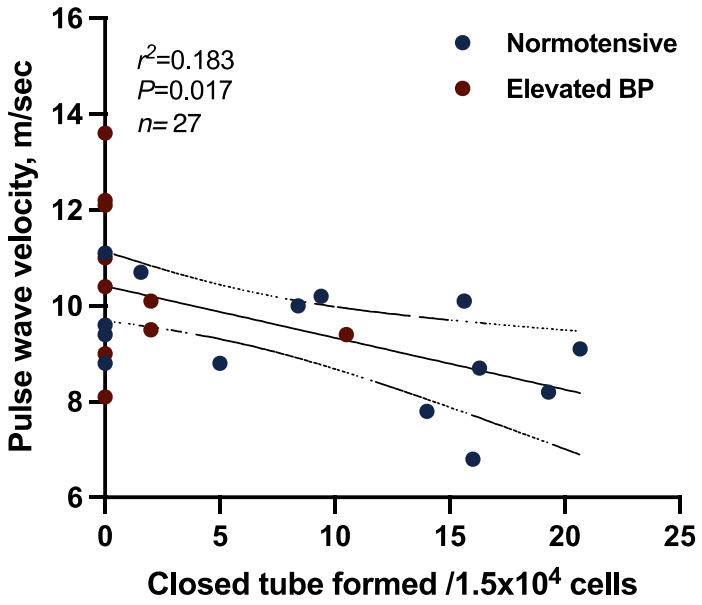


Figure 5.6. Linear regression between pulse wave velocity and endothelial colony-forming cells (ECFC) angiogenic capacity (closed tube formation).

PWV is negatively associated with ECFC closed tube formation. Linear regression adjusted for sex.

5.4.5 Relationship between systolic BP, EC function, micro-vasculature and PWV changes

5.4.5.1 Relationship between micro and macro-vascular changes

PWV was also significantly correlated with retinal vessel calibre (CRAE; r^2= 0.40, p=0.001**,** **Figure 5.7 a** and AVR; r^2= 0.269, p=0.006, **Figure 5.7 b**). The correlation between PWV and AVR remain statistically significant after correction for sex and glucose.

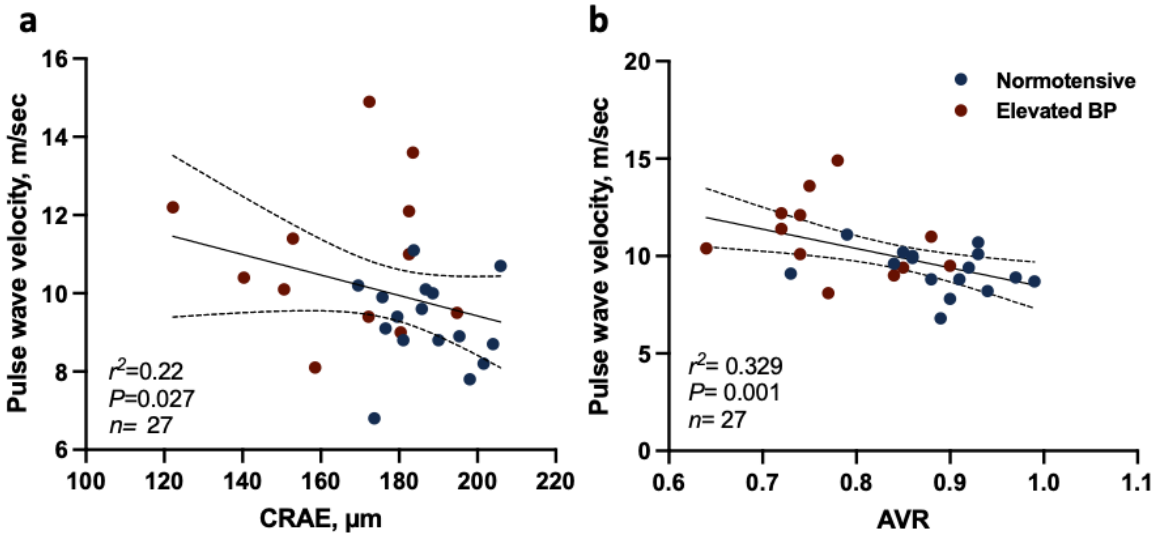


Figure 5.7. Linear regression between pulse wave velocity (PWV) and retinal micro-vasculature calibre.

PWV is negatively correlated with **(a)** central retinal arteriolar equivalent (CRAE) and **(b)** arteriolar-to-venular diameter ratio (AVR). Linear regression adjusted for sex. Normotensive and elevated blood pressure (BP) individuals are represented by blue and red circles, respectively.

5.4.5.2 Relationship between systolic BP and ECFC, micro and macro-vascular changes

Complete linear regression data of systolic BP and ECFCs function, micro-vascular changes or PWV are presented in **Supplementary Table S5.3** and summarised in **Figure 5.8**. Significant negative correlations were observed only either between systolic BP and ECFCs proliferation rate (r^2=0.155, p=0.036, **Figure 5.8 a**), CRAE (r^2= 0.505, P<0.001, **Figure 5.8 b**) or with AVR (r^2= 0.477, P<0.001, **Figure 5.8 c**). Negative correlation was observed between systolic BP and PWV (r^2=0.168, n=27, P<0.017, **Figure 5.8 d**). All interactions were still significant after correction for sex and glucose.

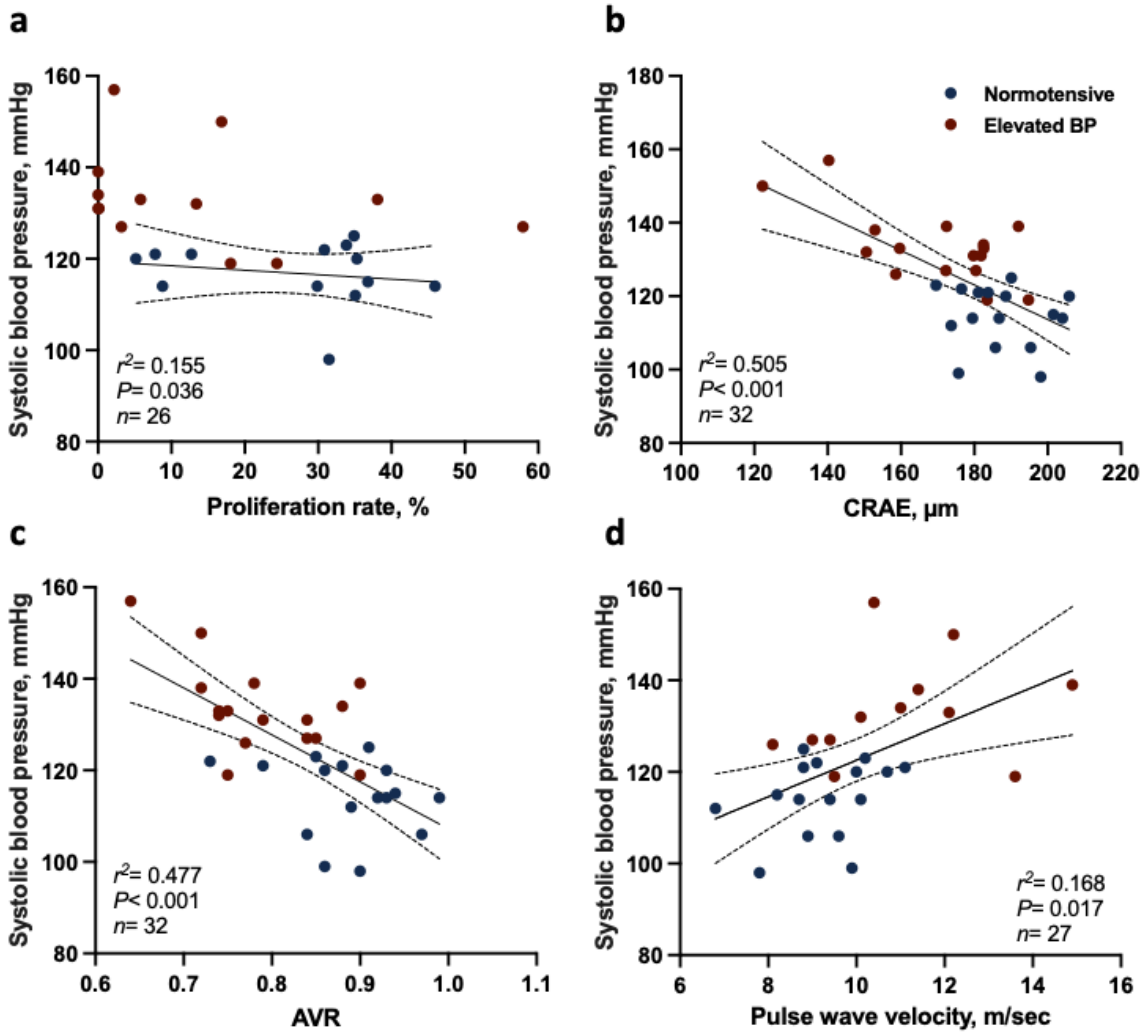


Figure 5.8. Relationship between systolic blood pressure (BP) and endothelial colony-forming cell (ECFC) function, micro-vascular structure, and pulse wave velocity in young adults.

Systolic BP negatively correlated with **(a)** proliferation rate (r^2= 0.155, n=26, P=0.036), **(b)** central retinal arteriolar equivalent (CRAE) (r^2= 0.505, n=32, P<0.001), **(b)** arteriole–venular ratio (AVR) (r^2= 0.477, n=32, P<0.001), and **(d)** pulse wave velocity (r^2=0.168, n=27, P<0.017). Linear regression adjusted for sex. Normotensive and elevated blood pressure (BP) individuals are represented by blue and red circles, respectively.

5.4.5.3 Multiple regression model of systolic BP

Multiple linear regression was then used to test models of clinical parameters potentially influencing BP in our study population (**Table 5.3)**. We used sex, significant ECFC, micro- and macro-vascular parameters in these models. Our results show that ECFC proliferation rate and CRAE can independently correlate with systolic BP (Model 1, P<0.001). However, in Model 2, when assessing

correlations with AVR, ECFC proliferation rate no longer correlates with systolic BP (P=0.25). We observed no significant correlation between systolic BP with ECFC proliferation in models including PWV (P=0.1, Model 3). To investigate the micro-vascular and PWV, our result showed that retinal micro-vasculature (CRAE and AVR) to me significant of predicting systolic BP (P<0.001). Furthermore, our data demonstrate that in all models, micro-vascular parameters CRAE and AVR have independently strongly correlated with systolic BP (P<0.001 in Models 1, 4 and 5, P=0.002 in Model 2).

Table 5.3. Multiple linear regression with systolic blood pressure (BP) as dependent variable.

Model	B_{model} (95% CI)	$r_{partial}$	P	Adjusted R^2	P
Model 1					
Sex	-0.14 (-10.83, 4.29)	-0.90	0.38		
ECFC proliferation rate, %	**-0.35 (-0.46, -0.06)**	**-2.64**	**0.015**	0.59	**<0.001**
CRAE	**-0.72 (-0.66, -0.26)**	**-4.84**	**<0.001**		
Model 2					
Sex	-0.17 (-14.83, 5.92)	-0.898	0.38		
ECFC proliferation rate, %	-0.197 (-0.431, 0.119)	-1.188	0.25	0.44	**0.001**
AVR	**-0.62 (-139.87, -33.87)**	**-3.596**	**0.002**		
Model 3					
Sex	0.22 (-4.71, 15.9)	0.22	0.27		
ECFC proliferation rate, %	-0.37 (-0.64, 0.06)	-0.37	0.1	0.26	**0.044**
PWV, m/s	0.36 (-0.68, 6.48)	0.36	0.11		
Model 4					
Sex	**-0.38 (-17.7, -2.52)**	**-2.75**	**0.011**		
CRAE	**-0.80 (-0.75, -0.36)**	**-5.86**	**<0.001**	0.65	**<0.001**
PWV, m/s	0.14 (-1.08, 3.25)	0.31	0.31		
Model 5					
Sex	-0.28 (-16.31, 1.24)	-1.78	0.09		
AVR	**-0.73 (-166.17, 3.11)**	**-4.21**	**<0.001**	0.51	**<0.001**
PWV, m/s	0.03 (-2.67, 3.11)	0.16	0.88		

Central retinal arteriolar equivalent (CRAE); arteriole–venular ratio (AVR); pulse wave velocity (PWV)

5.5.6 Proteomic signature of ECFCs from subjects with normal and elevated BP

5.5.6.1. Gene ontology, hierarchical and PCA analysis

A total of 2691 proteins were quantified, with 158 proteins demonstrating significant differential abundance between the compared conditions based on unique peptides ≥ 2 and either $\log_2$(fold change) ≥ 1.5 or ≤ -1.5 (145 upregulated and 13 downregulated proteins) from n=4 per group age and sex-matched **(Figure 5.9 a and b)**. Baseline clinical characteristics are described in **Supplementary Table S5.4** and ECFC, retinal micro-vasculature and vicorder parameters are presented in **Supplementary Table S5.5.**

The analysis of gene ontology revealed the top 10 enriched pathways being the following: 1) platelet degranulation, 2) regulated exocytosis, 3) regulation of haemostasis, 4) ECM organisation, 5) regulation of coagulation, 6) neutrophil-mediated immunity, 7) blood coagulation, 8) secretion by cell, 9) neutrophil degranulation, 10) negative regulation of wound healing **(Figure 5.9 a).** Heatmaps of proteins identified in each pathway are shown in **Supplementary Figure S5.1.**

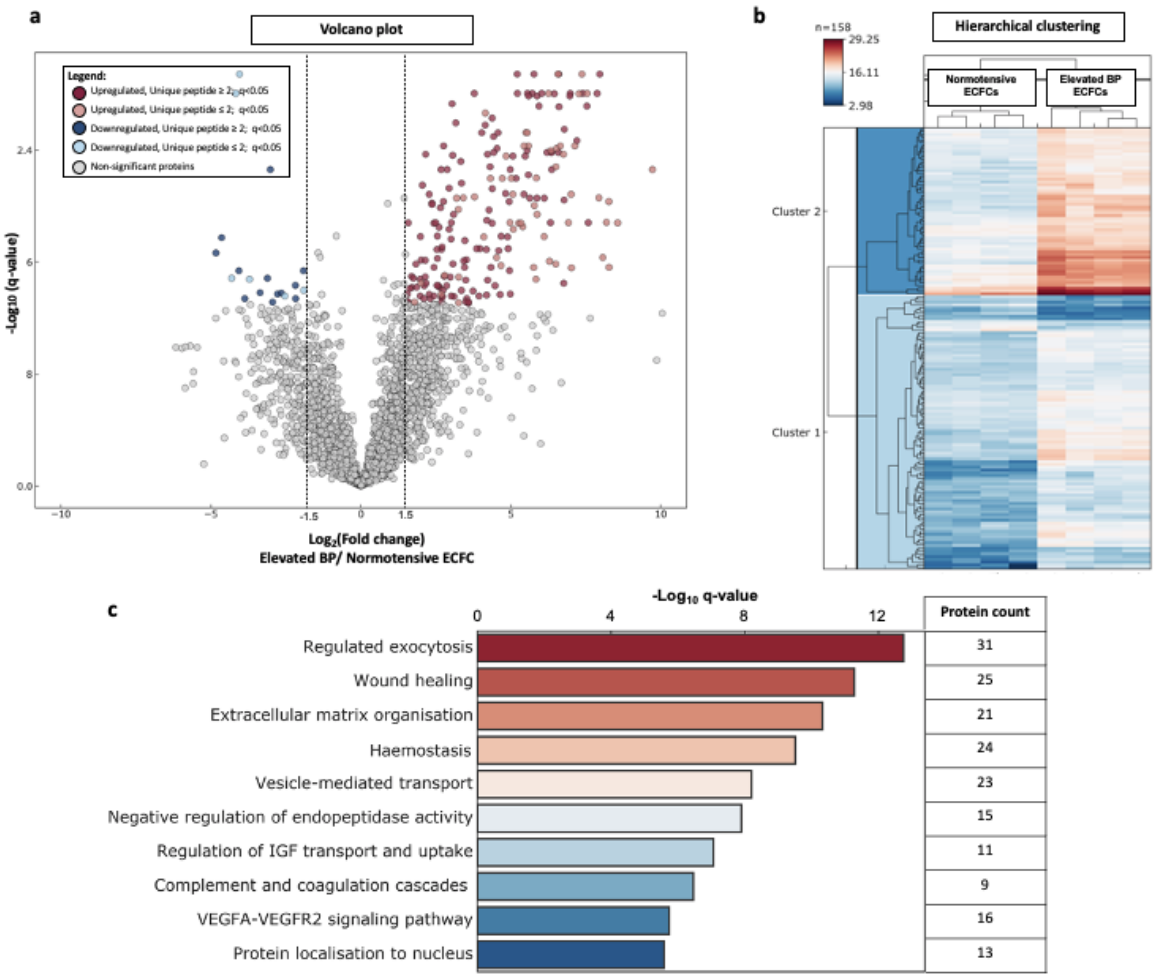


Figure 5.9. Proteomics analysis of normotensive and elevated blood pressure endothelial colony-forming cells (ECFCs).

(a) Volcano plot shows significantly regulated proteins between normotensive and elevated blood pressure ECFCs, after FDR correction for multiple testing. A total of 2691 proteins were quantified with 158 proteins demonstrating significant differential abundance between the compared conditions based on unique peptides ≥ 2 and either log_2(fold change) ≥ 1.5 or ≤ -1.5 (145 upregulated and 13 downregulated proteins). **(b)** Unsupervised hierarchical clustering (Euclidean distance) distinguishes samples according to their group and shows distinct protein abundance profiles indicative of grouping. **(c)** Significantly changed proteins show enrichment gene ontology biological pathways. Protein count represents the number of proteins involved in the respective biological pathway.

PCA of the ECFC proteomic data, clinical parameters including sex, fasting glucose levels, clinical BP, and ECFC function, micro and macro-vascular characteristics from normotensive and elevated BP individuals, exhibited a clear separation in PCA between the different BP groups

between PCA component 1, 2 and 3 **(Figure 5.10)**. With PC 1 capturing the largest variance of the data (87.4%), followed by PC2 (3.9%) and PC3 (3%).

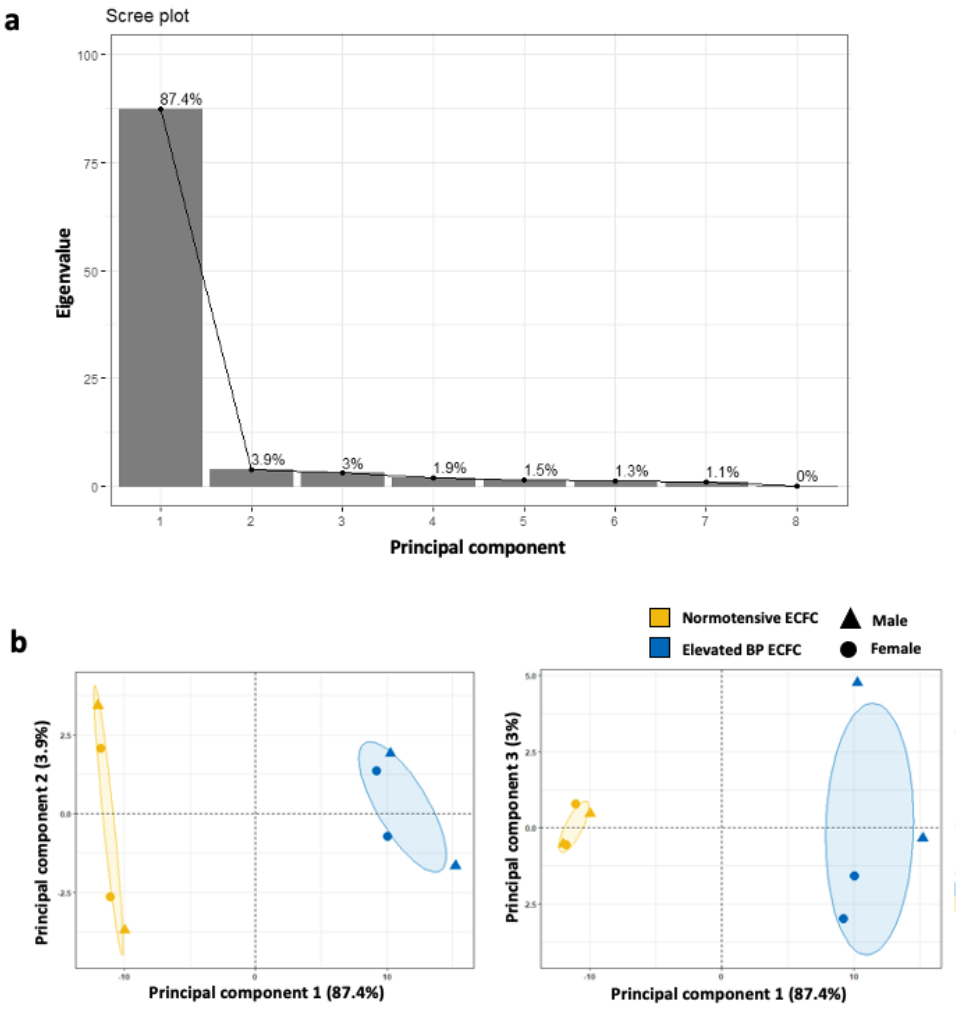


Figure 5.10. Principal component analysis (PCA) of functional and dysfunctional endothelial colony-forming cells (ECFCs).

(a) Scree plots showing the eigenvalue (%) of all the principal components for the analysis. **(b)** The PCA plot represents 8 participants that indicated clear proteomics profile differences between functional and dysfunctional ECFC are represented in yellow and blue colours respectively and sex are represented in matching symbols (male – triangle and female – circle).

Contributions of variables to the PCA component 1 to 3 are presented in **Figure 5.11**. The top-ranked contributors for PCA component 2 include clinical parameters such as diastolic BP, AVR, MAP, glucose level, systolic BP, CRAE and closed tube (**Figure 5.11 c).**

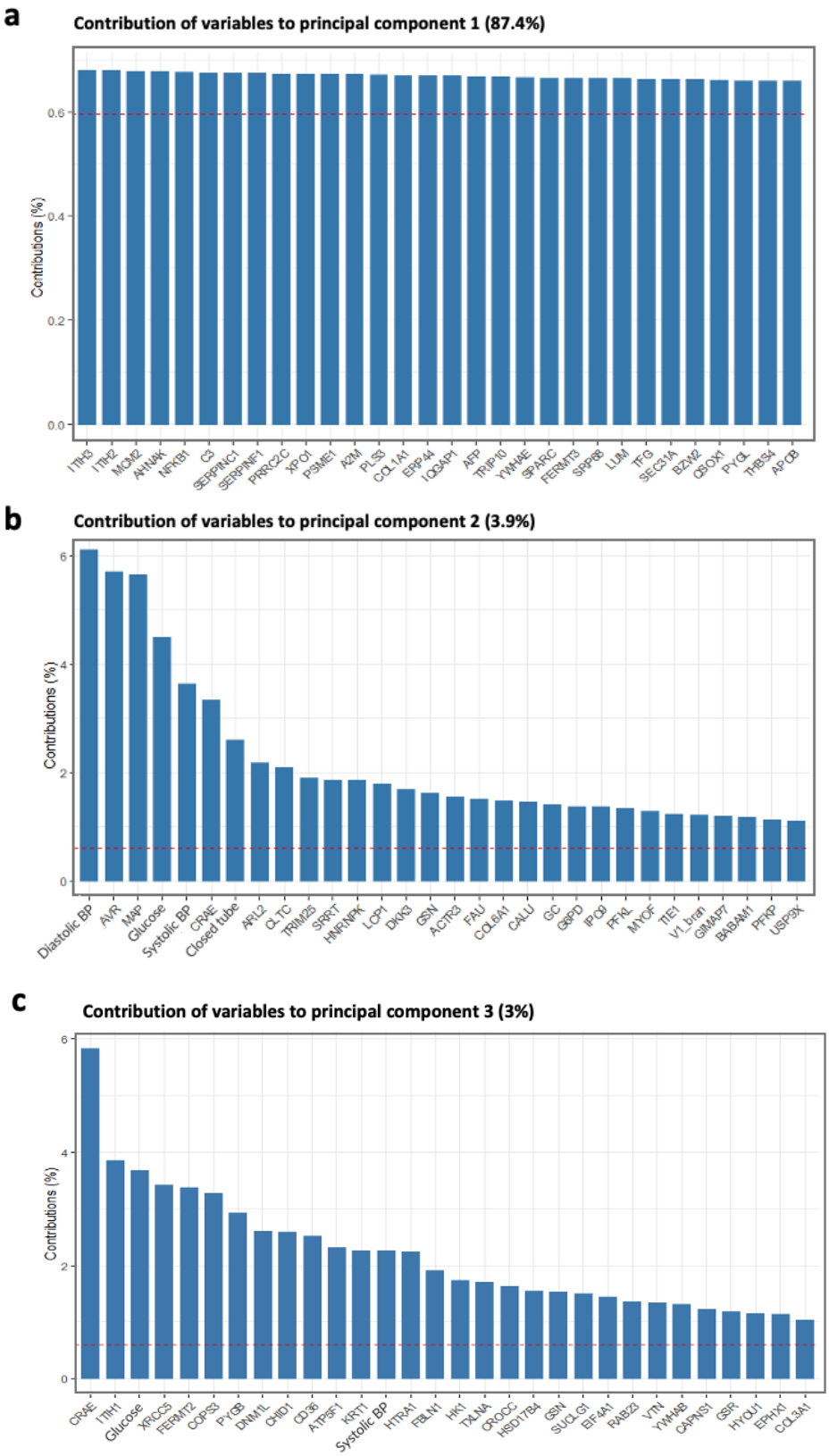
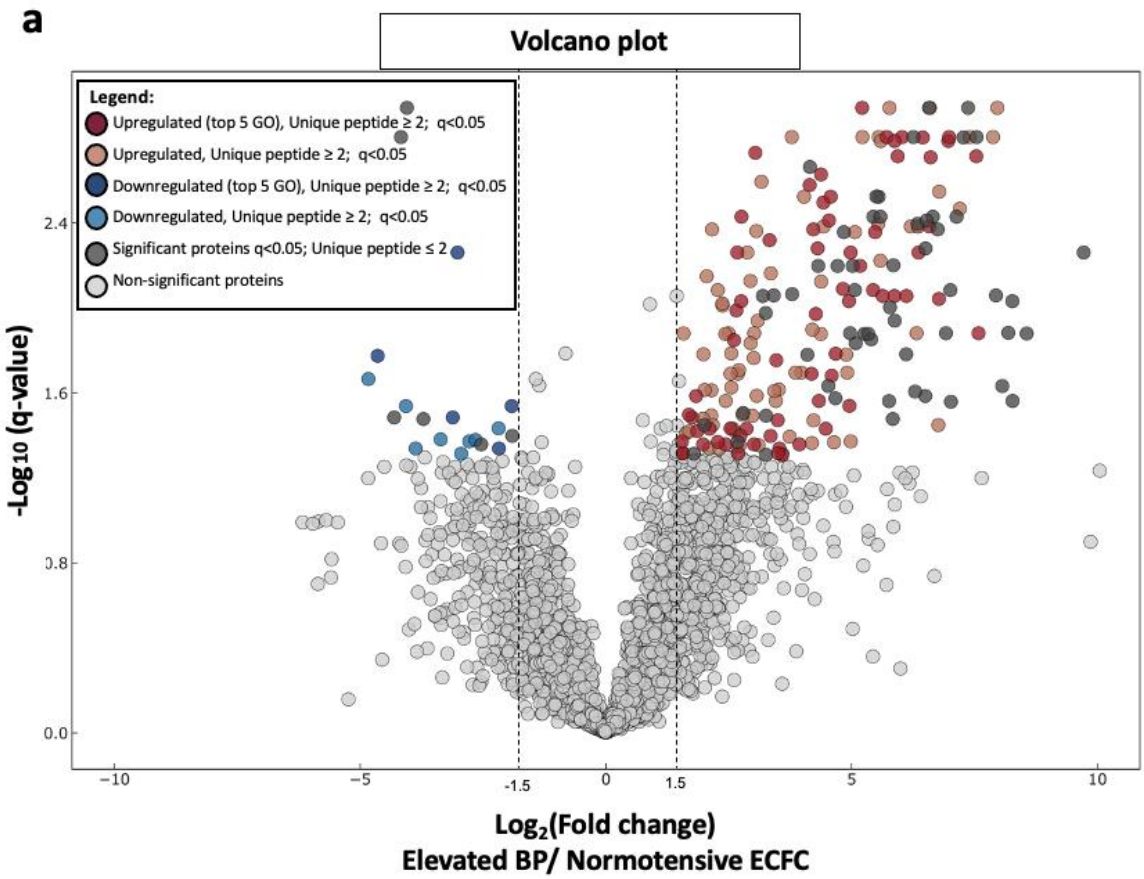


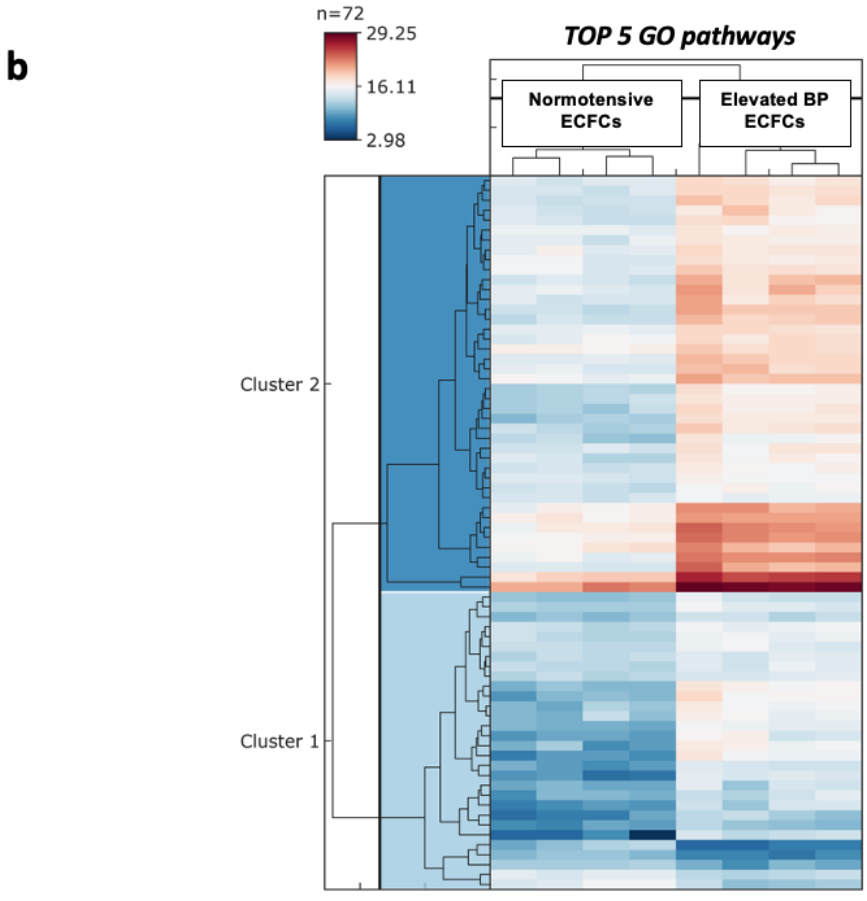
Figure 5.11. Contribution of variables to principal component 1 to 3.

The red dashed line on the graph above indicates the expected average contribution.

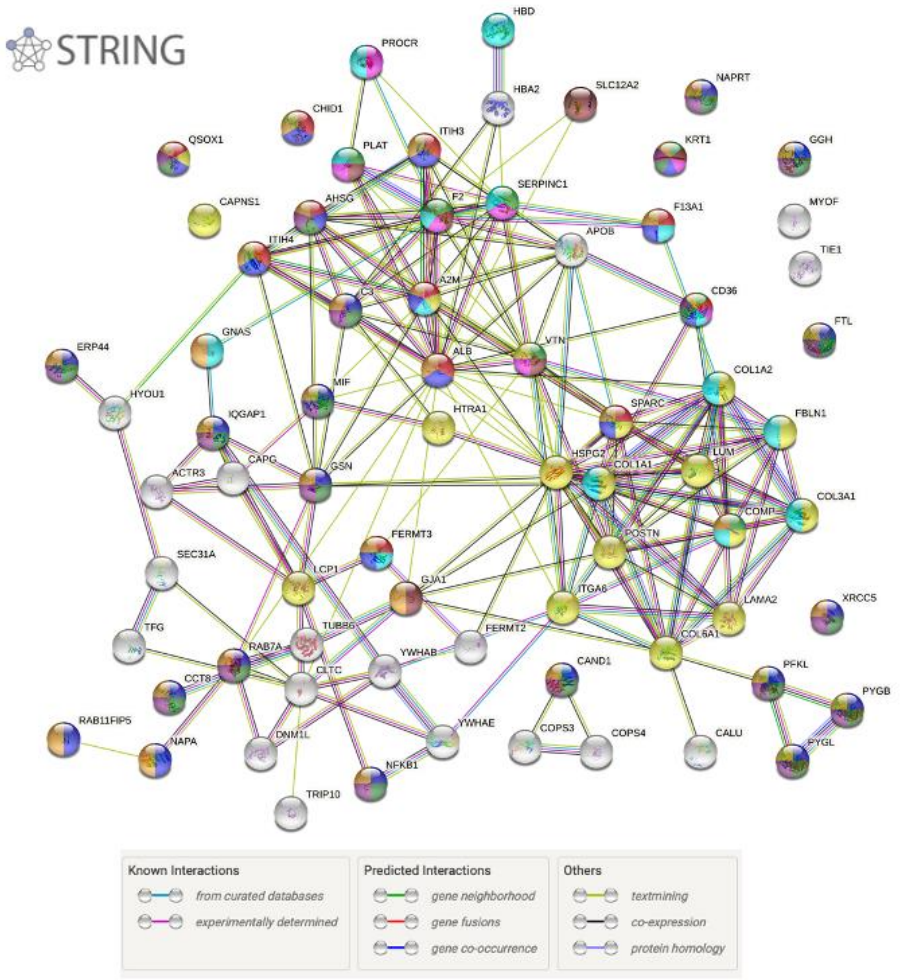
5.5.6.2 Gene ontology analysis of top 5 Gene Ontology biological pathway

The comparison of proteomic signatures of ECFCs identified 72 differentially expressed proteins between normal and elevated BP subjects, from the top 5 GO pathways (1) platelet degranulation, 2) regulated exocytosis, 3) regulation of haemostasis, 4) ECM organisation, 5) regulation of coagulation), with unique peptides ≥2 and either fold change ≥1.5 or ≤-1.5 (67 upregulated and 5 downregulated proteins) **(Figure 5.12 a)** and represented in a heatmap **(Figure 5.12 b)**. String™ interactive pathway analysis of proteins further revealed two main interactive clusters **(Figure 5.12 c)**, one cluster containing mainly proteins related to ECM organisation (yellow circles) and blood coagulation (light blue circles), and a second cluster containing proteins related to the regulation of coagulation (pink circles), exocytosis (purple circles) and haemostasis (green circles) **(Figure 5.12 d)**.


a
Volcano plot
Legend:
Upregulated (top 5 GO), Unique peptide ≥ 2; q<0.05
Upregulated, Unique peptide ≥ 2; q<0.05
Downregulated (top 5 GO), Unique peptide ≥ 2; q<0.05
Downregulated, Unique peptide ≥ 2; q<0.05
Significant proteins q<0.05; Unique peptide ≤ 2
Non-significant proteins
-Log10 (q-value)
2.4
1.6
0.8
0.0
−10
−5
-1.5
0
1.5
5
10
Log2(Fold change)
Elevated BP/ Normotensive ECFC


b
n=72
29.25
16.11
2.98
TOP 5 GO pathways
Normotensive ECFCs
Elevated BP ECFCs
Cluster 2
Cluster 1

c



d

STRING Functional biological process (Gene Ontology) enrichments

GO-Term	Description	Count in network	Strength	q-value	
GO:0002576	Platelet degranulation	11 of 129	1.36	1.18E-09	
GO:0045055	Regulated exocytosis	30 of 697	1.07	1.53E-20	
GO:1900046	Regulation of haemostasis	7 of 81	1.37	9.05E-06	
GO:0030198	Extracellular matrix organisation	18 of 338	1.16	3.98E-13	
GO:0050818	Regulation of coagulation	7 of 84	1.35	1.12E-05	
GO:0002446	Neutrophil mediated immunity	21 of 495	1.06	8.85E-14	
GO:0007596	Blood coagulation	15 of 303	1.13	2.01E-10	
GO:0032940	Secretion by cell	33 of 979	0.96	4.08E-20	
GO:0043312	Neutrophil degranulation	20 of 484	1.05	6.85E-13	
GO:0061045	Negative regulation of wound healing	6 of 70	1.37	7.15E-05	

Figure 5.12. Proteins identified in the top 5 enriched gene ontology (GO) pathways that are differently expressed between normotensive and elevated blood pressure (BP) of endothelial colony-forming cells (ECFCs).

(a) Volcano plot shows significantly regulated proteins between normotensive and elevated BP ECFCs, after FDR correction for multiple testing. A total of 2691 proteins were quantified with 158 proteins demonstrating significant differential abundance between the compared conditions based on unique peptides ≥ 2 and either $\log_2$(fold change) ≥ 1.5 or ≤ -1.5 (145 upregulated and 13 downregulated proteins). Among the 150 proteins, 71 proteins were identified as part of the top 5 GO pathways, with 67 upregulated proteins and 5 downregulated proteins. **(b)** Heatmaps of proteins involved in the top 5 enriched gene ontology pathways (n=72). Results are represented as a heatmap displaying protein expression levels on a logarithmic scale. Red indicates high expression, while dark blue indicates low or no expression. **(c)** String™ interactive pathway analysis of proteins (n=72) with **(d)** top 10 rank GO pathways.

We further identified 51 proteins of a total of 72 that significantly correlated with all four ECFC functional characteristics **(Supplementary Table S5.6)** Functional enrichment analysis revealed potential interactions between 51 identified proteins **(Figure 5.13 a)**. The interaction diagram of the 51 identified proteins indicates a potential central role of the growth factor receptor-bound protein-2 (GRB2) gene in regulating ECFC function in young adults with elevated BP **(Figure 5.13 b)**.

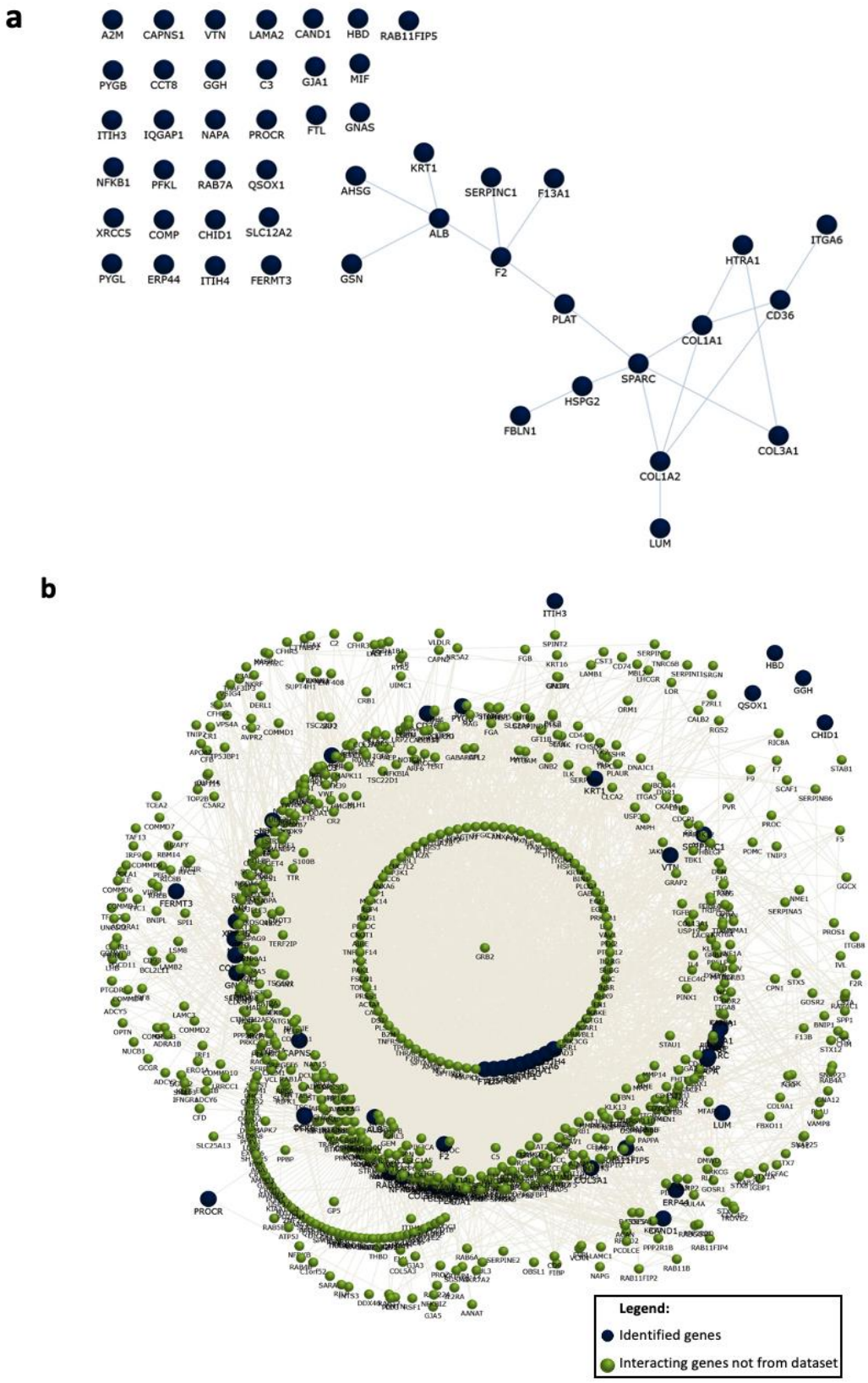


Figure 5.13. Interaction diagrams of identified proteins from proteome that significantly correlated with ECFC function.

(a) Functional enrichment analysis revealed potential interactions between identified proteins and **(b)** interactions between identified proteins (blue circles) with interacting genes/proteins not from dataset.

Detailed analysis of the 51 identified proteins revealed enrichments in GO biological pathways predominantly in vesicle-mediated transport and exocytosis and cellular component gene ontology domains, including cytoplasmic vesicle part **(Figure 5.14, Supplementary Table S5.7 and Supplementary Table S5.8).**

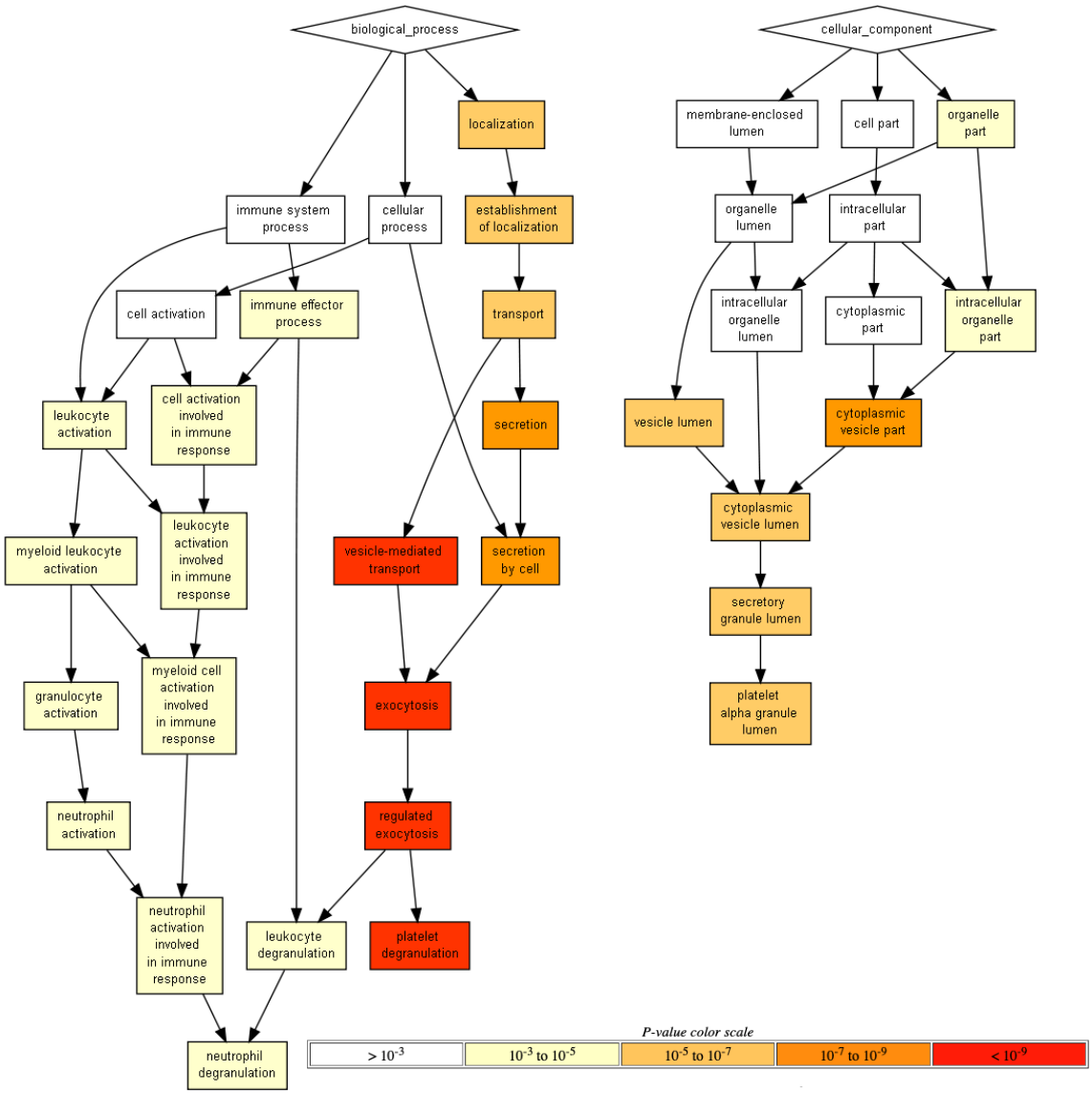


Figure 5.14. Gene Ontology enRIchement anaLysis and visuaLisAtion (GOrilla) reveals the gene ontology (GO) terms in biological process and cellular component GO domains, enriched with genes differentially expressed in elevated blood pressure endothelial colony cells (ECFCs) compared to normotensive ECFCs.

5.5 Discussion

5.5.1 Current findings

Young adults with elevated BP have a significant reduction in expansion, proliferative and vasculogenic potentials of ECFCs accompanied with adverse retinal micro-vascular endothelium dysfunction and increase in macro-vascular resistance. Of these variations, all the characteristics were adversely correlated to increase clinic systolic BP level. Furthermore, hierarchical functional clustering revealed distinct ECFC proteomic signatures between normotensive and elevated-BP ECFCs with changes in cellular mechanisms involved in exocytosis and vesicle transport. Our linear regression models demonstrated that retinal micro-vasculature is a very strong contributor to the increase in systolic BP compared to ECFCs and PVW measurements. We are one of the first to attempt to link endothelial, micro-vascular and macro-vascular interactions.

5.5.2 ECFC dysfunction, proteome, and elevated blood pressure

A recent review highlighted the crucial role of ECs in endothelial dysfunction and hypertension pathogenesis[113]. It has been suggested that endothelial dysfunction promotes arterial structural and functional abnormalities, including EC apoptosis or insufficient angiogenesis secondary to loss of endothelial nitric oxide-mediated properties that may both lead to micro-vascular rarefaction and phenotypical alteration of the endovascular lining of blood vessels that is characterised by a pro-thrombotic, pro-inflammatory, and pro-constrictive phenotype and ultimately vascular remodelling[126, 371-373]. These may explain the adverse phenotype alterations observed in the elevated BP individuals. Our study observed that ECFCs obtained elevated BP individuals to be dysfunctional (less proliferative and angiogenic). This is in line with studies showing a strong association between ECFC dysfunction and higher BP[10, 148, 318].

5.5.2.1 PCA reveals distinctive proteome between ECFC-derived from elevated BP vs normotensive individual.

The PCA scree plot of the first three principal components accounted for 94.3% of the total variance. The use of 2D representation allowed the effective separation of the samples based on the BP of individuals. The PC 1 captured the largest variance of the data (87.4%). The clinical parameters, including sex, fasting glucose levels, clinical BP, and ECFC function, micro and macro-vascular characteristics of normotensive and elevated BP individuals, that contributed to a distinctive separation in PCA between the different BP groups. This is supported by other published studies highlighting the involvement of BP, glucose, retinal micro-vasculature and EC function in regulating the overall proteome and elevated BP[5, 149, 159, 325, 358, 374-377].

5.5.2.2 ECFC dysfunction and extracellular vesicle transport

Other studies have shown that endothelial dysfunction triggers the release of EC-derived EVs that plays an increasing role in disease progression[113, 378-382]. EVs, which include apoptotic bodies, micro-vesicles, and exosomes, have emerged as essential players in cell-to-cell communication in normal physiology and pathological conditions[60]. EVs, convey these messages through their special cargoes consisting of cytokines, proteins, nucleic acids (mRNAs, and microRNAs) to recipient cells and lipids, which they transport from the donor cell to the recipient cell[61-63] and can modulate EC behaviour and angiogenesis *in vivo*[63-67].

Furthermore, translation of EV-associated mRNAs can occur in recipient cells[61] and has been implicated in the activation of ECs[63]. This may result in the genetically stable and quiescent endothelium being activated. When activated, the endothelium secretes different growth factors and cytokines that affect EC proliferation, apoptosis, coagulation, attract inflammatory cells, and/or affect vasoactivity to restore homeostasis [127, 383]. Prolonged or chronic activation of the endothelium leads to EC dysfunction, the loss of homeostatic functions, leading to pathological changes including vascular remodelling and increased vascular resistance resulting in the

development of CVDs[137, 138]. Despite the various deleterious effects of EVs in the pathogenesis of CVD, an increasing body of evidence highlights the beneficial effects of specific EVs on vascular function and endothelial regeneration[384]. Studies by our group have shown that endothelial EVs promote vascular endothelial repair and angiogenesis[67, 385-390]. These findings showed that endothelial EVs could stimulate endothelial repair by functionally influencing migration, proliferation, and wound healing capacities in target cells. This emphasised the need for characterisation of the ECFC-EVs to better understand its involvement in disease progression.

Consistent with the findings, our hierarchical functional clustering revealed a distinctive proteome profile of elevated-BP ECFCs with changes in proteins involved in exocytosis and vesicle transport. Further analysis of the proteins involved in TOP 5 GO biological pathways that significantly correlated with all four ECFC functional characteristics (n=51 proteins) revealed that the predominant involvement of vesicle mediated transport and exocytosis and also in pro-inflammatory pathways, including platelet and neutrophil degranulation, immune effector response. This may suggest the potential of an increase in exocytosis-mediated intercellular signalling by EVs to trigger inflammation, thereby contributing to endothelial remodelling and activation in adults with elevated BP. In line with our study, an increased concentration of EC-derived EVs inhibited angiogenesis in the cultured sections of hearts by inducing eNOS dysfunction[391]. Recently, it was shown that EC-derived EVs inhibit tube-like structure formation by micro-vascular EC *in vitro* and *in vivo*[392].

5.5.2.3 Role of GRB2 in the regulation ECFC function

Functional enrichment analysis demonstrated the interactions between the 51 proteins and non-identified proteins showed the involvement of a central protein (GRB2) that was not identified in the dataset. GRB2 signalling is critical for cell cycle progression and actin-based cell motility, and, consequently, more complex processes in regulating EC function, including proliferation, angiogenesis, migration, survival and vasculogenesis the activation of ERK, Mitogen-

activated Protein Kinase (MAPK), AKT and JNK pathways[393] [394-396]. Grb2 is also associated with the proline-rich domain of the son of sevenless (SOS), which is the guanyl nucleotide-exchange factor. This process triggers the transformation of inactive GDP-bound Ras into the active form of GTP-bound Ras. Active Ras stimulates serine/threonine kinase Raf, which phosphorylates and activates MEK1/2. MEK1/2 phosphorylate ERK, a member of the MAPK signalling enzymes that stimulate gene transcription[397]. MAPK pathway is also associated with ECs by mediating secretion of ET-1, and an imbalance of the PI3-K/Akt pathway that may release of inflammatory markers and finally initiates and accelerates endothelial dysfunction[398, 399]. This is supported by a study by Proctor *et al.,* which showed that heterozygous $Grb2^{+/-}$ mice conferred resistance to lesion formation via reducing foam cell formation[400]. These results implicate a fundamental role for Grb2 in atherosclerotic lesion formation. Another study showed that knock out of GRB2 in pulmonary artery smooth muscle cells attenuated proliferation, migration, and enhanced apoptosis as observed in pulmonary arterial hypertension (PAH)[401]. The expression levels of Ras, ERK, Cyclin D1, CDK4, c-Fos, PI3K and AKT were down-regulated, and pro-apoptotic Bax/Bcl2 ration was elevated by si-GRB2 transfection[401].

Grb2-associated binder 1 (Gab1) interacts with Grb2 to form a macromolecular complex that mediates many cellular signalling cascades[402]. Gab1 is a scaffolding adaptor protein, plays a vital role in transmitting key signals that control cell growth, migration, tube formation, micro-vessel sprouting, differentiation, and function from multiple tyrosine kinase receptors[403]. More recently, Gab2 has been show to regulate immune signalling and endothelial dysfunction[404]. Gab2 silencing in ECs markedly attenuated TNFα-induced, IL-1β–induced, and LPS-induced expression of TF, cell adhesion molecules, and inflammatory cytokines/chemokines[404]. Gab2 silencing suppressed TNFα-induced, IL-1β–induced, and LPS-induced phosphorylation and ubiquitination of TAK1 (transforming growth factor beta-activated kinase 1) and activation of MAPKs and NF-κB (nuclear factor kappa B)[404]. Gab2 integrates signalling from multiple inflammatory receptors and regulates vascular inflammation and thrombosis[404].

5.5.3 Retinal micro-vasculature and blood pressure

The remodelling of retinal vascular calibres and hypertension has been well-established[107, 162, 163, 167, 175, 376, 405-407]. Alterations characterise vascular remodelling in vasoconstriction, endothelium dysfunction, synthesis or degradation of extracellular matrix, inflammation, thrombosis lesions and neointima formation, leading to muscularisation, and elevation in vascular resistance clinical manifestation of CVD symptoms[127-130, 139, 140].

Data from several longitudinal cohort studies provided the first prospective clinical evidence showing that narrower arteriolar calibres, as reflected by a smaller CRAE and AVR, are inversely related to higher BP levels[122, 123, 154, 165, 376]. These data and our data suggest that early structural micro-arteriolar damage, visible in the retina, a sign of endothelial dysfunction, may further precede the development and progression of hypertension as early as during adulthood. On the other hand, our findings show a lack of association observed for venular calibre with BP and hypertension that is evident in several studies[408-411]. Other studies outlined increased retinal venular calibre associated with inflammatory markers (C-reactive protein and leukocyte count), smoking, and increased BMI[169, 412-414]. Thus, it is plausible that inflammation and these other factors are a mechanistic link between retinal venular changes and later CVD events. Our multiple regression model further underlined that retinal micro-vasculature to play significant role in modulating BP regulation after correction with factors including sex, EC function and macro-vasculature (PWV). This highlights that retinal micro-vasculature is a key characteristic of elevated BP and offers a potential platform to monitor disease progression and therapeutic development.

5.5.3.1 Retinal micro-vasculature and endothelial colony-forming cell proliferation capacity

The narrowing of the retinal arterioles was observed in individuals with elevated BP. The adverse phenotypic alterations may be stimulated by EC dysfunction, including altered proliferation, angiogenesis, and proteome profile. As prolonged or chronic activation of the

endothelium leads to EC dysfunction, loss of homeostatic functions, pathological pro-thrombotic, pro-inflammatory, and pro-constrictive vascular remodeling[113, 127, 137, 138]. This chapter shows the positive correlation between AVR and ECFC proliferation rate. Healthy individuals with normal vascular ageing are associated with higher AVR than healthy sedentary and at-risk individuals, with lower AVR that has been associated with increased CV events[9, 172, 173]. Similar is observed in ECFCs, where healthy individuals have a better ECFC function[148].

Retinal micro-vascular and EC dysfunction have been observed in hypertension manifestation and progression[107, 113, 114]. Our linear regression model outlined the relationship between the proliferation rate of ECFF and systolic BP with retinal micro-vasculature (CRAE). This has been observed in some studies that trigger endothelial dysfunction to be triggered by arteriole narrowing- induced shear-stress and inflammatory response[127, 382]. As a consequence, the endothelium switches from a quiescent to an overactive state, where it starts to secrete vasoconstrictive factors, like ET-1[415] and thromboxane[416], and proliferative factors, like VEGF, fibroblast growth factor 2[417], CXCL12[418], and reduce the secretion of vasodilators, like nitric oxide (NO) and prostacyclin, which indicates that EC dysfunction might play a central role in the pathogenesis of hypertension[127]. On the other hand, a study by Dellett *et al.* showed that intravitreally delivering EVs containing microRNAs secreted by ECFCs confer a pro-migratory and proliferation potential in human retinal micro-vascular ECs in the murine oxygen-induced retinopathy model[419].

5.5.4 Arterial stiffness and blood pressure

Macro-vasculature modifications in the form of aortic stiffening are associated with increased PWV, which depends on micro-vascular density, tone and structure[108]. The bidirectional relationship between aortic stiffness and systolic hypertension is well supported by epidemiologic evidence and our study, suggesting a precursor role of aortic stiffening in the incidence of hypertension[178]. Arterial stiffening may also cause substantial BP variability that will affect the

function of organs with low-resistance micro-vascular beds, including the brain, kidneys and placenta, by increasing pulsatile loads, and the heart by increasing left systolic ventricular load and abnormal ventricular and arterial interactions that promote left ventricular hypertrophy, dysfunction, and fibrosis[108, 179].

5.5.4.1 Pulse wave velocity and endothelial colony-forming cell angiogenic capacity

ECs that form a single monolayer in vivo to line the inner lumen of blood vessels respond to changes in the mechanics of their extracellular matrix (ECM), such as its stiffness, by changing their migration, proliferation and barrier integrity can contribute to the emergence of pathologies[198, 199]. We showed the association between increased PWV and reduced ECFC angiogenic capacity for the first time. Subendothelial stiffening often occurs with ageing and in multiple pathologies such as atherosclerosis and hypertension, constituting a risk factor for developing CVDs[420].

A study by Bastounis *et al.* has provided insights into the relationship between subendothelial stiffness, endothelial mechanics and variation of the EC transcriptome, altering endothelial cell mechanical behaviour[200]. Bastounis and colleagues measured traction force generation and performed gene expression profiling for two EC types grown in monolayers on soft or stiff matrices: primary HUVEC and immortalised human micro-vascular endothelial cell (HMEC-1). Both cell types respond to changes in subendothelial stiffness by increasing the traction stresses they exert on stiffer as compared to softer matrices and exhibit a range of altered protein phosphorylation or protein conformational changes previously implicated in mechano-transduction[200].

Angiogenesis is predominately mediated through the interaction of VEGF-A with VEGF receptor-2 (VEGFR-2)[421]. Activation of VEGFR-2, through ligand binding or mechanical stimuli such as shear stress, requires receptor dimerisation and trans-autophosphorylation on intracellular tyrosine residues [422]. Downstream signals such as focal adhesion kinase (FAK), extracellular signal-

regulated kinase (ERK) 1/2, protein kinase B (PKB/Akt), and eNOS are then activated and mediate EC behaviours, including migration, proliferation, survival, and permeability[423].

However, LaValley et al. highlighted that the matrix stiffness promoted downstream EC response to VEGF by altering VEGFR-2 internalisation, VEGF-induced signalling, and cell proliferation in HUVEC [198]. Other studies have otherwise shown that the VEGF binding to ECFC increases, but internalisation and level of activated β1 integrin are lowest in the stiffer matrix[424]. As stiffness changes, cells respond by modifying their traction forces and subsequent strain on individual fibres of the ECM. The result is a structural rearrangement of ECM proteins and the exposure of cryptic binding sites for proteins such as VEGF[425-427]. As stiffness increases, the proportion of β1 integrin binding and its ability to be engaged and internalised may decrease until β1 integrin can no longer engage the matrix and effectively participate in VEGFR-2 internalisation and subsequent VEGFR-2 activation and signalling of downstream targets[424]. We further hypothesise that β1 integrin complexed with VEGF-VEGFR-2 directs the internalisation and influences the fate (recycling versus degradation) of VEGF-VEGFR-2 complexes, which could mediate signalling intensity and kinetics and likely subsequent physiologic response[424].

5.5.4.2 Pulse wave velocity and retinal micro-vasculature

Large arterial and retinal micro-vascular intermediate phenotypes are individually recognised as CVD risk factors, including hypertension, yet the extent to which they impact one another is unclear[153]. Physiologically, they are part of the one circulatory system, sharing elements of pulsatile transmission of pressure and flow, but they capture different profiles of the vascular tree[153]. Limited evidence of an association was observed between retinal venular calibre and large arterial phenotypes across both populations[117]. Some recent studies have shown an association between narrower retinal arteriolar calibre (CRAE) and a faster PWV in middle-aged individuals[117, 160, 193, 408, 409]. Similar was observed in the young adult population in our study, and we showed a positive correlation between macro-vascular resistance and systolic BP was mediated by retinal

micro-vascular dysfunction (CRAE and AVR). These findings shed some insights into the alteration of micro-vascular changes mediating the macro-vascular changes that potentially resulted in the variation in BP.

Nevertheless, there was little evidence to suggest that retinal venular calibre was associated with PWV in hypertension states, as observed in our study and other published studies[117, 160, 408, 409]. This indicates that retinal venules adapt to the hypertensive state with a decrease in calibre[408, 409]. However, then there is a tipping point when the cardiometabolic disease becomes overt, and this adaption breaks down, leading to an increase in venular calibre[410, 411, 428]. Another explanation for the lack of association observed for venular calibre is different risk factors related to venular changes. Increased retinal venular calibre is associated with inflammatory markers, such as C-reactive protein and leukocyte count, smoking and increased BMI[169, 412-414]. Thus, it is plausible that inflammation and these other factors are a mechanistic link between changes in retinal venular calibre and later CVD events.

5.5.5 Study strengths and limitations

A strength of our study was the ability to link up cellular properties with clinical measurements, including dermal capillary density, retinal micro-vasculature, PWV and BP, despite the limited sample size. We showed EC function, micro-vasculature and macro-vasculature interaction and investigated their relationship with BP variation for the first time.

Furthermore, age and sex-matched individuals were used to minimise any potential bias for our proteomic investigations. One of the challenges faced in the study was the missing data, as some of the data were either lost due to human error or were not collected either due to logistics or faulty machines or participants' withdrawal of consent for specific measurements. In addition, due to the poor cell expansion capacity, there were limited cells to perform all the functional assessments. Another limitation was that only participants with ECFCs successfully isolated were included into the study for analysis. However, our findings and others[10, 311] suggest the ECFC growth

to be random, thereby limiting sampling bias. We acknowledge several limitations, many of which were unavoidable. Our study shed valuable and significant insight into the interactions between cellular, micro-vascular and macro-vascular interactions with clinical outcomes in young adults.

5.6 Conclusion

Our findings may indicate a potential mechanistic link between ECFC cell dysfunction and altered extracellular vesicles transport, retinal micro- and micro-vasculature and BP elevation and the compensatory response of the capillary adaptation in young adults as summarised in **Figure 5.15**. Our findings suggest that the retinal micro-vascular network may represent a promising therapeutic and preventive target, considering the vital role of micro-circulation on EC function, significant arteries dysfunction and potentially incident hypertension. Further suggests that the micro-vascular network may represent a promising therapeutic and preventive target, considering the vital role of micro-circulation on target organ damage, macro-vascular dysfunction, and potentially incident hypertension. Retinal imaging may be of utility in risk prediction of diseases with suspected micro-vascular pathology. It would also be a useful non-invasive quantitative tool in exploratory research studies where micro-vascular changes may occur.

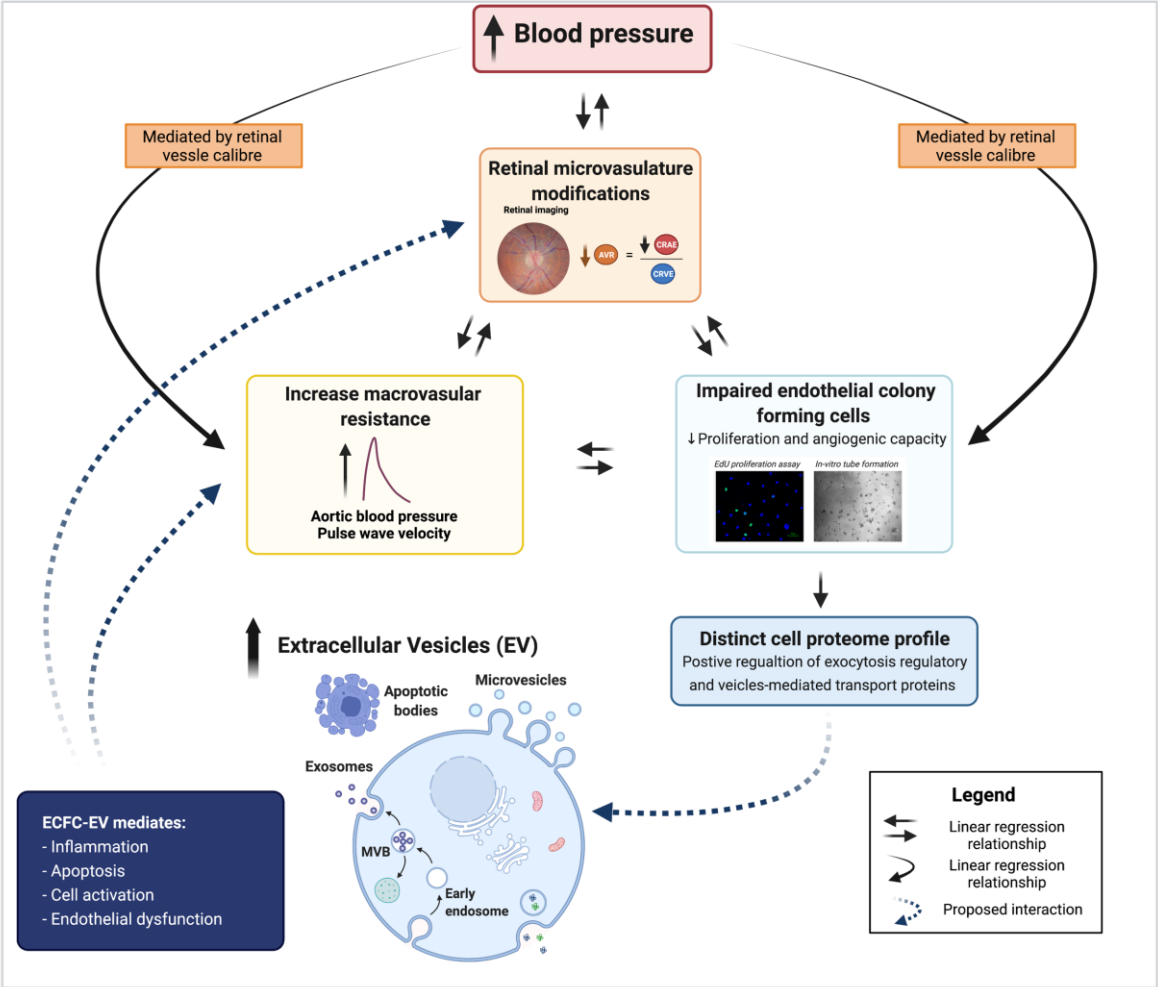


Figure 5.15. Summary of key findings - Association between endothelial colony-forming cell (ECFC) function, micro-vasculature, micro-vasculature and elevation in blood pressure.

An increase in BP results in retinal arterioles narrowing, an increase in macro-vascular resistance (pulse wave velocity) and EC dysfunction. The relationship between PWV, EC function with BP may be mediated via retinal vessel calibre. During the elevation of BP, ECFC dysfunction may stimulate extracellular vesicles production that may alter retinal micro-vasculature and micro-vasculature, and vice versa, thereby contributing to hypertension progression.

5.6 Supplemental materials

Supplementary Table S5.1

Table S5.1. Clinical characteristics of the study population of participants with or without ECFC colony formation.

Demographics and anthropometrics	Total (n=71)	ECFC colony formed (n=32)	No ECFC colony formed (n=39)	P-Value*
Male, n	37	17	20	<0.999
Female, n	34	15	19	
Age, years	27.86 ± 3.91	28.13 ± 4.4	27.64 ± 3.5	0.60
Height, cm	172.85 ± 9.72	172.96 ± 9.89	172.76 ± 9.71	0.97
Weight, kg	75.5 ± 14.42	75.7 ± 14.25	75.33 ± 14.75	0.97
BMI, kg/m^2	25.14 ± 3.6	25.18 ± 3.34	25.11 ± 3.84	0.95
Total body fat, %	26.09 ± 9.69 (66)	25.66 ± 9.67 (28)	26.4 ± 9.83 (38)	0.91
Total fat mass, kg	20.02 ± 9.1 (66)	19.59 ± 8.32 (28)	20.33 ± 9.74 (38)	0.83
Total fat free mass, kg	56.2 ± 11.76 (66)	56.63 ± 12.19 (28)	55.89 ± 11.59 (38)	0.98
Waist-hip ratio	0.86 ± 0.22 (67)	0.88 ± 0.31 (30)	0.84 ± 0.08 (37)	0.42
Gestational age, weeks	37.62 ± 3.58	37.88 ± 3.43	37.41 ± 3.73	0.60
Clinic seated BP				
Systolic BP, mmHg	122.68 ± 12.13	123.91 ± 13.24	121.67 ± 11.2	0.46
Diastolic BP, mmHg	76.46 ± 10.37	77.84 ± 11.2	75.33 ± 9.63	0.31
Mean arterial BP, mmHg	94.03 ± 10.23	95.13 ± 11.52	93.13 ± 9.09	0.43
Heart rate, beats per min	70.34 ± 10.35	70.81 ± 10.91	69.95 ± 9.99	0.72
Blood biochemistry				
Triglyceride, mmol/l	1.02 ± 0.58 (69)	1.07 ± 0.65 (30)	0.98 ± 0.52	0.52
Cholesterol, mmol/l	4.55 ± 0.78 (69)	4.58 ± 0.73 (30)	4.53 ± 0.82	0.80
High density lipoprotein, mmol/l	1.39 ± 0.3 (69)	1.39 ± 0.3 (30)	1.39 ± 0.31	0.93
Low density lipoprotein, mmol/l	2.67 ± 0.65 (69)	2.59 ± 0.67 (30)	2.73 ± 0.63	0.39
Glucose, mmol/l	54.56 ± 41.88 (69)	4.9 ± 0.36 (30)	4.8 ± 0.5 (38)	0.26
Insulin, pmol/l	4.85 ± 0.44 (68)	49.23 ± 26.7 (30)	58.66 ± 50.55	0.36
HOMA β-cell, %	101.18 ± 33.74 (63)	93.54 ± 25.99 (28)	107.29 ± 38.13 (35)	0.11
HOMA β-cell sensitivity, %	122.6 ± 55.98 (63)	126.39 ± 54.32 (28)	119.57 ± 57.89 (35)	0.63
HOMA Insulin resistance	1.07 ± 0.78 (63)	0.96 ± 0.49 (28)	1.17 ± 0.95 (35)	0.28
C-reactive protein, mg/l	2.32 ± 4.13 (64)	2.6 ± 4.38 (28)	2.1 ± 3.97 (36)	0.61
Retinal imaging				
CRAE, µm	179.89 ± 18.26 (69)	177.9 ± 18.51	181.62 ± 18.11 (37)	0.37
CRVE, µm	213.39 ± 18.17 (69)	213.64 ± 15.49	213.17 ± 20.42 (37)	0.93
AVR	0.85 ± 0.08 (69)	0.84 ± 0.09	0.86 ± 0.07 (37)	0.27
Vicorder parameters				
Peripheral systolic BP, mmHg	127.55 ± 11.68 (64)	128 ± 14.28 (28)	127.19 ± 9.37 (36)	0.85
Peripheral diastolic BP, mmHg	67.91 ± 7.76 (64)	68.39 ± 9.28 (28)	67.53 ± 6.46 (36)	0.66

Central aortic systolic BP, mmHg	121 ± 11.2 (64)	121.14 ± 13.95 (28)	120.89 ± 8.69 (36)	0.94
Central aortic diastolic BP, mmHg	67.88 ± 7.71 (64)	68.39 ± 9.28 (28)	67.47 ± 6.33 (36)	0.63
Pulse wave velocity, m/sec	9.72 ± 1.57 (62)	9.96 ± 1.76 (27)	9.55 ± 1.4 (35)	0.33

Data are expressed as mean ± standard deviation (SD). BP, blood pressure; BMI, body mass index; HOMA, Homeostasis Model Assessment. *Comparison between normotensive and Elevated-blood pressure (BP) participants and P-values corrected for sex. Atherosclerosis Risk in Communities (ARIC) study. Data are expressed as mean ± standard deviation (SD). Independent t-test or χ^2 test. Central Retinal Arteriolar Equivalent (CRAE), Central Retinal Venular Equivalent, (CRVE), Arteriole–venular ratio (AVR). Independent t-test or χ^2 test. Mean ± standard deviation (SD).

Supplementary Table S5.2

Table S5.2. Linear regression of endothelial colony-forming cell (ECFC) function and retinal micro-vascular and macro-vascular assessment

Linear regression	Days taken for ECFC colony formation			ECFC proliferation rate (%)			ECFC closed tube formation (n)			ECFC branches formation (n)		
	R^2	Standardised Beta	P-value	R^2	Standardised Beta	P-value	R^2	Standardised Beta	P-value	R^2	Standardised Beta	P-value
CRAE	0.129	-0.458	**0.016**	-0.006	0.231	0.321	0.041	0.312	0.156	0.048	0.317	0.149
CRVE	-0.069	-0.016	0.93	0.012	-0.242	0.238	-0.038	-0.054	0.784	-0.034	-0.052	0.793
AVR	0.12	-0.435	**0.019**	0.125	0.447	**0.042**	0.085	0.38	0.075	0.09	0.381	0.074
PWV	0.044	0.354	0.09	0.051	-0.371	0.109	0.183	-0.51	**0.017**	0.063	-0.383	0.083

Linear regression with P values adjusted for sex. Central retinal arteriolar equivalent (CRAE), central retinal venular equivalent (CRVE), arteriolar-to-venular-ratio (AVR) and pulse wave velocity (PWV).

Supplementary Table S5.3

Table S5.3. Linear regression with systolic blood pressure as dependent variable.

Cellular and micro-vascular parameters	B_{model} *(95% CI)*	*r partial*	*Adjusted* R^2	*P**	*P⁺*
ECFC characteristics					
Days taken for ECFC colony formation	0.179 (-0.438, 1.284)	1.005	0.023	0.323	0.433
ECFC proliferation rate, %	**-0.418 (-0.584, -0.022)**	**-2.233**	**0.155**	**0.036**	**0.021**
ECFC closed tube formation (n)	-0.323 (-1.069, 0.094)	-1.726	0.087	0.097	0.144
ECFC branches formation (n)	-0.358 (-0.543, 0.017)	-1.934	0.111	0.064	0.106
Retinal imaging					
Central retinal arteriolar equivalent	**-0.551 (-0.747, -0.354)**	**-5.728**	**0.505**	**<0.001**	**<0.001**
Central retinal venular equivalent	-0.017 (-0.34, 0.311)	-0.089	-0.054	0.812	0.861
Arteriolar-to-venular diameter ratio	**-0.73 (-155.09, -70.23)**	**-5.431**	**0.477**	**<0.001**	**<0.001**
Vicorder					
Pulse wave velocity	**0.479 (0.726, 6.74)**	**2.562**	**0.168**	**0.017**	0.081

P* adjusted for sex. P^+ adjusted for sex and glucose.

Supplementary Table S5.4

Table S5.4. Clinical characteristics of the study population that underwent proteomics analysis.

Demographics and anthropometrics	Total (n=8)	Normotensives (n=4)	Elevated BP (n=4)	P-Value*
Male, n	4	2	2	1
Female, n	4	2	2	
Age, years	25.25 ± 4.2	24.5 ± 1.73	26 ± 6.06	0.66
Height, cm	174.13 ± 7.41	176.75 ± 9.74	171.5 ± 3.87	0.37
Weight, kg	70.14 ± 8.05	67.2 ± 3.45	73.08 ± 10.79	0.36
BMI, kg/m^2	23.21 ± 3.04	21.59 ± 1.77	24.82 ± 3.38	0.16
Total body fat, %	15.76 ± 10.37	10.69 ± 2.09 (2)	27.18 ± 11.06 (3)	0.12
Total fat mass, kg	20.58 ± 11.99	7.5 ± 1.7 (2)	21.27 ± 10 (3)	0.13
Total fat free mass, kg	58.74 ± 6.4	62.35 ± 0.35 (2)	56.33 ± 7.76 (3)	0.31
Waist-hip ratio	0.79 ± 0.04	0.81 ± 0.04	0.75 ± 0.02 (3)	0.04
Gestational age, weeks	38.63 ± 2.97	36.75 ± 2.75	40.5 ± 1.91	0.09
Clinic seated BP				
Systolic BP, mmHg	128.12 ± 11.98	**119.25 ± 6.95**	**137 ± 8.76**	**0.03**
Diastolic BP, mmHg	81.25 ± 12.57	**72.5 ± 10.75**	**90 ± 6.98**	**0.05**
Mean arterial BP, mmHg	99 ± 12.62	**89.75 ± 9.32**	**108.25 ± 7.5**	**0.04**
Heart rate, beats per min	71.38 ± 11.75	70.25 ± 10.63	72.5 ± 14.34	0.82
Blood biochemistry				
Triglyceride, mmol/l	0.94 ± 0.45	0.87 ± 0.34	1 ± 0.59	0.73
Cholesterol, mmol/l	4.83 ± 0.76	4.32 ± 0.68	5.33 ± 0.43	0.07
High density lipoprotein, mmol/l	1.42 ± 0.25	1.35 ± 0.17	1.49 ± 0.32	0.49
Low density lipoprotein, mmol/l	2.5 ± 0.59	2.2 ± 0.56	2.8 ± 0.52	0.19
Glucose, mmol/l	4.86 ± 0.47	4.77 ± 0.37	4.96 ± 0.6	0.55
Insulin, pmol/l	46.29 ± 13.39	46.33 ± 12	46.25 ± 16.56	0.99
HOMA β-cell, %	93.84 ± 27.04	96.53 ± 22.09	91.15 ± 34.62	0.77

HOMA β-cell sensitivity, %	124.69 ± 33.85	123.57 ± 36.14	125.8 ± 36.94	0.94
HOMA Insulin resistance	0.86 ± 0.24	0.85 ± 0.22	0.86 ± 0.3	0.97
C-reactive protein, mg/l	2.01 ± 3.54	0.24 ± 0.05 (2)	2.9 ± 4.22	0.31

Data are expressed as mean ± standard deviation (SD). * Comparison between normotensive and Elevated-blood pressure (BP) participants and P-values adjusted for sex. Independent t-test or χ^2 test. Mean ± standard deviation (SD).

Supplementary Table S5.5

Table S5.5. Endothelial colony-forming cells, retinal imaging and Vicorder characteristics of the study population

ECFC characteristics	Total (n=8)	Normotensives (n=4)	Elevated BP (n=4)	P-Value*
Days for ECFC colony formation (n)	16.63 ± 3.96	13.25 ± 2.22	20 ± 1.15	**0.002**
Proliferation rate (%) (n)	23.3 ± 20.9	40.91 ± 11.41	5.69 ± 7.9	**0.003**
Closed tube formed, n per 1.5x10^4 (n)	6.9 ± 7.98	13.8 ± 4.67	0	**0.001**
Branches formed, n per 1.5x10^4 (n)	16.9 ± 12.91	28.37 ± 5.19	5.43 ± 3.28	**0.001**
Retinal imaging				
CRAE, µm	173.27 ± 22.89	179.25 ± 14.97	167.28 ± 30.05	0.50
CRVE, µm	208.44 ± 22.84	203.24 ± 7.91	213.64 ± 32.91	0.58
AVR	0.83 ± 0.08	0.88 ± 0.04	0.78 ± 0.07	0.06
Vicorder parameters				
Peripheral systolic BP, mmHg	128.43 ± 15.52 (7)	118.25 ± 6.70	142.00 ± 13.11 (3)	**0.025**
Peripheral diastolic BP, mmHg	68 ± 9.29 (7)	62.0 ± 2.16	76.0 ± 9.17 (3)	**0.029**
Central aortic systolic BP, mmHg	121.14 ± 12.27 (7)	122.25 ± 6.02	133.00 ± 5.29 (3)	**0.005**
Central aortic diastolic BP, mmHg	68 ± 9.29 (7)	62.0 ± 2.16	76.0 ± 9.17 (3)	**0.029**
Pulse wave velocity, m/sec	9.76 ± 1.96 (7)	8.65 ± 1.48	11.23 ± 1.59 (3)	0.08

Atherosclerosis Risk in Communities (ARIC) study. Data are expressed as mean ± standard deviation (SD). Independent t-test or χ^2 test. Mean ± standard deviation (SD). Central Retinal Arteriolar Equivalent (CRAE), Central Retinal Venular Equivalent, (CRVE), Arteriole–venular ratio (AVR).

Supplementary Table S5.6

Table S5.6. Pearson correlation of proteins with endothelial colony-forming cell (ECFC) characteristics.

Proteins	GO pathways	ECFC characteristics (n=8)							
		Days of colony formation (n)		Proliferation rate (%)		Tube formation (n)		Branches formation (n)	
		Pearson Correlation	P-value	Pearson Correlation	P-value	Pearson Correlation	P-value	Pearson Correlation	P-value
FERMT3	Platelet degranulation, regulated exocytosis, blood coagulation, secretion by cell	.907**	0.002	-.945**	0.000	-.855**	0.007	-.910**	0.002
ALB	Platelet degranulation, regulated exocytosis, secretion by cell	.839**	0.009	-.860**	0.006	-.969**	0.000	-.989**	<0.001
SPARC	Platelet degranulation, regulated exocytosis, extracellular matrix organisation, secretion by cell	.839**	0.009	-.871**	0.005	-.925**	0.001	-.972**	<0.001
A2M	Platelet degranulation, regulated exocytosis, extracellular matrix organisation, blood coagulation, secretion by cell	.933**	0.001	-.931**	0.001	-.860**	0.006	-.914**	0.001
ITIH3	Platelet degranulation, regulated exocytosis, secretion by cell	.907**	0.002	-.935**	0.001	-.887**	0.003	-.939**	0.001
AHSG	Platelet degranulation, regulated exocytosis, neutrophil mediated immunity, secretion by cell, neutrophil degranulation	.823*	0.012	-.913**	0.002	-.924**	0.001	-.975**	<0.001
CHID1	Platelet degranulation, regulated exocytosis, secretion by cell	.849**	0.008	-.813*	0.014	-.764*	0.027	-.805*	0.016

QSOX1	Platelet degranulation, regulated exocytosis, extracellular matrix organisation, neutrophil mediated immunity, secretion by cell, neutrophil degranulation	.923**	0.001	-.949**	0.000	-.859**	0.006	-.908**	0.002
F13A1	Platelet degranulation, regulated exocytosis, blood coagulation, blood coagulation, secretion by cell	.916**	0.001	-.950**	0.000	-.896**	0.003	-.938**	0.001
CD36	Platelet degranulation, regulated exocytosis, regulation of haemostasis, regulation of coagulation, neutrophil mediated immunity, blood coagulation, secretion by cell, neutrophil degranulation	.855**	0.007	-.789*	0.020	-.900**	0.002	-.895**	0.003
ITIH4	Platelet degranulation, regulated exocytosis, secretion by cell	.917**	0.001	-.940**	0.001	-.783*	0.022	-.866**	0.005
IQGAP1	Regulated exocytosis, neutrophil mediated immunity, secretion by cell, neutrophil degranulation	.866**	0.005	-.904**	0.002	-.937**	0.001	-.980**	<0.001
CCT8	Regulated exocytosis, neutrophil mediated immunity, secretion by cell, neutrophil degranulation	.816*	0.013	-.883**	0.004	-.756*	0.030	-.850**	0.008
KRT1	Regulated exocytosis, regulation of haemostasis, regulation of coagulation, neutrophil mediated immunity, secretion by cell, neutrophil degranulation, negative regulation of wound healing	.800*	0.017	-.886**	0.003	-.753*	0.031	-.846**	0.008
GSN	Regulated exocytosis, neutrophil mediated immunity, secretion by cell, neutrophil degranulation	.743*	0.035	-.727*	0.041	-.944**	0.000	-.938**	0.001

XRCC5	Regulated exocytosis, neutrophil mediated immunity, secretion by cell, neutrophil degranulation	.767*	0.026	-.819*	0.013	-.790*	0.020	-.841**	0.009
C3	Regulated exocytosis, neutrophil mediated immunity, secretion by cell, neutrophil degranulation	.906**	0.002	-.919**	0.001	-.883**	0.004	-.937**	0.001
CAND1	Regulated exocytosis, neutrophil mediated immunity, secretion by cell, neutrophil degranulation	.885**	0.004	-.920**	0.001	-.836**	0.010	-.888**	0.003
RAB7A	Regulated exocytosis, neutrophil mediated immunity, secretion by cell, neutrophil degranulation, neutrophil degranulation	.918**	0.001	-.971**	0.000	-.780*	0.022	-.841**	0.009
PFKL	Regulated exocytosis, neutrophil mediated immunity, secretion by cell, neutrophil degranulation	.878**	0.004	-.863**	0.006	-.707*	0.050	-.767*	0.026
NAPA	Regulated exocytosis, secretion by cell	.914**	0.001	-.961**	0.000	-.897**	0.003	-.948**	<0.001
PYGL	Regulated exocytosis, neutrophil mediated immunity, secretion by cell, neutrophil degranulation	.871**	0.005	-.877**	0.004	-.927**	0.001	-.965**	<0.001
PYGB	Regulated exocytosis, neutrophil mediated immunity, secretion by cell, neutrophil degranulation	.737*	0.037	-.822*	0.012	-.777*	0.023	-.868**	0.005
ERP44	Regulated exocytosis, neutrophil mediated immunity, secretion by cell, neutrophil degranulation	.910**	0.002	-.952**	0.000	-.845**	0.008	-.916**	0.001
GGH	Regulated exocytosis, neutrophil mediated immunity, secretion by cell, neutrophil degranulation	.928**	0.001	-.848**	0.008	-.723*	0.043	-.759*	0.029

FTL	Regulated exocytosis, neutrophil mediated immunity, secretion by cell, neutrophil degranulation	.946**	0.000	-.943**	0.000	-.794*	0.019	-.838**	0.009
NFKB1	Regulated exocytosis, neutrophil mediated immunity, secretion by cell, neutrophil degranulation	.877**	0.004	-.905**	0.002	-.912**	0.002	-.956**	<0.001
NAPRT	Regulated exocytosis, neutrophil mediated immunity, secretion by cell, neutrophil degranulation	.752*	0.031	-.864**	0.006	-.846**	0.008	-.910**	0.002
RAB11FIP5	Regulated exocytosis, secretion by cell	-.861**	0.006	.902**	0.002	.768*	0.026	.838**	0.009
F2	Regulation of haemostasis, regulation of coagulation, neutrophil mediated immunity, blood coagulation, negative regulation of wound healing	.835**	0.010	-.862**	0.006	-.918**	0.001	-.963**	<0.001
VTN	Regulation of haemostasis, extracellular matrix organisation, regulation of coagulation, negative regulation of wound healing	.895**	0.003	-.862**	0.006	-.849**	0.008	-.882**	0.004
PLAT	Regulation of haemostasis, regulation of coagulation, blood coagulation, negative regulation of wound healing	.829*	0.011	-.925**	0.001	-.793*	0.019	-.894**	0.003
SERPINC1	Regulation of haemostasis, regulation of coagulation, blood coagulation	.892**	0.003	-.917**	0.001	-.884**	0.004	-.946**	<0.001
COMP	Regulation of haemostasis, extracellular matrix organisation, blood coagulation, secretion by cell	.937**	0.001	-.917**	0.001	-.809*	0.015	-.863**	0.006
HSPG2	Extracellular matrix organisation	.836**	0.010	-.936**	0.001	-.882**	0.004	-.946**	<0.001
POSTN	Extracellular matrix organisation	.862**	0.006	-.891**	0.003	-.750*	0.032	-.839**	0.009

CAPNS1	Extracellular matrix organisation	.806*	0.016	-.771*	0.025	-.764*	0.027	-.805*	0.016
FBLN1	Extracellular matrix organisation, Blood coagulation	.813*	0.014	-.805*	0.016	-.899**	0.002	-.913**	0.002
ITGA6	Extracellular matrix organisation	.803*	0.016	-.829*	0.011	-.839**	0.009	-.866**	0.005
COL1A1	Extracellular matrix organisation, blood coagulation	.855**	0.007	-.876**	0.004	-.913**	0.002	-.963**	<0.001
HTRA1	Extracellular matrix organisation	.813*	0.014	-.743*	0.035	-.840**	0.009	-.847**	0.008
LUM	Extracellular matrix organisation	.840**	0.009	-.879**	0.004	-.910**	0.002	-.964**	<0.001
COL3A1	Extracellular matrix organisation, blood coagulation	.794*	0.019	-.866**	0.005	-.878**	0.004	-.950**	<0.001
COL1A2	Extracellular matrix organisation, blood coagulation	.773*	0.025	-.759*	0.029	-.841**	0.009	-.882**	0.004
LAMA2	Extracellular matrix organisation	.806*	0.016	-.853**	0.007	-.911**	0.002	-.942**	<0.001
PROCR	Regulation of coagulation, blood coagulation	-.832*	0.010	.797*	0.018	.749*	0.032	.825*	0.012
GNAS	Blood coagulation, secretion by cell	.880**	0.004	-.916**	0.001	-.804*	0.016	-.876**	0.004
HBD	Blood coagulation	.850**	0.008	-.891**	0.003	-.890**	0.003	-.955**	<0.001
MIF	Secretion by cell, neutrophil degranulation	0.687	0.060	-.808*	0.015	-.928**	0.001	-.970**	<0.001
GJA1	Secretion by cell, negative regulation of wound healing	-.898**	0.002	.856**	0.007	.926**	0.001	.914**	0.001
SLC12A2	Negative regulation of wound healing	.837**	0.010	-.878**	0.004	-.963**	0.000	-.990**	<0.001

Correlation is significant at the 0.05 level* and 0.01 level (2-tailed)**

Supplementary Table S5.7

Table S5.7. Gene Ontology enRIchement anaLysis and visuaLisAtion (GOrilla) analysis with enriched GO biological pathway.

GO term	Description	P-value	FDR q-value	Enrichment (N, B, n, b)	Proteins
GO:0006887	Exocytosis	3.01E-11	6.20E-08	1.69 (49,28,28,27)	A2M, F13A1, CCT8, FTL, GSN, PYGB, IQGAP1, FERMT3, ITIH3, ITIH4, SPARC, KRT1, CHID1, RAB7A, CD36, QSOX1, GGH, NFKB1, AHSG, PYGL, CAND1, C3, PFKL, ERP44, XRCC5, RAB11FIP5, ALB,
GO:0045055	Regulated exocytosis	3.01E-11	3.10E-08	1.69 (49,28,28,27)	A2M, FTL, CCT8, F13A1, GSN, PYGB, IQGAP1, FERMT3, ITIH3, ITIH4, SPARC, KRT1, CHID1, RAB7A, CD36, QSOX1, GGH, NFKB1, AHSG, PYGL, CAND1, C3, PFKL, ERP44, XRCC5, RAB11FIP5, ALB, [, A2M, CHID1, FERMT3, F13A1, ITIH3, CD36, ITIH4, SPARC, ALB, QSOX1, AHSG,
GO:0002576	Platelet degranulation	3.43E-11	2.36E-08	4.45 (49,11,11,11)	A2M, CHID1, FERMT3, F13A1, ITIH3, CD36, ITIH4, SPARC, ALB, QSOX1, AHSG,
GO:0016192	Vesicle-mediated transport	8.42E-10	4.33E-07	1.53 (49,32,30,30)	A2M, FTL, CCT8, F13A1, GSN, PYGB, IQGAP1, FERMT3, ITIH3, ITIH4, SPARC, KRT1, CHID1, RAB7A, CD36, QSOX1, GGH, NFKB1, NAPA, AHSG, PYGL, CAND1, C3, PFKL, ERP44, XRCC5, RAB11FIP5, F2, ALB, VTN,
GO:0046903	Secretion	2.91E-08	1.20E-05	1.52 (49,31,28,27)	A2M, F13A1, CCT8, FTL, GSN, PYGB, IQGAP1, FERMT3, ITIH3, ITIH4, SPARC, KRT1, CHID1, RAB7A, CD36, QSOX1, GGH, NFKB1, AHSG, PYGL, CAND1, C3, PFKL, ERP44, XRCC5, RAB11FIP5, ALB,
GO:0032940	Secretion by cell	5.96E-08	2.05E-05	1.58 (49,30,28,27)	A2M, FTL, CCT8, F13A1, GSN, PYGB, IQGAP1, FERMT3, ITIH3, ITIH4, SPARC, KRT1, CHID1, RAB7A, CD36, QSOX1, GGH, NFKB1, AHSG, PYGL, CAND1, C3, PFKL, ERP44, XRCC5, RAB11FIP5, ALB,
GO:0006810	Transport	8.29E-07	2.44E-04	1.29 (49,37,34,33)	A2M, F13A1, CCT8, FTL, GSN, PYGB, IQGAP1, FERMT3, ITIH3, ITIH4, SPARC, SERPINC1, KRT1, CHID1, RAB7A, CD36, QSOX1, GGH, NFKB1, NAPA, AHSG, PYGL, HSPG2, CAND1, C3, PFKL, COMP, ERP44, XRCC5, RAB11FIP5, F2, VTN, ALB,
GO:0051179	Localization	8.29E-07	2.13E-04	1.29 (49,37,34,33)	A2M, FTL, F13A1, CCT8, GSN, PYGB, IQGAP1, FERMT3, ITIH3, ITIH4, SPARC, SERPINC1, KRT1, CHID1, RAB7A, CD36, QSOX1, GGH, NFKB1, NAPA, AHSG, PYGL, HSPG2, CAND1, C3, PFKL, COMP, ERP44, XRCC5, RAB11FIP5, F2, ALB, VTN,
GO:0051234	Establishment of localization	8.29E-07	1.90E-04	1.29 (49,37,34,33)	A2M, FTL, CCT8, F13A1, GSN, PYGB, IQGAP1, FERMT3, ITIH3, ITIH4, SPARC, SERPINC1, KRT1, CHID1, RAB7A, CD36, GGH, QSOX1, NFKB1, NAPA, AHSG,

					PYGL, HSPG2, CAND1, C3, COMP, PFKL, ERP44, XRCC5, RAB11FIP5, F2, ALB, VTN,
GO:0043312	Neutrophil degranulation	1.64E-05	3.37E-03	1.72 (49,19,27,18)	KRT1, RAB7A, CCT8, FTL, CD36, GGH, QSOX1, GSN, NFKB1, AHSG, PYGL, CAND1, C3, PYGB, PFKL, IQGAP1, ERP44, XRCC5,
GO:0002366	Leukocyte activation involved in immune response	1.64E-05	3.06E-03	1.72 (49,19,27,18)	KRT1, RAB7A, CCT8, FTL, CD36, GGH, QSOX1, GSN, NFKB1, AHSG, PYGL, CAND1, C3, PFKL, PYGB, IQGAP1, ERP44, XRCC5,
GO:0002263	Cell activation involved in immune response	1.64E-05	2.81E-03	1.72 (49,19,27,18)	KRT1, RAB7A, CCT8, FTL, CD36, GGH, QSOX1, GSN, NFKB1, AHSG, PYGL, CAND1, C3, PYGB, PFKL, IQGAP1, ERP44, XRCC5,
GO:0002275	Myeloid cell activation involved in immune response	1.64E-05	2.59E-03	1.72 (49,19,27,18)	KRT1, RAB7A, CCT8, FTL, CD36, GGH, QSOX1, GSN, NFKB1, AHSG, PYGL, CAND1, C3, PYGB, PFKL, IQGAP1, ERP44, XRCC5,
GO:0002274	Myeloid leukocyte activation	1.64E-05	2.41E-03	1.72 (49,19,27,18)	KRT1, RAB7A, CCT8, FTL, CD36, GGH, QSOX1, GSN, NFKB1, AHSG, PYGL, CAND1, C3, PFKL, PYGB, IQGAP1, ERP44, XRCC5,
GO:0002283	Neutrophil activation involved in immune response	1.64E-05	2.25E-03	1.72 (49,19,27,18)	KRT1, RAB7A, CCT8, FTL, CD36, GGH, QSOX1, GSN, NFKB1, AHSG, PYGL, CAND1, C3, PFKL, PYGB, IQGAP1, ERP44, XRCC5,
GO:0036230	Granulocyte activation	1.64E-05	2.11E-03	1.72 (49,19,27,18)	KRT1, RAB7A, CCT8, FTL, CD36, GGH, QSOX1, GSN, NFKB1, AHSG, PYGL, CAND1, C3, PFKL, PYGB, IQGAP1, ERP44, XRCC5,
GO:0043299	Leukocyte degranulation	1.64E-05	1.98E-03	1.72 (49,19,27,18)	KRT1, RAB7A, CCT8, FTL, CD36, GGH, QSOX1, GSN, NFKB1, AHSG, PYGL, CAND1, C3, PFKL, PYGB, IQGAP1, ERP44, XRCC5,
GO:0045321	Leukocyte activation	1.64E-05	1.87E-03	1.72 (49,19,27,18)	KRT1, RAB7A, CCT8, FTL, CD36, GGH, QSOX1, GSN, NFKB1, AHSG, PYGL, CAND1, C3, PYGB, PFKL, IQGAP1, ERP44, XRCC5,
GO:0042119	Neutrophil activation	1.64E-05	1.77E-03	1.72 (49,19,27,18)	KRT1, RAB7A, CCT8, FTL, CD36, GGH, QSOX1, GSN, NFKB1, AHSG, PYGL, CAND1, C3, PYGB, PFKL, IQGAP1, ERP44, XRCC5,
GO:0002252	Immune effector process	6.00E-05	6.17E-03	1.61 (49,20,29,19)	KRT1, RAB7A, CCT8, FTL, CD36, GGH, QSOX1, GSN, NFKB1, AHSG, PYGL, CAND1, C3, PFKL, PYGB, IQGAP1, ERP44, XRCC5, F2

Enrichment (N, B, n, b) is defined as follows:
N - is the total number of genes
B - is the total number of genes associated with a specific GO term
n - is the number of genes in the top of the user's input list or in the target set when appropriate
b - is the number of genes in the intersection
Enrichment = (b/n) / (B/N)

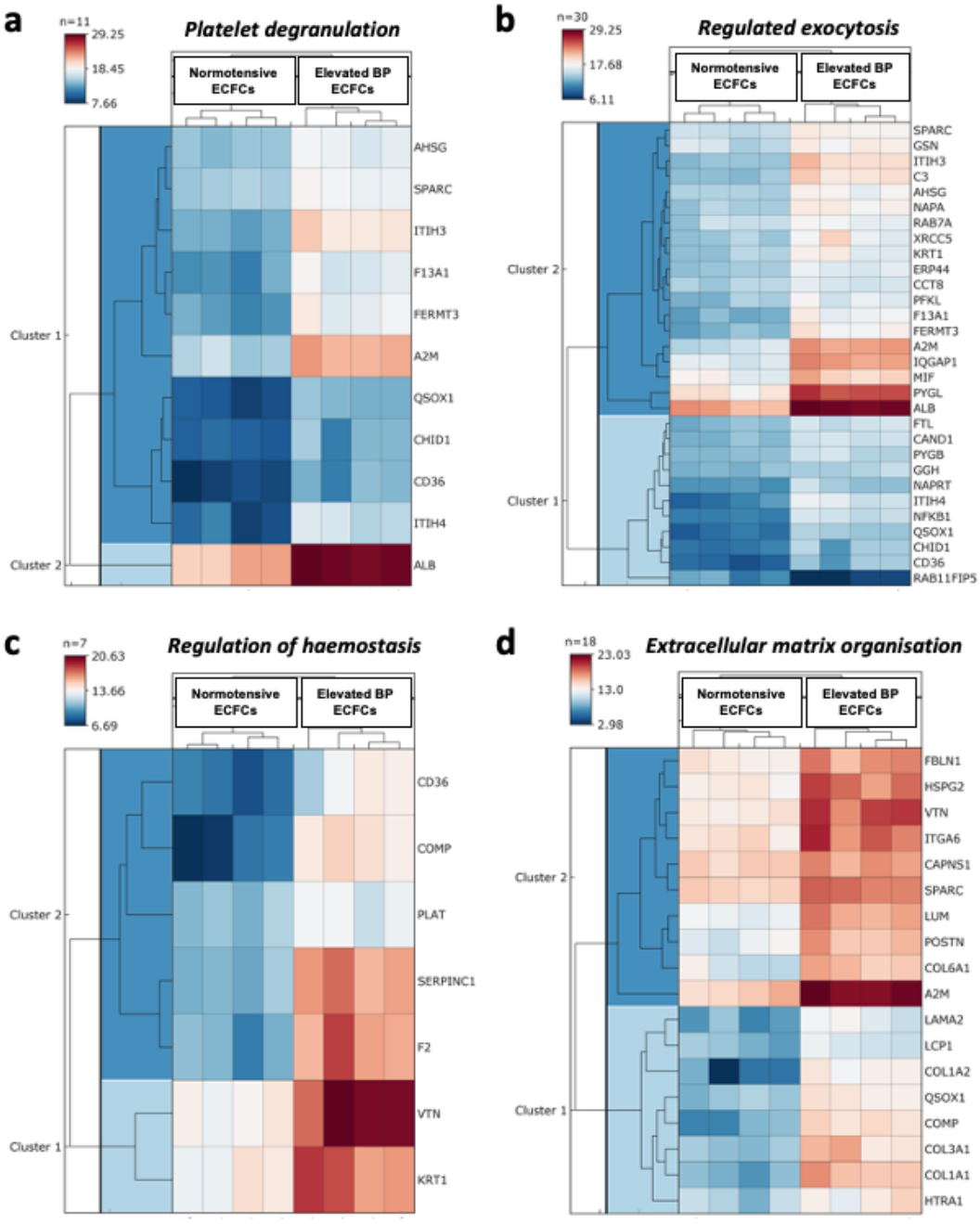
Supplementary Table S5.8

Table S5.8. Gene Ontology enRIchement anaLysis and visuaLisAtion (GOrilla) analysis with enriched GO cellular component pathway.

GO term	Description	P-value	FDR q-value	Enrichment (N, B, n, b)	Proteins
GO:0044433	Cytoplasmic vesicle part	2.91E-08	7.73E-06	1.57 (49,29,28,26)	A2M, CCT8, FTL, F13A1, GSN, PYGB, IQGAP1, FERMT3, ITIH3, ITIH4, SPARC, KRT1, RAB7A, CD36, QSOX1, GGH, NFKB1, AHSG, PYGL, CAND1, C3, PFKL, ERP44, XRCC5, RAB11FIP5, ALB,
GO:0034774	Secretory granule lumen	5.51E-07	7.32E-05	1.73 (49,22,27,21)	A2M, CCT8, FTL, F13A1, GGH, QSOX1, GSN, NFKB1, AHSG, PYGL, CAND1, C3, PYGB, PFKL, ERP44, FERMT3, ITIH3, XRCC5, ITIH4, SPARC, ALB,
GO:0031983	Vesicle lumen	5.51E-07	4.88E-05	1.73 (49,22,27,21)	A2M, CCT8, FTL, F13A1, GGH, QSOX1, GSN, NFKB1, AHSG, PYGL, CAND1, C3, PYGB, PFKL, ERP44, FERMT3, ITIH3, XRCC5, ITIH4, SPARC, ALB,
GO:0060205	Cytoplasmic vesicle lumen	5.51E-07	3.66E-05	1.73 (49,22,27,21)	A2M, CCT8, FTL, F13A1, GGH, QSOX1, GSN, NFKB1, AHSG, PYGL, CAND1, C3, PFKL, PYGB, ERP44, FERMT3, XRCC5, ITIH3, ITIH4, SPARC, ALB,
GO:0031093	Platelet alpha granule lumen	2.93E-06	1.56E-04	5.44 (49,7,9,7)	A2M, FERMT3, F13A1, SPARC, ALB, QSOX1, AHSG,
GO:0044422	Organelle part	2.41E-04	1.07E-02	1.22 (49,40,29,29)	A2M, CCT8, FTL, F13A1, GSN, PYGB, IQGAP1, FERMT3, ITIH3, ITIH4, SPARC, KRT1, CHID1, RAB7A, CD36, QSOX1, GGH, NFKB1, NAPA, AHSG, PYGL, CAND1, C3, PFKL, ERP44, XRCC5, RAB11FIP5, F2, ALB,
GO:0044446	Intracellular organelle part	2.41E-04	9.16E-03	1.22 (49,40,29,29)	A2M, CCT8, FTL, F13A1, GSN, PYGB, IQGAP1, FERMT3, ITIH3, ITIH4, SPARC, KRT1, CHID1, RAB7A, CD36, GGH, QSOX1, NFKB1, NAPA, AHSG, PYGL, CAND1, C3, PFKL, ERP44, XRCC5, RAB11FIP5, F2, ALB,

Enrichment (N, B, n, b) is defined as follows:
N - is the total number of genes
B - is the total number of genes associated with a specific GO term
n - is the number of genes in the top of the user's input list or in the target set when appropriate
b - is the number of genes in the intersection
Enrichment = (b/n) / (B/N)

Supplementary Figure S5.1



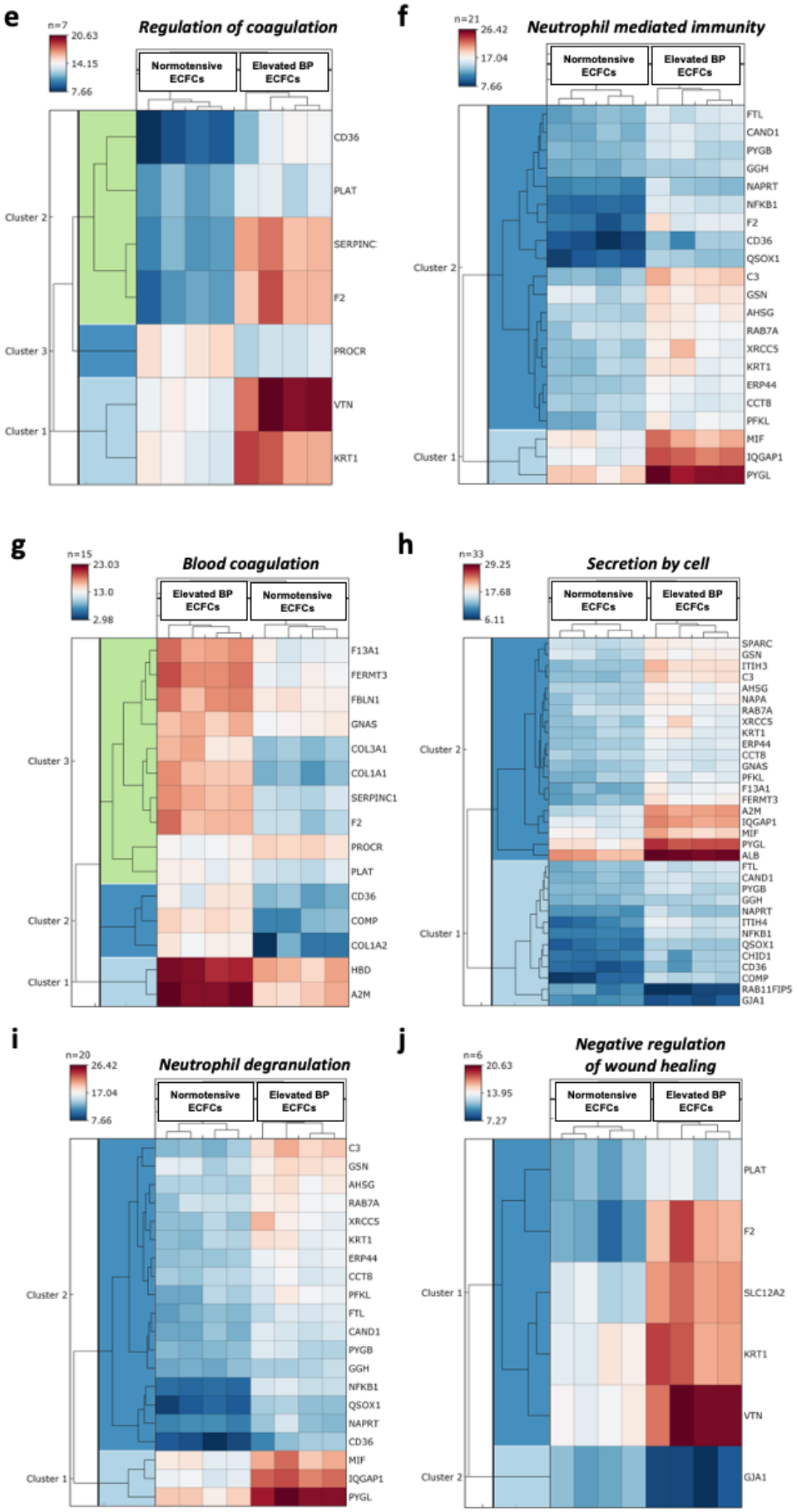

e
Regulation of coagulation
n=7
20.63
14.15
7.66
Normotensive ECFCs
Elevated BP ECFCs
CD36
PLAT
SERPINC
F2
PROCR
VTN
KRT1
Cluster 2
Cluster 3
Cluster 1
f
Neutrophil mediated immunity
n=21
26.42
17.04
7.66
Normotensive ECFCs
Elevated BP ECFCs
FTL
CAND1
PYGB
GGH
NAPRT
NFKB1
F2
CD36
QSOX1
C3
GSN
AHSG
RAB7A
XRCC5
KRT1
ERP44
CCT8
PFKL
MIF
IQGAP1
PYGL
Cluster 2
Cluster 1
g
Blood coagulation
n=15
23.03
13.0
2.98
Elevated BP ECFCs
Normotensive ECFCs
F13A1
FERMT3
FBLN1
GNAS
COL3A1
COL1A1
SERPINC1
F2
PROCR
PLAT
CD36
COMP
COL1A2
HBD
A2M
Cluster 3
Cluster 2
Cluster 1
h
Secretion by cell
n=33
29.25
17.68
6.11
Normotensive ECFCs
Elevated BP ECFCs
SPARC
GSN
ITIH3
C3
AHSG
NAPA
RAB7A
XRCC5
KRT1
ERP44
CCT8
GNAS
PFKL
F13A1
FERMT3
A2M
IQGAP1
MIF
PYGL
ALB
FTL
CAND1
PYGB
GGH
NAPRT
ITIH4
NFKB1
QSOX1
CHID1
CD36
COMP
RAB11FIP5
GJA1
Cluster 2
Cluster 1
i
Neutrophil degranulation
n=20
26.42
17.04
7.66
Normotensive ECFCs
Elevated BP ECFCs
C3
GSN
AHSG
RAB7A
XRCC5
KRT1
ERP44
CCT8
PFKL
FTL
CAND1
PYGB
GGH
NFKB1
QSOX1
NAPRT
CD36
MIF
IQGAP1
PYGL
Cluster 2
Cluster 1
j
Negative regulation of wound healing
n=6
20.63
13.95
7.27
Normotensive ECFCs
Elevated BP ECFCs
PLAT
F2
SLC12A2
KRT1
VTN
GJA1
Cluster 1
Cluster 2

Figure S5.1. Heatmaps of proteins identified from the String™ interactive pathway analysis.

The enriched pathways included: **(a)** platelet degranulation, **(b)** regulated exocytosis, **(c)** regulation of haemostasis, **(d)** extracellular matrix organisation, **(e)** regulation of coagulation, **(f)** neutrophil mediated immunity, **(g)** blood coagulation, **(h)** secretion by cell, **(i)** neutrophil degranulation, and **(j)** negative regulation of wound healing.

6

Effect of Exercise Training on ECFC function.



6. Effect of Exercise Training on ECFC function

6.1 Abstract

Background

The incidence of high BP is a significant public health concern that requires early population-level interventions. Numerous epidemiological and clinical studies have demonstrated that lifestyle modifications, including exercise, can significantly contribute to BP control and improve aerobic capacity, including oxygen uptake (VO_2), vascular endothelium, and EPCs in hypertensive patients and healthy individuals. However, most clinical studies have focussed on the benefits of exercise on individuals' general cardiovascular health in older populations. Little is known about the effects of exercise training in younger adults and whether there is an effect on ECFCs.

Methods

To examine the impact of 16-weeks of prescribed aerobic exercise training on ECFC function, 63 participants (n=28 controls and n=35 intervention) recruited into TEPHRA were included for the analysis in this chapter. All participants underwent baseline clinical assessments, including anthropometrics, BP, cardiopulmonary exercise testing (CPET) and blood tests. ECFCs were isolated from peripheral blood, and successfully isolated ECFCs were used to assess the functionality (proliferation and angiogenesis capacity). ECFCs were deemed dysfunctional if <1 closed tube formed during the in vitro tube formation assay and the proliferation rate <20%. All measurements were repeated at the post-intervention follow-up visit.

Results

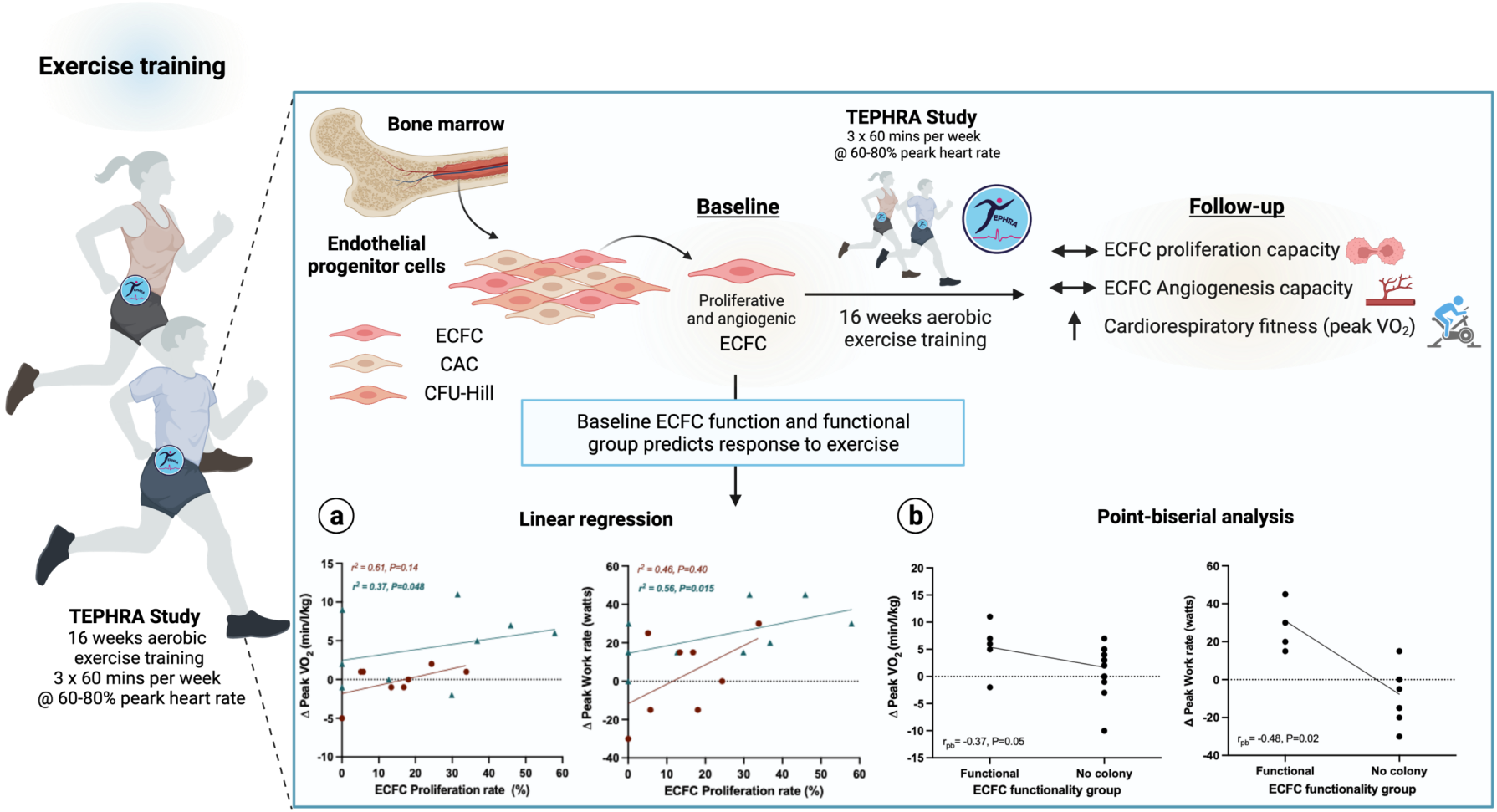
Individuals in the exercise arm displayed significant improvement in cardiopulmonary fitness (Δ Peak VO_2: 2.32 ± 4.76 ml/min/kg vs -1.12 ± 3.12 ml/min/kg, P=0.008, and Δ percentage of normal VO_2 at peak: 7.63 ± 14.61 % vs -2.61 ± 7.99 %, P=0.005) as compared to controls. Our

data demonstrated no significant changes in ECFC function before and after exercise intervention. Linear regression analysis of ECFC functional characteristics at baseline (pre-intervention) demonstrated a relationship with change in cardiopulmonary fitness. Positive correlations between pre-intervention ECFC proliferation rate with Δ peak VO_2 and Δ peak work rate (β=1.01, P<0.05, β=0.92, P=0.015) were found, respectively. A similar positive correlation was observed between pre-intervention ECFC angiogenic capacity and Δ peak work rate post-intervention (β=0.86, P=0.035). Individuals with functional ECFCs pre-intervention had significant improvements in peak VO_2 (r_{pb}= -0.37, P=0.05) and work rate (r_{pb}=-0.48, P=0.015) as compared to individuals with no colony formation.

Conclusion

Improvements in ECFC function did not underpin improvements in aerobic exercise-induced cardiopulmonary fitness. Our data demonstrated for the first time that baseline ECFC functional characteristics might predict response to exercise assessed by peak VO_2, indicating that subjects with functional ECFCs may develop positive responses to exercise compared to those with dysfunctional ECFCs. Nevertheless, the mechanisms underlying the link between ECFC function and physical adaptations to exercise have yet to be fully explored and warrant further research.

Graphical abstract



Abbreviations: ECFC, endothelial colony-forming cells; CAC, circulating angiogenic cells; CFU-Hill, colony-forming unit–Hill cells; ⟷ denotes no change; ↑denotes increase.

6.2 Introduction

Hypertension is regarded as a multifactorial condition; the aetiology and severity are influenced by dynamic interactions among genetic and environmental factors[429, 430]. It has been demonstrated that lifestyle modifications, including increased physical activity, can significantly contribute to BP control[431, 432]. A sedentary lifestyle increases the risk of many adverse health conditions, including CVDs, and shortens life expectancy[433, 434]. In contrast, increased occupational or leisure-time physical activity is associated with lower levels of BP[435]. Several intervention studies have been conducted so far, supporting the role of physical activity in modulating BP[436]. Physical training reduces BP, improves aerobic capacity, and shows beneficial effects for the vascular endothelium and EPCs in hypertensive patients and healthy individuals[211, 220, 257, 258].

VO_2 represents a measure of the body's capacity to supply oxygen to skeletal muscle to perform physical work[213]. VO_2 reflects the integration of multiple organ systems and cellular processes, including pulmonary ventilation, the oxygen-carrying capacity and transport through the circulatory system, cardiac output, central nervous system recruitment of motor units, oxygen diffusion and extraction at the capillary–skeletal muscle levels, as well as mitochondrial respiration[437]. Peak VO_2 defines the limits of these processes and is thus widely considered the gold-standard measure of cardiorespiratory fitness (CRF)[213, 438]. It is, therefore, not surprising that peak VO_2 (as a direct measure of CRF) has been firmly established as a powerful prognostic marker of CVD and all-cause mortality[439]. Peak VO_2's inverse relationship with CVD and mortality risk applies to both its baseline measure (intrinsic peak VO_2) and capacity to improve peak VO_2 through regular physical activity (adaptive peak VO_2; Δpeak VO_2)[440].

It is well established that hypertensive individuals have low numbers of functioning EPCs[441]. In turn, aerobic training increases the levels of EPCs in patients with cardiovascular risk or established CVD[442], balancing out endothelial injury and repair. Exercise training seems to increase the number of circulating EPCs, contributing to vascular regeneration and angiogenesis[232, 233, 255].

These positive effects of regular exercise seem to be closely related to increasing NO bioavailability, improving intracellular redox balance and mitochondrial health, increasing the number and recovering capability of circulating EPCs and lowering systemic inflammation[442].

Several clinical trials assessing the chronic effects of exercise have shown that an elevation in circulating EPCs coincides with an improvement in cardiopulmonary fitness capacity, including peak VO_2, 6-minute walk test and maximal walking distance[262, 273, 280-285]. This suggests that EPCs may positively affect cardiopulmonary fitness via changes in the altered micro-vasculature, which leads to an improvement in oxygen utilisation and aerobic power. However, no studies have yet investigated the association between aerobic exercise training and ECFCs, a subtype of EPCs, in young adults.

6.2.1 Study hypotheses, aims and clinical significance

This chapter seeks to investigate the effect of a 16-week aerobic exercise training intervention on the function and characteristics of ECFCs derived from peripheral blood of young adults with elevated BP or stage 1 hypertension and determine if ECFC function can predict the response to exercise training. We hypothesised that:

1. Exercise intervention will improve ECFC function and its relationship with other clinical measurements.
2. ECFC cellular function (proliferative and angiogenic capacity) can predict the response to the exercise intervention.

To address the hypothesis, we aimed to:

1. *Assess ECFC function pre- and post-exercise intervention and correlate it with clinical measurements to determine if ECFC functionality can predict the change in clinical measures after exercise intervention.*

This chapter will allow us to understand the potential impact of exercise training on ECFC function.

6.3 Methodology

6.3.1 Study population and general methods

Participants were recruited as part of a baseline assessment visit for the TEPHRA study. Ethical approval was provided by the Oxford Research Ethics Committee (Ethics reference: 16/SC/0016). For this study, we included 63 young adults aged between 18-35 years, body mass index (BMI) <30 kg/m^2, clinical BP 115mmHg > systolic BP <159 mmHg and/or 70mmHg> diastolic BP <99 mmHg without any clinical diagnosis of CVDs and medications. All participants provided written consent for the collection and subsequent experimental use of samples under appropriate ethical approvals. Details of the study are outlined in **Chapter 2 – Study population, Section 2.3.**

The following methods that were used for this chapter are described in detail in **Chapter 3**:

3.1 Anthropometric measurements

3.2 BP measurements

3.3 Blood sample collection and biochemistry analysis

3.4 ECFC isolation and cellular assessments

- 3.4.1 Fluorescence-activated cell sorting (FACS)
- 3.4.2 Immunofluorescence staining
- 3.4.3 EdU proliferation assay
- 3.4.4 In vitro tube formation assay

6.3.2 ECFC functionality classification

Cellular proliferation and angiogenic capacity were assessed to classify the functionality of ECFCs. Specifically, ECFCs with less than one closed tube formed on Matrigel and less than 20% proliferation rate was deemed dysfunctional[148]. The 20% proliferation cutoff was established based on previous published studies on the capacity of ECFCs to sufficiently expand in culture to form

cobblestone-shaped colonies after the first or second passages and reach at least 30% confluence[10, 148]. Cell functional assessments were performed using cells obtained from no more than two passages after PBMC culture.

6.3.3 Cardiopulmonary exercise testing

Cardiac function and oxygen requirements in response to an incremental workload were measured via CPET. CPET was carried out using the protocol described in a previously published study[443]. The exercise protocol is a validated incremental protocol with established use in clinical and research practice. The exercise protocol is currently utilised in ongoing ethically approved studies conducted by our lab and was performed on a stationary cycle ergometer. The test commences with resting measures of spirometry **(Figure 6.1)**.

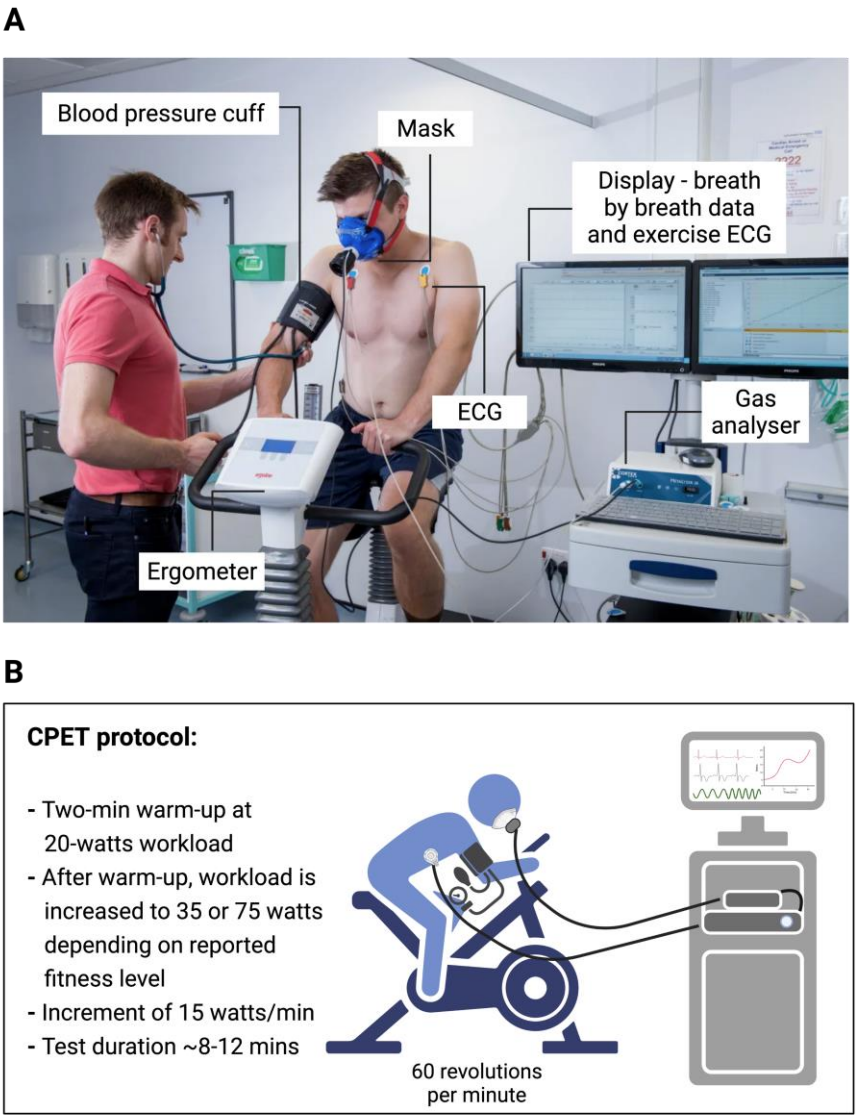


Figure 6.1. Standard cardiopulmonary exercise testing (CPET) set-up (A) and TEPHRA CPET protocol (B).

Resting spirometry was performed as a part of calibration prior to performing CPET on a seated stationary cycle ergometer (Ergoline GmbH, Germany) using a validated incremental protocol with respiratory gases and electrocardiogram monitoring (Metalyzer 3B, Cortex Biophysik, Germany). Heat rate and perceived exertion were recorded at a two-minute interval. BP was measured using a manual mercury sphygmomanometer at a four-minute interval. After one minute of resting measurements, participants proceeded to the two-minute warm-up with a 20-watt workload. Participants were instructed to maintain a rate of 60 revolutions per minute (rpm) for

the entire test. Post-warm-up, the workload increased to 35 watts. To normalise test duration to approximately 10–14 minutes, participants who reported higher activity or fitness levels had a workload increased to 75 watts after the warm-up period. The workload was automatically increased by 15 watts per minute for all participants. Participants cycled continuously until termination criteria were met, or fatigue prevented them from maintaining at least 50 rpm. Participants then completed a two-minute cooldown period at 35 watts at a workload of their preference.

6.3.4 Randomisation - Exercise intervention and control group

Participants meeting the main study inclusion criteria for the full trial were randomly allocated 1:1 to the two arms (exercise intervention or control group) as described in Williamson *et al.*, 2018 and **Chapter 2 – Study population, Section 2.3.2.** A minimisation algorithm (with a random element of 80%) is used to ensure balanced allocation across the two groups for key prognostic factors: sex, age and gestational age of participants. The categories for each prognostic factor were as follows:

- Sex: male/female;
- Age: < 24 years old, 24–29 years old, 30–35 years old;
- Gestational age: ≤32 weeks, 32–37 weeks, > 37 weeks.

ECFC functional characteristics were not included in the randomisation process.

Briefly, participants were recruited and randomised into either an exercise group (16-month exercise intervention) or a control group following routine lifestyle guidance **(Figure 6.2).** Participants were requested to return for the follow-up study visits at 16 weeks (post-intervention visit 2) with repeated measurements of the parameters performed at baseline.

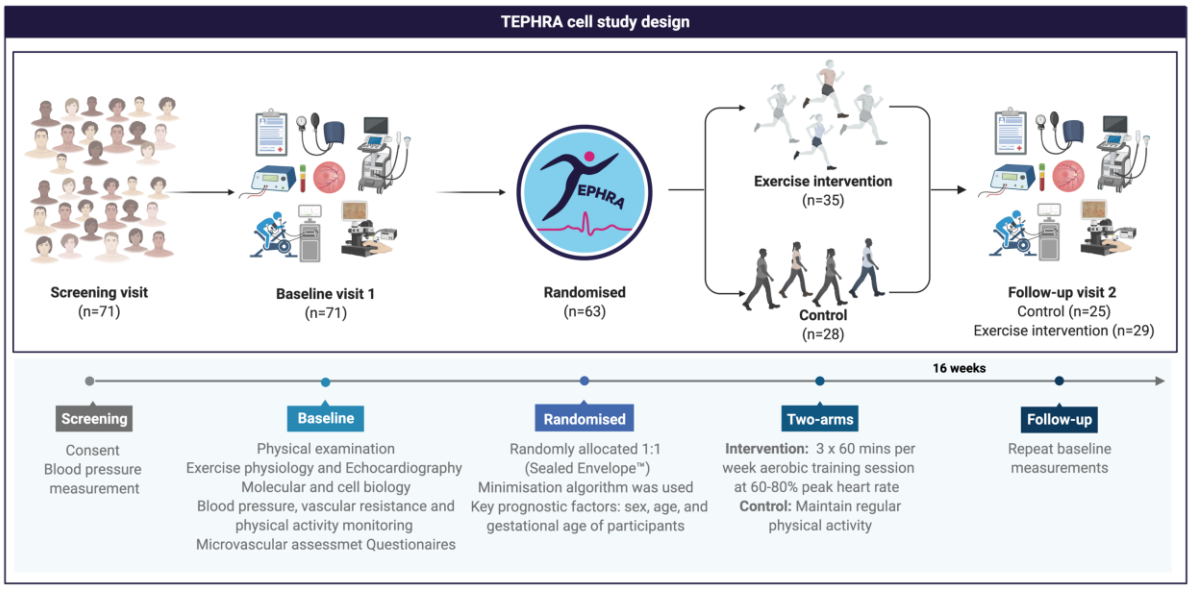


Figure 6.2. Schematic representation of TEPHRA cell study design.

6.3.5 Statistical analysis

All statistical analyses were performed using SPSS version 25 (IBM, North Castle, NY, USA). The Shapiro-Wilk test was used to assess the normality of variables. Dependent on the normality of sample distribution, comparisons between two groups were performed by either a parametric independent t-test or a non-parametric Mann-Whitney U test. The Kruskal-Wallis test was performed with a Bonferroni post hoc test to compare ECFC functionality groups (functional, dysfunctional and no colony). Categorical variables were compared by $\chi 2$ or Fisher's Exact tests. Results are presented as mean ± standard deviation (SD) unless stated otherwise. Pearson correlations (r) were used for bivariate associations. P values ≤ 0.05 were considered statistically significant.

6.4 Results

6.4.1 Study population

A total of 63 participants that had PBMCs isolated were randomised into the trial. Of the 63 participants, 28 and 35 were randomised into the control and exercise groups, respectively **(Figure 6.3)**. Of these, 13/28 (46.43%) control participants and 13/35 (37.14%) intervention participants had successfully isolated baseline ECFCs. Twenty-five (89.29%) control and 29 (82.85%) exercise participants completed the follow-up visit. Due to limited human resources and some participants not providing consent for the blood draw, we only managed to isolate PBMCs from 18 controls and 19 exercise group individuals, with 8/18 (44.44%) and 11/19 (57.89%) with ECFC colony formation in each respective group. There were nine matched visit 1 and visit 2 samples (n=6 controls and n=3 exercise intervention group).

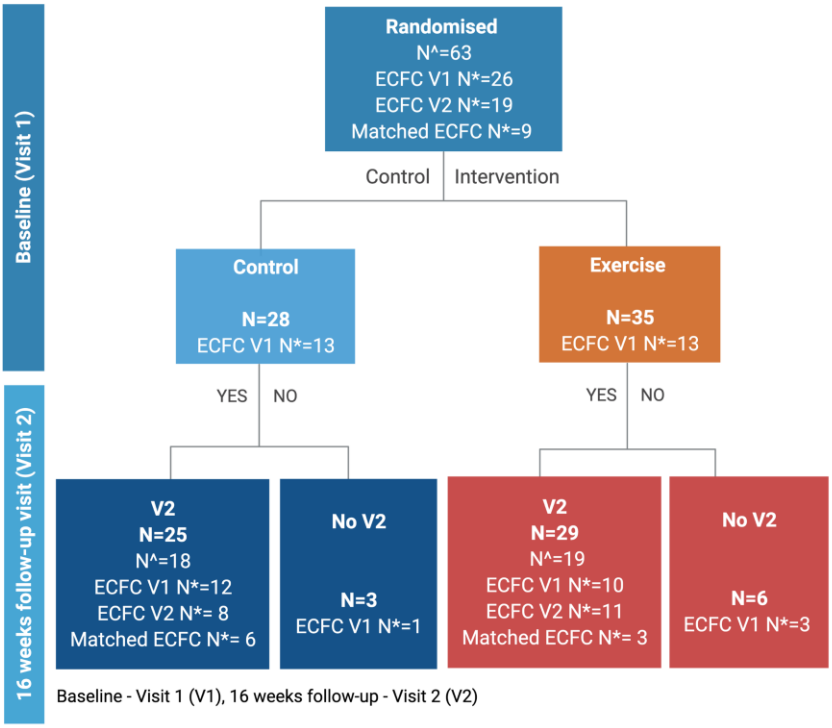


Figure 6.3. Flowchart of TEPHRA cell study participants that were randomised into the trial.

From the trial, 63 participants had their blood taken for ECFCs isolation at baseline and 37 participants 16 weeks follow-up visit, respectively. **N** (bold) represents the number of participants that participated in the visit. N^ represents the number of participants with blood collected for

ECFC culture. N* represents the number of ECFC successfully isolated from participants in the baseline visit (visit 1) or 16-week follow-up (visit 2).

6.4.2 Clinical characteristics and ECFC phenotype

The clinical characteristics of the participants with blood collection from both baseline and follow-up visits (n=18 in control and n=19 in the exercise intervention group) are presented in **Table 6.1 and Table 6.2,** respectively. Baseline characteristics were the same across controls and the intervention group. Differences in Δ BMI (0.39 ± 0.61 kg/m^2 and -0.13 ± 0.66 kg/m^2, P<0.02) and Δ systolic BP (-3.94 ± 9.46 mmHg and 1.95 ± 6.67mmHg, P=0.037) were observed in control and exercise intervention groups respectively. CPET revealed improvements in and peak VO_2 (34.11 ± 7.94 ml/min/kg and 36.42 ± 7.43 ml/min/kg, respectively, P=0.05) in individuals pre- and post-intervention **(Table 6.2)**. Significant differences were observed in controls vs the intervention group, with Δ Peak VO_2 not corrected for body weight (-0.07 ± 0.23 L/m and 0.15 ± 0.35 L/min respectively, P=0.02), Δ Peak VO_2 adjusted for body weight (-1.12 ± 3.12 ml/min/kg and 2.32 ± 4.76 ml/min/kg, respectively, P=0.008) and Δ percentage of normal VO_2 at peak (-2.61 ± 7.99 % and 7.63 ± 14.61 %, respectively, P=0.005). However, no changes were observed in the ECFC function **(Table 6.3).**

Table 6.1. Demographics and anthropometrics of the participants in TEPHRA study.

Demographics and anthropometrics	Control (n=18)			P-Value*	Exercise intervention (n=19)			P-Value*	P-Value^{v1}	P-Value$^{\Delta}$
	Baseline	Visit 2	Δ		Baseline	Visit 2	Δ			
Male, n	10				11			-	1	-
Female, n	8				8					
Age, years	27. 56 ± 4.05			-	27.37 ± 3.65			-	0.88	-
Height, cm	173.06 ± 10.24	172.87 ± 9.84	-0.19 ± 1.38	0.57	177.16 ± 8.03	177.22 ± 8.08	+0.053 ± 0.83	0.79	0.19	0.51
Weight, kg	75.01 ± 14.72	75.93 ± 13.97	+0.92 ± 2.1	0.081	79.39 ± 14.48	79.03 ± 15.15	-0.35 ± 1.85	0.42	0.36	0.06
BMI, kg/m^2	24.84 ± 2.98	25.23 ± 2.88	+0.39 ± 0.61	**0.015**	25.22 ± 3.93	25.09 ± 4.14	-0.13 ± 0.66	0.39	0.74	**0.02**
Total body fat, % (n)	26.08 ± 7.61 (16)	26.05 ± 7.06 (15)	+0.79 ± 1.56 (15)	0.069	23.86 ± 10.35 (18)	23.68 ± 8.89 (17)	+0 ± 1.58 (16)	1	0.48	0.17
Total fat free mass, kg (n)	56.99 ± 12.42 (16)	57.30 ± 12.51 (15)	-0.37 ± 1.34 (15)	0.3	60.88 ± 10.68 (18)	61.07 ± 11.62 (17)	+0.11 ± 0.89 (16)	0.62	0.34	0.25
Total fat mass, kg (n)	20.01 ± 7.35 (16)	20.05 ± 6.88 (15)	+0.65 ± 1.4 (15)	0.092	19.67 ± 10.81 (18)	19.35 ± 9.91 (17)	-0.02 ± 1.55 (16)	0.96	0.92	0.22
Birth gestational age, weeks	37.33 ± 4.78				37.21 ± 2.8			-	0.93	-
Clinic seated blood pressure (BP)										
Systolic BP, mmHg	125.72 ± 10.3	121.78 ± 11.93	-3.94 ± 9.46	0.095	122.05 ± 10.89	124 ± 12.77	+1.95 ± 6.67	0.22	0.30	**0.037**
Diastolic BP, mmHg	78.28 ± 7.47	75.61 ± 8.26	-2.67 ± 6.66	0.11	76.47 ± 9.62	77.68 ± 7.82	+1.21 ± 7.03	0.46	0.53	0.094
Mean arterial pressure, mmHg	96.22 ± 7.83	92.58 ± 9.26	-3.64 ± 6.44	**0.028**	94.21 ± 8.7	94.13 ± 8.74	-0.08 ± 7.12	0.96	0.46	0.12
Heart rate, beats per min	68.78 ± 8.54	73.14 ± 9.02	+4.36 ± 9.28	**0.03**	67.68 ± 8.15	66.18 ± 9.61	-1.5 ± 8.78	0.47	0.69	0.06
Blood Biochemistry										
Triglyceride, mmol/l	1.09 ± 0.65	1.02 ± 0.54	-0.065 ± 0.34	0.43	0.98 ± 0.38	0.79 ± 0.27	-0.19 ± 0.32	**0.019**	0.54	0.27
Cholesterol, mmol/l	4.6 ± 0.68	4.47 ± 0.69	-0.13 ± 1.09	0.61	4.29 ± 0.86	4.16 ± 0.79	-0.13 ± 0.85	0.52	0.22	0.99
High density lipoprotein, mmol/l	1.35 ± 0.33	1.35 ± 0.31	-0.0078 ± 0.2	0.87	1.35 ± 0.27	1.37 ± 0.28	+0.018 ± 0.24	0.75	0.96	0.72

Low density lipoprotein, mmol/l	2.71 ± 0.52	2.67 ± 0.7	-0.039 ± 0.54	0.77	2.49 ± 0.7	2.43 ± 0.61	-0.058 ± 0.52	0.63	0.29	0.91
Glucose, mmol/l	4.95 ± 0.42	5 ± 0.77	+0.048 ± 0.71	0.78	4.87 ± 0.45	4.65 ± 0.41 (15)	-0.12 ± 0.38 (15)	0.24	0.60	0.42
Insulin, pmol/l	58.51 ± 38.4	77.43 ± 84.56	+18.92 ± 85.82	0.36	55.77 ± 32.35	44.35 ± 21.3	-11.42 ± 31.96	0.14	0.82	0.17
HOMA β-cell, %	103.09 ± 35.99	117.11 ± 51.81 (16)	+14.02 ± 49.24 (16)	0.27	102.09 ± 30.49 (18)	98.28 ± 25.6 (15)	-3.78 ± 32.42 (14)	0.67	0.78	0.25
HOMA β-cell sensitivity, %	113.68 ± 59.40 (16)	102.52 ± 62.22 (16)	-11.16 ± 52.52 (16)	0.41	116.24 ± 52.59 (18)	139.94 ± 56.62(15)	+14.8 ± 47.72 (14)	0.27	0.69	0.17
HOMA Insulin resistance	1.09 ± 0.71	1.57 ± 1.59 (16)	+0.41 ± 1.66 (16)	0.34	1.08 ± 0.59 (18)	0.85 ± 0.43 (15)	-0.11 ± 0.43 (14)	0.36	0.96	0.25
C-reactive protein, mg/l	3.28 ± 5.83 (16)	2.73 ± 4.0	-0.55 ± 4.66 (16)	0.65	1.64 ± 2.2 (18)	1.75 ± 2.59	0.21 ± 1.46 (18)	0.55	0.30	0.54

Data are expressed as mean ± standard deviation (SD). Comparison between respective baseline (V1) and visit 2 (V2) data within the same group*; and comparison between Δ for control vs. intervention $^{\Delta}$. Independent t-test, paired sample t-test or χ^2 test. All P-values are not sex-adjusted.

Table 6.2. Cardiopulmonary exercise test of the participants in TEPHRA study.

Cardiopulmonary Exercise Testing	Control (n=18)			P-Value *	Exercise intervention (n=19)			P-Value*	P-Value^{v1}	P-Value$^{\Delta}$
	Baseline	Visit 2	Δ		Baseline	Visit 2	Δ			
At peak										
VO_2, L/ml	2.67 ± 0.77	2.64 ± 0.73 (17)	-0.07 ± 0.23 (17)	0.2	2.67 ± 0.69	2.82 ± 0.5	+0.15 ± 0.35	0.08	0.89	**0.02**
VO_2/kg, ml/min/kg	35.39 ± 6.94	34.82 ± 6.05 (17)	-1.12 ± 3.12 (17)	0.16	34.11 ± 7.94	36.42 ± 7.43	+2.32 ± 4.76	**0.05**	0.53	**0.008**
Oxygen pulse, ml/min/heartbeat	14.83 ± 4.4	14.18 ± 4.07 (17)	-0.82 ± 2.63 (17)	0.21	14.94 ± 3.72 (18)	15.37 ± 2.81	+0.39 ± 2.38 (18)	0.5	0.86	0.12
Heart rate, beats/min	185.76 ± 11.1 (17)	186.76 ± 7.94 (17)	-0.37 ± 9.21 (16)	0.87	178.22 ± 11.68 (18)	180.32 ± 11.05	+1.22 ± 5.79 (18)	0.38	0.06	0.55
Work rate, watts	221.94 ± 67.02	221.76 ± 62.67 (17)	-4.12 ± 18.22 (17)	0.37	223.16 ± 49.11	231.32 ± 41.33	+8.16 ± 23.52	0.15	0.99	0.07
Ventilatory equivalent for O_2 (V_E/VO_2)	37.56 ± 5.13	36.84 ± 5.38 (17)	-1.11 ± 5.56 (17)	0.42	36.31 ± 4.91	35.07 ± 5.52	-1.24 ± 3.83	0.18	0.46	0.96
Ventilatory equivalent for CO_2 (V_E/VCO_2)	32.3 ± 3.58	32.42 ± 3.47 (17)	-0.24 ± 3.81 (17)	0.8	31.72 ± 3.34	30.79 ± 3.43	-0.93 ± 2.31	0.1	0.62	0.52
Respiration exchange ratio (RER)	1.16 ± 0.06	1.15 ± 0.05 (17)	-0.01 ± 0.06 (17)	0.68	1.14 ± 0.05	1.14 ± 0.1	-0.01 ± 0.07	0.67	0.35	0.96
Minute ventilation (V_E), L/min	106.04 ± 27.48	104.11 ± 24.11 (17)	-4.3 ± 15.82 (17)	0.28	103.56 ± 27.96	105.68 ± 24.37	+2.12 ± 19.25	0.64	0.65	0.23
Ventilatory threshold , L	2.55 ± 0.65	2.51 ± 0.69 (17)	-0.08 ± 0.26 (17)	0.24	2.42 ± 0.58	2.56 ± 0.65	+0.13 ± 0.39	0.16	0.42	0.07
Respiratory rate, breaths/min	41.94 ± 5.1	42.76 ± 8.26 (17)	+0.41 ± 6.63 (17)	0.8	43.32 ± 10.22	43.11 ± 11.87	-0.21 ± 6.98	0.9	0.63	0.81

Data are expressed as mean ± standard deviation (SD). Comparison between respective baseline (V1) and visit 2 (V2) data*; Δ between V1 and V2 $^{\Delta}$; and comparison between baseline v1 measurements between control and exercise groupv1. Independent t-test, paired sample t-test or χ^2 test. All P-values are sex-adjusted, except for ccomparisons between respective V1 and V2*.

Table 6.3. Endothelial colony-forming cell (ECFC) characteristics of the participants in TEPHRA study

ECFC characteristics	Control (n=18)			P-Value*	Exercise intervention (n=19)			P-Value*	P-Value^{v1}	P-Value$^{\Delta}$
	Baseline	16 weeks	Δ		Baseline	16 week	Δ			
ECFC colony formed/n of cells collected, (%)	8/18 (44.4%)	8/18 (44.4%)	-	0.054	6/13 (46.2%)	11/18 (66.1%)	-	0.51	0.89	-
Days for ECFC colony formation (n)	17.25 ± 5.5 (8)	16.38 ± 6.52 (8)	-0.17 ± 5.91 (6)	0.95	14.83 ± 6.11 (6)	13 ± 4.24 (11)	-0.67 ± 7.37 (3)	0.89	0.40	0.93
Proliferation rate (%) (n)	20.26 ± 12.26 (7)	15.94 ± 10.3 (7)	-1.48 ± 12.85 (5)	0.81	19.91 ± 23.93 (6)	20.23 ± 11.01 (9)	-9.98 ± 23.07 (3)	0.53	0.89	0.56
Closed tube formed, n per $1.5x10^4$ (n)	3.11 ± 4.06 (7)	7.49 ± 9.04 (7)	+2.78 ± 6.76 (5)	0.41	6.8 ± 7.67 (6)	7.12 ± 7.66 (9)	-4.13 ± 3.74 (3)	0.2	0.24	0.13
Branches formed, n per $1.5x10^4$ (n)	13.96 ± 7.73 (7)	18 ± 15.46 (7)	+1.76 ± 11.56 (5)	0.75	17.79 ± 16.79 (6)	23.6 ± 19.3 (9)	-3.97 ± 10.7 (3)	0.59	0.36	0.54

Data are expressed as mean ± standard deviation (SD). Comparison between respective baseline (V1) and visit 2 (V2) data*; baseline data^; 16 weeks data$^{\#}$; and Δ between V1 and V2^{+}. Independent t-test, paired sample t-test or χ^2 test. All P-values are sex-adjusted, except for comparisons between respective V1 and V2*.

No ECFC colony formation was observed on eight participants from the control group at the baseline and visit 2 and five from the exercise intervention group at both the baseline and visit 2 **(Figure 6.4)**. Due to no EFCF colony formation for some participants, there was a low number of matched samples for analyses. We were, therefore, unable to make statistically powered comparisons.

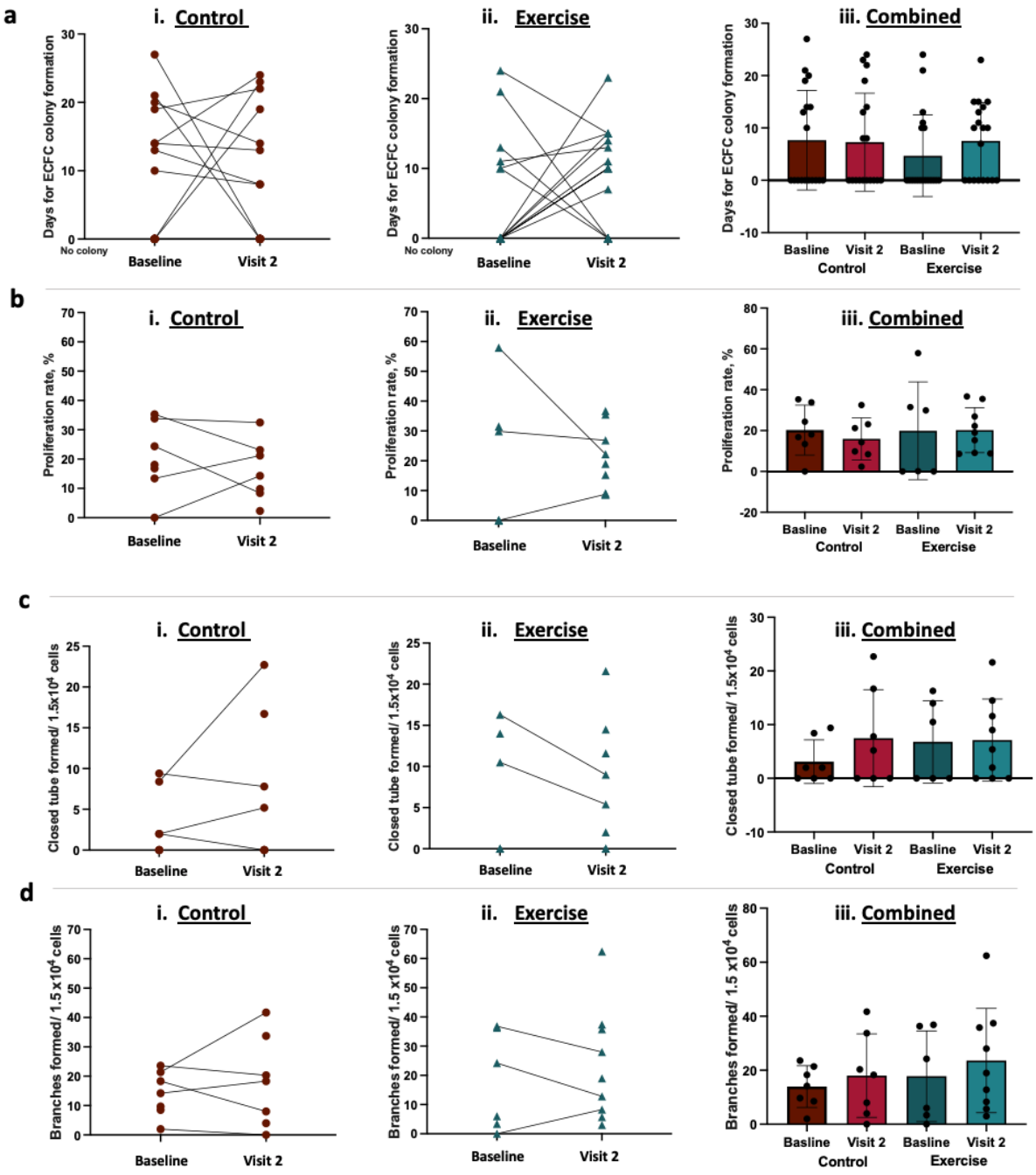


Figure 6.4.Characteristics of endothelial colony-forming cells collected from participants in the control group (n=18) and exercise intervention group (n=19).

Scatter plots representing days taken for ECFC colony formation **(a)**; proliferation rate **(b)**; closed tube formation **(c)**; and branches formed per $1.5x10^4$ cells **(d)** from pre-intervention (i. baseline) to post-intervention (ii. visit 2). Eight individuals from the control group had no colony formation for both baseline and visit 2; n=5 from the exercise intervention group had no colony formation for both baseline and visit 2. The combined data are represented in the box plot (iii.).

We further categorised the participants based on the functionality of ECFCs and no colony formation in the control and intervention groups to investigate if there was a change in the function and colony formation with and without exercise intervention **(Figure 6.5).** Our data showed no significant differences with the intervention despite an increase in ECFC colony formation and the number of functional and dysfunctional ECFCs. On the other hand, there was a significant difference in the control group ($P<0.01$), with three participants with adverse change in cell functionality, three participants with improvements in ECFC cell function and colony formation, and 10 individuals having shown no change in ECFC function or colony formation at baseline and follow-up.

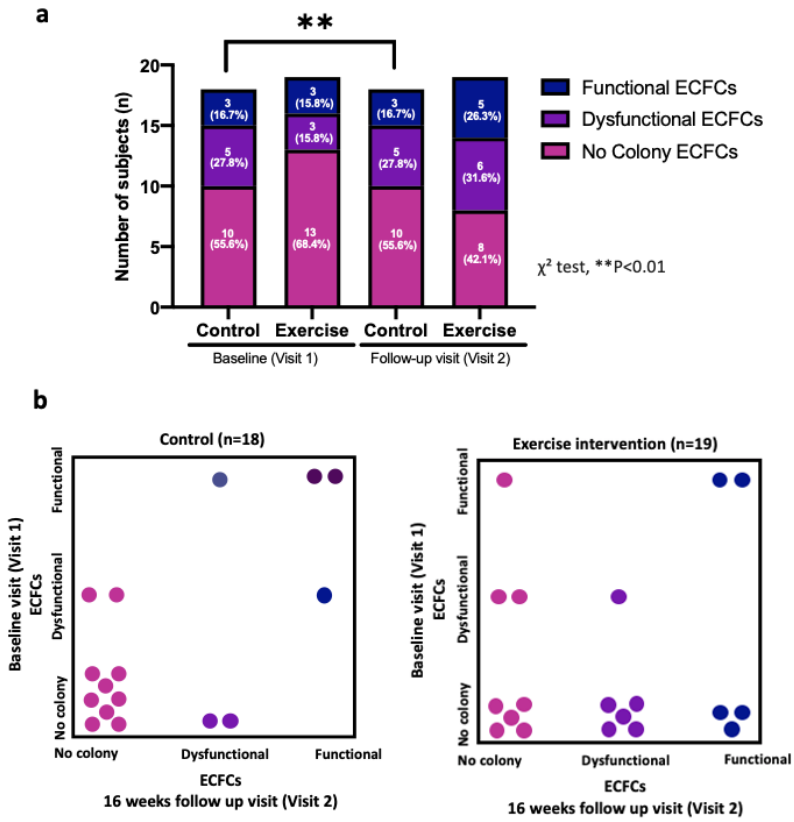


Figure 6.5. Classification of endothelial colony-forming cells (ECFCs) based on the cell functionality. Dysfunctional and functional cells were determined with a proliferation rate (% - Edu-stained cells/DAPI stained x 100) of below 20% and above 20%, respectively.
(a) Bar graph representation of participants with ECFCs collected in both the baseline and visit 2 categorised by their respective functional group (no colony, dysfunctional and functional group). **(b)** ECFC functional groups for baseline and visit 2 are plotted in a dot plot for the control and exercise intervention groups. χ^2 test, **P<0.01, sex-adjusted.

6.4.4 Baseline ECFC characteristics as a predictor of exercise response

To address the other hypothesis on the ability of the ECFC function at baseline to predict response to exercise, we investigated individuals with baseline ECFCs collected and who had completed the 16-week follow-up visit (n=12 controls and n=10 in the exercise intervention). The baseline characteristics of the participants are described in **Table 6.4**. Participants in the control group presented significant weight gain with an increase of 1.88 ± 2.66 kg, P=0.03 and an elevation in BMI (0.64 ± 0.91 kg/m^2, P=0.03). In contrast, individuals in the exercise intervention had improvements in Peak VO_2 (0.28 ± 0.25 L/m, P<0.01), peak VO_2 adjusted for weight (4.11 ± 4.59 ml/min/kg, P=0.03), and work rate at peak (23.89 ± 14.95 watts, P=0.01).

Table 6.4. Demographics and anthropometrics of the participants in TEPHRA study with Endothelial colony-forming cell (ECFC) cells growth at baseline.

Demographics and anthropometrics	Control (n=12)			P-Value*	Exercise intervention (n=10)			P-Value*	P-Value^{v1}	P-Value$^{\Delta}$
	Baseline	Visit 2	Δ		Baseline	Visit 2	Δ			
Male, n	6		-	-	7		-	-	0.42	-
Female, n	6				3					
Age, years	29.17 ± 4.09			-	28 ± 4			-	0.51	-
Height, cm	171.13 ± 8.51	171.15 ± 7.82	+0.025 ± 1.67	0.96	177.83 ± 10.14	178.02 ± 9.98	+0.19 ± 0.85	0.5	0.12	0.77
Weight, kg	73.35 ± 10.89	75.24 ± 10.18	+1.88 ± 2.66	**0.03**	76.8 ± 14.64	76.72 ± 16.32	-0.08 ± 3.7	0.95	0.55	0.18
Body mass index, kg/m²	25 ± 2.74	25.64 ± 2.58	+0.64 ± 0.91	**0.03**	24.16 ± 3.24	24.07 ± 3.79	-0.1 ± 1.26	0.81	0.53	0.14
Total body fat, %	25.19 ± 10.48 (10)	25.36 ± 10.42 (10)	+0.93 ± 2.7 (9)	0.33	22.07 ± 9.63	18.82 ± 6.26 (9)	-1.32 ± 6.27 (9)	0.55	0.50	0.34
Total fat free mass, kg	56.3 ± 10.21 (10)	56.9 ± 11.26 (10)	+0.83 ± 1.89 (9)	0.22	59.96 ± 13.2	62.42 ± 13 (9)	+1.27 ± 2.21 (9)	0.12	0.58	0.66
Total fat mass, kg	19.07 ± 9.05 (10)	19.13 ± 8.52 (10)	+0.96 ± 2.36 (9)	0.26	16.92 ± 7.93	14.64 ± 6.62 (9)	-0.62 ± 5.15 (9)	0.73	0.58	0.42
CPET										
<u>At peak</u>										
VO_2, L/ml	2.6 ± 0.61	2.7 ± 0.56 (11)	+0.04 ± 0.22 (11)	0.58	2.63 ± 0.6	2.99 ± 0.37 (9)	+0.28 ± 0.25 (9)	**0.01**	0.32	**0.011**
VO_2/kg, ml/min/kg	35.5 ± 7.14	36.09 ± 6.3 (11)	-0.27 ± 2.41 (11)	0.72	34.3 ± 5.31	38.67 ± 5.66 (9)	+4.11 ± 4.59 (9)	**0.03**	0.26	**0.004**

Oxygen pulse, ml/min/heartbeat	14.55 ± 3.78 (11)	14.64 ± 3.26 (11)	-0.8 ± 2.86 (10)	0.4	14.3 ± 3.27	15.67 ± 2.24 (9)	+0.89 ± 2.89 (9)	0.38	0.054	0.08
Heart rate, beats/min	185.73 ± 11.95 (11)	186.18 ± 11.05 (11)	-1.8 ± 16.73 (10)	0.74	180.9 ± 11.58	182.67 ± 12.39 (9)	+2.67 ± 7.28 (9)	0.3	0.32	0.49
Work rate, watts	220.42 ± 53.83	227.27 ± 46.06 (11)	+0.91 ± 19.98 (11)	0.88	219 ± 36.88	248.33 ± 28.5 (9)	+23.89 ± 14.95 (9)	**<0.01**	0.23	**0.004**
Ventilatory equivalent for O_2 (V_E/VO_2)	37.33 ± 4.51	38.09 ± 4.86 (11)	+0.19 ± 4.83 (11)	0.9	37.28 ± 3.45	36.56 ± 5.04 (9)	-0.83 ± 3.22 (9)	0.46	0.85	0.58
Ventilatory equivalent for CO_2 (V_E/VCO_2)	32.02 ± 3.14	32.76 ± 3.93 (11)	+0.22 ± 3.4 (11)	0.84	32.31 ± 2.75	31.97 ± 3.77 (9)	-0.53 ± 1.83 (9)	0.41	0.77	0.62
Respiration exchange ratio (RER)	1.16 ± 0.05	1.16 ± 0.04 (11)	+0 ± 0.07 (11)	0.97	1.15 ± 0.04	1.14 ± 0.07 (9)	-0.01 ± 0.07 (9)	0.71	0.96	**0.04**
Minute ventilation (V_E), L/min	102.58 ± 18.62	108.97 ± 19.15 (11)	+3.05 ± 15.27 (11)	0.52	104.88 ± 25.94	116.38 ± 21.7 (9)	+8.43 ± 15.57 (9)	0.14	0.62	0.69
Ventilatory threshold , L	2.48 ± 0.68	2.46 ± 0.69 (11)	-0.08 ± 0.25 (11)	0.32	2.5 ± 0.66	2.81 ± 0.72 (9)	+0.21 ± 0.5 (9)	0.24	0.54	0.37
Respiratory rate, breaths/min	42.67 ± 7.64	46.18 ± 8.7 (11)	+2.82 ± 6.29 (11)	0.17	42.8 ± 10	44 ± 13.41 (9)	+1.67 ± 6.44 (9)	0.46	0.92	0.12

Comparison between respective baseline (V1) and visit 2 (V2) data*; Δ between V1 and V2 $^{\Delta}$; and comparison between baseline v1 measurements between control and exercise group^{v1}. Independent t-test, paired sample t-test or χ^2 test. All P-values are not sex-adjusted. Independent t-test, paired sample t-test or χ^2 test. All P-values for demographics and anthropometrics are not sex-adjusted, whereas CPET P-values are sex adjusted.

The baseline characteristics of ECFCs are described in **Table 6.5**. The ECFCs obtained at baseline displayed similar functionality in both groups, except for higher closed tube capacity observed in the intervention group (8.97 ± 7.82 vs 2.34 ± 3.57, P=0.04).

Table 6.5. Baseline endothelial colony-forming cell (ECFC) characteristics of the participants in TEPHRA study.

ECFC characteristics	Control (n=12)	Exercise intervention (n=10)	P-Value
	Baseline	Baseline	
Days for ECFC colony formation (n)	17.83 ± 5.57	14.5 ± 4.62	0.15
Proliferation rate (%) (n)	16.97 ± 12.46 (9)	23.88 ± 21.61 (9)	0.38
Closed tube formed, n per $1.5x10^4$ (n)	2.34 ± 3.57 (10)	8.97 ± 7.82 (9)	**0.04**
Branches formed, n per $1.5x10^4$ (n)	11.18 ± 7.87 (10)	24 ± 17.12 (9)	0.06

Data are expressed as mean ± standard deviation (SD). Independent t-test, P-values are sex-adjusted.

We proceeded to assess the linear relationship of the baseline ECFC function in the exercise intervention group to change in CPET measurements from visit 1 to visit 2 **(Table 6.6)**. We observed significant relationships between baseline ECFC proliferation and angiogenic profiles with several CPET measurements.

Table 6.6.The correlation and regression*analysis between baseline endothelial colony-forming cell (ECFC) characteristics to physical exercise parameters.

	Control ECFC (N=10)						Exercise intervention ECFC (N=12)					
	Baseline proliferation rate		Baseline closed tube formation		Baseline branches formation		Baseline proliferation rate		Baseline closed tube formation		Baseline branches formation	
Regression analysis	***β***	***P-value***	***B***	***P-value***	***β***	***P-value***	***β***	***P-value***	***β***	***P-value***	***β***	***P-value***
Cardiopulmonary exercise test at peak												
Δ VO_2, L/ml	0.27	0.39	0.32	0.4	0.29	0.38	0.48	0.49	0.19	0.8	0.31	0.67
Δ VO_2/kg, ml/min/kg	0.42	0.14	0.25	0.51	0.38	0.24	**1.01**	**0.05**	0.65	0.26	0.65	0.26
Δ Oxygen pulse, ml/min/heartbeat	-0.12	0.79	0.29	0.57	0.055	0.91	0.016	0.97	-0.19	0.7	-0.2	0.69
Δ Heart rate, beats/min	-0.062	0.86	-0.03	0.99	0.11	0.77	0.36	0.39	0.028	0.95	0.32	0.44
Δ Work rate, watts	0.28	0.4	0.56	0.13	0.56	0.079	**0.92**	**0.015**	0.72	0.099	**0.86**	**0.035**
Δ Ventilatory equivalent for O_2 (V_E/VO_2)	-0.39	0.18	-0.32	0.37	-0.82	0.81	0.71	0.058	0.71	0.067	**0.88**	**0.01**
Δ Ventilatory equivalent for CO_2 (V_E/VCO_2)	-0.35	0.23	-0.28	0.44	-0.01	0.97	**0.81**	**0.013**	0.68	0.065	**0.71**	**0.049**
Δ Respiration exchange ratio (RER)	-0.38	0.3	-0.28	0.58	-0.31	0.45	0.21	0.64	0.28	0.53	0.51	0.23
Δ Minute ventilation (V_E), L/min	-0.29	0.34	-0.17	0.64	0.019	0.96	**0.9**	**0.045**	0.74	0.13	**0.97**	**0.028**
Δ Ventilatory threshold , L	-0.076	0.81	0.11	0.76	-0.13	0.7	-0.26	0.52	-0.3	0.48	-0.34	0.41
Δ Respiratory rate, breaths/min	-0.18	0.58	-0.18	0.62	0.17	0.62	0.57	0.16	0.55	0.18	**0.76**	**0.045**

r, Pearson correlation coefficient, β, Regression coefficient, *The regression model is adjusted for sex.

Linear regression of baseline ECFC proliferation rate to: Δ peak VO_2 (β=1.01, P=0.05) **(Figure 6.6a)**; Δ peak work rate (β=0.92, P=0.015) **(Figure 6.6b)**; Δ ventilatory equivalent for CO_2 (V_E/VCO_2) (β=0.81, P=0.0013); Δ minute ventilation (V_E) (β=0.9, P=0.045) are demonstrated **(Table 6.6)**. Similarly, linear regression analyses between baseline ECFC branches formed to: Δ peak work rate (β=0.86, P<0.035); Δ ventilatory equivalent for O_2 (V_E/VO_2) (β=0.88, P=0.01)**;** Δ ventilatory equivalent for CO_2 (V_E/VCO_2) (β=0.71, P=0.028); Δ minute ventilation (V_E) (β=0.97, P=0.028) and Δ respiratory rate (β=0.76, P=0.045) are also observed **(Table 6.6)**.

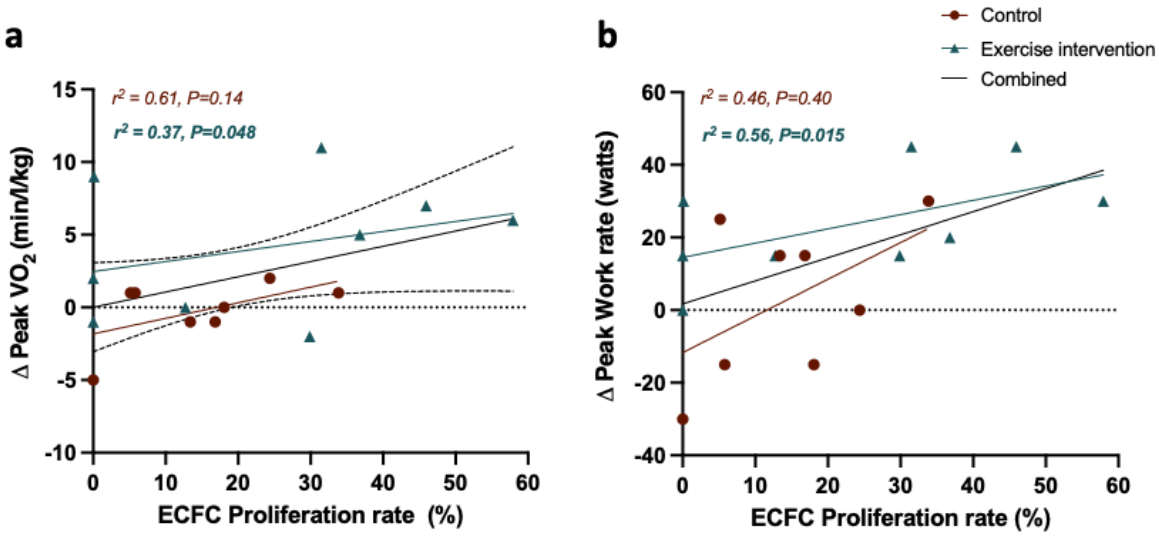


Figure 6.6. Relationship between ECFC characteristics to absolute change in clinical cardiopulmonary exercise testing parameters for oxygen uptake from baseline to 16-week follow up in control (red, circles) and intervention group (green, triangles).

Linear regression of baseline ECFC proliferation rate to: **(a)** Δ peak VO_2; **(b)** Δ peak work rate.

6.4.5 Baseline ECFC functional group as a predictor of exercise response

Individuals were divided based on ECFC functional groups, including those with no colony formation at V1. The baseline clinical characteristics are outlined in **Table S6.1** for the control group and **Table S6.2** for the intervention group. The baseline ECFC characteristics are outlined in **Table 6.7**. Based on the grouping criteria, the comparison of ECFC functional characteristics revealed that, in cells of subjects with dysfunctional ECFCs, the number of days for ECFC colony formation is longer, with a lower proliferation rate and angiogenic capacity (as indicated by the number of tube branches and the number of closed tubes formed *in vitro*). Significant differences were observed at baseline between the control and exercise intervention groups were observed in the ECFC angiogenic capacity (closed tube formation (6.60 ± 4.01 vs 16.95 ± 5.29, P=0.05) and branches formed (21.1 ± 2.66 vs 37.88 ± 9.27, P=0.003) for the functional ECFCs that could be explained by differences in sample size.

Table 6.7. Baseline Endothelial colony-forming cells (ECFC) characteristics of the participants in the TEPHRA cell sub-study based on ECFC functional group.

Exercise ECFC characteristics	Baseline control ECFC (n=28)			P-Value*	Baseline exercise ECFC (n=35)			P-Value*	P-Value[f]	P-Value[df]
	Functional (n=3)	Dysfunctional (n=10)	No colony (n=15)		Functional (n=6)	Dysfunctional (n=7)	No colony (n=22)			
Days for ECFC colony formation (n)	12.67 ± 2.31	18.9 ± 5.4	-	<0.01	12.33 ± 2.34	15.86 ± 4.63	-	0.12	0.57	0.25
Proliferation rate (%) (n)	**31.17 ± 5.92**	**8.92 ± 7.1 (7)**	**-**	**<0.01**	**40.03 ± 10.44**	**9.26 ± 13.61 (6)**	**-**	**<0.01**	0.72	0.96
Closed tube formed, n per $1.5x10^4$ (n)	**6.6 ± 4.01**	**0.45 ± 0.83 (8)**	**-**	**<0.01**	**16.95 ± 5.29**	**0.83 ± 2.04 (6)**	**-**	**<0.001**	**0.05**	0.65
Branches formed, n per $1.5x10^4$ (n)	**21.1 ± 2.66**	**6.23 ± 4.62 (8)**	**-**	**<0.01**	**37.88 ± 9.27**	**8.09 ± 9.75 (6)**	**-**	**<0.001**	**0.003**	0.66

Data are expressed as mean ± standard deviation (SD). Comparison between baseline endothelial colony-forming cells (ECFCs) functional groups in control and exercise group using independent t-test*. Comparison between control and intervention ECFC and its respective ECFC functional group: functional[f] and dysfunctional group[df] via independent t-test, P-values adjusted for sex.

The point-biserial analysis was used to investigate the relationship between baseline ECFC functional groups to physical exercise CPET parameters in the exercise intervention group **(Table 6.8)**. The results showed that individuals with functional ECFCs before the intervention had improvements in peak VO_2 (r_{pb}= -0.37, P=0.05) and peak watts (r_{pb}= -0.48, P=0.02) as compared to individuals with no colony formation **(Figure 6.7 a and b)**.

Table 6.8. The point-biserial analysis between baseline endothelial colony-forming cell (ECFC) characteristics to physical exercise parameters.

Point-biserial analysis Cardiopulmonary exercise test	Exercise intervention ECFC (N=29)					
	Functional vs no colony		Functional vs dysfunctional		Dysfunctional vs no colony	
	r_{pb}	*P-value*	r_{pb}	*P-value*	r_{pb}	*P-value*
At peak						
Δ VO_2, L/ml	-0.25	0.14	0.024	0.79	-0.25	0.12
Δ VO_2/kg, ml/min/kg	**-0.37**	**0.05**	-0.33	0.29	-0.08	0.48
Δ Work rate, watts	**-0.48**	**0.02**	-0.56	0.10	-0.19	0.29

r_{pb}, Point-biserial correlation coefficient. P-value adjusted for sex.

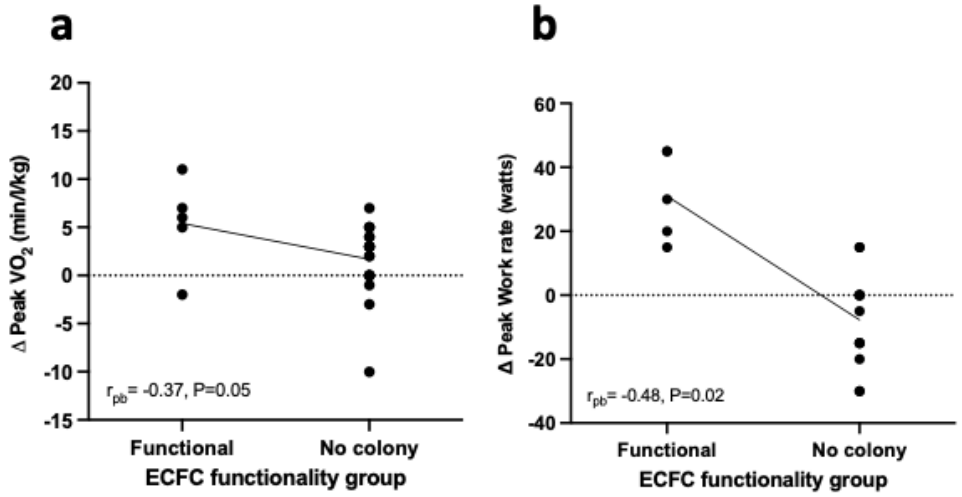


Figure 6.7. Point-biserial correlation between endothelial colony-forming cell (ECFC) functional group and cardiopulmonary exercise test parameters post-exercise intervention.

Point-biserial correlation between functional ECFC and no colony group to **(a)** Δ peak VO_2 and **(b)** Δ peak work rate.

6.5 Discussion

This is the first study to investigate the effect of 16 weeks of aerobic exercise training on ECFCs derived from young adults. The study showed the potential impact of exercise training on ECFC function that may provide some insights into the benefits of exercise in young adults that require further investigation. Furthermore, we showed the potential for using baseline ECFC cell function or functional groupings to predict their response to the exercise intervention.

6.5.1 Effect of exercise intervention on clinical measurements

Previous studies involving different populations demonstrated that overall health, comorbidities, and anthropometric characteristics might influence endothelial function and BP improvements induced by exercise training[444-446]. Study of Endothelial Function Response to Exercise Training in Hypertensive Individuals (SEFRET) is a randomised, evaluator-blinded, parallel-group clinical trial with three different modes of exercise training (aerobic, resistance, or combined) for 12 weeks in 81 subjects with systemic arterial hypertension aged 18 to 70 years[445]. The study noticed that BP was reduced in all three groups, and impacts on ambulatory BP appeared to vary in individuals with pre-hypertension or hypertension[445]. Consistent with Waclawovsky *et al.*, both studies observed that exercise intensity might influence the improvement, which should be further investigated[444].

In the TEPHRA trial, participants were subjected to three sessions of 1-hour aerobic exercise training sessions at 60-80% maximal heart rate as part of the exercise regime[293]. A slight increase in systolic BP in our young adult cohort was observed in the intervention arm at the follow-up visit. These adaptations may be due to a response to aerobic exercise training, which may act as a stimulus to increase vascular and sympathetic tone in younger people, thereby increasing BP[239, 447, 448]. Physical exercise is also known to initiate an increase in vascular oxidative stress and provides a challenge to tissues' antioxidative capacity, thereby increasing vascular shear stress and

hypoxia[239]. On the other hand, improvements in the CPET measurements were observed for individuals in the exercise intervention group for parameters including peak VO_2 and maximal workload. These findings were also in line with several clinical trials that reported a significant increase in fitness status post-exercise intervention[260, 262, 280, 282-284].

6.5.2 Impact of exercise on ECFC functionality

EPCs are a heterogeneous group of cells. There are two types of EPCs in circulation: early EPCs and outgrowth ECs (OEC), also known as ECFCs. It is important to note that most of the published studies on EPCs refer to early EPCs. EPCs are involved in neovasculogenesis and maintenance of vascular integrity[259]. An altered status of circulating EPCs represents a marker of endothelial dysfunction[26]. In fact, some studies have indicated that the number of circulating EPCs is an independent indicator of overall cardiovascular health[441, 449]. Exercise training is a vital physiological stimulus to mobilise EPCs in healthy individuals[260, 264].

Using paired sample analysis across V1 and V2, we showed no significant differences in the ECFC cellular function between individuals in the control arm and those in the exercise intervention arm. However, this may be explained by the small sample sizes of the groups. Despite not being statistically significant, we observed an increase in the number of individuals with the ECFC colony formation following the exercise intervention (more with either dysfunctional or functional ECFCs instead of no colony formation).

6.5.3 Baseline ECFC characteristics as a potential predictor to exercise response

6.5.3.1 ECFC cellular characteristics improve prediction of exercise responses

This chapter showed a significant relationship between the baseline ECFC proliferation and angiogenic profiles with several CPET measurements. The ECFC proliferation capacity was positively correlated to Δ peak VO_2, Δ peak work rate, Δ ventilatory equivalent for CO_2, and Δ minute

ventilation. Similarly, the ECFC's angiogenic capacity (is positively correlated to peak work rate, Δ ventilatory equivalent for O_2, ventilatory equivalent for CO_2, Δ minute ventilation and Δ respiratory rate.

In most of the trials assessing the chronic effects of exercise, the increase in circulating EPCs has coincided with an improvement in aerobic capacity (e.g., peak VO_2, 6 minutes walking test, maximal walking distance)[262, 273, 280-285]. However, the role of circulating EPCs in improving aerobic capacity is not clear. Mezzani *et al.* suggested EPCs possibly had a positive effect on peak VO_2 by mediating changes in the altered micro-vasculature, which improved oxygen utilisation and aerobic power[284]. However, the molecular determinants of interindividual differences in the baseline (intrinsic) peak VO_2 and increases of peak VO_2 in response to exercise training are largely unknown.

6.5.3.2 ECFC cellular functional group improve prediction of exercise responses

A point-biserial analysis was performed to compare the different ECFC categories (functional, dysfunctional and no colony formation). The result showed that individuals with functional baseline ECFCs had improvements in oxygen consumption (peak VO_2) and higher workload than individuals with no ECFC colony formation. This observation may suggest that mechanisms or substances modulating ECFC colony formation may be important factors that affect individuals' responses to exercise. A study by Clement *et al.* highlighted that the NO produced by the EC plays a physiological role in overall oxygen distribution, utilisation, consumption, and cellular respiration critical for EC adaptation to environmental changes, particularly hypoxia[450, 451]. Furthermore, EC can facilitate the delivery of oxygen and nutrients and response to VEGF that are released in hypoxic conditions (i.e. exercise) to attract new vessel sprouts to replenish oxygen, nutrient supply, and potentially response exercise[452]. EC metabolism is highly regulated and critical for meeting the cells' high demand for biosynthesis, redox, and energy, which may provide some cues to ECFC function, its ability to promote exercise adaptations[453]. Nonetheless, the mechanisms

behind ECFC colony formation have yet to be investigated. Thus, it warrants the need for more research.

6.5.4 Study strengths and limitations

For the first time, we demonstrated the potential of ECFCs characteristics to predict exercise response. However, the study has some limitations that need to be considered. First, TEPHRA is a randomised controlled trial, and thus, peak VO_2 adaptations may reflect unmeasured factors beyond the exercise-training stimuli. Leisure-time physical activity and diet were not measured for both arms of the study, only in the intervention arm. Based on the power calculation, the comparison between exercise and ECFC characteristics at the baseline and follow-up visits were not sufficiently powered. Therefore, no significant changes were observed. Furthermore, only participants with ECFC successfully isolated were included into the study for analysis.

6.6 Conclusion

In conclusion, despite no significant changes observed in ECFCs following the exercise intervention, our findings suggested for the first time that baseline ECFC functional characteristics may predict response to exercise training. This suggests that mechanisms or substances modulating the ECFC colony formation and function may be essential factors that affect an individual's response to exercise. Nevertheless, these underlying ECFC adaptation and response mechanisms have yet to be fully enlightened. All efforts are still needed to deepen our understanding of how exercise exerts beneficial effects on ECFCs and whether they can be used to predict exercise training response.

6.7 Supplemental materials

Supplementary Table S6.1

Table S6.1. Demographics and anthropometrics of the control participants in TEPHRA study.

Control Demographics and anthropometrics	Baseline (n=28)			P-Value*	Visit two (n=25)			P-Value*	P-Value^f	P-Value^df	P-Value^nc
	Functional (n=3)	Dysfunctional (n=10)	No colony (n=15)		Functional (n=3)	Dysfunctional (n=9)	No colony (n=13)				
Male, n	0	7	10	0.07	0	7	10	0.07	-	-	-
Female, n	3	3	5		3	3	5				
Age, years	30 ± 4	28.8 ± 4.08	27.4 ± 3.48	0.45	**34.33 ± 4.04***	29.56 ± 4.72	**27.54 ± 3.55 ***	**0.05**	0.38	0.08	**0.04**
Height, cm	162.5 ± 4.33	175.4 ± 8.42	173.37 ± 10.86	0.14	163.53 ± 3.85	173.69 ± 7.16	173 ± 11.01	0.25	0.083	0.62	0.25
Weight, kg	68.77 ± 6.1	78.2 ± 15.4	75.48 ± 17.63	0.68	72.02 ± 5.9	76.31 ± 11.34	73.44 ± 17.51	0.87	**0.004**	0.19	0.73
BMI, kg/m²	26.04 ± 2.01	25.24 ± 3.36	24.75 ± 3.34	0.81	26.93 ± 2.06	25.21 ± 2.7	24.15 ± 3.15	0.32	**0.001**	0.15	0.65
Total body fat, %	34.38 ± 5.86 (2)	22.95 ± 9.64 (9)	24.96 ± 6.41	0.19	32.68 (1)	24.55 ± 10.71	24.14 ± 4.97	0.58	-	0.48	0.15
Total fat free mass, kg	46.25 ± 0.78 (2)	61.1 ± 11.52 (9)	57.02 ± 13.21	0.31	47.1 (1)	57.99 ± 11.37	56.3 ± 13.32	0.71	-	0.32	0.09
Total fat mass, kg	24.5 ± 6.65 (2)	18.56 ± 9.15 (9)	19.05 ± 7.32	0.63	22.6 (1)	18.74 ± 8.94	17.85 ± 5.79	0.81	-	0.42	0.16
Clinic seated blood pressure (BP)											
Systolic BP, mmHg	120.67 ± 2.08	129.8 ± 12.38	120.53 ± 9.13	0.09	114.33 ± 7.51	127.89 ± 12.71	120.85 ± 10.03	0.15	0.19	0.54	0.95
Diastolic BP, mmHg	79.33 ± 6.11	81.9 ± 11.72	73.8 ± 7.72	0.11	73.33 ± 3.79	79.78 ± 12.31	73.77 ± 6.62	0.28	0.39	0.51	0.65
Mean arterial pressure, mmHg	94.67 ± 3.51	99.7 ± 10.69	91.67 ± 6.95	0.08	88 ± 5	98 ± 12.84	91.15 ± 7.38	0.18	0.31	0.56	0.93

Heart rate, beats per min	63 ± 4.58	69.4 ± 10.18	69.67 ± 9.63	0.54	66.5 ± 3.04	77.61 ± 11.36	68.92 ± 9.75	0.11	0.078	0.21	0.92
Cardiopulmonary Exercise Testing											
At peak											
VO_2, L/ml	2.28 ± 0.29	2.83 ± 0.72	2.65 ± 0.86	0.56	2.67 ± 0.12 (2)	2.71 ± 0.62	2.56 ± 0.85	0.90	0.04	0.97	0.07
VO_2/kg, ml/min/kg	33.67 ± 6.81	36.1 ± 7.11	34.67 ± 6.62	0.82	39 ± 1.41 (2)	35.44 ± 6.84	34.62 ± 5.32	0.62	0.20	0.45	0.15
Oxygen pulse, ml/min/heartbeat	12.33 ± 0.58	15.89 ± 4.2 (9)	14.6 ± 4.55	0.45	14 ± 1.41 (2)	14.78 ± 3.6	14.15 ± 4.67	0.93	0.20	0.23	0.23
Heart rate, beats/min	184.33 ± 15.89	187.33 ± 11.18 (9)	181.13 ± 14.5	0.56	191 ± 9.9 (2)	185.11 ± 11.55	179.85 ± 13.86	0.42	0.80	0.81	0.52
Work rate, watts	195 ± 37.75	236 ± 58.68	214.33 ± 69.07	0.55	230 ± 0 (2)	226.67 ± 51.48	208.08 ± 71.05	0.76	0.50	0.74	0.08
Ventilatory equivalents for O_2 (V_E/VO_2)	38.53 ± 7.06	37.33 ± 3.85	36.5 ± 6.2	0.83	40.95 ± 4.6 (2)	37.46 ± 4.94	34.82 ± 4.99	0.20	0.86	0.73	0.66
Ventilatory equivalents for CO_2 (V_E/VCO_2)	31.97 ± 5.44	32.3 ± 2.49	31.89 ± 4.32	0.97	35.25 ± 2.05 (2)	32.21 ± 4.11	30.72 ± 3.49	0.25	0.93	0.88	0.55
Respiration exchange ratio	1.2 ± 0.02	1.15 ± 0.05	1.14 ± 0.07	0.24	1.16 ± 0.07 (2)	1.16 ± 0.04	1.16 ± 0.06	1.00	0.50	0.62	0.19
Minute ventilation (V_E), L/min	95.17 ± 27.2	111.01 ± 24.31	103.09 ± 35.91	0.70	115.8 ± 9.33 (2)	107.46 ± 20.81	97.06 ± 31.19	0.53	0.78	0.64	0.30
Ventilatory threshold, L	2.32 ± 0.48	2.69 ± 0.86	2.52 ± 0.74	0.73	2.55 ± 0.39 (2)	2.44 ± 0.75	2.52 ± 0.79	0.97	0.80	0.33	0.66
Respiratory rate, breaths/min	40.33 ± 4.73	43.1 ± 8.08	41.07 ± 6.65	0.73	46.5 ± 10.61 (2)	46.11 ± 8.98	39.31 ± 7.47	0.15	0.69	0.24	0.70

Data are expressed as mean ± standard deviation (SD). Comparison between control endothelial colony-forming cells (ECFCs) functional groups in baseline and visit two using ANOVA plus Bonferroni post-hoc test*, P<0.05*. Comparison between baseline ECFC and its respective ECFC functional group: functional[f], dysfunctional[df] and no colony[nc] group via paired t-test.

Supplementary Table S6.2

Table S6.2. Demographics and anthropometrics of the exercise intervention participants in TEPHRA study.

Exercise Demographics and anthropometrics	Baseline (n=35)			P-Value*	Visit two (n=29)			P-Value*	P-Value^f	P-Value^df	P-Value^nc
	Functional (n=6)	Dysfunctional (n=7)	No colony (n=22)		Functional (n=5)	Dysfunctional (n=5)	No colony (n=19)				
Male, n	4	5	9	0.16	4	5	9	0.16	-	-	-
Female, n	2	2	13		2	2	13				
Age, years	28 ± 4.69	26.43 ± 4.5	27.64 ± 3.54	0.73	28.2 ± 6.87	28.2 ± 3.56	28.16 ± 3.56	1.00	0.85	0.07	**0.01**
Height, cm	175.63 ± 11.42	177.36 ± 9.18	172.09 ± 8.71	0.38	178.5 ± 10.04	177.54 ± 11.08	173.84 ± 7.5	0.46	0.80	0.39	0.36
Weight, kg	67.4 ± 11.74	83.8 ± 14.57	75.38 ± 13.25	0.10	69.06 ± 10.34	84.38 ± 18.58	73.85 ± 14.12	0.23	0.19	0.50	0.16
BMI, kg/m^2	21.72 ± 1.99	26.47 ± 2.77	25.47 ± 4.34	0.07	21.63 ± 2.08	26.51 ± 3.63	24.35 ± 3.98	0.13	0.18	0.63	0.13
Total body fat, %	19.25 ± 9.39	26.21 ± 7.81	27.7 ± 11.6 (21)	0.24	15.97 ± 6.88	22.37 ± 3.33 (4)	25.07 ± 9.11	0.11	0.39	0.72	0.19
Total fat free mass, kg	54.7 ± 12.31	61.94 ± 12.72	54.89 ± 9.86 (21)	0.32	58.42 ± 10.53	67.43 ± 15.58 (4)	55.73 ± 10.13 (18)	0.18	0.49	**0.02**	0.65
Total fat mass, kg	12.7 ± 6.21	21.97 ± 7.43	21.62 ± 11.42 (21)	0.15	10.84 ± 4.16	19.4 ± 6.3 (4)	19.12 ± 9.98 (18)	0.19	0.39	0.53	0.17
Clinic seated blood pressure (BP)											
Systolic BP, mmHg	116.83 ± 12.16	124.86 ± 10.49	122.95 ± 12.87	0.47	114.2 ± 10.26	124 ± 12.86	125.32 ± 12.45	0.21	0.90	0.50	0.39
Diastolic BP, mmHg	75.33 ± 14.22	74.71 ± 10.16	76.05 ± 11.06	0.96	72.4 ± 6.47	78.6 ± 9.02	77.32 ± 8.61	0.44	0.69	0.56	0.70
Mean arterial pressure, mmHg	90.83 ± 13.35	94.14 ± 10.4	94.18 ± 10.65	0.80	87.8 ± 7.66	93.4 ± 10.42	94.95 ± 9.16	0.32	0.87	0.52	0.97
Heart rate, beats per min	72.83 ± 12.43	73.14 ± 11.29	70.68 ± 10.35	0.83	62.7 ± 6.35	75.5 ± 11.03	67.03 ± 12.33	0.21	0.09	0.30	0.20

Exercise Cardiopulmonary Exercise Testing											
At peak											
VO_2, L/ml	2.47 ± 0.72	2.66 ± 0.52	2.44 ± 0.67	0.74	2.92 ± 0.39	3.08 ± 0.38 (4)	2.61 ± 0.55	0.19	0.10	0.09	0.19
VO_2/kg, ml/min/kg	36.17 ± 5.23	31.71 ± 4.03	32.86 ± 8.64	0.54	42.4 ± 4.34	34 ± 2.83 (4)	35.89 ± 7.77	0.14	0.06	0.35	0.07
Oxygen pulse, ml/min/heartbeat	13.5 ± 3.51	14.43 ± 3.15	13.85 ± 4.17 (20)	0.91	14.8 ± 2.17	16.75 ± 2.06 (4)	14.63 ± 3.15	0.42	0.82	0.18	0.50
Heart rate, beats/min	177.83 ± 10.46	183.86 ± 11.64	178.35 ± 9.91 (20)	0.45	181.6 ± 7.96	184 ± 17.91 (4)	179.21 ± 9.21	0.68	0.43	0.61	0.79
Work rate, watts	206.67 ± 49.26	221.43 ± 31.85	206.14 ± 52.78	0.77	251 ± 32.29	245 ± 27.39 (4)	218.42 ± 46.04	0.23	**0.01**	0.09	0.32
Ventilatory equivalents for O_2 (V_E/VO_2)	37.87 ± 4.42	35.44 ± 2.6	38.14 ± 6.23	0.52	39.06 ± 5.27	33.43 ± 2.66 (4)	36.34 ± 5.87	0.32	0.58	0.06	0.21
Ventilatory equivalents for CO_2 (V_E/VCO_2)	32.45 ± 3.54	31.07 ± 2.37	32.56 ± 4.13	0.66	33.34 ± 4.44	30.25 ± 2.1 (4)	31.22 ± 3.47	0.38	0.22	0.09	0.10
Respiration exchange ratio	1.17 ± 0.03	1.14 ± 0.04	1.17 ± 0.06	0.49	1.17 ± 0.06	1.11 ± 0.08 (4)	1.16 ± 0.1	0.56	1.00	0.49	0.81
Minute ventilation (V_E), L/min	101.05 ± 33.74	100.57 ± 19.77	98.56 ± 25.23	0.97	122.12 ± 25.11	109.2 ± 17.07 (4)	101.73 ± 26.18	0.28	0.14	0.80	0.79
Ventilatory threshold, L	2.27 ± 0.61	2.57 ± 0.66	2.25 ± 0.5	0.41	2.51 ± 0.28	**3.18 ± 0.97 (4)***	**2.37 ± 0.51***	**0.05**	0.63	0.34	0.19
Respiratory rate, breaths/min	44.67 ± 12.18	39.86 ± 4.85	44.5 ± 8.99	0.48	49.4 ± 13.33	37.25 ± 11.53 (4)	43.74 ± 9.77	0.25	0.09	0.78	0.80

Data are expressed as mean ± standard deviation (SD). Comparison between control endothelial colony-forming cells (ECFCs) functional groups in baseline and visit two using ANOVA plus Bonferroni post-hoc test*, P<0.05*. Comparison between baseline ECFC and its respective ECFC functional group: functional[f], dysfunctional[df] and no colony[nc] group via paired t-test.

Supplementary Table S6.3

Table S6.3. Absolute change in demographics and anthropometrics of the participants in TEPHRA study based on endothelial colony-forming cell (ECFC) functional group.

Demographics and anthropometrics	Control (n=25)			P-Value*	Exercise (n=29)			P-Value*	P-Value^f	P-Value^df	P-Value^nc
	Functional (n=3)	Dysfunctional (n=9)	No colony (n=13)		Functional (n=5)	Dysfunctional (n=5)	No colony (n=19)				
Δ Height, cm	1.03 ± 0.55	-0.31 ± 1.8	-0.46 ± 1.38	0.31	0.14 ± 1.14	0.24 ± 0.56	0.28 ± 1.31	0.97	0.77	0.53	0.12
Δ Weight, kg	**3.25 ± 0.35***	1.43 ± 2.97	**-0.13 ± 1.39***	0.04	-1.62 ± 2.3	1.46 ± 4.42	-0.79 ± 2.34	0.19	0.094	1	0.31
Δ BMI, kg/m²	0.89 ± 0.05	0.56 ± 1.06	0.08 ± 0.6	0.18	-0.56 ± 0.77	0.36 ± 1.56	-0.35 ± 0.96	0.34	0.12	0.76	0.14
Δ Total body fat, %	2.45 ± (1)	0.74 ± 2.82	0.69 ± 1.64	0.73	-3.12 ± 7.23	0.94 ± 4.77 (4)	-1.06 ± 3.21 (17)	0.40	0.85	0.94	0.17
Δ Total fat free mass, kg	1.4 ± (1)	0.76 ± 2.01 (8)	-0.58 ± 1.12	0.12	1.02 ± 3.03	1.58 ± 0.72 (4)	0.13 ± 1.15 (17)	0.22	0.78	0.47	0.17
Δ Total fat mass, kg	2.8 ± (1)	0.73 ± 2.42 (8)	0.56 ± 1.35	0.51	-2.36 ± 5.5	1.55 ± 4.36 (4)	-0.99 ± 2.87 (17)	0.29	0.76	0.69	0.14
Clinic seated blood pressure (BP)											
Δ Systolic BP, mmHg	-6.33 ± 5.51	-2.22 ± 10.53	-0.15 ± 9.52	0.60	0.6 ± 9.96	-1.6 ± 4.83	1.47 ± 7.31	0.72	0.32	0.90	0.59
Δ Diastolic BP, mmHg	-6 ± 9.64	-1.78 ± 7.68	0.92 ± 7.05	0.34	1.2 ± 6.3	2 ± 6.96	0.74 ± 8.18	0.95	0.24	0.38	0.95
Δ Mean arterial pressure, mmHg	-6.67 ± 8.5	-1.56 ± 7.62	-0.15 ± 6.51	0.38	0.6 ± 7.59	-2.4 ± 7.67	0.05 ± 6.96	0.76	0.25	0.85	0.93
Δ Heart rate, beats per min	3.5 ± 1.8	7.39 ± 16.35	-0.15 ± 5.23	0.28	-8.1 ± 8.13	3.1 ± 5.77	-2.87 ± 9.34	0.15	0.06	0.49	0.35
Cardiopulmonary Exercise Testing											
<u>At peak</u>											
Δ VO_2, L/ml	0.23 ± 0.02 (2)	0 ± 0.23	-0.13 ± 0.22	0.10	0.28 ± 0.29	0.29 ± 0.23 (4)	0.1 ± 0.3	0.31	0.26	0.06	0.08

Δ VO_2/kg, ml/min/kg	1.5 ± 0.71 (2)	-0.67 ± 2.5	-1.38 ± 3.28	0.43	5.4 ± 4.72	2.5 ± 4.51 (4)	1.68 ± 3.77	0.21	0.17	0.12	0.06
Δ Oxygen pulse, ml/min/heartbeat	1.5 ± 0.71 (2)	-1.38 ± 2.92 (8)	-0.69 ± 1.97	0.31	0.4 ± 3.71	1.5 ± 1.73 (4)	0.28 ± 1.71 (18)	0.60	0.85	0.078	0.27
Δ Heart rate, beats/min	-2.5 ± 10.61 (2)	-1.63 ± 18.54 (8)	-2 ± 10.82	1.00	3.4 ± 8.68	1.75 ± 6.24 (4)	0.33 ± 5.31 (18)	0.60	0.34	0.75	0.36
Δ Work rate, watts	15 ± 21.21 (2)	-2.22 ± 19.54	-7.69 ± 14.67	0.23	**31 ± 13.87***	15 ± 12.25 (4)	**5 ± 21.15***	**0.04**	0.25	0.13	0.13
Δ Ventilatory equivalents for O_2 (V_E/VO_2)	-1.35 ± 8.41 (2)	0.53 ± 4.43	-0.71 ± 5.66	0.83	0.84 ± 3.13	-2.93 ± 2.03 (4)	-1.33 ± 4.46	0.38	0.41	0.19	0.76
Δ Ventilatory equivalents for CO_2 (V_E/VCO_2)	0.4 ± 5.09 (2)	0.18 ± 3.35	-0.58 ± 3.44	0.85	0.64 ± 0.98	-2 ± 1.59 (4)	-1.09 ± 2.78	0.25	0.95	0.27	0.59
Δ Respiration exchange ratio	-0.05 ± 0.08 (2)	0.01 ± 0.06	0.03 ± 0.07	0.31	0 ± 0.09	-0.02 ± 0.05 (4)	0 ± 0.06	0.89	0.13	0.35	0.32
Δ Minute ventilation (V_E), L/min	5.9 ± 22.63 (2)	2.41 ± 15	-4.6 ± 15.14	0.48	13.68 ± 16.43	1.88 ± 13.54 (4)	1.1 ± 17.33	0.34	0.30	0.96	0.48
Δ Ventilatory threshold, L	-0.01 ± 0.02 (2)	-0.09 ± 0.27	-0.04 ± 0.29	0.85	0.1 ± 0.42	0.36 ± 0.63 (4)	0.06 ± 0.19	0.27	0.34	0.098	0.33
Δ Respiratory rate, breaths/min	3.5 ± 9.19 (2)	2.67 ± 6.22	-0.69 ± 6.3	0.42	4 ± 4.06	-1.25 ± 8.26 (4)	-0.37 ± 6.34	0.35	0.72	0.38	0.94

Data are expressed as mean ± standard deviation (SD). Comparison between endothelial colony-forming cells (ECFCs) functional groups in control and intervention group using ANOVA plus Bonferroni post-hoc test*, P<0.05*. Comparison between ECFCs (control vs intervention) and its respective ECFC functional group: functional[f], dysfunctional[df] and no colony[nc] group via t-test and P-value adjusted for sex.

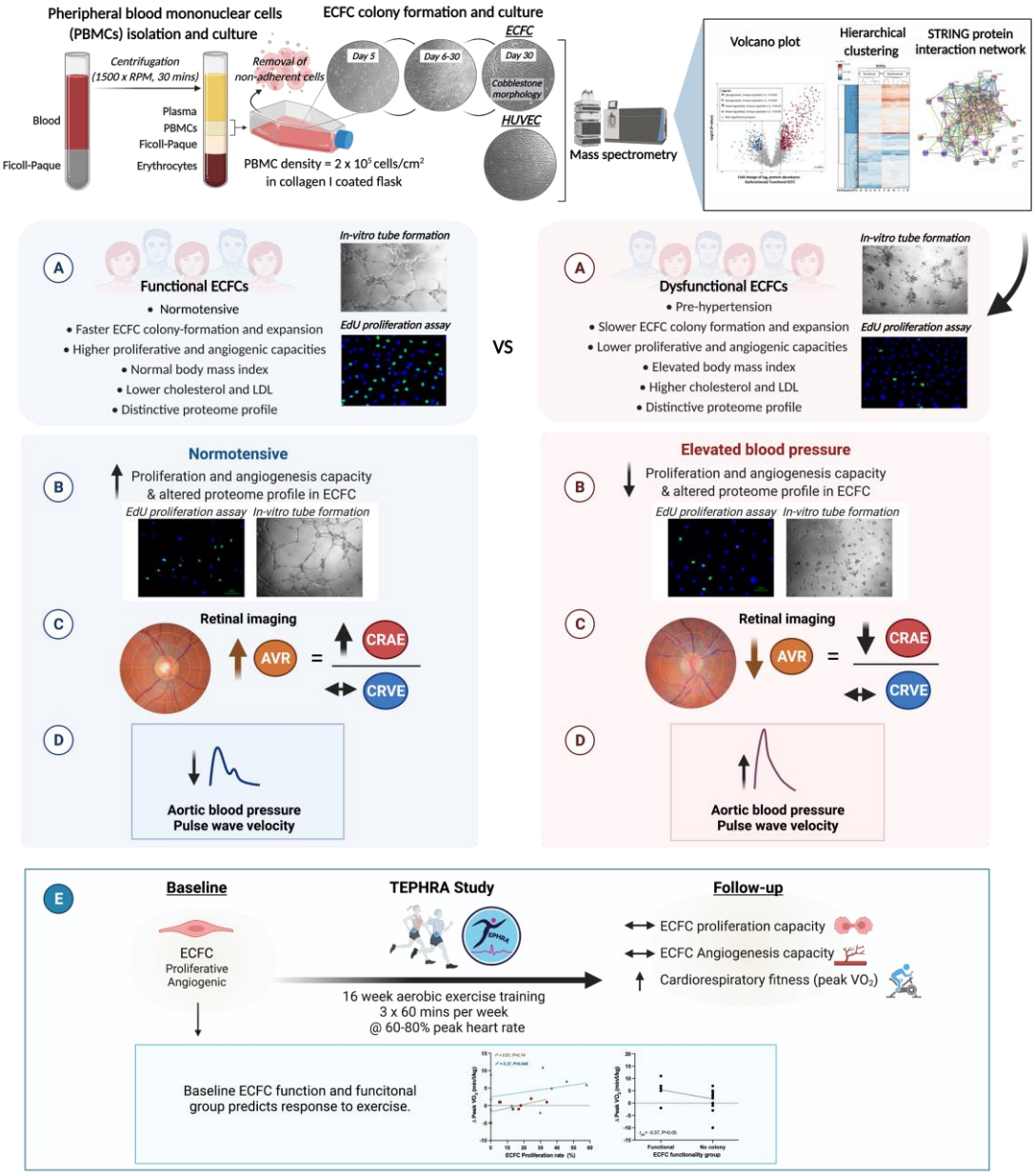
7
Conclusion



7. General conclusion

7.1 Main findings of the thesis

This thesis has provided a comprehensive insight into ECFCs as a platform for early cardiovascular risk assessment. Furthermore, it has been demonstrated that ECFCs can play a role in early-onset hypertension development and may provide a mechanistic understanding of exercise benefits in endothelial function, as summarised below.



Abbreviations: ECFC, endothelial colony-forming cells; AVR, arteriolar to venular diameter ratio; CRAE, central retinal arteriolar equivalent; CRVE, central retinal venular equivalent (CRVE) (↔ denotes no change; ↑denotes increase, ↓ denotes decrease)

Chapter 4 of this thesis compared the phenotype and proteomic signatures of functional and dysfunctional circulating ECFCs derived from the peripheral blood of young adults with no pre-existing CVDs and the influence of sex in cellular biological functions. Data in this chapter characterised a distinct proteomic signature with altered angiogenic and proliferation mechanisms in dysfunctional ECFCs. The disruption of crucial cellular mechanisms involved mainly in exocytosis, vesicle transport and ECM organisation, cell metabolism and apoptosis were identified in dysfunctional ECFCs, in addition to targeted anti-angiogenic proteins. Due to limited the sample size, this work could not conclude whether there was a significant contribution of sex on ECFC function and proteome profiles. Larger studies are needed to validate the targeted mechanisms described in this thesis and investigate sex dimorphism in ECFCs to enhance our understanding of the physiological function of ECFCs and establish a connection between experimental findings in this thesis and clinical characteristics considering potential sex differences.

Chapter 5 uncovered the relationship between EC function, retinal micro-vasculature, macro-vascular resistance (arterial stiffness, PWV) and BP changes. Young adults with elevated BP had significantly reduced expansion, proliferative and vasculogenic potentials of ECFCs and presented an adverse retinal micro-vascular endothelium dysfunction and macro-vascular resistance. Furthermore, hierarchical functional clustering revealed distinct ECFC proteomic signatures between normotensive and elevated BP ECFCs with changes in cellular mechanisms, including regulated exocytosis, wound healing, ECM organisation, haemostasis and vesicle-mediated transport. Our regression model highlighted the significance of retinal micro-vasculature with BP. These findings suggest that the retinal micro-vascular network may represent a promising therapeutic and preventative target, considering the vital role of micro-circulation on target organ damage, macro-vascular dysfunction, and incident hypertension.

Chapter 6 focused on the effect of a 16-week exercise training intervention on the function and characteristics of ECFCs derived from peripheral blood from young adults with elevated or stage 1 hypertension and determines if ECFC function can predict the response to exercise training. Despite no significant changes being observed in the ECFCs following exercise intervention, a potential exercise-induced proteome modification might exist that could have a positive effect on aerobic training, thereby improving cardiopulmonary fitness. The identified pathways highlight potential exercise sensors or courses that could be used as novel therapeutic targets. Furthermore, data in chapter 6 data demonstrated that baseline ECFC functional characteristics might predict responses to exercise training, suggesting that mechanisms or molecules modulating ECFC colony formation and function may be essential factors that affect how an individual responds to exercise training. Nevertheless, these underlying mechanisms for ECFC adaptation and response have yet to be fully investigated. Further research is needed to deepen the current understanding of how exercise exerts beneficial effects on ECFCs and their role as a potential predictor of cardiovascular response to exercise training.

Overall, this thesis has furthered our understanding of ECFCs and their potential as a platform for early cardiovascular risk assessment and has identified potential mechanisms that may interfere with the pathophysiology of hypertension. Potential mechanisms that may interfere with the pathophysiology of hypertension.

7.2 Experimental considerations and limitations

7.2.1 Impact of COVID-19 on research

Disruptions caused by the Covid-19 pandemic substantially impacted the progression of this thesis. Due to the suspension of research facilities and clinical research studies, proteins identified in the proteomic analysis could not be validated. Cell fractions and blood samples

collected could not undergo deep phenotyping and genotyping. Further exploration of the application of ECFCs was also limited due to delays and restrictions posed by COVID-19.

7.3 Future work

7.3.1 Protein validation

This thesis has identified the potential proteins and mechanisms associated with BP-induced EC dysfunction. Further investigation may provide insights into preventing disease progression and therapeutic development.

7.3.2 ECFC extracellular vesicles assessments

Proteomic analysis revealed enrichment in proteins involved in exocytosis, vesicle transport and immune response in individuals with dysfunctional ECFCs. This may suggest increased in exocytosis-mediated intercellular signalling by extracellular vesicles (EVs) to trigger inflammatory responses, thereby contributing to endothelial remodelling and activation in adults with elevated BP. EVs, including apoptotic bodies, micro-vesicles, and exosomes, have emerged as essential players in cell-to-cell communication in normal physiology and pathological conditions[60]. EVs can convey these messages through their special cargoes consisting of cytokines, proteins, and nucleic acids (mRNAs and microRNAs) to recipient cells and lipids, which they transport from a donor cell to the recipient cells[61-63] can modulate EC behaviour and angiogenesis in vivo [63-67]. Studies have shown that endothelial dysfunction triggers the release of EC-derived EVs that play an increasing role in disease progression[113, 378-382]. Increased concentrations of EC-derived EVs were shown to inhibit angiogenesis in the cultured sections of hearts by inducing eNOS dysfunction *in vitro* and *in vivo*[391, 392]. A recent study from Akbar *et al.,* also highlighted the mobilisation of neutrophils from the spleen to the peripheral blood by VCAM-1+ endothelial extracellular vesicles[383].

In addition, translation of EV-associated mRNAs can occur in recipient cells and has been implicated in the activation of ECs[61, 63]. This may result in the genetically stable and quiescent endothelium being activated to secrete different growth factors and cytokines that affect EC proliferation, apoptosis, coagulation, inflammatory cell recruitment, and/or affect vasoactivity to restore homeostasis[127]. Prolonged or chronic activation of the endothelium leads to EC dysfunction, the loss of homeostatic functions, leading to pathological changes, including vascular remodelling and increased vascular resistance resulting in the development of CVDs[137, 138]. Although the various deleterious effects of EVs in the pathogenesis of CVD, an increasing body of evidence highlights the beneficial effects of specific EVs on vascular function and endothelial regeneration, vascular endothelial repair, and angiogenesis[67, 384-390]. These findings showed that endothelial EVs could stimulate endothelial repair by functionally influencing migration, proliferation, and wound healing in target cells, which further emphasises the need for characterisation of the ECFC-EVs to understand their involvement in disease progression. Future work should address the isolation and characterisation of ECFC-EVs from cells isolated during the work described in this thesis as beneficial in pursuing a deeper understanding of the role of ECFC-EVs.

7.3.3 Other clinical applications of ECFCs

7.3.3.1 ECFCs and pre-eclamptic pregnancy

Dysregulation of the vascular endothelium and ECs has been observed in the pathogenesis and progression of several CVDs, including hypertension and hypertensive pregnancy disorders[307, 454-459]. Studies have demonstrated significant peripartum inflammation, endothelial dysfunction and angiogenic imbalance that extends beyond delivery and is observed up to five to 10 years post-partum[460-462]. The role of endothelial dysfunction in the pathogenesis of pre-eclampsia is widely accepted and micro-vascular rarefaction has been considered a hallmark for the elevation in peripheral resistance and precedes hypertension pathogenesis[306, 463]. Nitric oxide-dependent

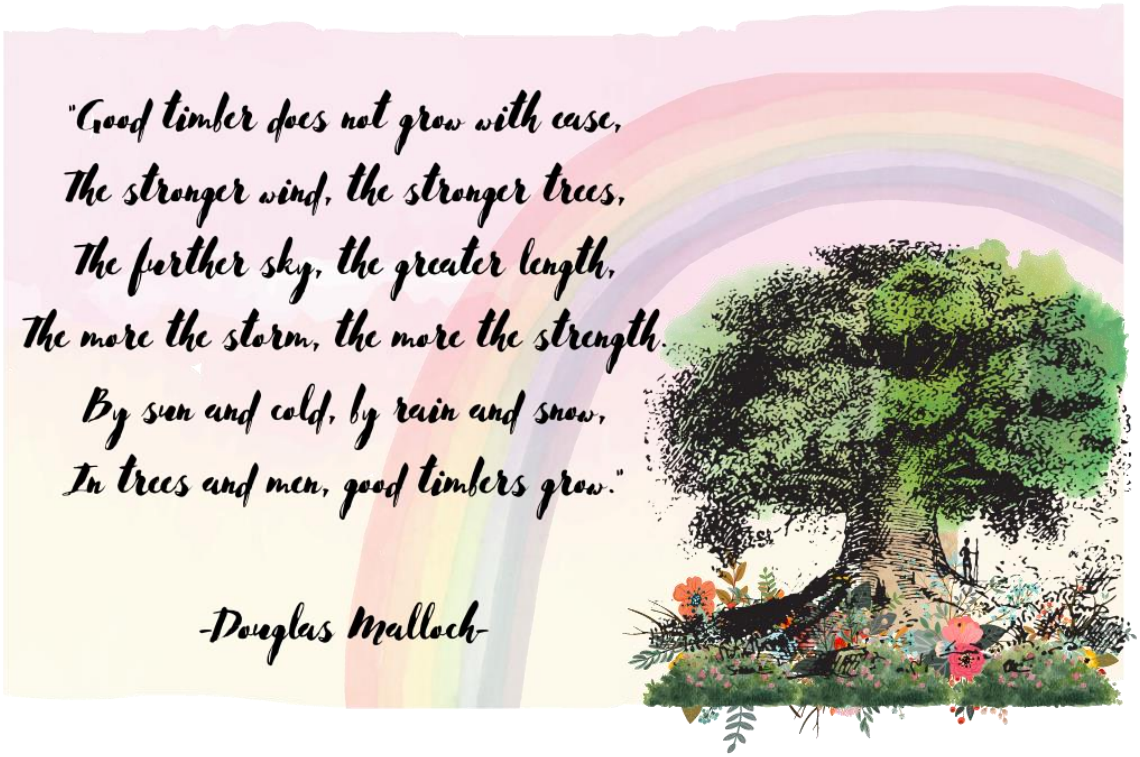
vasodilation has been shown to be reduced in myometrial arteries isolated from pre-eclamptic pregnancies[464]. BH4 is a required cofactor for the enzyme eNOS responsible for nitric oxide generation. A deficiency of BH4 has been demonstrated to have an important role in certain vascular diseases disease states through this pathway[465, 466].

Chuaiphichai *et al.* recently demonstrated differences in BH4 and eNOS activity levels in HUVECs collected from pre-eclamptic pregnancies. BH4 levels as measured by HPLC were significantly reduced in pre-eclamptic compared with normotensive pregnancies[467]. Critically, treatment with BH4 precursor, sepiapterin, normalised BH4 levels and NOS activity and restored tube formation capacity in HUVECs from hypertensive pregnancies. Furthermore, a causal role of BH4 has been established in a selective EC BH4 deficiency animal model, generated by EC-specific deletion of Gch1, that encodes the BH4 biosynthetic enzyme - GTP cyclohydrolase 1 (GTPCH). Mice with EC Gch1 deletion developed a pre-eclamptic-like syndrome with increased BP and intrauterine growth restriction (IUGR) due to placental insufficiency mediated by defective uteroplacental vascular remodelling[467]. Nonetheless the role of BH4 on ECFC function is still unknown. Besides, ECFCs also offers a novel platform to investigate the endothelial function during a pre-eclampsia pregnancy. Investigating the ECFC function during a pre-eclamptic pregnancy and its interaction with the BH4 pathway may offer us a cue to potential therapeutics development.

7.3.3.2 3D ECFC-cardiomyocyte organoids (Cardiospheres)

Another potential application of ECFCs includes the development of advanced cellular technology platforms such as three-dimensional (3D) organoid cell cultures. Despite the advances in organoid technology, developing an efficient 3D induced pluripotent stem cell-derived cardiomyocyte (iPSC-CM) organoid cell culture has been challenging[468]. This is in part due to the maturity of the iPSC-CMs. The maturity of CMs in the organoid structure is critical for achieving physiological function, significantly affecting its role in drug predictability, toxicity, metabolic assay response, apoptosis sensitivity, and regenerative capability[468]. Several mechanisms have been

highlighted to enhance the maturity of CMs, including the interaction with ECs[469]. A study by Giacomelli *et al.* revealed that microtissue composed of 15% cardiac mesoderm derived ECs and 85% iPS-CMs resulted in better EC organisation and distribution and that a culture time of 20 days promoted CM maturation[469]. Herein, we propose using readily attainable and proliferative circulating ECFCs to induce the maturation of iPSC-CMs in the organoid model. We hypothesised that co-culturing ECFCs and iPSC-CMs may promote synergistic maturation of both cell types, and the cellular function of ECFCs may alter the maturation of iPSC-CMs, providing a novel cardiac organoid with increased maturation. These technologies would potentially provide a robust and accurate in-vitro disease model and drug testing platform, more closely mimicking human cardiac physiology in a dish.


"Good timber does not grow with ease,
The stronger wind, the stronger trees,
The further sky, the greater length,
The more the storm, the more the strength.
By sun and cold, by rain and snow,
In trees and men, good timbers grow."
-Douglas Malloch-

References

1. Aird, W.C. Phenotypic heterogeneity of the endothelium: I. Structure, function, and mechanisms. *Circulation research* **100**, 158-173 (2007).
2. Pober, J.S. & Tellides, G. Participation of blood vessel cells in human adaptive immune responses. *Trends in immunology* **33**, 49-57 (2012).
3. Chistiakov, D.A., Orekhov, A.N. & Bobryshev, Y.V. Effects of shear stress on endothelial cells: go with the flow. *Acta Physiologica* **219**, 382-408 (2017).
4. Dharmashankar, K. & Widlansky, M.E. Vascular endothelial function and hypertension: insights and directions. *Current hypertension reports* **12**, 448-455 (2010).
5. Delva, P. *et al.* Endothelial progenitor cells in patients with essential hypertension. *Journal of hypertension* **25**, 127-132 (2007).
6. Munoz-Hernandez, R. *et al.* Decreased level of cord blood circulating endothelial colony-forming cells in preeclampsia. *Hypertension* **64**, 165-171 (2014).
7. Duong, H.T. *et al.* High Proliferative Endothelial Colony-Forming Cells Among Human Pulmonary Artery Endothelial Cells In Pulmonary Arterial Hypertension, in *C96. BONE MARROW AND MICROPARTICLES IN THE PATHOGENESIS OF PULMONARY ARTERIAL HYPERTENSION* A5092-A5092 (American Thoracic Society, 2012).
8. Grace Z, Y. *et al.* Neonatal MicroRNA Profile Determines Endothelial Function in Offspring of Hypertensive Pregnancies. *Hypertension* **72**, 937-945 (2018).
9. Gopinath, B. *et al.* Blood pressure is associated with retinal vessel signs in preadolescent children. *J Hypertens* **28**, 1406-1412 (2010).
10. Bertagnolli, M. *et al.* Endothelial Colony-Forming Cells in Young Adults Born Preterm: A Novel Link Between Neonatal Complications and Adult Risks for Cardiovascular Disease. *Journal of the American Heart Association* **7**, e009720 (2018).
11. Lewandowski, A.J. *et al.* Elevated blood pressure in preterm-born offspring associates with a distinct antiangiogenic state and microvascular abnormalities in adult life. *Hypertension* **65**, 607-614 (2015).
12. Ingram, D.A., Caplice, N.M. & Yoder, M.C. Unresolved questions, changing definitions, and novel paradigms for defining endothelial progenitor cells. *Blood* **106**, 1525-1531 (2005).
13. Martin-Ramirez, J., Hofman, M., Van Den Biggelaar, M., Hebbel, R.P. & Voorberg, J. Establishment of outgrowth endothelial cells from peripheral blood. *nature protocols* **7**, 1709 (2012).
14. Reinisch, A. *et al.* Humanized large-scale expanded endothelial colony-forming cells function in vitro and in vivo. *Blood* **113**, 6716-6725 (2009).
15. Asahara, T. *et al.* Isolation of putative progenitor endothelial cells for angiogenesis. *Science* **275**, 964-966 (1997).
16. Lin, Y., Weisdorf, D.J., Solovey, A. & Hebbel, R.P. Origins of circulating endothelial cells and endothelial outgrowth from blood. *The Journal of clinical investigation* **105**, 71-77 (2000).
17. Hirschi, K.K., Ingram, D.A. & Yoder, M.C. Assessing identity, phenotype, and fate of endothelial progenitor cells. *Arteriosclerosis, thrombosis, and vascular biology* **28**, 1584-1595 (2008).
18. Jujo, K., Ii, M. & Losordo, D.W. Endothelial progenitor cells in neovascularization of infarcted myocardium. *J Mol Cell Cardiol* **45**, 530-544 (2008).
19. Alphonse, R.S. *et al.* Existence, functional impairment, and lung repair potential of endothelial colony-forming cells in oxygen-induced arrested alveolar growth. *Circulation* **129**, 2144-2157 (2014).
20. Ingram, D.A. *et al.* Identification of a novel hierarchy of endothelial progenitor cells using human peripheral and umbilical cord blood. *Blood* **104**, 2752-2760 (2004).
21. Paradis, A. & Zhang, L. Role of endothelin in uteroplacental circulation and fetal vascular function. *Current vascular pharmacology* **11**, 594-605 (2013).
22. Melero-Martin, J.M. *et al.* In vivo vasculogenic potential of human blood-derived endothelial progenitor cells. *Blood, The Journal of the American Society of Hematology* **109**, 4761-4768 (2007).
23. Au, P. *et al.* Differential in vivo potential of endothelial progenitor cells from human umbilical cord blood and adult peripheral blood to form functional long-lasting vessels. *Blood, The Journal of the American Society of Hematology* **111**, 1302-1305 (2008).

24. Yoon, C.H. *et al.* Synergistic neovascularization by mixed transplantation of early endothelial progenitor cells and late outgrowth endothelial cells: the role of angiogenic cytokines and matrix metalloproteinases. *Circulation* **112**, 1618-1627 (2005).
25. Friedman, A. & Fahey, J. in Seminars in perinatology, Vol. 17 106-121 (1993).
26. Recchioni, R. *et al.* Physical activity and progenitor cell-mediated endothelial repair in chronic heart failure: Is there a role for epigenetics? *Mech Ageing Dev* **159**, 71-80 (2016).
27. De Biase, C. *et al.* Effects of physical activity on endothelial progenitor cells (EPCs). *Frontiers in physiology* **4**, 414 (2014).
28. Asahara, T. & Kawamoto, A. Endothelial progenitor cells for postnatal vasculogenesis. *American Journal of Physiology-Cell Physiology* **287**, C572-C579 (2004).
29. Yoder, M.C. Defining human endothelial progenitor cells. *J Thromb Haemost* **7 Suppl 1**, 49-52 (2009).
30. Urbich, C. & Dimmeler, S. Endothelial progenitor cells: characterization and role in vascular biology. *Circ Res* **95**, 343-353 (2004).
31. Dimmeler, S. & Zeiher, A.M. Endothelial cell apoptosis in angiogenesis and vessel regression. *Circulation research* **87**, 434-439 (2000).
32. Rehman, J. *et al.* Exercise acutely increases circulating endothelial progenitor cells and monocyte-/macrophage-derived angiogenic cells. *J Am Coll Cardiol* **43**, 2314-2318 (2004).
33. Dimmeler, S. *et al.* HMG-CoA reductase inhibitors (statins) increase endothelial progenitor cells via the PI 3-kinase/Akt pathway. *The Journal of clinical investigation* **108**, 391-397 (2001).
34. Medina, R.J. *et al.* Molecular analysis of endothelial progenitor cell (EPC) subtypes reveals two distinct cell populations with different identities. *BMC medical genomics* **3**, 18 (2010).
35. Prasain, N., Meador, J.L. & Yoder, M.C. Phenotypic and functional characterization of endothelial colony forming cells derived from human umbilical cord blood. *JoVE (Journal of Visualized Experiments)*, e3872 (2012).
36. Mund, J.A., Estes, M.L., Yoder, M.C., Ingram Jr, D.A. & Case, J. Flow cytometric identification and functional characterization of immature and mature circulating endothelial cells. *Arteriosclerosis, thrombosis, and vascular biology* **32**, 1045-1053 (2012).
37. Yoder, M.C. Is endothelium the origin of endothelial progenitor cells? *Arterioscler Thromb Vasc Biol* **30**, 1094-1103 (2010).
38. Bompais, H. *et al.* Human endothelial cells derived from circulating progenitors display specific functional properties compared with mature vessel wall endothelial cells. *Blood* **103**, 2577-2584 (2004).
39. Yoder, M.C. *et al.* Redefining endothelial progenitor cells via clonal analysis and hematopoietic stem/progenitor cell principals. *Blood* **109**, 1801-1809 (2007).
40. Banno, K. & Yoder, M.C. Tissue regeneration using endothelial colony-forming cells: promising cells for vascular repair. *Pediatric research* **83**, 283-290 (2018).
41. Medina, R.J. *et al.* Endothelial progenitors: a consensus statement on nomenclature. *Stem cells translational medicine* **6**, 1316-1320 (2017).
42. Bouvard, C. *et al.* α6-integrin subunit plays a major role in the proangiogenic properties of endothelial progenitor cells. *Arteriosclerosis, thrombosis, and vascular biology* **30**, 1569-1575 (2010).
43. Palii, C.G. *et al.* Trichostatin A enhances vascular repair by injected human endothelial progenitors through increasing the expression of TAL1-dependent genes. *Cell Stem Cell* **14**, 644-657 (2014).
44. Saif, J. *et al.* Combination of injectable multiple growth factor–releasing scaffolds and cell therapy as an advanced modality to enhance tissue neovascularization. *Arteriosclerosis, thrombosis, and vascular biology* **30**, 1897-1904 (2010).
45. Schwarz, T.M. *et al.* Vascular incorporation of endothelial colony-forming cells is essential for functional recovery of murine ischemic tissue following cell therapy. *Arteriosclerosis, thrombosis, and vascular biology* **32**, e13-e21 (2012).
46. Gomes, K., Jadli, A. & Patel, V. ENDOTHELIAL COLONY-FORMING CELL-DERIVED EXOSOMES PROMOTE ANGIOGENESIS AND CARDIAC REPAIR POST-MYOCARDIAL INFARCTION. *Canadian Journal of Cardiology* **37**, S117 (2021).
47. Lin, R.-Z. *et al.* Human endothelial colony-forming cells serve as trophic mediators for mesenchymal stem cell engraftment via paracrine signaling. *Proceedings of the National Academy of Sciences* **111**, 10137-10142 (2014).
48. Egorova, A.D. *et al.* Endothelial colony-forming cells show a mature transcriptional response to shear stress. *In Vitro Cellular & Developmental Biology-Animal* **48**, 21-29 (2012).

49. Cooke, J.P. & Losordo, D.W. Modulating the vascular response to limb ischemia: angiogenic and cell therapies. *Circulation research* **116**, 1561-1578 (2015).
50. Fraineau, S., Palii, C.G., Allan, D.S. & Brand, M. Epigenetic regulation of endothelial-cell-mediated vascular repair. *The FEBS journal* **282**, 1605-1629 (2015).
51. Park, K.M. & Gerecht, S. Harnessing developmental processes for vascular engineering and regeneration. *Development* **141**, 2760-2769 (2014).
52. Shantsila, E., Watson, T. & Lip, G.Y. Endothelial progenitor cells in cardiovascular disorders. *J Am Coll Cardiol* **49**, 741-752 (2007).
53. Liao, G., Zheng, K., Shorr, R. & Allan, D.S. Human endothelial colony-forming cells in regenerative therapy: A systematic review of controlled preclinical animal studies. *Stem cells translational medicine* **9**, 1344-1352 (2020).
54. Zhang, X. *et al.* Increased expression of microRNA-221 inhibits PAK1 in endothelial progenitor cells and impairs its function via c-Raf/MEK/ERK pathway. *Biochem Biophys Res Commun* **431**, 404-408 (2013).
55. Huang, X.-T. *et al.* Intracerebroventricular transplantation of ex vivo expanded endothelial colony-forming cells restores blood–brain barrier integrity and promotes angiogenesis of mice with traumatic brain injury. *Journal of neurotrauma* **30**, 2080-2088 (2013).
56. Ding, J. *et al.* Bioluminescence imaging of transplanted human endothelial colony-forming cells in an ischemic mouse model. *Brain Research* **1642**, 209-218 (2016).
57. Moubarik, C. *et al.* Transplanted late outgrowth endothelial progenitor cells as cell therapy product for stroke. *Stem Cell Reviews and Reports* **7**, 208-220 (2011).
58. Garrigue, P. *et al.* Erythropoietin pretreatment of transplanted endothelial colony-forming cells enhances recovery in a cerebral ischemia model by increasing their homing ability: a SPECT/CT study. *Journal of Nuclear Medicine* **57**, 1798-1804 (2016).
59. Medina, R.J., O'Neill, C.L., Humphreys, M.W., Gardiner, T.A. & Stitt, A.W. Outgrowth endothelial cells: characterization and their potential for reversing ischemic retinopathy. *Investigative ophthalmology & visual science* **51**, 5906-5913 (2010).
60. Todorova, D., Simoncini, S., Lacroix, R., Sabatier, F. & Dignat-George, F. Extracellular vesicles in angiogenesis. *Circulation research* **120**, 1658-1673 (2017).
61. Valadi, H. *et al.* Exosome-mediated transfer of mRNAs and microRNAs is a novel mechanism of genetic exchange between cells. *Nature cell biology* **9**, 654-659 (2007).
62. Viñas, J.L. *et al.* Transfer of microRNA-486-5p from human endothelial colony forming cell–derived exosomes reduces ischemic kidney injury. *Kidney international* **90**, 1238-1250 (2016).
63. Deregibus, M.C. *et al.* Endothelial progenitor cell–derived microvesicles activate an angiogenic program in endothelial cells by a horizontal transfer of mRNA. *Blood* **110**, 2440-2448 (2007).
64. Salomon, C. *et al.* Exosomal signaling during hypoxia mediates microvascular endothelial cell migration and vasculogenesis. *PloS one* **8**, e68451 (2013).
65. van Balkom, B.W. *et al.* Endothelial cells require miR-214 to secrete exosomes that suppress senescence and induce angiogenesis in human and mouse endothelial cells. *Blood, The Journal of the American Society of Hematology* **121**, 3997-4006 (2013).
66. Zhang, Y. *et al.* Secreted monocytic miR-150 enhances targeted endothelial cell migration. *Molecular cell* **39**, 133-144 (2010).
67. Cantaluppi, V. *et al.* Microvesicles derived from endothelial progenitor cells enhance neoangiogenesis of human pancreatic islets. *Cell transplantation* **21**, 1305-1320 (2012).
68. Liu, W. *et al.* Distinct anti-fibrotic effects of exosomes derived from endothelial colony-forming cells cultured under normoxia and hypoxia. *Medical science monitor: international medical journal of experimental and clinical research* **24**, 6187 (2018).
69. Zeng, C.-Y., Xu, J., Liu, X. & Lu, Y.-Q. Cardioprotective Roles of Endothelial Progenitor Cell-Derived Exosomes. *Frontiers in Cardiovascular Medicine* **8** (2021).
70. Burger, D. *et al.* Human endothelial colony-forming cells protect against acute kidney injury: role of exosomes. *The American journal of pathology* **185**, 2309-2323 (2015).
71. Vasa, M. *et al.* Increase in circulating endothelial progenitor cells by statin therapy in patients with stable coronary artery disease. *Circulation* **103**, 2885-2890 (2001).
72. Hill, J.M. *et al.* Circulating endothelial progenitor cells, vascular function, and cardiovascular risk. *New England Journal of Medicine* **348**, 593-600 (2003).
73. Ingram, D.A. *et al.* In Vitro Hyperglycemia or a Diabetic Intrauterine Environment Reduces Neonatal Endothelial Colony-Forming Cell Numbers and Function. *Diabetes* **57**, 724-731 (2008).

74. Oliveras, A. *et al.* Endothelial progenitor cells are reduced in refractory hypertension. *Journal of human hypertension* **22**, 183-190 (2008).
75. Berezin, A., Zulli, A., Kerrigan, S., Petrovic, D. & Kruzliak, P. Predictive role of circulating endothelial-derived microparticles in cardiovascular diseases. *Clin Biochem* **48**, 562-568 (2015).
76. Liang, J. *et al.* Systemic microvascular rarefaction is correlated with dysfunction of late endothelial progenitor cells in mild hypertension: a substudy of EXCAVATION-CHN1. *Journal of translational medicine* **17**, 1-11 (2019).
77. Tan, K., Cutler, A., Nerone, P. & Anand-Apte, B. Dysfunction of Circulating Endothelial Progenitor Cells in Patients With Diabetic Retinopathy. *Investigative Ophthalmology & Visual Science* **49**, 4385-4385 (2008).
78. Hernandez-Lopez, R. *et al.* Reduced proliferation of endothelial colony-forming cells in unprovoked venous thromboembolic disease as a consequence of endothelial dysfunction. *Plos one* **12**, e0183827 (2017).
79. Alvarado-Moreno, J.A. *et al.* Endothelial colony-forming cells: Biological and functional abnormalities in patients with recurrent, unprovoked venous thromboembolic disease. *Thrombosis research* **137**, 157-168 (2016).
80. Lyons, C.J. & O'Brien, T. The Functionality of Endothelial-Colony-Forming Cells from Patients with Diabetes Mellitus. *Cells* **9**, 1731 (2020).
81. Wang, H.-W. *et al.* MicroRNA-134 contributes to glucose-induced endothelial cell dysfunction and this effect can be reversed by far-infrared irradiation. *PLoS One* **11**, e0147067 (2016).
82. Sipos, P.I. *et al.* Endothelial colony-forming cells derived from pregnancies complicated by intrauterine growth restriction are fewer and have reduced vasculogenic capacity. *The Journal of Clinical Endocrinology & Metabolism* **98**, 4953-4960 (2013).
83. Baker, C.D. *et al.* Endothelial colony-forming cells from preterm infants are increased and more susceptible to hyperoxia. *American journal of respiratory and critical care medicine* **180**, 454-461 (2009).
84. Wang, J., Bingaman, S. & Huxley, V.H. Intrinsic sex-specific differences in microvascular endothelial cell phosphodiesterases. *American Journal of Physiology-Heart and Circulatory Physiology* **298**, H1146-H1154 (2010).
85. Huang, A. & Kaley, G. Gender-specific regulation of cardiovascular function: estrogen as key player. *Microcirculation* **11**, 9-38 (2004).
86. Kunert, M.P., Dwinell, M.R., Drenjancevic Peric, I. & Lombard, J.H. Sex-specific differences in chromosome-dependent regulation of vascular reactivity in female consomic rat strains from a SS× BN cross. *American Journal of Physiology-Regulatory, Integrative and Comparative Physiology* **295**, R516-R527 (2008).
87. Rodford, J.L. *et al.* Endothelial dysfunction and reduced antioxidant protection in an animal model of the developmental origins of cardiovascular disease. *The Journal of physiology* **586**, 4709-4720 (2008).
88. Mudrovcic, N., Arefin, S., Van Craenenbroeck, A.H. & Kublickiene, K. Endothelial maintenance in health and disease: Importance of sex differences. *Pharmacological research* **119**, 48-60 (2017).
89. Kublickiene, K. & Luksha, L. Gender and the endothelium. *Pharmacol Rep* **60**, 49-60 (2008).
90. Sumanasekera, W.K. *et al.* Estradiol and dihydrotestosterone regulate endothelial cell barrier function after hypergravity-induced alterations in MAPK activity. *American Journal of Physiology-Cell Physiology* **293**, C566-C573 (2007).
91. Villar, I.C., Hobbs, A.J. & Ahluwalia, A. Sex differences in vascular function: implication of endothelium-derived hyperpolarizing factor. *The Journal of endocrinology* **197**, 447-462 (2008).
92. Addis, R. *et al.* Human umbilical endothelial cells (HUVECs) have a sex: characterisation of the phenotype of male and female cells. *Biology of sex differences* **5**, 1-12 (2014).
93. Lorenz, M. *et al.* Does cellular sex matter? Dimorphic transcriptional differences between female and male endothelial cells. *Atherosclerosis* **240**, 61-72 (2015).
94. Malorni, W., Campesi, I., Straface, E., Vella, S. & Franconi, F. Redox features of the cell: a gender perspective. *Antioxidants & redox signaling* **9**, 1779-1802 (2007).
95. James, B.D. & Allen, J.B. Sex-Specific Response to Combinations of Shear Stress and Substrate Stiffness by Endothelial Cells In Vitro. *Advanced Healthcare Materials*, 2100735 (2021).
96. Boscaro, C. *et al.* Sex differences in the pro-angiogenic response of human endothelial cells: Focus on PFKFB3 and FAK activation. *Frontiers in pharmacology* **11** (2020).

97. Cattaneo, M.G. *et al.* Sex-specific eNOS activity and function in human endothelial cells. *Scientific reports* **7**, 1-13 (2017).
98. Witt, E. *et al.* Sex-specific differences in the intracellular proteome of human endothelial cells from dizygotic twins. *Journal of proteomics* **201**, 48-56 (2019).
99. Hartman, R.J. *et al.* Intrinsic transcriptomic sex differences in human endothelial cells at birth and in adults are associated with coronary artery disease targets. *Scientific reports* **10**, 1-12 (2020).
100. Cvitic, S. *et al.* Sexual dimorphism of miRNA signatures in feto-placental endothelial cells is associated with altered barrier function and actin organization. *Clinical Science* **134**, 39-51 (2020).
101. Cattaneo, M.G., Banfi, C., Brioschi, M., Lattuada, D. & Vicentini, L.M. Sex-dependent differences in the secretome of human endothelial cells. *Biology of Sex Differences* **12**, 1-15 (2021).
102. Shah, K., McCormack, C.E. & Bradbury, N.A. Do you know the sex of your cells? *American Journal of Physiology-Cell Physiology* **306**, C3-C18 (2014).
103. Woitowich, N.C. & Woodruff, T.K. Opinion: Research community needs to better appreciate the value of sex-based research. *Proceedings of the National Academy of Sciences* **116**, 7154-7156 (2019).
104. Taylor, K.E., Vallejo-Giraldo, C., Schaible, N.S., Zakeri, R. & Miller, V.M. Reporting of sex as a variable in cardiovascular studies using cultured cells. *Biology of sex differences* **2**, 1-7 (2011).
105. Ventura-Clapier, R. *et al.* Sex in basic research: concepts in the cardiovascular field. *Cardiovascular research* **113**, 711-724 (2017).
106. Franklin, S.S. & Wong, N.D. Hypertension and cardiovascular disease: contributions of the Framingham Heart Study. *Global heart* **8**, 49-57 (2013).
107. Xu, Q., Sun, H., Huang, X. & Qu, Y. Retinal microvascular metrics in untreated essential hypertensives using optical coherence tomography angiography. *Graefe's Archive for Clinical and Experimental Ophthalmology* **259**, 395-403 (2021).
108. Mitchell, P. *et al.* Blood pressure and retinal arteriolar narrowing in children. *Hypertension* **49**, 1156-1162 (2007).
109. Forouzanfar, M.H. *et al.* Global burden of hypertension and systolic blood pressure of at least 110 to 115 mm Hg, 1990-2015. *Jama* **317**, 165-182 (2017).
110. Whelton, P.K. *et al.* 2017 ACC/AHA/AAPA/ABC/ACPM/AGS/APhA/ASH/ASPC/NMA/PCNA guideline for the prevention, detection, evaluation, and management of high blood pressure in adults: a report of the American College of Cardiology/American Heart Association Task Force on Clinical Practice Guidelines. *Journal of the American College of Cardiology* **71**, e127-e248 (2018).
111. Brettler, J. Essential hypertension. *BMJ Best Practice* (2019).
112. BHF British Heart Foundation Annual Report. (2021).
113. Evans, C.E., Cober, N.D., Dai, Z., Stewart, D.J. & Zhao, Y.-Y. Endothelial cells in the pathogenesis of pulmonary arterial hypertension. *European Respiratory Journal* (2021).
114. Nørrelund, H. *et al.* Early narrowed afferent arteriole is a contributor to the development of hypertension. *Hypertension* **24**, 301-308 (1994).
115. McCarron, P., Smith, G.D., Okasha, M. & McEwen, J. Blood pressure in young adulthood and mortality from cardiovascular disease. *The Lancet* **355**, 1430-1431 (2000).
116. Berenson, G.S. *et al.* Association between multiple cardiovascular risk factors and atherosclerosis in children and young adults. *New England journal of medicine* **338**, 1650-1656 (1998).
117. Liu, M. *et al.* Associations of retinal microvascular caliber with intermediate phenotypes of large arterial function and structure: a systematic review and meta-analysis. *Microcirculation* **26**, e12557 (2019).
118. Tapp, R.J. *et al.* Impact of blood pressure on retinal microvasculature architecture across the lifespan: the Young Finns Study. *Microcirculation* **22**, 146-155 (2015).
119. Zhang, Y., Lacolley, P., Protogerou, A.D. & Safar, M.E. Arterial stiffness in hypertension and function of large arteries. *American journal of hypertension* **33**, 291-296 (2020).
120. Levy, B.I. *et al.* Impaired tissue perfusion: a pathology common to hypertension, obesity, and diabetes mellitus. *Circulation* **118**, 968-976 (2008).
121. Feihl, F.o., Liaudet, L., Waeber, B. & Levy, B.I. Hypertension: a disease of the microcirculation? *Hypertension* **48**, 1012-1017 (2006).
122. Kawasaki, R. *et al.* Retinal vessel diameters and risk of hypertension: the Multiethnic Study of Atherosclerosis. *Journal of hypertension* **27**, 2386 (2009).
123. Smith, W. *et al.* Retinal arteriolar narrowing is associated with 5-year incident severe hypertension: the Blue Mountains Eye Study. *Hypertension* **44**, 442-447 (2004).

124. Levy, B., Ambrosio, G., Pries, A. & Struijker-Boudier, H. Microcirculation in hypertension: a new target for treatment? *Circulation* **104**, 735-740 (2001).
125. Cheung, C.Y.-l., Ikram, M.K., Sabanayagam, C. & Wong, T.Y. Retinal microvasculature as a model to study the manifestations of hypertension. *Hypertension* **60**, 1094-1103 (2012).
126. Celermajer, D.S. *et al.* Non-invasive detection of endothelial dysfunction in children and adults at risk of atherosclerosis. *The lancet* **340**, 1111-1115 (1992).
127. Kurakula, K. *et al.* Endothelial Dysfunction in Pulmonary Hypertension: Cause or Consequence? *Biomedicines* **9**, 57 (2021).
128. Renna, N.F., De Las Heras, N. & Miatello, R.M. Pathophysiology of vascular remodeling in hypertension. *International journal of hypertension* **2013** (2013).
129. Gohlke, P. *et al.* Vascular remodeling in systemic hypertension. *The American journal of cardiology* **71**, E2-E7 (1993).
130. Feihl, F., Liaudet, L., Levy, B.I. & Waeber, B. Hypertension and microvascular remodelling. *Cardiovascular research* **78**, 274-285 (2008).
131. Tucker, W.D., Arora, Y. & Mahajan, K. Anatomy, blood vessels. (2017).
132. Chen, B.P. *et al.* DNA microarray analysis of gene expression in endothelial cells in response to 24-h shear stress. *Physiological genomics* **7**, 55-63 (2001).
133. Malek, A.M., Alper, S.L. & Izumo, S. Hemodynamic shear stress and its role in atherosclerosis. *Jama* **282**, 2035-2042 (1999).
134. Szulcek, R. *et al.* Delayed microvascular shear adaptation in pulmonary arterial hypertension. Role of platelet endothelial cell adhesion molecule-1 cleavage. *American journal of respiratory and critical care medicine* **193**, 1410-1420 (2016).
135. Lerman, A. & Zeiher, A.M. Endothelial function: cardiac events. *Circulation* **111**, 363-368 (2005).
136. de la Sierra, A. & Larrousse, M. Endothelial dysfunction is associated with increased levels of biomarkers in essential hypertension. *J Hum Hypertens* **24**, 373-379 (2010).
137. Hadi, H.A., Carr, C.S. & Al Suwaidi, J. Endothelial dysfunction: cardiovascular risk factors, therapy, and outcome. *Vascular health and risk management* **1**, 183 (2005).
138. Budhiraja, R., Tuder, R.M. & Hassoun, P.M. Endothelial dysfunction in pulmonary hypertension. *Circulation* **109**, 159-165 (2004).
139. Humbert, M. *et al.* Cellular and molecular pathobiology of pulmonary arterial hypertension. *Journal of the American College of Cardiology* **43**, S13-S24 (2004).
140. Humbert, M. *et al.* Endothelial cell dysfunction and cross talk between endothelium and smooth muscle cells in pulmonary arterial hypertension. *Vascular pharmacology* **49**, 113-118 (2008).
141. Czernichow, S. *et al.* Microvascular dysfunction in healthy insulin-sensitive overweight individuals. *Journal of hypertension* **28**, 325-332 (2010).
142. Jonk, A.M. *et al.* Microvascular dysfunction in obesity: a potential mechanism in the pathogenesis of obesity-associated insulin resistance and hypertension. *Physiology* **22**, 252-260 (2007).
143. Yoon, C.-H. *et al.* Synergistic neovascularization by mixed transplantation of early endothelial progenitor cells and late outgrowth endothelial cells: the role of angiogenic cytokines and matrix metalloproteinases. (2005).
144. Friedrich, E.B., Walenta, K., Scharlau, J., Nickenig, G. & Werner, N. CD34−/CD133+/VEGFR-2+ endothelial progenitor cell subpopulation with potent vasoregenerative capacities. *Circulation research* **98**, e20-e25 (2006).
145. Oliveras, A. *et al.* Endothelial progenitor cells are reduced in refractory hypertension. *J Hum Hypertens* **22**, 183-190 (2008).
146. Giannotti, G. *et al.* Impaired endothelial repair capacity of early endothelial progenitor cells in prehypertension: relation to endothelial dysfunction. *Hypertension* **55**, 1389-1397 (2010).
147. António, N. *et al.* Reduced levels of circulating endothelial progenitor cells in acute myocardial infarction patients with diabetes or pre-diabetes: accompanying the glycemic continuum. *Cardiovascular diabetology* **13**, 1-17 (2014).
148. Tan, C.M. *et al.* Proteomic Signature of Dysfunctional Circulating Endothelial Colony-Forming Cells of Young Adults. *Journal of the American Heart Association* **10**, e021119 (2021).
149. Brunner, H. *et al.* Working Group on Endothelins and Endothelial Factors of the European Society of Hypertension. Endothelial function and dysfunction. Part II: Association with cardiovascular risk factors and diseases. A statement by the Working Group on Endothelins and Endothelial Factors of the European Society of Hypertension. *J Hypertens* **23**, 233-246 (2005).

150. Chun, H.J., Bonnet, S. & Chan, S.Y. Translational Advances in the Field of Pulmonary Hypertension. Translating MicroRNA Biology in Pulmonary Hypertension. It Will Take More Than "miR" Words. *American journal of respiratory and critical care medicine* **195**, 167-178 (2017).
151. Badorff, C. *et al.* Transdifferentiation of blood-derived human adult endothelial progenitor cells into functionally active cardiomyocytes. *Circulation* **107**, 1024-1032 (2003).
152. De Miguel, C., Rudemiller, N.P., Abais, J.M. & Mattson, D.L. Inflammation and hypertension: new understandings and potential therapeutic targets. *Curr Hypertens Rep* **17**, 507 (2015).
153. Ikram, M.K., Ong, Y.T., Cheung, C.Y. & Wong, T.Y. Retinal vascular caliber measurements: clinical significance, current knowledge and future perspectives. *Ophthalmologica* **229**, 125-136 (2013).
154. Wong, T.Y. *et al.* Retinal arteriolar diameter and risk for hypertension. *Annals of internal medicine* **140**, 248-255 (2004).
155. Sun, C., Wang, J.J., Mackey, D.A. & Wong, T.Y. Retinal vascular caliber: systemic, environmental, and genetic associations. *Survey of ophthalmology* **54**, 74-95 (2009).
156. Seidelmann, S.B. *et al.* Retinal vessel calibers in predicting long-term cardiovascular outcomes: the atherosclerosis risk in communities study. *Circulation* **134**, 1328-1338 (2016).
157. Li, L.J. *et al.* Assessing the Causality between Blood Pressure and Retinal Vascular Caliber through Mendelian Randomisation. *Sci Rep* **6**, 22031 (2016).
158. Nguyen, T.T. *et al.* Retinal arteriolar narrowing predicts incidence of diabetes: the Australian Diabetes, Obesity and Lifestyle (AusDiab) Study. *Diabetes* **57**, 536-539 (2008).
159. Cheung, C.Y. *et al.* Retinal vascular tortuosity, blood pressure, and cardiovascular risk factors. *Ophthalmology* **118**, 812-818 (2011).
160. Triantafyllou, A. *et al.* Association between retinal vessel caliber and arterial stiffness in a population comprised of normotensive to early-stage hypertensive individuals. *American journal of hypertension* **27**, 1472-1478 (2014).
161. Delles, C. *et al.* Impaired endothelial function of the retinal vasculature in hypertensive patients. *Stroke* **35**, 1289-1293 (2004).
162. Hubbard, L.D. *et al.* Methods for evaluation of retinal microvascular abnormalities associated with hypertension/sclerosis in the Atherosclerosis Risk in Communities Study. *Ophthalmology* **106**, 2269-2280 (1999).
163. Wong, T.Y. *et al.* Retinal arteriolar narrowing and risk of coronary heart disease in men and women: the Atherosclerosis Risk in Communities Study. *Jama* **287**, 1153-1159 (2002).
164. Wong, T.Y. & Mitchell, P. Hypertensive retinopathy. *New England Journal of Medicine* **351**, 2310-2317 (2004).
165. Ikram, M.K. *et al.* Retinal vessel diameters and risk of hypertension: the Rotterdam Study. *hypertension* **47**, 189-194 (2006).
166. Wong, T.Y. *et al.* Retinal microvascular abnormalities and incident stroke: the Atherosclerosis Risk in Communities Study. *The Lancet* **358**, 1134-1140 (2001).
167. McGeechan, K. *et al.* Risk prediction of coronary heart disease based on retinal vascular caliber (from the Atherosclerosis Risk In Communities [ARIC] Study). *The American journal of cardiology* **102**, 58-63 (2008).
168. Zheng, Y., Huang, W., Zhang, J. & He, M. Phenotypic and genetic correlation of blood pressure and body mass index with retinal vascular caliber in children and adolescents: the Guangzhou twin eye study. *Investigative ophthalmology & visual science* **54**, 423-428 (2013).
169. Gishti, O. *et al.* Retinal microvasculature and cardiovascular health in childhood. *Pediatrics* **135**, 678-685 (2015).
170. Imhof, K., Zahner, L., Schmidt-Trucksass, A. & Hanssen, H. Association of body composition and blood pressure categories with retinal vessel diameters in primary school children. *Hypertens Res* **39**, 423-429 (2016).
171. Owen, C.G. *et al.* Retinal arteriolar tortuosity and cardiovascular risk factors in a multi-ethnic population study of 10-year-old children; the Child Heart and Health Study in England (CHASE). *Arterioscler Thromb Vasc Biol* **31**, 1933-1938 (2011).
172. Hanssen, H. *et al.* Retinal vessel diameter, obesity and metabolic risk factors in school children (JuvenTUM 3). *Atherosclerosis* **221**, 242-248 (2012).
173. Kannenkeril, D. *et al.* Retinal vascular resistance in arterial hypertension. *Blood Press* **27**, 82-87 (2018).
174. Rijks, J. *et al.* Characteristics of the retinal microvasculature in association with cardiovascular risk markers in children with overweight, obesity and morbid obesity. *Scientific reports* **8**, 1-8 (2018).

175. Owen, C.G. *et al.* Retinal vasculometry associations with cardiometabolic risk factors in the european prospective investigation of cancer—norfolk study. *Ophthalmology* **126**, 96-106 (2019).
176. Li, L.J., Ikram, M.K. & Wong, T.Y. Retinal vascular imaging in early life: insights into processes and risk of cardiovascular disease. *The Journal of physiology* **594**, 2175-2203 (2016).
177. Vicaut, E. Hypertension and the microcirculation: a brief overview of experimental studies. *Journal of hypertension. Supplement: official journal of the International Society of Hypertension* **10**, S59-68 (1992).
178. Yannoutsos, A., Levy, B.I., Safar, M.E., Slama, G. & Blacher, J. Pathophysiology of hypertension: interactions between macro and microvascular alterations through endothelial dysfunction. *Journal of hypertension* **32**, 216-224 (2014).
179. Chirinos, J.A., Segers, P., Hughes, T. & Townsend, R. Large-artery stiffness in health and disease: JACC state-of-the-art review. *Journal of the American College of Cardiology* **74**, 1237-1263 (2019).
180. Boutouyrie, P., Chowienczyk, P., Humphrey, J.D. & Mitchell, G.F. Arterial stiffness and cardiovascular risk in hypertension. *Circulation Research* **128**, 864-886 (2021).
181. Williams, B. *et al.* 2018 Practice guidelines for the management of arterial hypertension of the European Society of Cardiology and the European Society of Hypertension. *Blood pressure* **27**, 314-340 (2018).
182. Mancia, G. *et al.* Reappraisal of European guidelines on hypertension management: a European Society of Hypertension Task Force document. *Blood pressure* **18**, 308-347 (2009).
183. Najjar, S.S. *et al.* Pulse wave velocity is an independent predictor of the longitudinal increase in systolic blood pressure and of incident hypertension in the Baltimore Longitudinal Study of Aging. *Journal of the American College of Cardiology* **51**, 1377-1383 (2008).
184. O'Rourke, M.F. & Nichols, W.W. Aortic diameter, aortic stiffness, and wave reflection increase with age and isolated systolic hypertension. *Hypertension* **45**, 652-658 (2005).
185. Sun, Z. Aging, arterial stiffness, and hypertension. *Hypertension* **65**, 252-256 (2015).
186. Prenner, S.B. & Chirinos, J.A. Arterial stiffness in diabetes mellitus. *Atherosclerosis* **238**, 370-379 (2015).
187. Safar, M.E., London, G.r.M. & Plante, G.r.E. Arterial stiffness and kidney function. *Hypertension* **43**, 163-168 (2004).
188. Vanfleteren, L.E. *et al.* Arterial stiffness in patients with COPD: the role of systemic inflammation and the effects of pulmonary rehabilitation. *European Respiratory Journal* **43**, 1306-1315 (2014).
189. Ikonomidis, I., Makavos, G. & Lekakis, J. Arterial stiffness and coronary artery disease. *Current opinion in cardiology* **30**, 422-431 (2015).
190. Chen, Y., Shen, F., Liu, J. & Yang, G.-Y. Arterial stiffness and stroke: de-stiffening strategy, a therapeutic target for stroke. *Stroke and vascular Neurology* **2** (2017).
191. Ben-Shlomo, Y. *et al.* Aortic pulse wave velocity improves cardiovascular event prediction: an individual participant meta-analysis of prospective observational data from 17,635 subjects. *Journal of the American College of Cardiology* **63**, 636-646 (2014).
192. Rezaeian, M., Golzan, S.M., Avolio, A.P., Graham, S. & Butlin, M. The association between retinal and central pulse wave velocity in the elderly. *Artery Research* **26**, 148-153 (2020).
193. Kawashima-Kumagai, K. *et al.* Association of retinal vessel calibers and longitudinal changes in arterial stiffness: the Nagahama study. *Journal of hypertension* **36**, 587-593 (2018).
194. Tapp, R.J. *et al.* Associations of retinal microvascular diameters and tortuosity with blood pressure and arterial stiffness: United Kingdom Biobank. *Hypertension* **74**, 1383-1390 (2019).
195. Tomiyama, H. *et al.* Longitudinal association among endothelial function, arterial stiffness and subclinical organ damage in hypertension. *International journal of cardiology* **253**, 161-166 (2018).
196. Maruhashi, T. *et al.* Endothelial dysfunction, increased arterial stiffness, and cardiovascular risk prediction in patients with coronary artery disease: FMD-J (Flow-Mediated Dilation Japan) Study A. *Journal of the American Heart Association* **7**, e008588 (2018).
197. Liew, G. *et al.* Relative importance of systemic determinants of retinal arteriolar and venular caliber: the atherosclerosis risk in communities study. *Archives of ophthalmology* **126**, 1404-1410 (2008).
198. LaValley, D.J. *et al.* Matrix stiffness enhances VEGFR-2 internalization, signaling, and proliferation in endothelial cells. *Convergent Science Physical Oncology* **3**, 044001 (2017).
199. Birukova, A.A. *et al.* Endothelial barrier disruption and recovery is controlled by substrate stiffness. *Microvascular research* **87**, 50-57 (2013).
200. Bastounis, E.E., Yeh, Y.-T. & Theriot, J.A. Subendothelial stiffness alters endothelial cell traction force generation while exerting a minimal effect on the transcriptome. *Scientific reports* **9**, 1-16 (2019).

201. WHO Global health risks: mortality and burden of disease attributable to selected major risks. *World Health Organization.* (2009).
202. Schoenborn, C.A. & Stommel, M. Adherence to the 2008 adult physical activity guidelines and mortality risk. *American journal of preventive medicine* **40**, 514-521 (2011).
203. Bamman, M.M. *et al.* in Mayo Clinic Proceedings, Vol. 89 148-153 (Elsevier, 2014).
204. Christianson, M.S. & Shen, W. Osteoporosis prevention and management: nonpharmacologic and lifestyle options. *Clinical obstetrics and gynecology* **56**, 703-710 (2013).
205. Di Francescomarino, S., Sciartilli, A., Di Valerio, V., Di Baldassarre, A. & Gallina, S. The effect of physical exercise on endothelial function. *Sports medicine* **39**, 797-812 (2009).
206. Luan, X. *et al.* Exercise as a prescription for patients with various diseases. *Journal of sport and health science* **8**, 422-441 (2019).
207. Bernardo, B.C., Ooi, J.Y., Weeks, K.L., Patterson, N.L. & McMullen, J.R. Understanding key mechanisms of exercise-induced cardiac protection to mitigate disease: current knowledge and emerging concepts. *Physiological Reviews* **98**, 419-475 (2018).
208. Wang, L., Wang, J., Cretoiu, D., Li, G. & Xiao, J. Exercise-mediated regulation of autophagy in the cardiovascular system. *Journal of Sport and Health Science* **9**, 203-210 (2020).
209. Mancia, G. *et al.* 2013 ESH/ESC practice guidelines for the management of arterial hypertension: ESH-ESC the task force for the management of arterial hypertension of the European Society of Hypertension (ESH) and of the European Society of Cardiology (ESC). *Blood pressure* **23**, 3-16 (2014).
210. James, P.A. *et al.* 2014 evidence-based guideline for the management of high blood pressure in adults: report from the panel members appointed to the Eighth Joint National Committee (JNC 8). *Jama* **311**, 507-520 (2014).
211. Beck, D.T., Casey, D.P., Martin, J.S., Emerson, B.D. & Braith, R.W. Exercise training improves endothelial function in young prehypertensives. *Experimental biology and medicine* **238**, 433-441 (2013).
212. Fernandes, T., Magalhães, F.d.C., Carmo, E.C.d. & Oliveira, E.M.d. Aerobic exercise training inhibits skeletal muscular apoptotic signaling mediated by VEGF-VEGR2 in spontaneously hypertesive rats. *Revista Brasileira de Medicina do Esporte* **18**, 412-418 (2012).
213. Hawley, J.A., Hargreaves, M., Joyner, M.J. & Zierath, J.R. Integrative biology of exercise. *Cell* **159**, 738-749 (2014).
214. Neufer, P.D. *et al.* Understanding the cellular and molecular mechanisms of physical activity-induced health benefits. *Cell metabolism* **22**, 4-11 (2015).
215. Safdar, A., Saleem, A. & Tarnopolsky, M.A. The potential of endurance exercise-derived exosomes to treat metabolic diseases. *Nature Reviews Endocrinology* **12**, 504-517 (2016).
216. Walz, W. From Functional Linkage to Integrative Physiology, in *Integrative Physiology in the Proteomics and Post-Genomics Age* 1-5 (Springer, 2005).
217. Gatta, L. *et al.* Effects of a short-term exercise training on serum factors involved in ventricular remodelling in chronic heart failure patients. *International journal of cardiology* **155**, 409-413 (2012).
218. Volaklis, K.A., Tokmakidis, S.P. & Halle, M. Acute and chronic effects of exercise on circulating endothelial progenitor cells in healthy and diseased patients. *Clin Res Cardiol* **102**, 249-257 (2013).
219. Williamson, W. *et al.* Will exercise advice be sufficient for treatment of young adults with prehypertension and hypertension? A systematic review and meta-analysis. *Hypertension* **68**, 78-87 (2016).
220. Braith, R.W. & Stewart, K.J. Resistance exercise training: its role in the prevention of cardiovascular disease. *Circulation* **113**, 2642-2650 (2006).
221. Pescatello, L.S. Exercise and hypertension: recent advances in exercise prescription. *Current hypertension reports* **7**, 281-286 (2005).
222. Ntanasis-Stathopoulos, J., Tzanninis, J., Philippou, A. & Koutsilieris, M. Epigenetic regulation on gene expression induced by physical exercise. *J Musculoskelet Neuronal Interact* **13**, 133-146 (2013).
223. Wang, R. *et al.* Impacts of exercise intervention on various diseases in rats. *Journal of sport and health science* **9**, 211-227 (2020).
224. Gielen, S., Schuler, G. & Hambrecht, R. Exercise training in coronary artery disease and coronary vasomotion. *Circulation* **103**, e1-e6 (2001).
225. Cerqueira, É., Marinho, D.A., Neiva, H.P. & Lourenço, O. Inflammatory effects of high and moderate intensity exercise—A systematic review. *Frontiers in physiology*, 1550 (2020).

226. Sun, D., Huang, A., Koller, A. & Kaley, G. Short-term daily exercise activity enhances endothelial NO synthesis in skeletal muscle arterioles of rats. *Journal of Applied Physiology* **76**, 2241-2247 (1994).
227. Davies, P.F., Spaan, J. & Krams, R. Shear stress biology of the endothelium. *Annals of biomedical engineering* **33**, 1714-1718 (2005).
228. Resnick, N. *et al.* Fluid shear stress and the vascular endothelium: for better and for worse. *Progress in biophysics and molecular biology* **81**, 177-199 (2003).
229. Green, D.J., Maiorana, A., O'Driscoll, G. & Taylor, R. Effect of exercise training on endothelium-derived nitric oxide function in humans. *The Journal of physiology* **561**, 1-25 (2004).
230. Widder, J.D. *et al.* Regulation of tetrahydrobiopterin biosynthesis by shear stress. *Circulation research* **101**, 830-838 (2007).
231. Hambrecht, R. *et al.* Regular physical activity improves endothelial function in patients with coronary artery disease by increasing phosphorylation of endothelial nitric oxide synthase. *Circulation* **107**, 3152-3158 (2003).
232. Balligand, J.-L., Feron, O. & Dessy, C. eNOS activation by physical forces: from short-term regulation of contraction to chronic remodeling of cardiovascular tissues. *Physiological reviews* **89**, 481-534 (2009).
233. Haram, P.M., Kemi, O.J. & Wisloff, U. Adaptation of endothelium to exercise training: insights from experimental studies. *Front Biosci* **13**, 336-346 (2008).
234. Yang, Z. *et al.* Acute exercise-induced nitric oxide production contributes to upregulation of circulating endothelial progenitor cells in healthy subjects. *Journal of human hypertension* **21**, 452-460 (2007).
235. Seo, D.Y. *et al.* Exercise as a potential therapeutic target for diabetic cardiomyopathy: insight into the underlying mechanisms. *International journal of molecular sciences* **20**, 6284 (2019).
236. Gao, J., Pan, X., Li, G., Chatterjee, E. & Xiao, J. Physical exercise protects against endothelial dysfunction in cardiovascular and metabolic diseases. *Journal of cardiovascular translational research*, 1-17 (2021).
237. Downey, R.M. *et al.* Endothelial dysfunction correlates with exaggerated exercise pressor response during whole body maximal exercise in chronic kidney disease. *American Journal of Physiology-Renal Physiology* **312**, F917-F924 (2017).
238. Vona, M. *et al.* Effects of different types of exercise training followed by detraining on endothelium-dependent dilation in patients with recent myocardial infarction. *Circulation* **119**, 1601-1608 (2009).
239. Suvorava, T. & Kojda, G. Prevention of transient endothelial dysfunction in acute exercise: a friendly fire? *Thromb Haemost* **97**, 331-333 (2007).
240. Tao, J. *et al.* Shear stress increases Cu/Zn SOD activity and mRNA expression in human endothelial progenitor cells. *Journal of human hypertension* **21**, 353-358 (2007).
241. Tanaka, L.Y. *et al.* Exercise improves endothelial function: a local analysis of production of nitric oxide and reactive oxygen species. *Nitric Oxide* **45**, 7-14 (2015).
242. Gu, Q. *et al.* Chronic aerobic exercise training attenuates aortic stiffening and endothelial dysfunction through preserving aortic mitochondrial function in aged rats. *Experimental gerontology* **56**, 37-44 (2014).
243. Gioscia-Ryan, R.A. *et al.* Voluntary aerobic exercise increases arterial resilience and mitochondrial health with aging in mice. *Aging (Albany NY)* **8**, 2897 (2016).
244. Tao, L., Bei, Y., Zhang, H., Xiao, J. & Li, X. Exercise for the heart: signaling pathways. *Oncotarget* **6**, 20773-20784 (2015).
245. Van Craenenbroeck, E.M. & Conraads, V.M. Mending injured endothelium in chronic heart failure: a new target for exercise training. *Int J Cardiol* **166**, 310-314 (2013).
246. Lesniewski, L.A. *et al.* Aerobic exercise reverses arterial inflammation with aging in mice. *American Journal of Physiology-Heart and Circulatory Physiology* **301**, H1025-H1032 (2011).
247. Sousa, A.S., Sponton, A., Trifone, C.B. & Delbin, M.A. Aerobic exercise training prevents perivascular adipose tissue-induced endothelial dysfunction in thoracic aorta of obese mice. *Frontiers in Physiology*, 1009 (2019).
248. Palmefors, H., DuttaRoy, S., Rundqvist, B. & Börjesson, M. The effect of physical activity or exercise on key biomarkers in atherosclerosis–a systematic review. *Atherosclerosis* **235**, 150-161 (2014).
249. Lee, J.S. & Feldman, A.M. Gene therapy for therapeutic myocardial angiogenesis: a promising synthesis of two emerging technologies. *Nature medicine* **4**, 739-742 (1998).

250. Gustafsson, T., Puntschart, A., Kaijser, L., Jansson, E. & Sundberg, C.J. Exercise-induced expression of angiogenesis-related transcription and growth factors in human skeletal muscle. *American Journal of Physiology-Heart and Circulatory Physiology* **276**, H679-H685 (1999).
251. Richardson, R. *et al.* Exercise adaptation attenuates VEGF gene expression in human skeletal muscle. *American Journal of Physiology-Heart and Circulatory Physiology* **279**, H772-H778 (2000).
252. Strehlow, K. *et al.* Estrogen increases bone marrow–derived endothelial progenitor cell production and diminishes neointima formation. *Circulation* **107**, 3059-3065 (2003).
253. Gevaert, A.B. *et al.* Endothelial dysfunction and cellular repair in heart failure with preserved ejection fraction: response to a single maximal exercise bout. *European journal of heart failure.-Place of publication unknown* **21**, 125-127 (2019).
254. Djohan, A.H., Sia, C.-H., Lee, P.S. & Poh, K.-K. Endothelial progenitor cells in heart failure: an authentic expectation for potential future use and a lack of universal definition. *Journal of cardiovascular translational research* **11**, 393-402 (2018).
255. Kaushik, K. & Das, A. Endothelial progenitor cell therapy for chronic wound tissue regeneration. *Cytotherapy* **21**, 1137-1150 (2019).
256. Fadini, G.P., Sartore, S., Agostini, C. & Avogaro, A. Significance of endothelial progenitor cells in subjects with diabetes. *Diabetes care* **30**, 1305-1313 (2007).
257. Dzau, V.J., Braun-Dullaeus, R.C. & Sedding, D.G. Vascular proliferation and atherosclerosis: new perspectives and therapeutic strategies. *Nature medicine* **8**, 1249 (2002).
258. Werner, N. *et al.* Circulating Endothelial Progenitor Cells and Cardiovascular Outcomes. *New England Journal of Medicine* **353**, 999-1007 (2005).
259. Leone, A.M. *et al.* From bone marrow to the arterial wall: the ongoing tale of endothelial progenitor cells. *Eur Heart J* **30**, 890-899 (2009).
260. Sandri, M. *et al.* Effects of exercise and ischemia on mobilization and functional activation of blood-derived progenitor cells in patients with ischemic syndromes: results of 3 randomized studies. *Circulation* **111**, 3391-3399 (2005).
261. Brehm, M. *et al.* Effects of exercise training on mobilization and functional activity of blood-derived progenitor cells in patients with acute myocardial infarction. *European journal of medical research* **14**, 393-405 (2009).
262. Sarto, P. *et al.* Effects of exercise training on endothelial progenitor cells in patients with chronic heart failure. *J Card Fail* **13**, 701-708 (2007).
263. Yang, Z. *et al.* Regular exercise-induced increased number and activity of circulating endothelial progenitor cells attenuates age-related decline in arterial elasticity in healthy men. *Int J Cardiol* **165**, 247-254 (2013).
264. Cavalcante, S.L. *et al.* Effects of exercise on endothelial progenitor cells in patients with cardiovascular disease: A systematic review and meta-analysis of randomized controlled trials. *Revista Portuguesa de Cardiologia* **38**, 817-827 (2019).
265. Hoetzer, G.L. *et al.* Aging, exercise, and endothelial progenitor cell clonogenic and migratory capacity in men. *Journal of applied physiology* **102**, 847-852 (2007).
266. Özüyaman, B. *et al.* Nitric oxide differentially regulates proliferation and mobilization of endothelial progenitor cells but not of hematopoietic stem cells. *Thrombosis and haemostasis* **94**, 770-772 (2005).
267. Silva, J.F.R.d., Rocha, N.G. & Nóbrega, A.C.L.d. Mobilization of endothelial progenitor cells with exercise in healthy individuals: a systematic review. *Arquivos brasileiros de cardiologia* **98**, 182-191 (2012).
268. Tsai, H.-H., Lin, C.-P., Lin, Y.-H., Hsu, C.-C. & Wang, J.-S. High-intensity Interval training enhances mobilization/functionality of endothelial progenitor cells and depressed shedding of vascular endothelial cells undergoing hypoxia. *European journal of applied physiology* **116**, 2375-2388 (2016).
269. Umpierre, D., Stein, R., Vieira, P.J. & Ribeiro, J.P. Blunted vascular responses but preserved endothelial vasodilation after submaximal exercise in chronic heart failure. *European Journal of Preventive Cardiology* **16**, 53-59 (2009).
270. Van Craenenbroeck, E.M. *et al.* A maximal exercise bout increases the number of circulating CD34+/KDR+ endothelial progenitor cells in healthy subjects. Relation with lipid profile. *Journal of applied physiology* **104**, 1006-1013 (2008).
271. Möbius-Winkler, S. *et al.* Time-dependent mobilization of circulating progenitor cells during strenuous exercise in healthy individuals. *Journal of Applied Physiology* **107**, 1943-1950 (2009).

272. Kalka, C. *et al.* Vascular endothelial growth factor165 gene transfer augments circulating endothelial progenitor cells in human subjects. *Circulation research* **86**, 1198-1202 (2000).
273. Laufs, U. *et al.* Physical training increases endothelial progenitor cells, inhibits neointima formation, and enhances angiogenesis. *Circulation* **109**, 220-226 (2004).
274. Steiner, S. *et al.* Endurance training increases the number of endothelial progenitor cells in patients with cardiovascular risk and coronary artery disease. *Atherosclerosis* **181**, 305-310 (2005).
275. Schlager, O. *et al.* Exercise training increases endothelial progenitor cells and decreases asymmetric dimethylarginine in peripheral arterial disease: a randomized controlled trial. *Atherosclerosis* **217**, 240-248 (2011).
276. Van Craenenbroeck, E.M. *et al.* The effect of acute exercise on endothelial progenitor cells is attenuated in chronic heart failure. *Eur J Appl Physiol* **111**, 2375-2379 (2011).
277. Valgimigli, M. *et al.* CD34+ and endothelial progenitor cells in patients with various degrees of congestive heart failure. *Circulation* **110**, 1209-1212 (2004).
278. Tan, Q., Li, Y. & Guo, Y. Exercise Training Improves Functions of Endothelial Progenitor Cells in Patients with Metabolic Syndrome. *Arquivos Brasileiros de Cardiologia* **117**, 108-117 (2021).
279. Xia, W.H. *et al.* Physical exercise attenuates age-associated reduction in endothelium-reparative capacity of endothelial progenitor cells by increasing CXCR4/JAK-2 signaling in healthy men. *Aging cell* **11**, 111-119 (2012).
280. Erbs, S. *et al.* Exercise training in patients with advanced chronic heart failure (NYHA IIIb) promotes restoration of peripheral vasomotor function, induction of endogenous regeneration, and improvement of left ventricular function. *Circulation: Heart Failure* **3**, 486-494 (2010).
281. Adams, V. *et al.* Adiponectin promotes the migration of circulating angiogenic cells through p38-mediated induction of the CXCR4 receptor. *International journal of cardiology* **167**, 2039-2046 (2013).
282. Cesari, F. *et al.* Impact of a cardiac rehabilitation program and inflammatory state on endothelial progenitor cells in acute coronary syndrome patients. *International journal of cardiology* **167**, 1854-1859 (2013).
283. Eleuteri, E. *et al.* Aerobic training and angiogenesis activation in patients with stable chronic heart failure: a preliminary report. *Biomarkers* **18**, 418-424 (2013).
284. Mezzani, A. *et al.* Speeding of pulmonary VO2 on-kinetics by light-to-moderate-intensity aerobic exercise training in chronic heart failure: clinical and pathophysiological correlates. *International journal of cardiology* **167**, 2189-2195 (2013).
285. Kourek, C. *et al.* The acute and long-term effects of a cardiac rehabilitation program on endothelial progenitor cells in chronic heart failure patients: Comparing two different exercise training protocols. *IJC Heart & Vasculature* **32**, 100702 (2021).
286. Ma, C. *et al.* Moderate exercise enhances endothelial progenitor cell exosomes release and function. *Medicine and science in sports and exercise* **50**, 2024-2032 (2018).
287. Frühbeis, C., Helmig, S., Tug, S., Simon, P. & Krämer-Albers, E.-M. Physical exercise induces rapid release of small extracellular vesicles into the circulation. *Journal of extracellular vesicles* **4**, 28239 (2015).
288. Li, X. *et al.* Exosomes derived from endothelial progenitor cells attenuate vascular repair and accelerate reendothelialization by enhancing endothelial function. *Cytotherapy* **18**, 253-262 (2016).
289. Wu, K. *et al.* The effects of microvesicles on endothelial progenitor cells are compromised in type 2 diabetic patients via downregulation of the miR-126/VEGFR2 pathway. *American Journal of Physiology-Endocrinology and Metabolism* **310**, E828-E837 (2016).
290. Cantaluppi, V. *et al.* Microvesicles derived from endothelial progenitor cells protect the kidney from ischemia–reperfusion injury by microRNA-dependent reprogramming of resident renal cells. *Kidney international* **82**, 412-427 (2012).
291. Wang, Y. *et al.* MicroRNA-126 attenuates palmitate-induced apoptosis by targeting TRAF7 in HUVECs. *Molecular and cellular biochemistry* **399**, 123-130 (2015).
292. Fish, J.E. *et al.* miR-126 regulates angiogenic signaling and vascular integrity. *Developmental cell* **15**, 272-284 (2008).
293. Williamson, W. *et al.* Trial of exercise to prevent HypeRtension in young adults (TEPHRA) a randomized controlled trial: study protocol. *BMC cardiovascular disorders* **18**, 1-16 (2018).
294. Nguyen, Q.C. *et al.* Discordance in national estimates of hypertension among young adults. *Epidemiology (Cambridge, Mass.)* **22**, 532 (2011).

295. Zhang, Y. *et al.* Associations of Blood Pressure and Cholesterol Levels During Young Adulthood With Later Cardiovascular Events. *Journal of the American College of Cardiology* **74**, 330 (2019).
296. Chen, V. *et al.* Lifetime Risks for Hypertension by Contemporary Guidelines in African American and White Men and Women. *JAMA Cardiology* **4**, 455-459 (2019).
297. Yano, Y. *et al.* Association of Blood Pressure Classification in Young Adults Using the 2017 American College of Cardiology/American Heart Association Blood Pressure Guideline With Cardiovascular Events Later in LifeAssociation Between Young Adult Hypertension and Cardiovascular Events in Middle AgeAssociation Between Young Adult Hypertension and Cardiovascular Events in Middle Age. *JAMA* **320**, 1774-1782 (2018).
298. Carson April, P. *et al.* Evaluating the Framingham Hypertension Risk Prediction Model in Young Adults. *Hypertension* **62**, 1015-1020 (2013).
299. Sheppard, J.P. *et al.* Benefits and Harms of Antihypertensive Treatment in Low-Risk Patients With Mild HypertensionBenefits and Harms of Antihypertensive Treatment in Low-Risk Patients With Mild HypertensionBenefits and Harms of Antihypertensive Treatment in Low-Risk Patients With Mild Hypertension. *JAMA Internal Medicine* **178**, 1626-1634 (2018).
300. Whelton Paul, K. *et al.* 2017 ACC/AHA/AAPA/ABC/ACPM/AGS/APhA/ASH/ASPC/NMA/PCNA Guideline for the Prevention, Detection, Evaluation, and Management of High Blood Pressure in Adults: Executive Summary: A Report of the American College of Cardiology/American Heart Association Task Force on Clinical Practice Guidelines. *Hypertension* **71**, 1269-1324 (2018).
301. Kajantie, E. & Hovi, P. Is very preterm birth a risk factor for adult cardiometabolic disease? *Seminars in fetal & neonatal medicine* **19**, 112-117 (2014).
302. de Jong, F., Monuteaux, M.C., van Elburg, R.M., Gillman, M.W. & Belfort, M.B. Systematic review and meta-analysis of preterm birth and later systolic blood pressure. *Hypertension* **59**, 226-234 (2012).
303. Davis, E.F. *et al.* Cardiovascular risk factors in children and young adults born to preeclamptic pregnancies: a systematic review. *Pediatrics* **129**, e1552-1561 (2012).
304. Crump, C., Winkleby, M.a., Sundquist, K. & Sundquist, J. Risk of hypertension among young adults who were born preterm: a Swedish national study of 636,000 births. *American journal of epidemiology* **173**, 797-803 (2011).
305. Bonamy, A.-K.E., Källén, K. & Norman, M. High blood pressure in 2.5-year-old children born extremely preterm. *Pediatrics* **129**, e1199-1204 (2012).
306. Lewandowski, A.J. *et al.* Elevated blood pressure in preterm-born offspring associates with a distinct antiangiogenic state and microvascular abnormalities in adult life. *Hypertension* **65**, 607-614 (2015).
307. Lewandowski, A.J. *et al.* Preterm heart in adult life: cardiovascular magnetic resonance reveals distinct differences in left ventricular mass, geometry, and function. *Circulation* **127**, 197-206 (2013).
308. Davis, E.F. *et al.* Clinical cardiovascular risk during young adulthood in offspring of hypertensive pregnancies: insights from a 20-year prospective follow-up birth cohort. *BMJ Open* **5**, e008136 (2015).
309. Smadja, D.M. *et al.* Standardization of methods to quantify and culture endothelial colony-forming cells derived from peripheral blood: Position paper from the International Society on Thrombosis and Haemostasis SSC. *Journal of thrombosis and haemostasis: JTH* **17**, 1190 (2019).
310. Lapidos, K.A., Sprague, S.M. & Ameer, G.A. Impact of serum source and inflammatory cytokines on the isolation of endothelial colony-forming cells from peripheral blood. *Journal of tissue engineering and regenerative medicine* **8**, 747-756 (2014).
311. van de Pol, V. *et al.* Endothelial colony forming cells as an autologous model to study endothelial dysfunction in patients with a bicuspid aortic valve. *International journal of molecular sciences* **20**, 3251 (2019).
312. Holman, R. *et al.* A calculator for HOMA. *Diabetologia* **47**, A222 (2004).
313. Wessel, D.m. & Flügge, U. A method for the quantitative recovery of protein in dilute solution in the presence of detergents and lipids. *Analytical biochemistry* **138**, 141-143 (1984).
314. Davis, S. *et al.* Expanding proteome coverage with CHarge Ordered Parallel Ion aNalysis (CHOPIN) combined with broad specificity proteolysis. *Journal of proteome research* **16**, 1288-1299 (2017).
315. Zhou, Y. *et al.* Metascape provides a biologist-oriented resource for the analysis of systems-level datasets. *Nature communications* **10**, 1-10 (2019).
316. Nolte, H., MacVicar, T.D., Tellkamp, F. & Krüger, M. Instant Clue: A Software Suite for Interactive Data Visualization and Analysis. *Scientific Reports* **8**, 12648 (2018).

317. Yu, G.Z. *et al.* Association of Maternal Antiangiogenic Profile at Birth With Early Postnatal Loss of Microvascular Density in Offspring of Hypertensive Pregnancies. *Hypertension (Dallas, Tex. : 1979)* **68**, 749-759 (2016).
318. Bertagnolli, M., Nuyt, A.M., Thébaud, B. & Luu, T.M. Endothelial progenitor cells as prognostic markers of preterm birth-associated complications. *Stem cells translational medicine* **6**, 7-13 (2017).
319. Lee, S.H. *et al.* Hypoxia accelerates vascular repair of endothelial colony-forming cells on ischemic injury via STAT3-BCL3 axis. *Stem cell research & therapy* **6**, 1-13 (2015).
320. Tsukada, S. *et al.* Identification of mouse colony-forming endothelial progenitor cells for postnatal neovascularization: a novel insight highlighted by new mouse colony-forming assay. *Stem cell research & therapy* **4**, 1-13 (2013).
321. Critser, P.J. & Yoder, M.C. Endothelial colony forming cell role in neoangiogenesis and tissue repair. *Current opinion in organ transplantation* **15**, 68 (2010).
322. Giurgiu, M. *et al.* CORUM: the comprehensive resource of mammalian protein complexes—2019. *Nucleic acids research* **47**, D559-D563 (2019).
323. Cline, M.S. *et al.* Integration of biological networks and gene expression data using Cytoscape. *Nature protocols* **2**, 2366-2382 (2007).
324. Kutikhin, A.G. *et al.* Human Peripheral Blood-Derived Endothelial Colony-Forming Cells Are Highly Similar to Mature Vascular Endothelial Cells yet Demonstrate a Transitional Transcriptomic Signature. *Cells* **9**, 876 (2020).
325. Carty, D., Schiffer, E. & Delles, C. Proteomics in hypertension. *Journal of Human Hypertension* **27**, 211-216 (2013).
326. Berezin, A.E. & Berezin, A.A. Extracellular endothelial cell-derived vesicles: emerging role in cardiac and vascular remodeling in heart failure. *Frontiers in cardiovascular medicine* **7**, 47 (2020).
327. Nightingale, T. & Cutler, D. The secretion of von W illebrand factor from endothelial cells; an increasingly complicated story. *Journal of thrombosis and haemostasis* **11**, 192-201 (2013).
328. Lowenstein, C.J., Morrell, C.N. & Yamakuchi, M. Regulation of Weibel–Palade body exocytosis. *Trends in cardiovascular medicine* **15**, 302-308 (2005).
329. Spiel, A.O., Gilbert, J.C. & Jilma, B. von Willebrand factor in cardiovascular disease: focus on acute coronary syndromes. *Circulation* **117**, 1449-1459 (2008).
330. Fan, M. *et al.* Prognostic value of plasma von Willebrand factor levels in major adverse cardiovascular events: a systematic review and meta-analysis. *BMC cardiovascular disorders* **20**, 72 (2020).
331. Zhang, X. *et al.* Endothelial cell dysfunction and glycocalyx–A vicious circle. *Matrix Biology* **71**, 421-431 (2018).
332. Gai, C., Carpanetto, A., Deregibus, M.C. & Camussi, G. Extracellular vesicle-mediated modulation of angiogenesis. (2016).
333. Schorey, J.S. & Harding, C.V. Extracellular vesicles and infectious diseases: new complexity to an old story. *The Journal of clinical investigation* **126**, 1181-1189 (2016).
334. Tracy, L.E., Minasian, R.A. & Caterson, E. Extracellular matrix and dermal fibroblast function in the healing wound. *Advances in wound care* **5**, 119-136 (2016).
335. Dawson, D.W. *et al.* CD36 mediates the in vitro inhibitory effects of thrombospondin-1 on endothelial cells. *The Journal of cell biology* **138**, 707-717 (1997).
336. Liu, A., Mosher, D.F., Murphy-Ullrich, J.E. & Goldblum, S.E. The counteradhesive proteins, thrombospondin 1 and SPARC/osteonectin, open the tyrosine phosphorylation-responsive paracellular pathway in pulmonary vascular endothelia. *Microvascular research* **77**, 13-20 (2009).
337. Kupprion, C., Motamed, K. & Sage, E.H. SPARC (BM-40, osteonectin) inhibits the mitogenic effect of vascular endothelial growth factor on microvascular endothelial cells. *Journal of Biological Chemistry* **273**, 29635-29640 (1998).
338. Niewiarowska, J. *et al.* Lumican inhibits angiogenesis by interfering with α2β1 receptor activity and downregulating MMP-14 expression. *Thrombosis research* **128**, 452-457 (2011).
339. Williams, K.E., Fulford, L.A. & Albig, A.R. Lumican reduces tumor growth via induction of fas-mediated endothelial cell apoptosis. *Cancer Microenvironment* **4**, 115-126 (2011).
340. Presta, M., Foglio, E., Churruca Schuind, A. & Ronca, R. Long Pentraxin-3 modulates the angiogenic activity of fibroblast growth factor-2. *Frontiers in immunology* **9**, 2327 (2018).
341. Rusnati, M. *et al.* Selective recognition of fibroblast growth factor-2 by the long pentraxin PTX3 inhibits angiogenesis. *Blood* **104**, 92-99 (2004).

342. Tamura, Y. *et al.* Human pentraxin 3 (PTX3) as a novel biomarker for the diagnosis of pulmonary arterial hypertension. *PloS one* **7** (2012).
343. Peri, G. *et al.* PTX3, A prototypical long pentraxin, is an early indicator of acute myocardial infarction in humans. *Circulation* **102**, 636-641 (2000).
344. Suzuki, S. *et al.* Pentraxin 3, a new marker for vascular inflammation, predicts adverse clinical outcomes in patients with heart failure. *American heart journal* **155**, 75-81 (2008).
345. Rolph, M.S. *et al.* Production of the long pentraxin PTX3 in advanced atherosclerotic plaques. *Arteriosclerosis, thrombosis, and vascular biology* **22**, e10-e14 (2002).
346. Duong, H.T. *et al.* Pulmonary artery endothelium resident endothelial colony-forming cells in pulmonary arterial hypertension. *Pulmonary circulation* **1**, 475-486 (2011).
347. Ward, M.R., Stewart, D.J. & Kutryk, M.J. Endothelial progenitor cell therapy for the treatment of coronary disease, acute MI, and pulmonary arterial hypertension: current perspectives. *Catheterization and cardiovascular interventions* **70**, 983-998 (2007).
348. Berezin, A.E. & Kremzer, A.A. Circulating endothelial progenitor cells as markers for severity of ischemic chronic heart failure. *Journal of cardiac failure* **20**, 438-447 (2014).
349. Sargento-Freitas, J. *et al.* Endothelial Progenitor Cells influence acute and subacute stroke hemodynamics. *J Neurol Sci* **385**, 119-125 (2018).
350. MacEneaney, O.J. *et al.* Endothelial progenitor cell number and colony-forming capacity in overweight and obese adults. *International journal of obesity* **33**, 219-225 (2009).
351. Tobler, K. *et al.* Reduction of both number and proliferative activity of human endothelial progenitor cells in obesity. *International Journal of Obesity* **34**, 687-700 (2010).
352. Müller-Ehmsen, J. *et al.* Decreased number of circulating progenitor cells in obesity: beneficial effects of weight reduction. *European heart journal* **29**, 1560-1568 (2008).
353. Rossi, F. *et al.* HDL cholesterol is a strong determinant of endothelial progenitor cells in hypercholesterolemic subjects. *Microvascular research* **80**, 274-279 (2010).
354. MacEneaney, O.J. *et al.* Endothelial progenitor cell function, apoptosis, and telomere length in overweight/obese humans. *Obesity* **18**, 1677-1682 (2010).
355. Wang, J.J. *et al.* Retinal vascular calibre and the risk of coronary heart disease-related death. *Heart* **92**, 1583-1587 (2006).
356. Lundberg, K. *et al.* Retinal vascular diameters in relation to physical activity in Danish children - The CHAMPS Eye Study. *Scand J Med Sci Sports* **28**, 1897-1907 (2018).
357. Noon, J.P. *et al.* Impaired microvascular dilatation and capillary rarefaction in young adults with a predisposition to high blood pressure. *The Journal of clinical investigation* **99**, 1873-1879 (1997).
358. Antonios, T.F., Singer, D.R., Markandu, N.D., Mortimer, P.S. & MacGregor, G.A. Rarefaction of skin capillaries in borderline essential hypertension suggests an early structural abnormality. *Hypertension* **34**, 655-658 (1999).
359. Antonios, T. *et al.* Rarefaction of skin capillaries in normotensive offspring of individuals with essential hypertension. *Heart* **89**, 175-178 (2003).
360. Antonios, T.F., Singer, D.R., Markandu, N.D., Mortimer, P.S. & MacGregor, G.A. Structural skin capillary rarefaction in essential hypertension. *Hypertension* **33**, 998-1001 (1999).
361. Williams, S. *et al.* Capillary hypertension and abnormal pressure dynamics in patients with essential hypertension. *Clinical Science* **79**, 5-8 (1990).
362. Shore, A.C. Capillaroscopy and the measurement of capillary pressure. *British journal of clinical pharmacology* **50**, 501-513 (2000).
363. Angouras, D. *et al.* Effect of impaired vasa vasorum flow on the structure and mechanics of the thoracic aorta: implications for the pathogenesis of aortic dissection. *European journal of cardio-thoracic surgery* **17**, 468-473 (2000).
364. Halcox, J.P. *et al.* Prognostic value of coronary vascular endothelial dysfunction. *Circulation* **106**, 653-658 (2002).
365. Ott, C., Raff, U., Harazny, J.M., Michelson, G. & Schmieder, R.E. Central pulse pressure is an independent determinant of vascular remodeling in the retinal circulation. *Hypertension* **61**, 1340-1345 (2013).
366. Muiesan, M.L. *et al.* Pulsatile hemodynamics and microcirculation: evidence for a close relationship in hypertensive patients. *Hypertension* **61**, 130-136 (2013).
367. Hanssen, H. *et al.* Exercise-induced alterations of retinal vessel diameters and cardiovascular risk reduction in obesity. *Atherosclerosis* **216**, 433-439 (2011).

368. Boardman, H. *et al.* Aortic stiffness and blood pressure variability in young people: a multimodality investigation of central and peripheral vasculature. *Journal of hypertension* **35**, 513 (2017).
369. Lewandowski, A.J., Pitcher, A., Banerjee, R. & Leeson, P. Arterial stiffness: using simple surrogate measures to make sense of a biologically complex phenomenon. *Hypertension Research* **35**, 155-156 (2012).
370. Eden, E., Navon, R., Steinfeld, I., Lipson, D. & Yakhini, Z. GOrilla: a tool for discovery and visualization of enriched GO terms in ranked gene lists. *BMC bioinformatics* **10**, 1-7 (2009).
371. Vion, A.-C. *et al.* Shear stress regulates endothelial microparticle release. *Circulation research* **112**, 1323-1333 (2013).
372. Tian, S. *et al.* Shear stress inhibits apoptosis of ischemic brain microvascular endothelial cells. *International journal of molecular sciences* **14**, 1412-1427 (2013).
373. dela Paz, N.G., Walshe, T.E., Leach, L.L., Saint-Geniez, M. & D'Amore, P.A. Role of shear-stress-induced VEGF expression in endothelial cell survival. *Journal of cell science* **125**, 831-843 (2012).
374. Delles, C., Carrick, E., Graham, D. & Nicklin, S.A. Utilizing proteomics to understand and define hypertension: where are we and where do we go? *Expert review of proteomics* **15**, 581-592 (2018).
375. Delles, C., Neisius, U. & Carty, D.M. Proteomics in hypertension and other cardiovascular diseases. *Annals of medicine* **44**, S55-S64 (2012).
376. Chew, S.K., Xie, J. & Wang, J.J. Retinal arteriolar diameter and the prevalence and incidence of hypertension: a systematic review and meta-analysis of their association. *Current hypertension reports* **14**, 144-151 (2012).
377. Chen, Z.-Z. & Gerszten, R.E. Metabolomics and proteomics in type 2 diabetes. *Circulation research* **126**, 1613-1627 (2020).
378. Dignat-George, F. & Boulanger, C.M. The many faces of endothelial microparticles. *Arteriosclerosis, thrombosis, and vascular biology* **31**, 27-33 (2011).
379. Koga, H. *et al.* Elevated levels of VE-cadherin-positive endothelial microparticles in patients with type 2 diabetes mellitus and coronary artery disease. *Journal of the American College of Cardiology* **45**, 1622-1630 (2005).
380. Jansen, F., Nickenig, G. & Werner, N. Extracellular vesicles in cardiovascular disease: potential applications in diagnosis, prognosis, and epidemiology. *Circulation research* **120**, 1649-1657 (2017).
381. Dignat-George, F. & Boulanger Chantal, M. The Many Faces of Endothelial Microparticles. *Arteriosclerosis, Thrombosis, and Vascular Biology* **31**, 27-33 (2011).
382. Li, M., Tan, Y., Stenmark, K.R. & Tan, W. High pulsatility flow induces acute endothelial inflammation through overpolarizing cells to activate NF-κB. *Cardiovascular engineering and technology* **4**, 26-38 (2013).
383. Akbar, N. *et al.* Rapid neutrophil mobilisation by VCAM-1+ endothelial extracellular vesicles. *Cardiovascular Research*, cvac012 (2022).
384. Boulanger, C.M., Loyer, X., Rautou, P.-E. & Amabile, N. Extracellular vesicles in coronary artery disease. *Nature reviews cardiology* **14**, 259-272 (2017).
385. Jansen, F. *et al.* Intercellular transfer of miR-126-3p by endothelial microparticles reduces vascular smooth muscle cell proliferation and limits neointima formation by inhibiting LRP6. *Journal of molecular and cellular cardiology* **104**, 43-52 (2017).
386. Jansen, F. *et al.* Endothelial microparticle–mediated transfer of microRNA-126 promotes vascular endothelial cell repair via SPRED1 and is abrogated in glucose-damaged endothelial microparticles. *Circulation* **128**, 2026-2038 (2013).
387. Ranghino, A. *et al.* Endothelial progenitor cell-derived microvesicles improve neovascularization in a murine model of hindlimb ischemia. *Int J Immunopathol Pharmacol* **25**, 75-85 (2012).
388. Zhang, J. *et al.* Exosomes derived from human endothelial progenitor cells accelerate cutaneous wound healing by promoting angiogenesis through Erk1/2 signaling. *International journal of biological sciences* **12**, 1472 (2016).
389. Li, X., Jiang, C. & Zhao, J. Human endothelial progenitor cells-derived exosomes accelerate cutaneous wound healing in diabetic rats by promoting endothelial function. *Journal of Diabetes and its Complications* **30**, 986-992 (2016).
390. Schuster, J., Cheng, S.B., Padbury, J. & Sharma, S. Placental extracellular vesicles and pre-eclampsia. *American Journal of Reproductive Immunology* **85**, e13297 (2021).
391. Ou, Z.-J. *et al.* Endothelium-derived microparticles inhibit angiogenesis in the heart and enhance the inhibitory effects of hypercholesterolemia on angiogenesis. *American Journal of Physiology-Endocrinology and Metabolism* **300**, E661-E668 (2011).

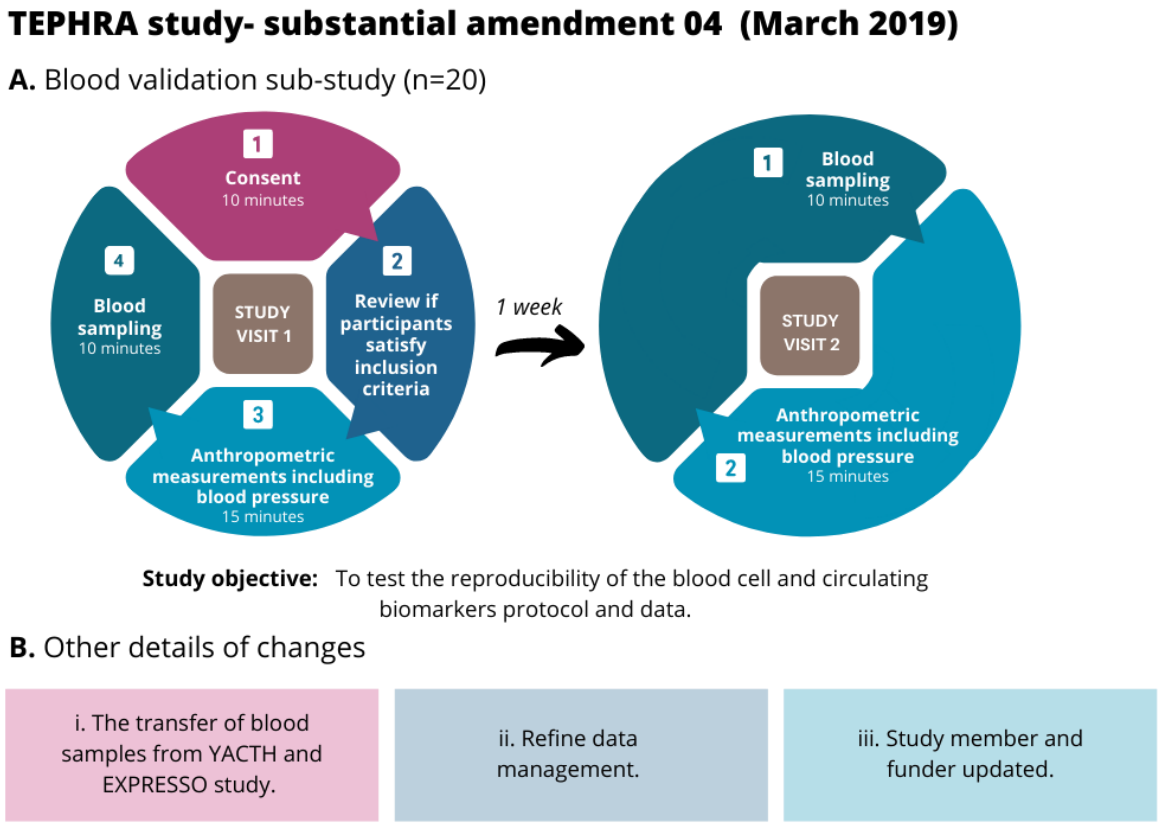
392. Ramakrishnan, D.P., Hajj-Ali, R.A., Chen, Y. & Silverstein, R.L. Extracellular vesicles activate a CD36-dependent signaling pathway to inhibit microvascular endothelial cell migration and tube formation. *Arteriosclerosis, thrombosis, and vascular biology* **36**, 534-544 (2016).
393. Giubellino, A., Burke, T.R. & Bottaro, D.P. Grb2 signaling in cell motility and cancer. *Expert opinion on therapeutic targets* **12**, 1021-1033 (2008).
394. Salameh, A., Galvagni, F., Bardelli, M., Bussolino, F. & Oliviero, S. Direct recruitment of CRK and GRB2 to VEGFR-3 induces proliferation, migration, and survival of endothelial cells through the activation of ERK, AKT, and JNK pathways. *Blood* **106**, 3423-3431 (2005).
395. Kroll, J. & Waltenberger, J. The vascular endothelial growth factor receptor KDR activates multiple signal transduction pathways in porcine aortic endothelial cells. *Journal of Biological Chemistry* **272**, 32521-32527 (1997).
396. Baizabal-Aguirre, V.M., Rosales, C., López-Macías, C. & Gómez, M.I., Vol. 2016 (Hindawi, 2016).
397. Rubinfeld, H. & Seger, R. The ERK cascade. *Molecular biotechnology* **31**, 151-174 (2005).
398. Hsueh, W.A. & Quiñones, M.J. Role of endothelial dysfunction in insulin resistance. *The American journal of cardiology* **92**, 10-17 (2003).
399. Montagnani, M. *et al.* Inhibition of phosphatidylinositol 3-kinase enhances mitogenic actions of insulin in endothelial cells. *Journal of Biological Chemistry* **277**, 1794-1799 (2002).
400. Proctor, B.M. *et al.* Grb2 is required for atherosclerotic lesion formation. *Arteriosclerosis, thrombosis, and vascular biology* **27**, 1361-1367 (2007).
401. Yang, Y. *et al.* Protective effects of dioscin on vascular remodeling in pulmonary arterial hypertension via adjusting GRB2/ERK/PI3K-AKT signal. *Biomedicine & Pharmacotherapy* **133**, 111056 (2021).
402. McDonald, C.B. *et al.* Bivalent binding drives the formation of the Grb2–Gab1 signaling complex in a noncooperative manner. *The FEBS journal* **279**, 2156-2173 (2012).
403. Zhao, J. *et al.* Endothelial Grb2-associated binder 1 is crucial for postnatal angiogenesis. *Arteriosclerosis, thrombosis, and vascular biology* **31**, 1016-1023 (2011).
404. Kondreddy, V., Magisetty, J., Keshava, S., Rao, L.V.M. & Pendurthi, U.R. Gab2 (Grb2-Associated Binder2) Plays a Crucial Role in Inflammatory Signaling and Endothelial Dysfunction. *Arteriosclerosis, thrombosis, and vascular biology* **41**, 1987-2005 (2021).
405. Ikram, M.K. *et al.* Retinal vessel diameters and risk of impaired fasting glucose or diabetes: the Rotterdam study. *Diabetes* **55**, 506-510 (2006).
406. Gepstein, R. *et al.* Association of retinal microvascular caliber with blood pressure levels. *Blood pressure* **21**, 191-196 (2012).
407. Wong, T.Y. *et al.* Retinal microvascular abnormalities and their relationship with hypertension, cardiovascular disease, and mortality. *Survey of ophthalmology* **46**, 59-80 (2001).
408. Aissopou, E.K. *et al.* Ambulatory aortic stiffness is associated with narrow retinal arteriolar caliber in hypertensives: the SAFAR study. *American journal of hypertension* **29**, 626-633 (2016).
409. Daien, V. *et al.* Retinal vascular caliber associated with cardiac and renal target organ damage in never-treated hypertensive patients. *Microcirculation* **24**, e12344 (2017).
410. Wang, S.B. *et al.* A spectrum of retinal vasculature measures and coronary artery disease. *Atherosclerosis* **268**, 215-224 (2018).
411. Yatsuya, H. *et al.* Retinal microvascular abnormalities and risk of lacunar stroke: Atherosclerosis Risk in Communities Study. *Stroke* **41**, 1349-1355 (2010).
412. Liew, G. *et al.* Measurement of retinal vascular caliber: issues and alternatives to using the arteriole to venule ratio. *Investigative ophthalmology & visual science* **48**, 52-57 (2007).
413. Klein, R., Klein, B.E., Knudtson, M.D., Wong, T.Y. & Tsai, M.Y. Are inflammatory factors related to retinal vessel caliber?: The Beaver Dam Eye Study. *Archives of ophthalmology* **124**, 87-94 (2006).
414. Yim-Lui Cheung, C. *et al.* C-reactive protein and retinal microvascular caliber in a multiethnic asian population. *American journal of epidemiology* **171**, 206-213 (2010).
415. Stewart, D.J., Levy, R.D., Cernacek, P. & Langleben, D. Increased plasma endothelin-1 in pulmonary hypertension: marker or mediator of disease? *Annals of internal medicine* **114**, 464-469 (1991).
416. Christman, B.W. *et al.* An imbalance between the excretion of thromboxane and prostacyclin metabolites in pulmonary hypertension. *New England Journal of Medicine* **327**, 70-75 (1992).
417. Tu, L. *et al.* Autocrine fibroblast growth factor-2 signaling contributes to altered endothelial phenotype in pulmonary hypertension. *American journal of respiratory cell and molecular biology* **45**, 311-322 (2011).

418. Dai, Z. *et al.* Endothelial and smooth muscle cell interaction via FoxM1 signaling mediates vascular remodeling and pulmonary hypertension. *American journal of respiratory and critical care medicine* **198**, 788-802 (2018).
419. Dellett, M. *et al.* MicroRNA-containing extracellular vesicles released from endothelial colony-forming cells modulate angiogenesis during ischaemic retinopathy. *Journal of cellular and molecular medicine* **21**, 3405-3419 (2017).
420. Liao, D. *et al.* Arterial Stiffness and the Development of Hypertension. *Hypertension* **34**, 201-206 (1999).
421. Carmeliet, P. & Jain, R.K. Molecular mechanisms and clinical applications of angiogenesis. *Nature* **473**, 298-307 (2011).
422. Simons, M., Gordon, E. & Claesson-Welsh, L. Mechanisms and regulation of endothelial VEGF receptor signalling. *Nature reviews Molecular cell biology* **17**, 611-625 (2016).
423. Holmes, K., Roberts, O.L., Thomas, A.M. & Cross, M.J. Vascular endothelial growth factor receptor-2: structure, function, intracellular signalling and therapeutic inhibition. *Cellular signalling* **19**, 2003-2012 (2007).
424. Sack, K.D., Teran, M. & Nugent, M.A. Extracellular matrix stiffness controls VEGF signaling and processing in endothelial cells. *Journal of cellular physiology* **231**, 2026-2039 (2016).
425. Mitsi, M., Forsten-Williams, K., Gopalakrishnan, M. & Nugent, M.A. A catalytic role of heparin within the extracellular matrix. *Journal of Biological Chemistry* **283**, 34796-34807 (2008).
426. Smith, M.L. *et al.* Force-induced unfolding of fibronectin in the extracellular matrix of living cells. *PLoS biology* **5**, e268 (2007).
427. Antia, M., Baneyx, G., Kubow, K.E. & Vogel, V. Fibronectin in aging extracellular matrix fibrils is progressively unfolded by cells and elicits an enhanced rigidity response. *Faraday discussions* **139**, 229-249 (2008).
428. Wang, J.J. *et al.* Retinal vessel diameter and cardiovascular mortality: pooled data analysis from two older populations. *European heart journal* **28**, 1984-1992 (2007).
429. Gong, M. & Hubner, N. Molecular genetics of human hypertension. *Clinical Science* **110**, 315-326 (2006).
430. Franceschini, N. & Le, T.H. Genetics of hypertension: discoveries from the bench to human populations. *American Journal of Physiology-Renal Physiology* **306**, F1-F11 (2014).
431. Elmer, P.J. *et al.* Effects of comprehensive lifestyle modification on diet, weight, physical fitness, and blood pressure control: 18-month results of a randomized trial. *Annals of internal medicine* **144**, 485-495 (2006).
432. Dusek, J.A. *et al.* Stress management versus lifestyle modification on systolic hypertension and medication elimination: a randomized trial. *The journal of alternative and complementary medicine* **14**, 129-138 (2008).
433. Lee, I.-M. *et al.* Effect of physical inactivity on major non-communicable diseases worldwide: an analysis of burden of disease and life expectancy. *The lancet* **380**, 219-229 (2012).
434. Kyu, H.H. *et al.* Physical activity and risk of breast cancer, colon cancer, diabetes, ischemic heart disease, and ischemic stroke events: systematic review and dose-response meta-analysis for the Global Burden of Disease Study 2013. *bmj* **354** (2016).
435. Bakker, E.A., Sui, X., Brellenthin, A.G. & Lee, D.-c. Physical activity and fitness for the prevention of hypertension. *Current Opinion in Cardiology* **33**, 394-401 (2018).
436. Pagonas, N. *et al.* The impact of aerobic exercise on blood pressure variability. *Journal of human hypertension* **28**, 367-371 (2014).
437. Robbins, J.M. *et al.* Human plasma proteomic profiles indicative of cardiorespiratory fitness. *Nature metabolism* **3**, 786-797 (2021).
438. Hawkins, M.N., Raven, P.B., Snell, P.G., Stray-Gundersen, J. & Levine, B.D. Maximal oxygen uptake as a parametric measure of cardiorespiratory capacity. *Medicine and science in sports and exercise* **39**, 103-107 (2007).
439. Ross, R. *et al.* Importance of assessing cardiorespiratory fitness in clinical practice: a case for fitness as a clinical vital sign: a scientific statement from the American Heart Association. *Circulation* **134**, e653-e699 (2016).
440. Myers, J. *et al.* Exercise capacity and mortality among men referred for exercise testing. *New England journal of medicine* **346**, 793-801 (2002).

441. Schmidt-Lucke, C. *et al.* Reduced number of circulating endothelial progenitor cells predicts future cardiovascular events: proof of concept for the clinical importance of endogenous vascular repair. *Circulation* **111**, 2981-2987 (2005).
442. Ribeiro, F. *et al.* Effects of exercise training on endothelial progenitor cells in cardiovascular disease: a systematic review. *American Journal of Physical Medicine & Rehabilitation* **92**, 1020-1030 (2013).
443. Huckstep, O.J. *et al.* Physiological stress elicits impaired left ventricular function in preterm-born adults. *Journal of the American College of Cardiology* **71**, 1347-1356 (2018).
444. Waclawovsky, G., Pedralli, M.L., Eibel, B., Schaun, M.I. & Lehnen, A.M. Effects of different types of exercise training on endothelial function in prehypertensive and hypertensive individuals: a systematic review. *Arquivos brasileiros de cardiologia* **116**, 938-947 (2021).
445. Pedralli, M.L. *et al.* Different exercise training modalities produce similar endothelial function improvements in individuals with prehypertension or hypertension: A randomized clinical trial. *Scientific reports* **10**, 1-9 (2020).
446. Boeno, F.P. *et al.* Effect of aerobic and resistance exercise training on inflammation, endothelial function and ambulatory blood pressure in middle-aged hypertensive patients. *Journal of Hypertension* **38**, 2501-2509 (2020).
447. Tahir, E. *et al.* Myocardial Fibrosis in Competitive Triathletes Detected by Contrast-Enhanced CMR Correlates With Exercise-Induced Hypertension and Competition History. *JACC: Cardiovascular Imaging* **11**, 1260-1270 (2018).
448. Vongpatanasin, W. *et al.* Functional sympatholysis is impaired in hypertensive humans. *J Physiol-London* **589**, 1209-1220 (2011).
449. Werner, N. *et al.* Endothelial progenitor cells correlate with endothelial function in patients with coronary artery disease. *Basic Res Cardiol* **102**, 565-571 (2007).
450. Clementi, E., Brown, G.C., Foxwell, N. & Moncada, S. On the mechanism by which vascular endothelial cells regulate their oxygen consumption. *Proceedings of the National Academy of Sciences* **96**, 1559-1562 (1999).
451. Victor, V.M. *et al.* Regulation of oxygen distribution in tissues by endothelial nitric oxide. *Circulation research* **104**, 1178-1183 (2009).
452. Eelen, G. *et al.* Endothelial cell metabolism. *Physiological reviews* **98**, 3-58 (2018).
453. Alhayaza, R., Haque, E., Karbasiafshar, C., Sellke, F.W. & Abid, M.R. The relationship between reactive oxygen species and endothelial cell metabolism. *Frontiers in Chemistry*, 1043 (2020).
454. Yu, G.Z. *et al.* Association of Maternal Antiangiogenic Profile at Birth With Early Postnatal Loss of Microvascular Density in Offspring of Hypertensive Pregnancies. *Hypertension* **68**, 749-759 (2016).
455. Lewandowski, A.J. *et al.* Elevated Blood Pressure in Preterm-Born Offspring Associates With a Distinct Antiangiogenic State and Microvascular Abnormalities in Adult Life. *Hypertension* **65**, 607-614 (2015).
456. Lewandowski, A.J. *et al.* Right ventricular systolic dysfunction in young adults born preterm. *Circulation* **128**, 713-720 (2013).
457. Davis, E.F. *et al.* Pre-eclampsia and offspring cardiovascular health: mechanistic insights from experimental studies. *Clinical science* **123**, 53-72 (2012).
458. Aye, C.Y.L. *et al.* Disproportionate cardiac hypertrophy during early postnatal development in infants born preterm. *Pediatr Res* **82**, 36-46 (2017).
459. Turbeville, H.R. & Sasser, J.M. Preeclampsia beyond pregnancy: Long-term consequences for mother and child. *American Journal of Physiology-Renal Physiology* **318**, F1315-F1326 (2020).
460. Agatisa, P.K. *et al.* Impairment of endothelial function in women with a history of preeclampsia: an indicator of cardiovascular risk. *American Journal of Physiology-Heart and Circulatory Physiology* **286**, H1389-H1393 (2004).
461. Kvehaugen, A.S. *et al.* Endothelial function and circulating biomarkers are disturbed in women and children after preeclampsia. *Hypertension* **58**, 63-69 (2011).
462. Sandvik, M.K. *et al.* Preeclampsia in healthy women and endothelial dysfunction 10 years later. *American journal of obstetrics and gynecology* **209**, 569. e561-569. e510 (2013).
463. Bonamy, A.K., Martin, H., Jorneskog, G. & Norman, M. Lower skin capillary density, normal endothelial function and higher blood pressure in children born preterm. *Journal of internal medicine* **262**, 635-642 (2007).
464. Kublickiene, K.R., Lindblom, B., Kruger, K. & Nisell, H. Preeclampsia: evidence for impaired shear stress-mediated nitric oxide release in uterine circulation. *Am J Obstet Gynecol* **183**, 160-166 (2000).

465. Crabtree, M.J. *et al.* Quantitative regulation of intracellular endothelial nitric-oxide synthase (eNOS) coupling by both tetrahydrobiopterin-eNOS stoichiometry and biopterin redox status: insights from cells with tet-regulated GTP cyclohydrolase I expression. *J Biol Chem* **284**, 1136-1144 (2009).
466. Vasquez-Vivar, J., Martasek, P., Whitsett, J., Joseph, J. & Kalyanaraman, B. The ratio between tetrahydrobiopterin and oxidized tetrahydrobiopterin analogues controls superoxide release from endothelial nitric oxide synthase: an EPR spin trapping study. *Biochem J* **362**, 733-739 (2002).
467. Chuaiphichai, S. *et al.* Endothelial GTPCH (GTP cyclohydrolase 1) and tetrahydrobiopterin regulate gestational blood pressure, uteroplacental remodeling, and fetal growth. *Hypertension* **78**, 1871-1884 (2021).
468. Nugraha, B., Buono, M.F. & Emmert, M.Y. (Oxford University Press, 2018).
469. Giacomelli, E. *et al.* Three-dimensional cardiac microtissues composed of cardiomyocytes and endothelial cells co-differentiated from human pluripotent stem cells. *Development* **144**, 1008-1017 (2017).

Appendices



Appendix Figure 1. TEPHRA study amendment

Appendix Table 1. TEPHRA study objectives, outcome measures and measurement time-points.

Objectives to compare the effect of aerobic exercise intervention and physical activity self-monitoring versus control	**Measures**	**Time-points**		
Benefits of exercise		**Baseline**	**16 weeks**	**52 weeks**
Short-term and sustained blood pressure response	- Systolic and diastolic blood pressure measured during ambulatory blood pressure monitoring	✓	✓	✓
Cardiovascular Fitness	- CPET - Exercise stress echocardiography (subgroup)	✓	✓	✓
Physical function based on walking gait, walking cadence and global physical function.	- Measurement of physical activity (1-week activity monitor) - Gait analysis - Questionnaire	✓	✓	✓
Cardiac, cerebrovascular, hepatic remodellings and adaptations	- Cardiac echocardiography - Brain MRI - Liver MRI	✓	✓	✓ (Echo only)

Metabolic Function:	- Fasting glucose, insulin and lipid profile	✓	✓	✓
Retinal and Dermal micro-vascular structure	- Retinal imaging arteriolar and venular indices - Dermal capillary density	✓	✓	✓
Mediators of Exercise Adaptation and Blood Pressure Response		**Baseline**	**16 weeks**	**52 weeks**
Physical activity behaviours	- Objective measure of physical activity (7 day wear of activity monitor)	✓	✓	✓
Molecular endothelial and angiogenic function	- Circulatory markers of angiogenic function - ECFC colony growth and functionality - Systolic and diastolic blood pressure - CPET	✓	✓	
Vascular remodelling	- Pulse wave velocity - Augmentation index - Central blood pressure - Retinal imaging arteriolar and venular indices - Dermal capillary density	✓	✓	
Predictors of Response to Exercise and Blood Pressure Change		**Baseline**	**16 weeks**	**52 weeks**
Track intervention compliance and characterise participants' subjective and qualitative experience of intervention and correlate with intervention effects to clinical measurements to assess efficacy of the intervention.	- Exercise log and Fitbit step counts via Fitabase - Structured interview of participants		✓	✓
Baseline cardiovascular and cerebrovascular phenotypes in response to exercise intervention across outcomes.	- Baseline ambulatory blood pressure - CPET - Cardiac echocardiography - Brain and cardiac MRI	✓	✓	✓
Tertiles of blood pressure and cardiovascular risk scores in response to exercise intervention.	- Baseline ambulatory blood pressure - CPET - Cardiac echocardiography - Brain and cardiac MRI - Questionnaire	✓	✓	✓
ECFC function - Investigate if baseline molecular and cellular mechanisms in ECFC predict response to exercise intervention across outcomes.	- ECFC proteomics and functionality - Baseline ambulatory blood pressure - CPET	✓	✓	